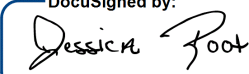


Distribution Agreement

In presenting this thesis or dissertation as a partial fulfillment of the requirements for an advanced degree from Emory University, I hereby grant to Emory University and its agents the non-exclusive license to archive, make accessible, and display my thesis or dissertation in whole or in part in all forms of media, now or hereafter known, including display on the world wide web. I understand that I may select some access restrictions as part of the online submission of this thesis or dissertation. I retain all ownership rights to the copyright of the thesis or dissertation. I also retain the right to use in future works (such as articles or books) all or part of this thesis or dissertation.

DocuSigned by:
Signature: 
E6BDC12821CD458...

Jessica Root
Name

6/23/2023 | 3:14 PM EDT
Date

Title Elucidating the Lysosomal Function of Granulins

Author Jessica Root

Degree Doctor of Philosophy

Program Biological and Biomedical Sciences
Neuroscience

Approved by the Committee

DocuSigned by:

Thomas Kukar

B00F10A6BF034AD...

Thomas Kukar

Advisor

DocuSigned by:

Victor Faundez

8525D8A9E8FE4A0...

Victor Faundez

Committee Member

DocuSigned by:

Chadwick Hales

7FA65C0C808C4C1...

Chadwick Hales

Committee Member

DocuSigned by:

Eric Ortlund

523BA27634FF4E6...

Eric Ortlund

Committee Member

DocuSigned by:

Nicholas Seyfried

4DDA20DAD30547B...

Nicholas Seyfried

Committee Member

Committee Member

Accepted by the Laney Graduate School:

Kimberly Jacob Arriola, Ph.D, MPH
Dean, James T. Laney Graduate School

Date

Elucidating the Lysosomal Function of Granulins

By

Jessica Turner Root
B.S., Emory University, 2015

Advisors:
Thomas Kukar, Ph.D.

An abstract of a dissertation submitted to the Faculty of the
James T. Laney School of Graduate Studies of Emory University
in partial fulfillment of the requirements for the degree of
Doctor of Philosophy
in Neuroscience
2023

Abstract: Loss of function mutations in the gene granulin (GRN) decrease levels of the protein progranulin (PGRN) and cause the neurodegenerative diseases frontotemporal dementia (FTD) and neuronal ceroid lipofuscinosis (CLN11). Although, lysosomal dysfunction is a common feature of PGRN deficiency disorders, the underlying function of PGRN and its constituent granulin subunits in the lysosome remains unclear. The studies detailed below demonstrate that granulins have the ability to rescue disease-like phenotypes *in vivo*, and that these phenotypes of interest are conserved across models of PGRN deficiency. This work contributes to the field's understanding of the molecular mechanisms underlying lysosomal dysfunction in models of PGRN deficiency, and provide insight into novel therapeutic avenues for PGRN based therapies.

Elucidating the Lysosomal Function of Granulins

By

Jessica Turner Root
B.S., Emory University, 2015

Advisors:
Thomas Kukar, Ph.D.

A dissertation submitted to the Faculty of the
James T. Laney School of Graduate Studies of Emory University
in partial fulfillment of the requirements for the degree of
Doctor of Philosophy
in Neuroscience
2023

1	<i>Introduction:</i>	6
1.1	A Brief History of Frontotemporal Dementia (FTD).....	7
1.2	FTD Clinical Subtypes	8
1.3	Pathology of Frontotemporal Lobar Degeneration.....	10
1.3.1	FTLD-Tau	11
1.3.2	FTLD-TDP	11
1.3.3	FTLD-FET	12
1.4	Genetics of FTD	12
1.4.1	C9orf72.....	13
1.4.2	MAPT.....	14
1.4.3	GRN.....	14
1.4.4	GRN in other Neurodegenerative Diseases	16
1.5	Functions of PGRN.....	17
1.6	PGRN and Neuronal Ceroid Lipofuscinosis	19
1.6.1	Overlap Between CLN11 and FTD-GRN.....	20
1.7	Lysosomal Functions of PGRN.....	20
1.8	Gene Therapy PGRN Treatments.....	24
1.9	Granulins	26
1.10	Production of Granulins	29
1.11	Functions of GRNs.....	32
1.11.1	Granulins in the Lysosome	34
1.11.2	Contrasting Functions of GRN and PGRNs.....	35
1.12	GRNs in FTD-GRN.....	37
1.13	Dissertation Aims and Hypothesis.....	38
2	<i>Granulins rescue inflammation, lysosome dysfunction, and neuropathology in a mouse model of progranulin deficiency</i>	40
2.1	Abstract.....	40
2.2	Introduction	40
2.3	RESULTS: ICV injection of rAAV at birth leads to widespread expression of granulins, PGRN, and GFP throughout the mouse brain.	42
2.4	Proteome-wide dysregulation in the thalamus of <i>Grn</i> ^{-/-} mice is ameliorated by expression of granulins.....	46
2.5	Individual granulins rescue dysregulated proteins in the thalamus of <i>Grn</i> ^{-/-} mice.....	48
2.6	Markers of Lysosomal Dysfunction are rescued by granulin expression across brain regions.....	51
2.7	Microglial activation and inflammatory markers are reduced by hGRNs	56
2.8	Lysosomal lipid dysregulation is rescued by a single granulin.....	60

2.9	Lipofuscin accumulation in <i>Grn</i> ^{-/-} brains is alleviated by expression of human granulins.	62
2.10	Behavioral Phenotypes.....	64
2.11	Discussion.....	66
2.12	Acknowledgements.....	69
2.13	Supplemental Figures.....	70
2.14	Experimental models and subject details.....	70
2.15	Methods.....	71
	Sample preparation for lipidomics and metabolomics analyses.....	76
	Lipidomics analysis.....	76
	Metabolomics analysis.....	77
	Analysis of glucosyl- and galactosyl-sphingolipids.....	78
3	<i>Chapter 3: HeLa cells Recapitulate Phenotypes of Lipid Dysregulation after loss of PGRN.....</i>	86
3.1	Introduction.....	86
3.2	Confirming that HeLa <i>GRN</i> ^{-/-} cell line is PGRN deficient.....	88
3.3	Characterizing Levels of lysosomal Proteins in <i>GRN</i> ^{-/-} HeLas.....	89
3.4	Activity of Cysteine Cathepsins are dysregulated in <i>GRN</i> ^{-/-} HeLa cells.....	91
3.5	Levels of LMP proteins and Lysosomal Membrane Integrity.....	92
3.6	Lipid Dysregulation is a characteristic of <i>GRN</i> ^{-/-} HeLa cells.....	96
3.7	Discussion.....	99
3.8	Methods.....	103
	Sample preparation for lipidomics and metabolomics analyses.....	106
3.9	Lipidomics analysis.....	106
4	<i>Discussion and Future Directions.....</i>	108
4.1	Summary of Findings:.....	108
4.2	Shared phenotypes between models:.....	108
4.3	GRNs are beneficial proteins in the lysosome.....	109
4.4	A New Model of GRN Function.....	110
4.5	Role of GRNs in Lipid Metabolism:.....	112
4.5.1	BMP.....	112
4.5.2	Glycosylsphingosines.....	117
4.6	The roles of individual GRNs, interchangeable, or divergent?.....	120
4.7	Reconciling findings that GRNs are beneficial with previous findings.....	122

4.8	Autonomous vs. Non-cell Autonomous Benefits of GRN expression.....	125
4.9	Therapeutic Role of GRNs, Outstanding Questions and Future pre-clinical studies.	128
4.9.1	Time of administration.....	128
4.9.2	Peripheral administration.....	129
4.9.3	Limitations of PGRN Deficient Mouse Models.....	131
4.9.4	Patient Derived iPSC lines as a platform for assessing therapeutic potential of GRNs.....	132
4.10	Investigating Proposed mechanisms for GRNs.....	133
4.11	Isolation of Lysosomes for PGRN deficient iPSCs.....	135
4.12	Exploring Cell Type Specific Effects	136
4.13	Understanding Inflammatory Roles of GRNs.....	137
4.14	Closing Remarks.....	138
5	<i>References</i>	<i>141</i>

1 Introduction:

Frontotemporal dementia (FTD) is the second most common dementia diagnosis after Alzheimer's disease, and the most common among people under the age of 60 (6). Over 100 different mutations in the granulin gene (*GRN*) encoding progranulin (PGRN) are known to cause FTD (7). All pathogenic *GRN* mutations reduce levels of PGRN, or are loss of function, however why decreased levels of PGRN cause disease remains unclear (8). PGRN is a multifunctional secreted protein composed of 7.5 tandem granulin domains expressed primarily in neurons and microglia in the CNS (9). PGRN has been associated with many functions including neurotrophic and anti-inflammatory activity (10-13), but its precise function is unclear.

While PGRN has been canonically understood as an extracellular protein, the discovery that homozygous *GRN* mutations cause a rare lysosomal storage disease CLN11 (14-16), revealed that PGRN may play a functional role intracellularly in the lysosome. Subsequent work has suggested PGRN may regulate activity of lysosomal hydrolases (17-20), influence the abundance of lysosomal lipids (21), and contribute to the maintenance of lysosome morphology (22). Loss of PGRN leads to lipofuscin accumulation, lysosomal dysfunction, and neuronal death (23, 24).

Work by the Kukar lab and others demonstrated that PGRN traffics to the lysosome where it is cleaved into the constitutive granulin subunits (25, 26). The granulin subunits are stable in the lysosome for many hours compared to PGRN which is cleaved within 30 minutes (25). Taken together, these data support the idea that cleaved granulin subunits carry out the functional role of PGRN in the lysosome. However individual granulins are not well understood, with various functions reported since they were first described in 1990 (27-29), some of which are conflicting (30, 31). These gaps in knowledge have stirred debate over whether granulins play a beneficial

role in the cell and contributed to the current lack of successful treatments for FTD-*GRN* patients. In this dissertation work, I will investigate the mechanisms underlying lysosomal dysfunction in disease relevant PGRN-deficient systems to further understand the etiology that leads to disease. The experiments detailed here assess the bioactive nature of granulins, and contribute to the basic understanding of lipid phenotypes and the tractability of HeLa cells lines to model FTD and CLN11. **These findings are significant because they advance our fundamental understanding of the role of PGRN and granulins in the lysosome.**

1.1 A Brief History of Frontotemporal Dementia (FTD)

The first case of FTD was described by Arnold Pick in 1892 (32). By 1906 Pick described 4 additional cases with language disturbances and temporal lobe atrophy and another patient that presented with behavioral disinhibition and mixed apraxia (33-35). All patients showed progressive mental deterioration, anomia and had pathology related to the degeneration of the left temporal lobe. Though Pick did not describe any histopathological changes, the histopathology associated with FTD was described a few years later in 1911 by Alois Alzheimer. While Alzheimer specifically characterized the argyrophilic intracellular inclusions and ballooned cells (36), it was A. Gans, a pupil of Pick's, who was the first to coin the term "Pick's Disease" to describe distinctive lobar cortical atrophy (37). While Pick believed that he had described an atypical case of senile dementia, work by Onari and Spatz (38), and Carl Schneider (39, 40) showed that Pick's Disease was a separate diagnosis, characterized by areas of degeneration and phases of clinical progression.

Pick's Disease remained a rare diagnosis until the second half of the 20th century when interest was rekindled as cases matching the clinical description were described in various patients. More evidence that these cases were Pick's disease was found at the histological level

where these cases were characterized into three types: the previously described argyrophilic inclusions and ballooned neurons (type A), ballooned neurons but not inclusions (type B) and cases lacking both ballooned neurons and inclusion (type C)(41). Concurrently, groups in Sweden and the UK described cohorts of patients with dementia and frontal lobe degeneration that did not present with either the plaques and tangles characteristic of Alzheimer's Disease or the inclusion pathology associated with Pick's Disease. The two groups independently termed these cases as "frontal degeneration non-Alzheimer type" (42, 43), and "dementia of the frontal type" (44). These two groups worked together to outline the first clinical and neuropathological criteria for frontotemporal dementia diagnoses (45). As clinical approaches, neuroimaging, neuropathology, and genetics have advanced, these criteria were later revised to encompass the heterogenous nature of FTD (46, 47). Our current understanding is that FTD is a clinically heterozygous disorder with substantial heritability. The heterogeneity of FTD can be classified according to 1) clinical presentation, 2) histopathological findings, and 3) genetic consultation.

1.2 FTD Clinical Subtypes

Frontotemporal dementia is an umbrella diagnostic term that encompasses two clinical subtypes classified by symptom presentation: behavioral-variant FTD (bvFTD), and primary progressive aphasia (PPA) (48). Each clinical variant is associated with a specific pattern of atrophy (49) and to a lesser degree a particular pattern of histopathology (section 1.3). Although presenting symptoms may differ, as the disease progresses symptoms often converge as the disease progresses and patients begin to develop more global cognitive impairment (50).

bvFTD comprises over 50% of all FTD cases (51). One of the most salient symptoms of bvFTD is behavioral disinhibition which can include socially inappropriate behavior, loss of manners, and impulsive actions (52). These changes are observed in concert with a relative sparing of memory functions. More cognitive symptoms include poor attention, distractibility,

disorganization, and loss of the ability to plan (53). Because of this presentation about half of bvFTD patients are first diagnosed with a primary psychiatric disorder prior to being diagnosed with a neurodegenerative disease (54). Neuroimaging studies show the earliest structural and functional changes in bvFTD patient brains include the anterior cingulate, orbitofrontal and fronto-insular cortices (55), and that these are generally lateralized to the right hemisphere, however, there is heterogeneity between individuals (56, 57).

The second common clinical presentation associated with FTD is primary progressive aphasia (PPA) which presents with an isolated language deficiency (58-60). Most diagnoses of PPA (~60%) are attributed to FTD disease processes, accounting for about 25% of FTD cases. The remaining 40% of PPA diagnoses are attributed to AD-type-neuropathology, highlighting how heterogenous and diverse FTD presents clinically (61). There are three recognized syndromes that are included under the diagnosis of PPA: semantic variant (svPPA) (62), progressive non-fluent variant (nfvPPA) (63), and logopenic progressive aphasia (64). Each subtype is characterized by a specific presentation in word loss, speech production difficulties, and word retrieval deficits.

svPPA, also known as semantic dementia, is characterized by difficulty reading words, irregular pronunciations, and surface dyslexia in the absence of speech fluency (65). Importantly, the gradual impairment of language focuses on object knowledge in comparison to other PPA subtypes (66). In contrast, lvPPA is characterized by an impairment in naming while object knowledge and single word comprehension is preserved (59). Though word finding difficulties may be present resulting in slower speech, lvPPA patients do not display the agrammatism typical of nfvPPA (59, 64). Lastly, nfvPPA is characterized by effortful speech and agrammatism (67). Agrammatism may be accompanied by a reduction in phrase length and syntactic complexity. For

example nfvPPA patients often employ fewer verbs than healthy controls (68). Interestingly, Pick's first descriptions of patients at the turn of the 20th century include patients whose symptoms would be considered both probable bvFTD and PPA diagnoses by today's criteria.

1.3 Pathology of Frontotemporal Lobar Degeneration

In gross pathological studies FTD patients' brains show frontal and anterior temporal lobe atrophy. Atrophy can be extensive, though there is marked sparing of posterior regions until the later stages of disease (69). Microscopically, the gray matter shows neuronal loss and gliosis, while white matter characteristically displays a loss of myelin and astrocytic gliosis (47). Though the patterns of atrophy and the cellular changes may be broadly generalizable between FTD clinical presentations and patients, FTD pathology is typically described as frontotemporal lobar degeneration (FTLD).

FTLD is the term fused to describe the various underlying pathological processes that cause the clinical manifestations of FTD. FTLD can be further broken down into three main neuropathological categories. The subdivisions of pathological presentations are categorized by the presence of inclusion bodies. The three recognized pathological designations are FTLD with tau inclusions (FTD-tau), FTLD with TDP-43 inclusions (FTLD-TDP) and FTLD with FET inclusions (FTLD-FET) (70). There are a few rare FTLD cases (<1%) where the major inclusion protein has not yet been identified. These cases are named for the proteins related to the ubiquitin proteasome system (UPS) found in the inclusions such as ubiquitin and p62 and termed FTD-UPS (71, 72). While the precise pattern and progression of degeneration correlates reasonably with clinical presentations, the pathology underlying each clinical presentation can vary making it difficult to accurately predict the neuropathology in individual patients. However, there are correlations between some clinical syndromes and neuropathological subtypes (73-75).

1.3.1 FTLD-Tau

Tau is a microtubule-associated protein that is highly expressed in neurons and functions to bind and stabilize microtubules (76). Abnormal accumulation of hyper phosphorylated tau is a feature of several neurodegenerative disorders, collectively referred to as tauopathies, a number of which can be classified as FTLD-tau (77, 78). Accumulation of hyperphosphorylated tau in neurofibrillary tangles (NFTs) is present in 45% of all FTD cases (79, 80). Pathological subtypes of FTD-tau include Pick's Disease (PiD), corticobasal degeneration (CBD), progressive supranuclear palsy (PSP), and argyrophilic grain disease (AGD) (75, 81). Tauopathies may be further subdivided by the primary isoform of the tau protein included in the inclusions either 3R tau (PiD), 4R tau (CBD, PSP, AGD), or a mixture of both (74, 78).

1.3.2 FTLD-TDP

TDP-43 pathology, characterized by hyperphosphorylated protein and cleaved c-terminal fragments, is the most common pathology present in FTD cases (81, 82). Transactivation-response DNA-binding protein of 43 kDa (TDP-43) is a ubiquitously expressed RNA/DNA binding protein with diverse functions including DNA and RNA homeostasis, transcriptional activation, mRNA splicing, transport, translation, and degradation (83-85). Four histopathological TDP-43 subtypes have been identified based on the distribution and morphology of the inclusions (86). Type A is characterized by TDP-43 neuronal cytoplasmic inclusions (NCI) and dystrophic neurites. It is most commonly associated with bvFTD and some nvPPA cases. Type B cases have moderate numbers of neuronal cytoplasmic inclusions, with few dystrophic neurites and most commonly identified in bvFTD cases. Type C pathology have high levels of dystrophic neurites and few neuronal cytoplasmic inclusions. There is a strong correlation between svPPA and type C pathology. Finally, type D pathology is marked by lentiform neuronal intranuclear inclusions of TDP-43 and short dystrophic neurites. This pathology is exclusively observed in patients with

VCP mutations, which is usually diagnosed as bvFTD (82, 87). Taken together one of these 4 FTLD-TDP pathologies is observed in about 50-60% of FTD cases (88, 89).

1.3.3 FTLD-FET

Inclusions in cases of FTLD-FET are positive for all three members of the FET family of proteins which includes fused in sarcoma (FUS), TATA-box binding protein associated factor 15 (TAF15), and Ewing's sarcoma (EWS)(90-92). Like TDP-43, they are ubiquitously expressed, homologous DNA/RNA-binding proteins, involved in various aspects of DNA and RNA metabolism (93). Compared to FTLD-tau and FTLD-TDP, FTLD-FET is less common representing about 5-10% of cases (75, 94). There are several histopathological variants of FTLD-FET known as Neuronal Intermediated Filament Inclusion Body Disease (NIFID), Basophilic Inclusion Body Disease (BIBD), and atypical FTLD-U (95-97). NIFID is characterized by FUS positive NCIs in a variety of brain regions (cortex, hippocampus, striatum, etc.) (98, 99). BIBD is characterized by strong FUS positive NCIs found in fewer brain regions (neocortex, hippocampus, globus pallidus, thalamus, midbrain, pons, and inferior olivary nucleus) and consistent ubiquitin positive staining (97, 100). Atypical FTLD-U has the most restrictive FUS positive immunoreactive staining (highest staining in frontal cortex) and is characterized by FUS positive neuronal intranuclear inclusions, NCI, and glial cytoplasmic inclusions (99, 100). Clinically most FTLD-FUS cases are sporadic, meaning no genetic heritability can be traced for these patients. These cases are also generally considered severe, with the age of onset occurring before the age of 50 (75).

1.4 Genetics of FTD

Clinicians observed the familial nature of FTD shortly after it was first described (101). 40-50% of bvFTD patients have a family history of disease, suggesting that there is a strong

genetic component (102, 103). This contrasts with other forms of dementia like AD for which only 5% of early onset patients have an identified autosomal-dominant mutation (104). Although the inheritance pattern varies between clinical diagnoses, family history is most prominent in patients with bvFTD (~45%) (103), and is less common in PPA (105). The majority of familial FTD cases can be attributed to mutations in three different genes: granulin (*GRN*), chromosome 9 open reading frame 72 (*C9orf72*), and microtubule-associated protein tau (*MAPT*) which together account for up to 40% of familial FTD (106). A list of pathogenic and other variants in these genes has been collated online in the AD&FTD Mutation Database (107).

1.4.1 C9orf72

C9orf72 was originally linked to FTD when multiple groups reported a strong linkage between a locus on chromosome 9 and the development of FTD as well as a related neurodegenerative disease, amyotrophic lateral sclerosis (ALS) (108-110). Following this, two groups independently discovered that FTD was caused by a hexanucleotide repeat expansion in the non-coding region of *C9orf72* gene was a major cause of FTD and ALS (111, 112). The *C9orf72* gene of most healthy individuals contains between two and twenty G4C2 repeats. Disease typically occurs in patients that have a repeat expansion of 100 or more G4C2 repeats (113). These repeat expansions of *C9orf72* are the most common genetic cause of FTD, accounting for about 25% of hereditary cases (113, 114). While the normal function of the protein encoded by *C9orf72* is still under investigation, it has been proposed that the toxicity of the G4C2 repeat expansion arises from dipeptide repeat (DRP) proteins, disrupted intracellular membrane trafficking, and/or RNA mediated toxicity (115-117). *C9orf72* cases are positive for TDP-43 pathology as it is thought that *C9orf72* expansions lead to the inappropriate exit of TDP-43 from the nucleus into pathological inclusions, typically either FTLD-TDP type B or type A (118). As we see with other genetic causes of FTD, the clinical presentation of *C9orf72* mutation carriers can be diverse. The

most common clinical diagnosis is bvFTD. Further, if ALS symptoms are seen in an individual with familial FTD it is likely that they carry an *C9orf72* mutation (119).

1.4.2 MAPT

Pathogenic mutations in the *MAPT* gene were the first to be linked to FTD (120-122). Since its description in the late 1990s, over 60 dominantly inherited mutations *MAPT* have been identified accounting for 5%–20% of familial FTD (fFTD) and 0%–3% of sporadic FTD (sFTD) (94, 123, 124). Patients with *MAPT* mutations present with FTLD-tau (125). Based on their mode of action, two different types of *MAPT* mutations are described: the first type deregulates gene splicing altering ratios of 3R and 4R isoforms, while the second type disturbs microtubule binding (126, 127). bvFTD is the most common diagnosis for families with *MAPT* mutations, typically with an early age of onset between 45 and 55 years old (119).

1.4.3 GRN

MAPT mutations were first identified in a group of patients with FTD and parkinsonism linked to chromosome 17 (128, 129). After *MAPT* was identified there were still several families that were negative for *MAPT* mutations and tau pathology but did display autosomal-dominant FTD linked to the same region on chromosome 17. This suggested that there was another gene on chromosome 17 that caused FTD. In 2006, mutations in the granulin gene (*GRN*), which encodes PGRN, were found to cause FTD with ubiquitinated inclusions that contained TDP-43 (130-133). Since the first description over 90 mutations have been reported in the *GRN* gene including frameshift, splice site, nonsense signal peptide, Kozak sequence disruptions, and missense mutations (https://coppolalab.ucla.edu/lovd_gift/view/GRN). Despite the diversity of mutation types, all pathogenic *GRN* mutations cause disease through haploinsufficiency which leads to ~50% or greater reduction in PGRN mRNA and protein (134). In healthy controls the levels of circulating PGRN in human plasma is about 200 ng/mL (135) and in CSF it is found

at a lower concentration around 6 ng/mL (136). Patients with FTD-GRN generally have plasma PGRN levels of 120 ng/mL or lower (135). It has been suggested that decreased protein levels may be mediated by nonsenses mediated degradation of the *GRN* mRNA transcript (137, 138). However, point mutations have also been shown to reduce the amount of CSF PGRN below the threshold for healthy function (135), indicated that further investigation into the mechanism via which *GRN* mutations lead to decreased protein requires further study. Depending on the patient population, *GRN* mutations account for 5–20% familial FTD and 1–5% of sporadic FTD patients

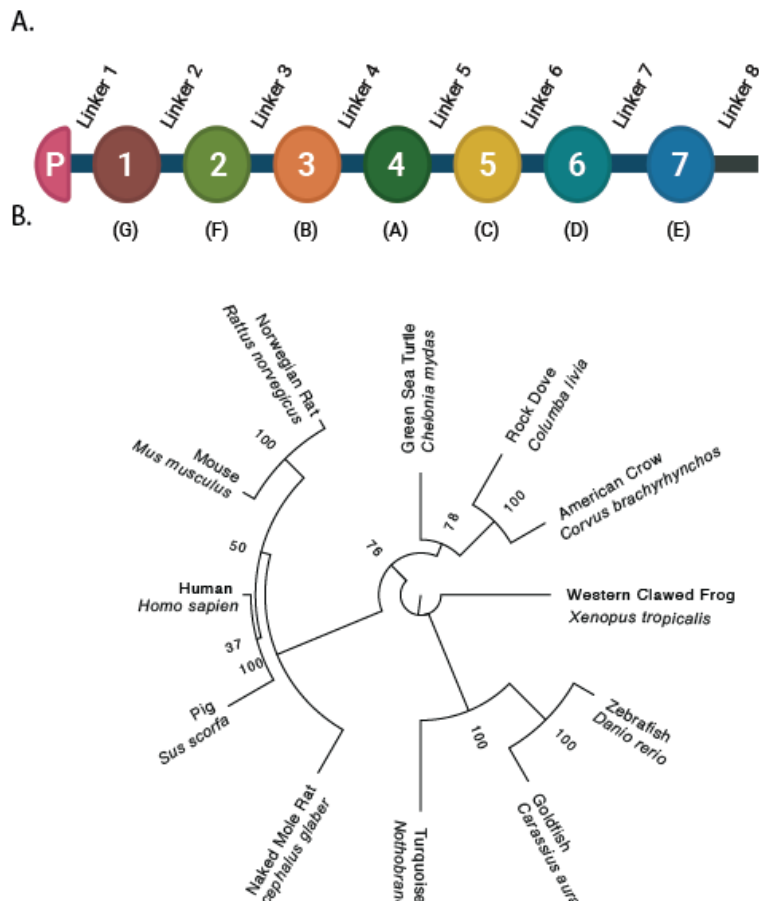


Figure 1.1: PGRN structure and Phylogeny

A) Schematic of PGRN and linker regions

B) Phylogenetic Tree with GRN human protein sequence and homologs. Maximum-Likelihood tree with bootstrap values displayed at nodes.

(113, 132).

At a pathological level, *GRN* mutations have been associated with FTLT-DTP subtype A pathology (133, 139, 140). Even so, *GRN* mutations carriers present with the widest clinical spectrum of genetic FTD. bvFTD and nfvPPA are the most common clinical presentation of *GRN* mutation carriers. However, clinical diagnosis of Alzheimer's disease, Lewy Body Dementia, and CBD have all been reported in *GRN* mutation carriers (119, 141). Interestingly, variants in the *GRN* gene have been identified as risk factors for both AD and PD (142-145), underlining the multifaceted and heterogeneous nature of *GRN* mutations and their clinical implications.

Encoded by the *GRN* gene, progranulin (PGRN) was originally discovered as a component of the granule fraction of mammalian phagocytic leukocytes (27). PGRN is also known as PC cell derived growth factor (146), acrogranin (147), proepithelin (148), granulin-epithelin precursor (149) or epithelial transforming growth factor (150). PGRN is a pleiotropic glycoprotein protein that is composed of 7.5 tandem cysteine rich granulin (GRN) domains (**Fig 1.1A**). Progranulin is phylogenetically ancient and granulin-domain containing proteins are found in organisms from slime molds (151) to mammals (27) (**Fig 1.1B**). Interestingly, multiple proteins containing granulin-domain are found in fish and invertebrates, whereas mammals possess only one copy of a granulin-domain containing gene (152). Taken together, this phylogenetic history suggests that progranulin is one of the first extracellular regulatory proteins still utilized by multicellular organisms (153).

1.4.4 *GRN* in other Neurodegenerative Diseases

Beyond FTD, a common genetic variant in *GRN*, the T allele of rs5848, has been associated with an increased risk of developing AD (142, 143, 154) and Parkinson's Disease (PD) (144, 145). Loss of function mutations have also been associated with Lewy Body Dementia (LBD), a rare neurodegenerative disorder associated with alpha synuclein pathology

(155). Variants within the *GRN* gene have also recently been associated with limbic predominant age associated TDP 43 encephalopathy (LATE) (156).

1.5 Functions of PGRN

PGRN is expressed throughout the body and CNS including epithelial cells, neurons, myeloid cells, immune cells, and adipocytes (157-159). Progranulin's broad expression profile suggests a role in basic cellular functions, and it has been implicated in several roles including: neurotrophic activity, wound healing, cancer progression, modulation of inflammation, and lysosome homeostasis (160).

Progranulin was originally described as a growth factor that regulates wound healing (27). Since these first observations, our understanding of PGRN's role in tissue growth, development and remodeling has expanded. PGRN has been detected at some of the earliest stages of development both before implantation where it plays a role in cavitation and blastocyst development (161, 162), and after where PGRN is particularly crucial to the development of epithelial and neural tissues (163). Following development PGRN is likely important for wound healing as expression increases in epithelial cells after injury and adding PGRN to wounds in mice increase the number of fibroblasts and capillaries (30). In the brain, PGRN is neurotrophic in that it promotes neurite outgrowth (11), and increases cell survival and axon growth in a model of nerve injury (164) and ischemic stroke (165).

In addition to promoting growth during development and wound healing, PGRN can enhance the colony forming ability of tumor cells (166) and regulate the proliferation of several types of cancer (167-169). PGRN has been studied in the context of several mechanisms of cancer progression (170, 171) including regulation of apoptosis (172), mediation of cell migration and invasion (173), the modulation of angiogenesis (174, 175), the promotion of chemoresistance (176, 177), and tumor cell immune evasion (178). Serum PGRN levels are currently being

investigated as a potential biomarker or prognostic indicator in ovarian cancer (179, 180), breast cancer (181), glioblastoma (182), and others (171).

Concordantly with its role in tumor cell immune evasion, PGRN may act as an immunomodulator. PGRN is elevated in chronic inflammatory conditions like atherosclerosis (183), diabetes mellitus (184), metabolic syndrome (185), multiple sclerosis (186), rheumatoid arthritis (187), and asthma (188). Studies suggest that PGRN can modulate the expression and release of chemokines, small secreted proteins that stimulate cell migration and play a central role in the immune system (189), including IL-8 (190), and the loss of PGRN increases levels of IL7 and IL-10 (191). Progranulin also reduces reactive oxygen species production by immune complex-activated neutrophils, inhibiting neutrophilic inflammation (192, 193). Although the mechanisms through which PGRN exerts this anti-inflammatory effect is not well understood some have asserted that it could be through PGRN's interaction with TNFR (194-196). However, there are conflicting reports on whether TNFR is truly a PGRN receptor (197-200).

While PGRN levels increase in chronic inflammatory diseases, the loss of PGRN has been shown to promote signs of inflammation in several models of neurodegenerative disease including models of FTD (201-203). Although these findings may seem disparate, taken together these data suggest that PGRN plays a role in the modulation of the immune response. It is possible that PGRN levels require careful regulation as both too much or too little PGRN have been found to be associated with increased inflammation.

PGRN has also been suggested to act as an adipokine, which are secreted factors produced by adipose tissue that can affect metabolic homeostasis, satiety, and reproduction (204). PGRN is found to be upregulated in differentiating adipocytes and is increased by LPS treatment and other inflammatory signaling molecules (205). Further, in the identifying report PGRN

expression is increased as a consequence of insulin resistance. *Grn*^{-/-} mice fed a high fat diet were protected from developing insulin resistance (206). Lastly, PGRN levels are increased in patients with obesity and metabolic disorder, and positively correlate with levels of insulin resistance (207, 208). In mice inhibition of PGRN expression in the hypothalamus increased feeding behaviors and obesity (209). These findings suggest that PGRN expression shifts in response to metabolic regulation, though the mechanism of action require further study (205).

Overall, PGRN has been implicated in several processes, but the proposed functions generally focus on the PGRN as a secreted factor localized to the extracellular space. However, recent genetic studies suggest PGRN plays a major functional role intracellularly.

1.6 PGRN and Neuronal Ceroid Lipofuscinosis

One of the first pieces of evidence that PGRN may be involved in lysosome function arose when homozygous *GRN* mutations were discovered to cause neuronal ceroid lipofuscinosis (NCL) type 11 (CLN11) (210). NCLs, also known as Batten's disease, are a group of lysosomal storage disorders that has been distinguished from other LSDs by the presence of lipofuscin, an auto-fluorescent storage material in enlarged nerve cells (211). Tissues throughout the body display abnormal accumulation of vacuolated lipoproteins in autolysosomes. CLN11 patients produced no detectable PGRN, had retinal dystrophy, seizures, cerebellar ataxia, and early signs of cognitive deterioration in their 20s. Electron micrographs of patient skin biopsy showed ultrastructure abnormalities and fingerprint accumulation of lipofuscin, the marker indicative for a diagnosis of NCL. The ultrastructure of the storage deposits differs between subtypes of NCL, though the mechanism behind this variation remains unknown. For some NCL subtypes some components of the storage material lipofuscin are known (212) and include sphingolipid activator proteins (SAPs) and subunit C of mitochondrial adenosine triphosphate synthase (SCMAS), however, for CLN11 the makeup of the lipofuscin in human patients remains unclear

(212, 213).

In addition to these pathological findings CLN11 patients have clinical features related to neurodegeneration including cerebellar ataxia, seizures, and progressive decline in cognitive and motor functions (23). Since the original case report, other cases of CLN11 have been documented (14, 15, 214-216), including families with both FTD-*GRN* and CLN11 cases (14). Recently, new patients from 9 unrelated families with homozygous *GRN* mutations were reported to present with variable clinical phenotypes (16, 217) including juvenile onset NCL, and bvFTD, including behavioral disinhibition and apathy. The observed heterogeneity in phenotype aligns with other NCL subtypes caused by mutations in 12 other genes related to lysosomal function (218, 219).

1.6.1 Overlap Between CLN11 and FTD-*GRN*

The clinical and genetic overlap between FTD-*GRN* and CLN11 patients led to further comparison of pathological findings between FTD-*GRN* patients and models of complete PGRN deficiency. One of the first reported similarities was the presence of retinal degeneration in FTD-*GRN* patients similar to CLN11 patients (220). Lipofuscinosis and ultrastructural abnormalities were found in the retinal and cortical tissue of FTD-*GRN* patients and patient derived iPSC neurons (19, 221). FTD-*GRN* patient brains and NCL patients had increased levels of the lysosomal membrane protein LAMP2, the lysosomal hydrolase cathepsin D, and astrocyte marker GFAP (17). Furthermore, SAPD and SCMAS are elevated in FTD-*GRN* patients' brains which are components of lipofuscin in several NCL subtypes (17). Taken together, this data suggests that FTD and NCL caused by *GRN* mutations are clinical phenotypes with a common mechanism of etiology and exist on a spectrum of severity related to the role of PGRN in lysosomal function (16, 210).

1.7 Lysosomal Functions of PGRN

Among the earliest findings linking PGRN to the lysosome was the discovery that PGRN co-localized to the lysosomal compartment and active cysteine cathepsins detected using immunocytochemistry (222, 223). Several endocytosis receptors mediate PGRN trafficking to the lysosome including direct trafficking via sortilin (SORT1) (Fig 1.2) (222) and indirect trafficking with prosaposin via its receptors cation-independent manose-6 phosphate receptor (CI-MP6R) and low-density lipoprotein receptor-related protein 1 (LRP1) (157). However, it is possible that other receptors remain to be discovered. Because PGRN is found in the lysosome it has been proposed that PGRN may regulate lysosomal function by several mechanisms including the modulation of lysosomal hydrolases, controlling lysosomal acidity, and regulation of lysosomal biogenesis signaling (224-226).

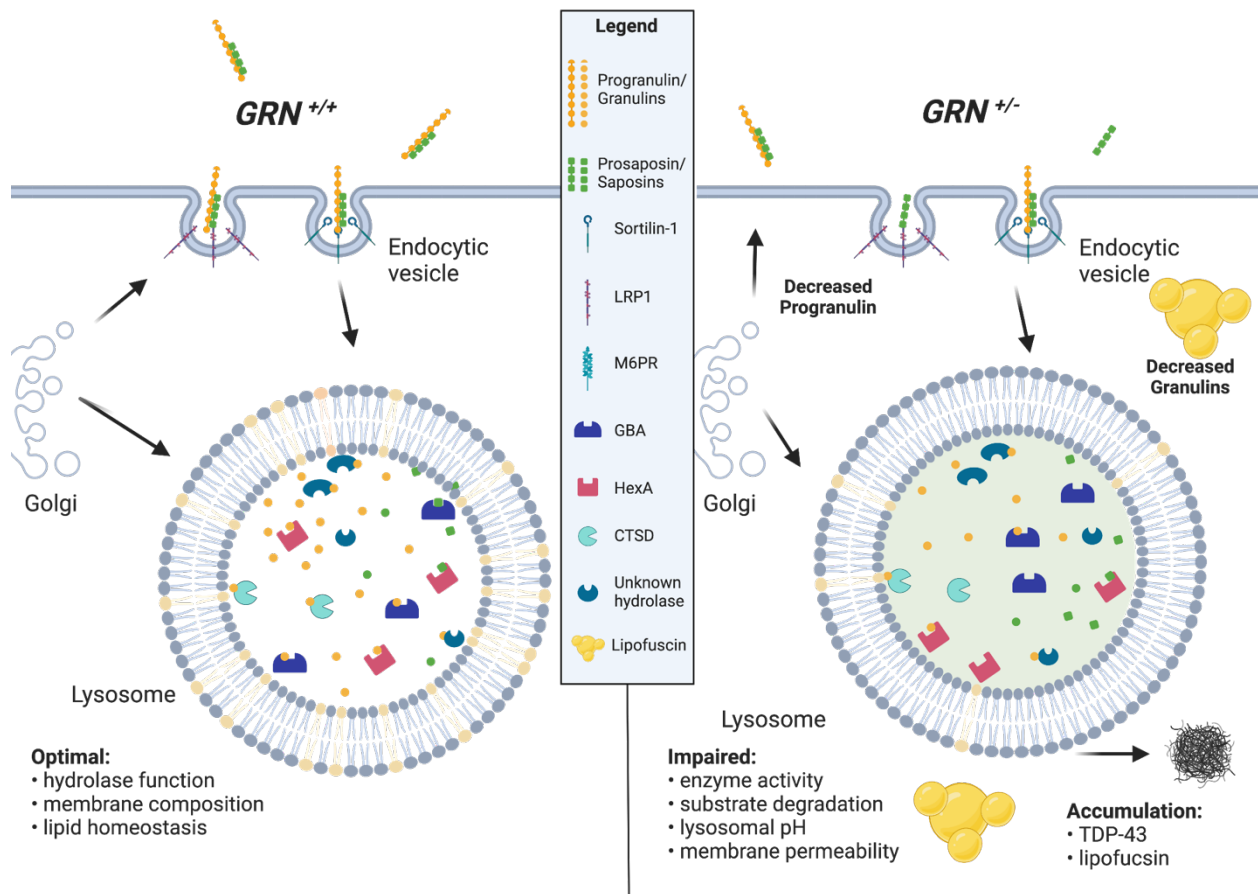


Figure 1.2: PGRN and GRNs function Intracellularly

A) Representative diagram of proposed lysosomal function with and without PGRN/GRNs

Mounting evidence suggests that PGRN can play a direct, or indirect role, on the activity of lysosomal enzymes. Patient derived induced pluripotent stem cells (iPSCs) and patient derived primary fibroblasts, as well as and preclinical mouse model of FTD-GRN show upregulation of lysosomal cathepsins (19, 221, 227). Specifically, PGRN has been shown to bind to cathepsin D (CTSD) and regulate its function (228, 229). Cathepsin D is a unique lysosomal aspartic protease that is also implicated in NCL, as mutations in the CTSD gene cause CLN10 (230). PGRN can also regulate other lysosomal enzymes including glucocerebrosidase (GBA) also known as GCase (18, 20, 231, 232) and β -hexosaminidase A (HexA) (233). PGRN is reported to bind

directly to GBA (231) and HexA (233) in order to regulate their enzymatic activity. Mutations in *GBA* cause Gaucher's Disease (234), the most common LSD. While *HexA* mutations lead cause Tay-Sachs Disease (235), both enzymes help degrade sphingolipids in the lysosome (236). This pattern shows that dysregulation of proteins known to interact with PGRN cause multiple LSDs with sphingolipid accumulation. Work included in this dissertation and others have shown that the loss of PGRN leads to dysregulated sphingolipid levels as well (237, 238). This suggests that a common mechanism, such as dysregulation of enzymes related to lipid metabolism, could underlie sphingolipid accumulation of in served FTD-*GRN* and LSDs.

Lysosomes are important for maintaining lipid homeostasis within the cell and play a role in lipid catabolism, and trafficking (239, 240). PGRN's role in lipid metabolism was first indirectly suggested when it was discovered that PGRN binds to prosaposin (PSAP) (157). PSAP is a precursor protein that is processed in the lysosome into individual saposin peptides (SapA-D), which activate various lysosomes lipases and facilitate glycosphingolipid degradation (241). The main substrates of GBA, which PGRN is known to interact with, glucosylceramide (GlcCer) and glucosylsphingosine (GlcSph), are not found to be dysregulated in FTD-*GRN* brains though levels of GlcSph are elevated in patient plasma (238). FTD-*GRN* patients brains display an accumulation of gangliosides (242), a decrease in overall white matter volume, and an accumulation of white matter cholesterol (243). Furthermore, immortalized human cell lines lacking PGRN show an accumulation of polyunsaturated triacylglycerides (21) and gangliosides (242), as well as a reduction of diacylglycerides, phosphatidylserine (21), and bis(monoacylglycerol)phosphate (BMP) (216, 242, 244), an atypical endo-lysosomal lipid. Additional enzymes involved in lipid metabolism are dysregulated in preclinical models of PGRN deficiency (227), enrichment of lipid droplet associated microglia (245), and lipid

dysregulation in *Grn*^{-/-} mice can be rescued by the exogenous addition of PGRN (238, 242).

There are several pieces of evidence that suggests PGRN may be important in the maintenance of lysosomal membranes. Loss of PGRN triggers to the recruitment of galectin-3, a marker of lysosomal membrane permeability (LMP), to the lysosomal membrane (246). Galectin-3 acts as a sensor of endo-lysosomal damage and LMP by binding lysosomal β -galactosides that are exposed on the cytosolic side of the lysosomal membrane as a consequence of LMP (247). Membrane integrity is crucial to the ability of the lysosome to maintain acidity, and lysosomes with elevated galectin-3 are likely to have dysregulated pH (248). PGRN has been proposed to directly influence lysosome acidification via its interaction with both SORT1 and CI-MP6R (249). Further, PGRN may be a part the Coordinated Lysosomal Expression and Regulation (CLEAR) response, which are genes involved in lysosomal function and autophagy (250). In addition, the *GRN* gene contains sequences that can bind the transcription factor EB (TFEB) (251, 252) a master regulator of lysosomal genes implicated in lysosomal structure and function and part of the CLEAR response (253). These observations suggest that PGRN is an essential protein for lysosomal homeostasis, and PGRN haploinsufficiency due to heterozygous *GRN* mutations may cause lysosomal dysfunction that underlies the characteristic neurodegeneration in both NCL11 and FTD-*GRN* (Fig 1.2).

1.8 Gene Therapy PGRN Treatments

Preclinically, FTD-*Grn* is commonly modeled *in vivo* using *Grn*^{-/-} mice. These mice develop disease related pathology including neuroinflammation, lysosome dysfunction, synaptic loss, and lipofuscin accumulation that increases with age (254). *Grn*^{-/-} mice brains accumulate lipofuscin and have increased levels and activity of HexA and GBA (20, 231, 255). As previously mentioned, *Grn*^{-/-} mice show signs of sphingolipid metabolism abnormalities, and BMP depletion (227, 238, 242). In addition to lysosomal dysfunction, *Grn*^{-/-} mice display signs

of neuroinflammation including, increases in proteins associated with microglial activation like CD68, astrogliosis, and elevated cytokine levels (256-258). Elevated inflammation and pathology are particularly prominent in the thalamus, where excessive pruning of inhibitory synapses is observed (259). It is important to note, these mice lack TDP-43 pathology present in human patients until a very advanced age (260). Taken together, these disease-like phenotypes may lead to decreased median survival of *Grn*^{-/-} mice compared to *Grn*^{+/+} mice (261).

In addition to biochemical recapitulation, *Grn*^{-/-} mice also phenocopy behavioral deficits associated with selective degeneration of the salience network (257, 262). They display compulsive behaviors such as over grooming and decreased sociability (257, 259). Some behaviors like decreased social dominance are actually more prominent in heterozygous compared to homozygous knock out mice (263).

Grn^{-/-} mouse models have been used to evaluate therapies targeting PGRN, several of which have progressed to clinical trials (264). This includes indirect approaches to increase PGRN levels such as anti-sortilin antibodies (265, 266) which have progressed to stage-3 clinical trials (NCT04374136). Other approaches include ASOs that block premature termination codons (137), or target miRNAs that regulate PGRN levels (267) and nonsense mediated decay inhibitors (137, 268). Other groups have utilized *Grn*^{-/-} mice to test the efficacy of strategies to directly replace PGRN. First, a protein transport vehicle (PTV) conjugated progranulin (PTV:PGRN) leverages an Fc domain that binds the human transferrin receptor (huTfR) to transport PGRN across the blood brain barrier. It can be delivered peripherally and has been shown to rescue several disease-like phenotypes including lysosomal and lipid regulation dysfunction (238). A phase 1 & 2 clinical trial is currently enrolling participants (NCT05262023).

In contrast to direct protein replacement, which may require ongoing administration, gene therapy could provide a one-time treatment approach to increase PGRN levels. Delivery of PGRN preferentially to neurons using AAV1 in the mPFC of *Grn*^{-/-} mice rescued signs of lysosomal and microglial dysfunction (244, 256). These benefits were not limited to the PFC and were also observed in the thalamus and hippocampus suggesting local delivery and expression of PGRN could have far reaching beneficial effects. Groups have also used PGRN's biology as a secreted protein to deliver the gene therapy intracerebroventricularly (ICV) (269). Using capsids that generalize delivery to additional cell types such as AAV9 lead to increased inflammation and hippocampal degeneration compared to AAV1 (270). However, immunogenic reactions observed in AAV can be dependent on species, time of delivery and delivery route (271), underlining the importance of optimizing these factors in therapeutic development. Several early-stage clinical trials testing intra-cisternal magna delivery of AAV9-hPGRN (NCT04408625) and AAV1-hPGRN (NCT04747431) are underway.

Multiple therapeutic modalities increasing levels of PGRN have been assessed in pre-clinical, and in ongoing clinical trials. However, no intervention specifically focusing on PGRN's subunits, the granulins have been investigated. Understanding the clinical significance of individual granulins is important, as there are PGRN based therapies in the clinical pipeline that both increase levels of granulins, like AAV approaches, and decrease levels of granulins, like anti-sortilin antibodies. Understanding the function of granulins will inform not only the design of treatments moving forwards but could inform outcomes of interest in ongoing trials.

1.9 Granulins

Granulins (GRNs) are ~6 kDa proteins that were first isolated from the granules of leukocytes in the 1990s (27, 28). It was later apparent that these individual granulins peptides were subunits of a single precursor protein, PGRN, encoded by the gene known as *GRN* (148). In total

the human *GRN* gene contains 12 coding exons and is translated into a protein containing 7.5 tandem repeats called granulins (GRNs). GRNs contain a uniquely high percentage of cysteine residues (~17%) (272), the average in the human proteome is around 3% (273). The granulin domain belongs to a larger group of cysteine rich protein domains known as knottin-II class domains (272). Knottin domain containing proteins are found in many species and are generally cysteine rich small proteins that are characterized by at least 3 interwoven disulfide bonds. These domains are functionally resistant to high temperature, enzymatic degradation, extreme pH and mechanical stress (274). Although the redox state of GRNs in the lysosome is unclear, it is known that GRNs have a high level of thermal stability (25, 31, 275). The granulin repeat is structurally defined by the cysteine-rich sequence X2-3CX5-6CX5CCX8CCX6CCXDXXHCCPX4CX5-6CX, where X can be any amino acid (153). The granulins are named, from the N terminus of progranulin to the C terminus, numerically p, granulin 1-7 with the p denoting the half-length paraganulin domain (Fig. 1.1A). Alternatively, some refer to the granulins using alphabetical nomenclature which are named starting at the N terminal: p, G, F, B, A, C, D, and E. For the remainder of this work, I will refer to the granulins using the numerical nomenclature. Granulins are separated by divergent linker regions. Protease cleavage occurs within these linker regions to produce the individual granulins (Fig 1.3A, 1.3C) (10, 276, 277).

Although the three-dimensional structure of full-length PGRN is unknown, the template structure of human granulins based on the known structure of carp granulin-1 has been determined using high resolution NMR spectroscopy (Fig 1.3B) (31, 278). Each granulin consists of parallel stacked β -hairpin turns held together by 6 disulfide bonds formed between the conserved cysteines within each subunit (30). These disulfide bonds are critical residues for the structure of GRNs (279), and mutations to these crucial cysteines interfere with the protein folding and function (135).

The high number of disulfide bonds leads to each individual GRN being compact, and may mediate protease resistance of GRNs in the lysosome compared to full length PGRN which is rapidly cleaved to GRNs (280).

Although each GRN shares conserved cysteine residues, there are marked differences between the individual granulins in structure and biochemistry. Sequence comparison of all full GRNs show that no two share more than 60% sequence identity (**Table 1**). This variation likely

<i>Table 1</i>	hGRN5	hGRN2	hGRN3	hGRN4	hGRN6	hGRN1	hGRN7
hGRN5	100.0%	46.3%	55.6%	59.3%	53.7%	40.7%	38.9%
hGRN2	46.3%	100.0%	51.8%	50.0%	49.1%	33.9%	41.1%
hGRN3	55.6%	51.8%	100.0%	52.7%	40.0%	34.5%	38.2%
hGRN4	59.3%	50.0%	52.7%	100.0%	52.7%	39.3%	48.2%
hGRN6	53.7%	49.1%	40.0%	52.7%	100.0%	38.2%	41.8%
hGRN1	40.7%	33.9%	34.5%	39.3%	38.2%	100.0%	33.9%
hGRN7	38.9%	41.1%	38.2%	48.2%	41.8%	33.9%	100.0%

contributes to differences in electrostatic charges at neutral pH and hydrophobicity observed between the granulins (281, 282). However three-dimensional structure and the pH of surrounding environment can influence ionizable groups and affect the net charge and hydrophobicity of a protein significantly (283). All human granulins contain 12 cysteine residues, with the exception of granulin 1 which contains 10 (31). While the general structure of the granulins has been reported, subsequent studies have highlighted differences in NMR spectroscopy and levels of internal disorder within individual granulins, particularly in the C-terminal region of GRN4 (31) and GRN3 (275, 279). It is important to note that the generalizability of these conclusions to *in vivo* systems may be limited as these proteins were produced recombinantly in non-mammalian cells, or assessed under reducing conditions which could change outcomes observed endogenously in mammalian cells or tissue.

While full length PGRN is a heavily glycosylated at asparagine residues, not all granulin subunits are glycosylated (284, 285). Specifically, GRNs 3, 5, 7, and the linker 2 region between GRN1 and GRN2 are N-linked glycosylated (285, 286). There is also evidence that the pattern of glycosylation could be tissue specific as levels of glycosylated GRN5 differed in mouse liver and spleen tissue extracts (286). This could be significant because glycosylation modifies protein structure and folding as well as interactions and recognition of other proteins and molecules (287). In addition to glycosylation one group has reported that a multi-granulin peptide containing GRNs 5-7 is serine phosphorylation, however precise residues have not been reported (288). This work suggests that GRNs may be differentially modified post-translationally. However, further work is needed to understand if any post-translational modifications effect granulin function.

1.10 Production of Granulins

The production of GRNs is a complex process that depends on the linker regions connecting the granulins and proteins that interact with PGRN. Cleavage of each granulin subunit is dependent on the divergent linker regions between the GRNs (7, 276, 277). Just as the general sequence of each granulin differs, each linker region has a unique amino acid sequence (Fig 1.3C). The divergent linker sequences that separate the granulin subunits can be cleaved by extracellular and intracellular proteases. Although PGRN is cleaved within the multiple linker regions between the granulin domains there isn't a clear consensus sequences for a specific protease. Taken together with the existence of multi-granulin fragments this suggests that PGRN can be cleaved by multiple proteases (10).

Indeed, progranulin can be proteolytically cleaved by several extracellularly localized enzymes including neutrophil elastase (193), proteinase 3 (a neutrophil protease) (192), MMP-12 (matrix metalloproteinase 12; macrophage elastase) (289), MMP-14 (290), and ADAMTS-7 (291). In addition to primarily extracellular proteases, several lysosomal enzymes can cleave PGRN to GRNs. As previously discussed, PGRN was first understood as a protein that functioned

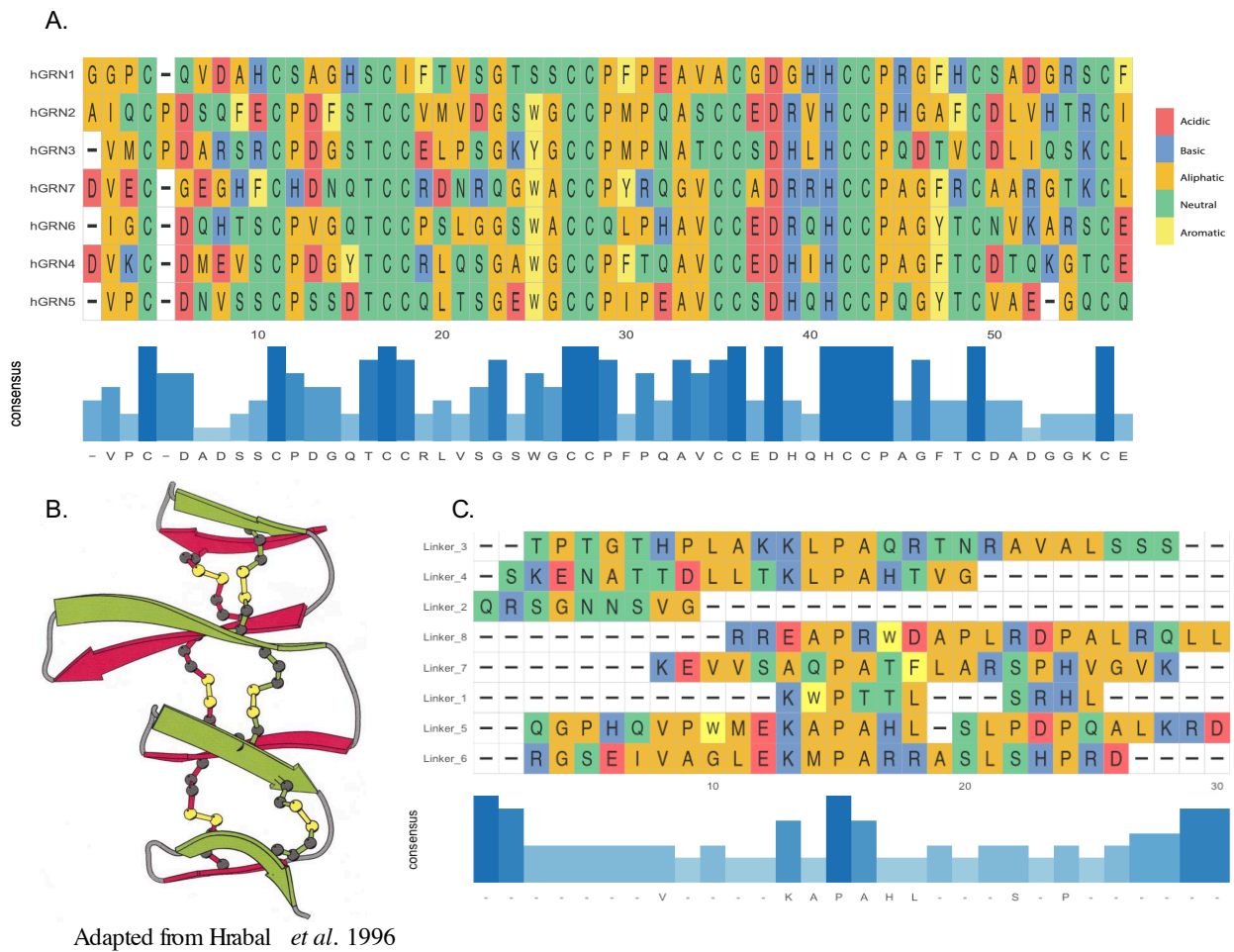


Figure 1.3: GRN Linkers and structure of GRNs

- A) ClustalOmega alignment of granulins 1-7 from the human PGRN protein. Amino acids colored by base chemistry and consensus residues from each site displayed above alignment
B) Representative model of GRN structure from Hrabal *et al.* 1996 (3)
C) ClustalOmega alignment of linker regions 1-8 from the human PGRN protein. Amino acids colored by base chemistry and consensus residues from each site displayed above alignment

extracellularly, however recent work has re-shaped this paradigm and focused interest on PGRN and GRNs intracellularly.

Intracellularly, PGRN traffics to the lysosomal compartment as previously described. Much like its trafficking partner PSAP, PGRN is processed to its constitutive granulins in the lysosome. The Kukar lab and others have independently shown that intracellular processing of PGRN into granulins also occurs in a lysosome dependent manner (280, 292, 293). PGRN was found to be present in cell lysates and media, while GRNs were detected in the cell lysates but were present at very low levels extracellularly. This suggests that PGRN is endocytosed and processed into GRNs, and that GRNs are primarily being produced intracellularly in the lysosome in these models (280, 292). Furthermore, inhibition of lysosomal function using autophagy inhibitors, or trafficking via SORT1 or PSAP decreased GRN levels while simultaneously increasing the abundance of full length PGRN (280, 294).

Cathepsin L (CatL) was the first lysosomal enzyme shown to cleave PGRN into GRNs and multi-granulin peptides *in vitro* (26). This was followed up by the discovery that the activity of Cathepsin L was pH dependent, and an acidic lysosomal pH is required for CatL to cleave PGRN (26, 280, 292). Since these initial findings other lysosomal enzymes that process PGRN have been identified. These include additional cysteine proteases like cathepsin B (CatB) (277, 280, 292), asparagine endopeptidase (AEP), aspartyl protease cathepsin E (CatE) and serine protease cathepsin G (CatG) (277). Interestingly expression of proteases known to cleave PGRN is not uniform suggesting that the regulation of PGRN processing into GRNs may be tissue or cell type specific (153, 289, 295). Further, *in vitro* incubation of PGRN with proteases produces not only 6kDa fragments but intermediate fragments between 15 kDa and 25 kDa (192, 193, 289). Adding an additional level of regulation, interactions with proteins like SLPI and high-density lipoprotein

(HDL) can modulate the ability of proteases to cleave PGRN (193, 296). When PGRN binds SLPI and cleavage by elastase is prevented (193). Similarly, the interaction of HDL and PGRN leads to a reduction in GRN production, though the mechanism is unclear (296). The multistep process of PGRN cleavage to GRNs remains poorly understood. Continued work is required to understand the cleavage of PGRN *in vivo* and the localization of GRNs throughout the cleavage process. Overall, the production of GRNs is dependent not only on the ability of PGRN to traffic to the lysosome, but also potentially on the tissue, cell type, and cellular localization of the protein.

1.11 Functions of GRNs

Most studies investigating the function of PGRN do not address any distinction between the precursor protein and the individual granulins. This has led to an incomplete understanding of the role GRNs play biologically. This may be due to technical limitations because until recently antibodies that detect individual granulins were not available. However, several groups including ours is working to address this shortcoming (280, 286). With these limitations in mind, work has been done to investigate the role of GRNs, but most do not include all GRNs, and the majority focus on the C-terminal GRN 7. Due to its position at the c-terminus of the PGRN protein, and its localization of the SORT1 binding domain and ability to be detected with commercially available antibodies, the majority of information surrounding the function of an individual GRN has focused on GRN 7 (GRN E) (297). GRN 7 exerts neurotrophic properties on cortical and motor neurons (11, 164), hippocampal neurons (10), and Schwann cells (164). Interestingly these neurotrophic effects have also been observed in a SORT1 independent manner (298), suggesting that GRN7's sortilin binding domain may not be the only factor enabling its neurotrophic properties.

Other granulins have also been implicated in neurotrophic functions. GRN5 and was found to increase motor neuron survival and axon outgrowth while also conferring a protective effect on Schwann cells in co-culture (164). A study delivering PGRN with point mutations in either GRN2,

GRN3 or, the linker region following GRN5, linker 6 to *GRN*^{-/-} cells found that the wildtype protein, but not the mutants were able to enhance neuronal outgrowth and neurite branching (10). A separate study leveraging *GRN* point mutations found GRN2 had a similar role in neurite growth stimulation in cell culture (299), suggesting that individual GRNs or the irregular processing of these granulins contributes to the observed neurotrophic effect (10). Finally, granulin and multi-granulin peptides less than 50 kDa have been shown to protect retinal photoreceptors from degeneration (300). While these findings all demonstrate that GRNs can be neurotrophic, or the loss of GRNs can be anti-trophic, there were also variations observed in the efficacy between GRNs. For example, neurotrophic effects comparing GRN7 and GRN5 were recapitulated in hippocampal neurons, but not the cortical neurons (10). While the mechanisms underlying tissue specific differences is unclear, recent work has shown that the ratio of GRNs differs in various tissues, brain regions, and cell types (286). This may indicate that while GRNs may have overlapping or redundant functions, there may be differences in cell type or tissue that characterize an individual GRNs role.

Outside of the brain GRN4 has been implicated in both pro-proliferative and anti-proliferative functions. GRN4 was shown to promote rodent keratinocyte and fibroblast proliferation (28, 148). Interestingly in these same studies GRN3 was found to be anti-proliferative. Independent groups found that GRN4 was found to have a more robust anti-proliferative effect than GRN3 in cancer cell lines (28, 301), and in the same cancer cell lines GRN2 was found to have the opposite effect of GRN4 and stimulated breast cancer cell growth (31). These findings must be interpreted with care, as they primarily focus on cancer cell lines, which can be difficult to translate to other model systems. Additionally, these studies assess GRNs added extracellularly to cells with no known PGRN deficiency. Further investigation is required

to understand the role of individual GRNs on lysosomal functions, and expansion to other models outside of overexpression in cancer will be important to understand the effects of GRNs in the context of deficiency.

In addition to regulating cell growth and neurotrophic functions, GRNs have been reported to regulate nucleic acids and transcription factors. Specifically, GRNs regulates DNA synthesis in models of breast cancer (GRN4) (301) as well as glioma and cultured astrocytes (GRN6) (302). These functions seem specific to certain GRNs as GRN6 (303) and GRN 7 (304), but not the other granulins (304, 305), bind the cysteine-rich activation domain of Tat, part of the Tat/P-TEFb complex that regulates the human immunodeficiency virus type 1 (HIV-1) transcription (304).

1.11.1 Granulins in the Lysosome

Granulins are known to be produced in the lysosome and are stable in the acidic compartment. Although GRNs localize to the lysosomal intracellularly, it's unclear what role granulins play in the lysosomal compartment. GRN2 or GRN3 has been shown to localize to the inner leaflet of LAMP1 positive lysosomes (280). Additionally, GRN7 was found to bind CD68 (306). In addition to associating with lysosomal membrane proteins, GRNs have been reported to bind lysosomal proteases. GRN7 has been shown to interact with GBA (18, 19, 229). In another study surveying all GRNs only GRN2 or GRN4 co-transfected with GBA immunoprecipitated with the enzyme (20). However, this experiment relied on an overexpression system, which can lead to improper protein folding and other artifacts (307). When GRNs in conditioned media from the same co-transfection paradigm were assayed all GRNs weakly associated with GBA except GRN1 (20). While it was asserted that the secreted GRNs are properly folded, this is not directly addressed and studies have found that overexpression can lead to non-canonical secretion of unfolded proteins (308).

Similar to studies showing differences in GRNs propensity to interact with GBA, Cathepsin D does not interact with all GRNs in a conserved manner. While GRN7 and multi-granulin peptides were shown to enhance the conversion of the pro-form of CatD to the mature protease, GRN5 did not (19, 282). However, after a selective reduction of GRN7 caused by the loss of CD68 CatD activity remains consistent (306). Although, it is not clear if this is mediated by the other multi-GRN fragments previously described, or another compensatory pathway. While granulins have been shown to associate with lysosomal membrane proteins and lysosomal enzymes our understanding of the role of these granulins in the lysosome remains incomplete. Further, the ability of individual granulins to rescue or replace PGRN function in models of PGRN deficiency have not been directly assessed.

1.11.2 Contrasting Functions of GRN and PGRNs

While there is evidence that GRNs share the same or similar neurotrophic and lysosomal functions with full-length PGRN, there are other publications suggestion GRNs have the opposing activity of PGRN (148). In particular, GRNs have been suggested to be pro-inflammatory, and anti-proliferative. GRNs levels increase in *C elegans* with age (281) and their overexpression promotes TDP-43 toxicity (309). Two studies have suggested that the abundance of multi-GRN fragments increases (309), and the ratio of PGRN to GRNs is dysregulated in FTD-GRN patient brains (277). PGRN is known to be cleaved to GRNs by several proteases that are released to the extracellular space by inflammatory stimuli including matrix metalloproteinase-9 (MMP-9) (310), MMP-12 (289), MMP-14 (290), neutrophil elastase (311), and proteinase 3 (PRTN3) (192). Though increased GRNs have not been quantified after inflammatory stimuli, it has been hypothesized that they could potentiate inflammation.

While PGRN has been reported to inhibit neutrophil activation and degranulation by blocking activity of TNF- α (193), recombinant granulins were found to either have a neutral or

enhancing effect (193, 312). Two GRNs were also suggested to induce the release of pro-inflammatory IL-8, from epithelial cells (190, 193). There are several limitations to these studies. Firstly, GRNs in these studies were produced using insect cells, therefore it is possible that the posttranslational modifications such as glycosylation of the GRNs are not produced the same way as they would be in human cells (313). Second, the purity of recombinant GRNs in the studies is poorly characterized, raising the possibility that contaminants are present, which may induce an immune response, as reported with other proteins made using baculovirus (314). Further these cell-based studies add GRNs to culture media, therefore these effects could be attributed to extracellularly localized GRNs. The abundance of extracellular GRNs in homeostatic conditions is not well understood. Further, while appropriate inflammatory responses are crucial for the maintenance of a healthy system, inappropriate or excessive inflammation can be detrimental. Understanding GRNs role in disease related inflammation vs. adaptive inflammatory responses will be important to further understand the complex biological role of PGRN and GRNs.

While there are reports that PGRN and GRNs have neurotrophic activity, there are conflicting publications suggesting that GRNs may be neurotoxic and anti-proliferative. Recombinant GRN4 was found to be anti-proliferative in a cancer cell model (31). However, like the previous cell-based assays discussed, these GRNs were purified from *E. coli*, and added to cell culture media, limiting the scope of these findings' translatability to homeostatic *in vivo* function. In a *Caenorhabditis elegans* model of TDP-43 proteinopathy, complete loss of the *pgrn-1* gene did not exacerbate TDP-43 toxicity, but *pgrn-1* heterozygosity did (309). If granulins were co-expressed with TDP-43 in *C. elegans*, the toxicity of TDP-43 was amplified and the granulins increased TDP-43 levels via a post-translational mechanism. Granulin peptides were also found to increase in abundance after aging and impair lysosomal cathepsins (281) and learning behavior in

C. elegans (309). These findings however, have not been recapitulated in a mammalian model suggesting that this may be a response that varies between biological model systems, and may not be applicable in mammals.

In general, granulins have been described as having the opposite, or antagonistic activity, compared to PGRN (276, 298, 315). However, these assumptions are based on a small number of studies that directly compare the function of PGRN and GRNs. These studies do identify differences between PGRN and GRNs, however this work was conducted in cell culture using protein produced in insect cells or *E. coli* or *C. elegans* and has yet to be translated to an *in vivo* mammalian model. This gap in understanding of GRN function is a major unmet need, because it has critical implications for how GRNs are assessed in therapeutic approaches for PGRN based diseases and changes the landscape for the exploration of potential GRN functions.

1.12 GRNs in FTD-GRN

Point mutations within the *GRN* gene that affect single GRNs decrease levels of PGRN in patient plasma below a pathogenic threshold (316). These mutations both affect one of the conserved cysteine residues and migration of native protein in non-reducing conditions is altered, suggesting that the tertiary structure of the protein may be compromised. Further it was observed that the C139R mutation affected neutrophil elastase cleavage of PGRN. This data suggests that the loss of cleaved PGRN may be sufficient to cause disease. Though information about the function of individual GRNs is limited, several studies provide insights into the biological function of the GRNs and how they either converge, or conflict with that of the full length PGRN precursor protein.

While the precise functions of GRNs remain unclear, and in some cases contradictory, it is important to note that in cases of FTD-*GRN* our lab published that both PGRN and individual granulins (GRN2, 3, 4) are decreased by similar amounts (280, 292). In contrast, Salazar *et. al*,

reported that a 33 kDa GRN fragment that contained GRN7 was specifically increased in regions of AD and FTD brains that had degeneration and gliosis (309). Further, they measured levels of GRN2 peptides in FTD-*GRN* patient brains from areas with neurodegeneration and concluded that GRN2 levels were increased compared to non-degenerating areas. However, this needs to be interpreted with caution, as GRN2 levels were not different between healthy controls and FTD-*GRN* patients was not changed (277). These studies suggest that the ratio of PGRN to GRN2 varied between healthy controls and FTD-*GRN* patient brains, but it is unclear whether the increase in GRNs is pathological or compensatory, especially as the overall abundance does not differ between cases and controls.

1.13 Dissertation Aims and Hypothesis

In summary, we know that decreased expression of PGRN leads to clinical presentation of FTD or NCL in human patients as a function of gene dose. PGRN is a secreted protein that has been implicated in decreasing inflammation, and modulating cell growth pathways. Though much work has been done to characterize the function of PGRN, it remains unclear why the loss of PGRN leads to lipofuscin accumulation, TDP-43 inclusions, neuroinflammation, and neuronal death in patients.

Previous studies have generally focused on the extracellular role of PGRN because it is secreted. Recently, work by the Kukar lab and others has shown that PGRN is also trafficked to the lysosome and cleaved into the individual GRNs (25). These GRNs were found to be stable in the lysosome for up to 16 hours, much longer than the precursor protein which was cleaved within minutes. Further, as GRNs are reduced in FTD-*GRN* patients, **we propose that GRNs are the bioactive component of PGRN that function intracellularly in the lysosome.** Understanding the role of GRNs, and whether they are biologically beneficial and homeostatic will address several outstanding questions regarding PGRN and GRN biology.

To investigate this gap in knowledge, I carried two aims. In AIM 1 I examined how expression of individual granulins effected lysosomal dysregulation, glial activation, and lipid accumulation in *Grn*^{-/-} mice. This aim provides insight into the functional role of granulins in a mouse model of progranulin deficiency and helps to determine whether these proteins are protective or toxic *in vivo*. This will be discussed in **Chapter 2**.

While the assessment of GRNs *in vivo* provides crucial insight into the role of GRNs in cellular survival, understanding the function of GRNs in the lysosome is challenging in a murine model. To overcome this challenge, in AIM 2 I investigate the function of lysosomes in PGRN deficient HeLa cells. These experiments validate a highly tractable cell-based model to study the cellular functions of GRNs. This will be discussed in **Chapter 3**.

We propose a paradigm shift in our understanding of the role of PGRN. This change is of particular importance as previous work has proposed that GRNs may have the opposite activity of full length PGRN and be pro-inflammatory and toxic. We investigate this both pre-clinically in mice and mechanistically in HeLa cells. These studies provide insight into the beneficial role of GRNs but also help to define individual role of the GRNs, and direct the development of new therapeutic approaches and clinical readouts in PGRN related disorders. The impact and future directions of this work will be considered in **Chapter 4**.

2 Granulins rescue inflammation, lysosome dysfunction, and neuropathology in a mouse model of progranulin deficiency

2.1 Abstract

Progranulin (PGRN) deficiency is linked to neurodegenerative diseases including frontotemporal dementia, Alzheimer's disease, Parkinson's disease, and neuronal ceroid lipofuscinosis. Proper PGRN levels are critical to maintain brain health and neuronal survival, however the function of PGRN is not well understood. PGRN is composed of 7.5 tandem repeat domains, called granulins, and is proteolytically processed into individual granulins inside the lysosome. The neuroprotective effects of full-length PGRN are well-documented, but the role of granulins is still unclear. Here we report, for the first time, that expression of single granulins is sufficient to rescue the full spectrum of disease pathology in mice with complete PGRN deficiency (*Grn*^{-/-}). Specifically, rAAV delivery of either human granulin-2 or granulin-4 to *Grn*^{-/-} mouse brain ameliorates lysosome dysfunction, lipid dysregulation, microgliosis, and lipofuscinosis similar to full-length PGRN. These findings support the idea that individual granulins are the functional units of PGRN, likely mediate neuroprotection within the lysosome, and highlight their importance for developing therapeutics to treat FTD-*GRN* and other neurodegenerative diseases.

2.2 Introduction

The granulin (*GRN*) gene encodes progranulin (PGRN), an ancient, evolutionarily conserved protein that is critical for brain health and neuronal survival (153). Specifically,

haploinsufficiency of PGRN due to *GRN* mutations causes frontotemporal dementia (FTD), a common neurodegenerative disease in people under the age of 60(132, 133, 170). Complete deficiency of PGRN causes neuronal ceroid lipofuscinosis (NCL), a neurodegenerative lysosomal storage disorder (LSD).(16, 210) Moreover, genetic variants in *GRN* decrease PGRN levels and have been associated with an increased risk of developing Alzheimer's disease, Parkinson's disease, or limbic-predominant age-related TDP-43 encephalopathy (LATE).(142, 143, 154, 317) Multiple therapeutic strategies are being pursued to treat the various neurodegenerative diseases associated with decreased PGRN.(224, 318) Despite these advances, the fundamental function of PGRN is still unresolved and presents a roadblock for developing efficacious therapies for neurodegeneration.

PGRN is a ~88 kDa secreted glycoprotein that is ubiquitously expressed and enriched in microglia and neurons in the brain.(289, 293, 319) Mammalian PGRN is composed of 7.5 tandem repeat proteins, called granulins. Within PGRN, each granulin is joined together by short linear sequences or linkers, which can be cleaved by proteases to release mature granulins (192, 193, 289). We refer to each granulin numbered 1 through 7 based on the UniProtKB (P28799) database, rather than the colloquial A through G nomenclature. The relationship between the activity of PGRN and individual granulins has been debated and is still unclear. Multiple functions have been associated with full-length PGRN including cell growth, neurotrophic signaling, and anti-inflammatory activity. The pleiotropic activity of PGRN may occur through binding extracellular signaling receptors (170, 320), however some PGRN-receptor interactions have not been widely replicated (198, 199, 321), raising the possibility of other mechanisms of action. Furthermore, the function of individual granulins, also called epithelins, is also controversial and unresolved. Depending on the model system, the reported activity of granulins is paradoxical, ranging from

enhancing neurotrophic activity(298), to promoting inflammation(193), inducing neurotoxicity (309) or impairing lysosome function.(281)

The discovery by our lab, and others, that granulins are made constitutively inside lysosomes led us to reevaluate the functional relationship between PGRN and granulins (25, 26, 292). Because complete loss of granulins in humans and mice causes an LSD, with more severe neurodegeneration than observed in PGRN haploinsufficiency, we reasoned that granulins have an intra-lysosomal function. This idea is supported by the known function of other lysosomal proteins, such as saposins, which are generated from the prosaposin precursor protein.(322) Here we test the hypothesis that PGRN serves as a precursor to granulins, which are the functional units that mediate lysosomal homeostasis and are neuroprotective. We used recombinant adeno-associated virus (rAAV2/1) to assess whether expression of individual granulins in the brain of PGRN deficient mice can correct disease-associated phenotypes. Our data show that neuronal expression of a single granulin fully rescues a range of phenotypes including lysosomal dysfunction, microglial activation, lipid abnormalities, and lipofuscin accumulation to the same extent as full-length PGRN. These findings provide compelling evidence that granulins are the bioactive subunits of PGRN and indicate that potential therapeutic approaches for FTD-GRN should consider their effect on granulin levels. Furthermore, this work supports the potential use of granulins themselves for the treatment of diseases associated with PGRN deficiency.

2.3 RESULTS: ICV injection of rAAV at birth leads to widespread expression of granulins, PGRN, and GFP throughout the mouse brain.

To test the hypothesis that granulins are functionally active and neuroprotective, we utilized *Grn*^{-/-} mice, which lack PGRN and develop pathology including neuroinflammation, lysosome dysfunction, and synaptic loss that increases with age. In these experiments, we compared human granulins 2 and 4, as previous studies suggested they have opposing functional

activity.(31) Furthermore, human granulin-2 (hGRN2) and human granulin-4 (hGRN4) share only 50% identity at the amino acid level, and we reasoned this would be sufficient to reveal differences in bioactivity if present (**Supp. Fig. 1A, B**). Human progranulin (hPGRN) and GFP served as positive and negative controls, respectively. For granulins and PGRN, we engineered expression constructs to include an N-terminal signal peptide (SP), to

direct trafficking through the secretory pathway, followed by epitope tags (twin-Strep tag and V5 or FLAG) to facilitate detection preceding the coding region of interest (**Fig. 2.1A**). We validated these constructs in HeLa *GRN^{-/-}* cells and found that hGRN2, hGRN4, and hPGRN were properly trafficked to the lysosome as well as secreted into the media (**Supp. Fig. 2**). Then, we

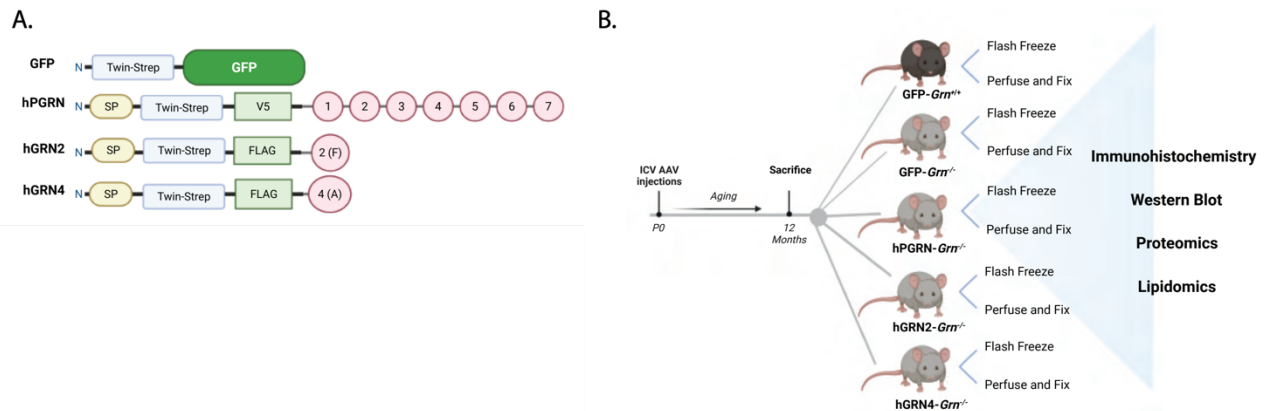


Figure 2.1: ICV injection constructs and experimental timeline

- A) Diagram of all expression constructs including coding region of interest, domains, and epitope tags that were packaged into rAAV2/1 (twin-Strep-tag (TST); V5 epitope tag; FLAG epitope tag; SP= signal peptide; granulin-1; granulin-2; granulin-3; granulin-4; granulin-5; granulin-6; granulin-7).
- B) Diagram of experimental workflow including ICV injection of rAAV, mouse aging, sample collection, and sample analysis.

generated recombinant hybrid Adeno-Associated Virus 2/1 (rAAV2/1) encoding hGRN2, hGRN4, hPGRN, and GFP and performed bilateral intracerebroventricular (ICV) injections of rAAV2/1

vector into newly born (P0) litters of *Grn*^{-/-} and *Grn*^{+/+} mice (**Fig. 2.1B**). This experimental paradigm, termed somatic brain transgenesis (SBT), preferentially transduces neurons when using AAV vectors packaged in the capsid 1 serotype and leads to widespread and long-term expression of genes of interest in the mouse brain.(323-325)

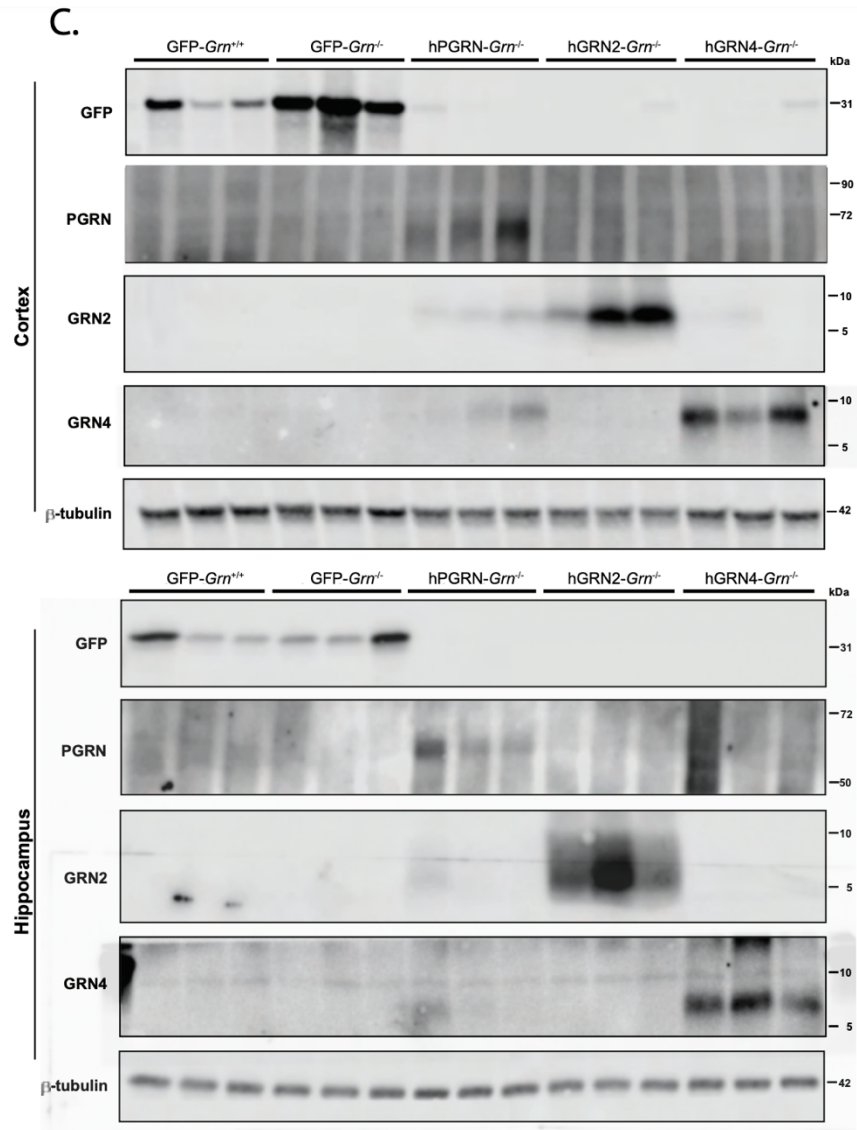


Figure 2.2: Immunoblot confirms expression of granulins in cortex and hippocampus

A) *Immunoblot verifying expression of encoded proteins following rAAV injection and aging. Cortical and hippocampal lysates were probed for GFP, hPGRN, hGRN2, hGRN4, with β-tubulin loading control.*

All mice were aged to 12-months, when substantial neuropathological changes are present in *Grn*^{-/-} mice. Next, we characterized the distribution and expression of each rAAV2/1 vector throughout the brain of injected *Grn*^{-/-} and *Grn*^{+/+} mice. To confirm the specific identity of expressed proteins, we performed immunoblotting of lysates from flash frozen cortical and

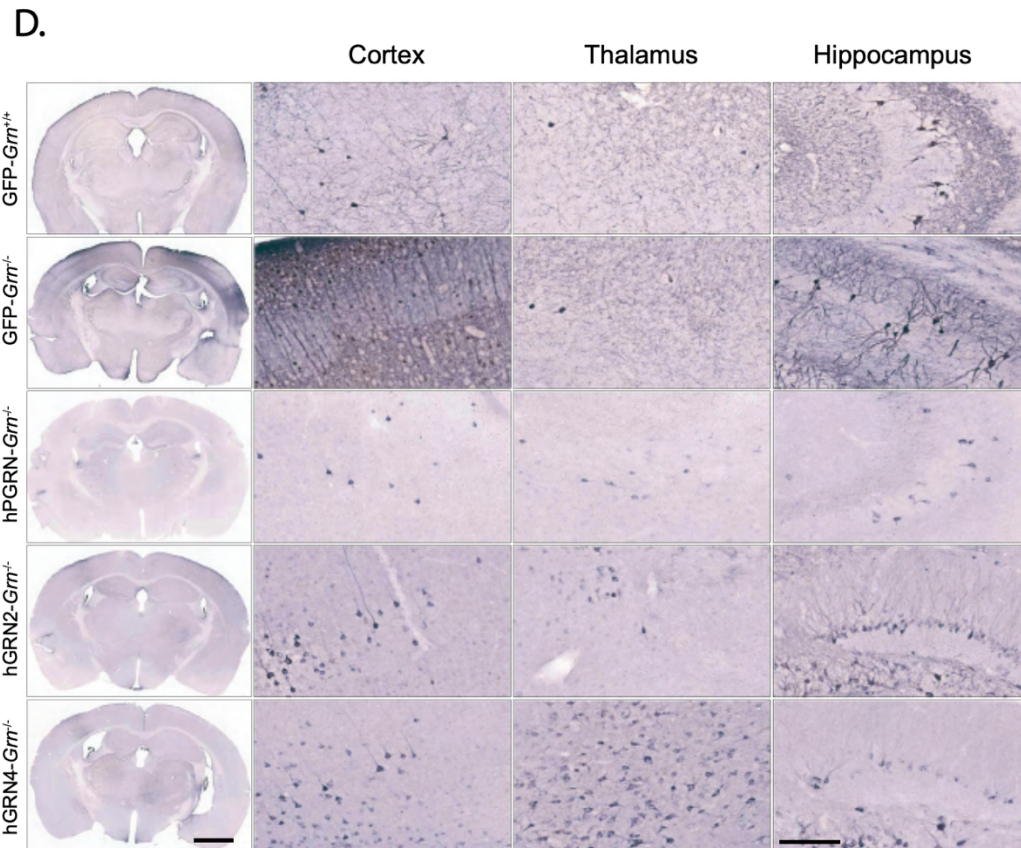


Figure 2.3: Strep-tag identified throughout the injected brains

A) Representative immunohistochemistry (IHC) images for twin-Strep tag to visualize expression of GFP, hPGRN, hGRN2, and hGRN4 following AAV injection in whole coronal

hippocampal brain tissue. Using specific antibodies, we confirmed expression of human progranulin in hPGRN-*Grn*^{-/-} mice, human GRN2 in hGRN2-*Grn*^{-/-} mice, human GRN4 in hGRN4-*Grn*^{-/-} mice and GFP in GFP-*Grn*^{-/-} and *Grn*^{+/+} mice in both the hippocampus and cortex (**Fig. 2.2A**). Immunostaining of serial coronal sections for the twin-Strep tag, which is shared across expression constructs, visualized, and verified widespread expression of all encoded

proteins in the hippocampus, thalamus, and cortex across injected mice (**Fig. 2.3A**).

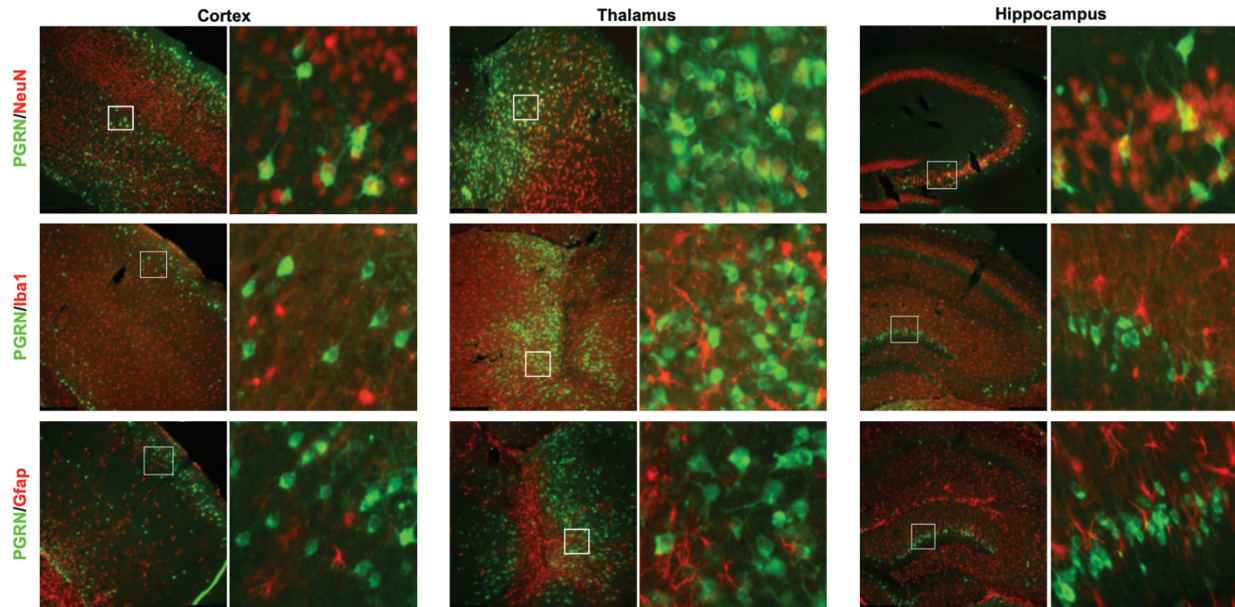


Figure 2.4: Immunohistochemistry co-localizes hPGRN and NeuN

A) Representative immunofluorescent images co-staining for hPGRN and antibody markers for neurons (NeuN), microglia (Iba1), and astrocytes (GFAP) in the cortex, hippocampus, and thalamus of an hPGRN-Grn^{-/-} mouse. White box highlights section of tissue enlarged on the right.

Next, we assessed which cell types in the brain were transduced by rAAV2/1 and expressed specific transgenes. We utilized immunofluorescent staining to co-label hPGRN with the neuronal marker NeuN, the microglial marker Iba1, or the astrocytic marker GFAP in hPGRN-Grn^{-/-} mice. We find that AAV-mediated transgene expression positively co-localized with the neuronal marker NeuN throughout the cortex, thalamus, and hippocampus. In contrast, we did not detect co-localization with Iba1 or GFAP (**Fig. 2.4A**). Thus, neonatal ICV injection of rAAV2/1 produced robust and stable neuronal expression of hGRN2, hGRN4, hPGRN, and GFP in mouse brains over the 12-month period of our experiments.

2.4 Proteome-wide dysregulation in the thalamus of Grn^{-/-} mice is ameliorated by expression of granulins.

The thalamus is a major site of pathologic changes in *Grn*^{-/-} mice(227) and FTD-*GRN* patients(326, 327), however the underlying pathogenic mechanisms are still poorly defined. To provide deeper insight into dysfunction of the thalamus caused by PGRN deficiency, we performed proteomics on flash frozen thalamic tissue of 12-month-old *Grn*^{-/-} mice injected with rAAV2/1 encoding hGRN2, hGRN4, hPGRN, or GFP and *Grn*^{+/+} mice injected with rAAV2/1 encoding GFP (**Fig. 2.1B**). Then, we performed quantitative proteomics of lysates of dissected thalamus using Tandem Mass Tagged (TMT) isobaric labeling followed by off-line electrostatic repulsion-hydrophilic interaction chromatography (ERLIC) fractionation prior to LC-MS/MS resulting in the identification and quantification of 9,255 proteins across all samples (**Supp. Fig. 3A**).

We next compared the GFP-*Grn*^{+/+} and GFP-*Grn*^{-/-} thalamic proteomes to identify differentially expressed proteins. In GFP-*Grn*^{-/-} mice we identified 131 proteins that increased and 9 proteins that decreased in abundance in the thalamus compared to GFP-*Grn*^{+/+} mice (≥ 1.2 -fold change; FDR $q < 0.05$; **Fig. 2.5A**). Gene ontology (GO) analysis of the top 100 differentially expressed proteins using Metascape found a significant enrichment ($-\log_{10}(p) > 10$) of proteins involved in lysosome function (Kegg mmu04142), glycosphingolipid metabolism (R-MMU-1660662), and protein catabolic processes in the vacuole (GO:0007039) (**Fig. 2.5B**). Some of the most significantly dysregulated proteins in *Grn*^{-/-} mice included lysosomal hydrolases (*Arsa*, *Gns*, *Hexa*, *Hexb*, *Manba*) and proteases (*Ctsd*, *Dpp7*, *Lgmn*, *Tpp1*). Additionally, modules related to inflammatory processes were significantly enriched ($-\log_{10}(p) > 5$), including MHC class II antigen presentation (R-MMU-2132295), regulation of complement cascade (R-MMU-977606),

which include C1Qa, C1Qb, C1Qc, and C1Qb.

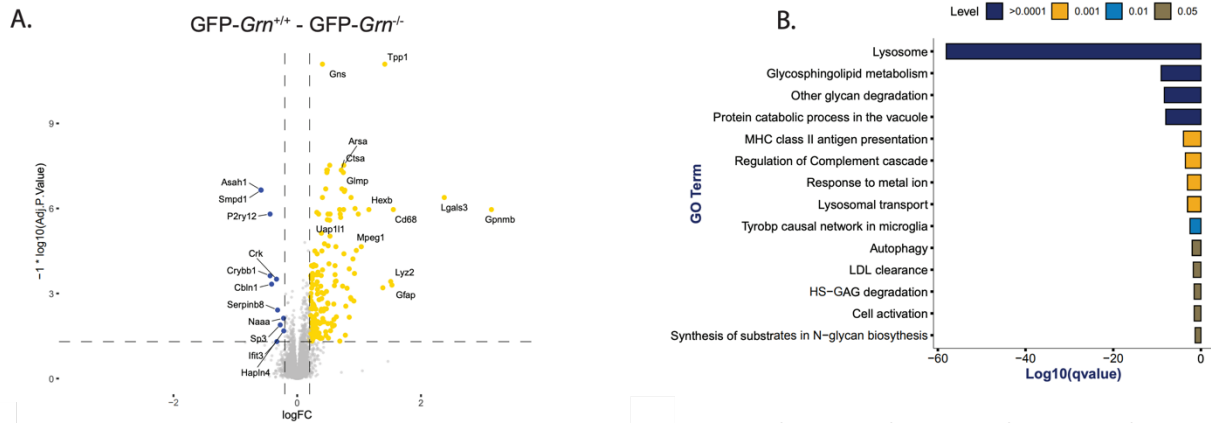


Figure 2.5: Proteomic analysis reveals differences in the proteome of *Grn*^{-/-} and *Grn*^{+/+} mice

- A) Volcano plot of differentially expressed proteins in the thalamus of *GFP-Grn*^{-/-} mice compared to *GFP-Grn*^{+/+} mice. Upregulated protein in *GFP-Grn*^{-/-} (yellow; right side) and downregulated in *GFP-Grn*^{-/-} (blue; left side) are shown ($FC > 1.2$, $p < 0.05$).
- B) Bar graph of the most significantly enriched Gene Ontology (GO) terms describing the differentially expressed proteins in Fig. 2A (*GFP-Grn*^{-/-} mice versus *GFP-Grn*^{+/+} mice; $FC > 1.2$ and adjusted p value 0.05). Displaying all significant changed modules (p value < 0.05).

2.5 Individual granulins rescue dysregulated proteins in the thalamus of *Grn*^{-/-} mice.

After characterizing differences in the proteome between *Grn*^{-/-} and *Grn*^{+/+} mice, we asked if expression of granulins or hPGRN could ameliorate changes observed in *Grn*^{-/-} thalamus. First, principal component analysis (PCA) was performed, extracting 10 components from the proteomics dataset, accounting for 93% of variance (Supp. Fig. 3B). Comparing principal components 1 and 2 (PC1 and PC2) revealed a clear separation of *GFP-Grn*^{+/+} and *GFP-Grn*^{-/-} samples with no overlap observed between groups (Fig. 2.6A). Samples from hPGRN-*Grn*^{-/-}, hGRN4-*Grn*^{-/-}, and hGRN2-*Grn*^{-/-} mice overlap and cluster closer together with *GFP-Grn*^{+/+} mice, revealing a shift towards wild-type mice, and away from *Grn*^{-/-} mice, suggesting a general

correction of altered protein levels.

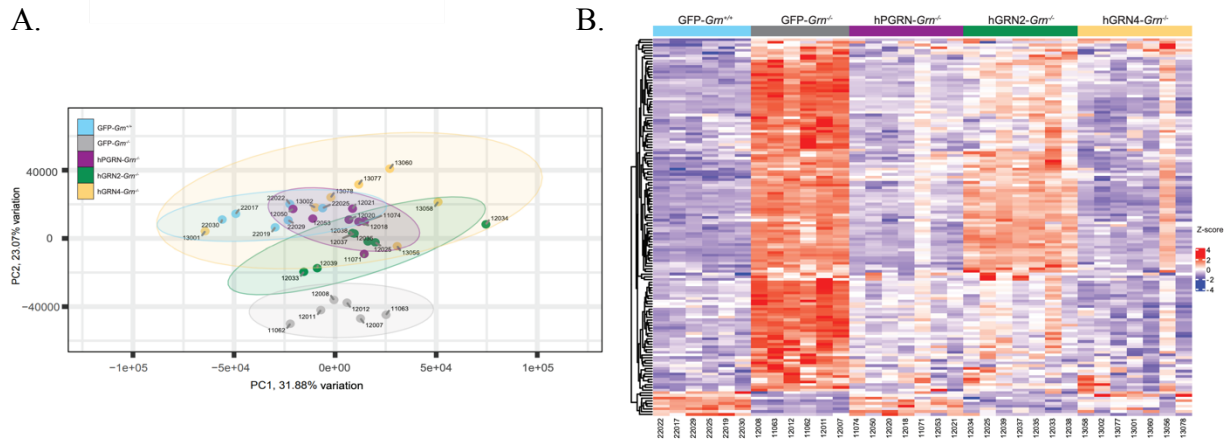


Figure 2.6: Proteomic analysis across injection groups show that GRNs rescue signs of dysfunction in *Grn*^{-/-} mice.

- Volcano plot of differentially expressed proteins in the thalamus of *GFP-Grn*^{-/-} mice compared to *GFP-Grn*^{+/+} mice. Upregulated protein in *GFP-Grn*^{-/-} (yellow; right side) and downregulated in *GFP-Grn*^{-/-} (blue; left side) are shown ($FC > 1.2$, $p < 0.05$).
- Bar graph of the most significantly enriched Gene Ontology (GO) terms describing the differentially expressed proteins in Fig. 2A (*GFP-Grn*^{-/-} mice versus *GFP-Grn*^{+/+} mice; $FC 1.2$ and adjusted p value 0.05). Displaying all significant changed modules (p value < 0.05).

To evaluate rescue of disease-linked phenotypes in more detail, we created a heatmap containing the 140 differentially expressed proteins from the *GFP-Grn*^{-/-} and *GFP-Grn*^{+/+} proteomics comparison and included *hGRN2-Grn*^{-/-}, *hGRN4-Grn*^{-/-}, *hPGRN-Grn*^{-/-} samples (**Fig. 2.6B**). Visually the groups of *Grn*^{-/-} mice treated with hGRN2, hGRN4, and PGRN are more like *GFP-Grn*^{+/+} than *GFP-Grn*^{-/-} mice. To provide a quantitative measurement of rescue, we compared expression levels of the most upregulated (2-fold; $p < 0.001$) proteins (GFAP, HEXB, SERPINA3N, TPP1, LYZ2, GPNMB, LGALS3, MPEG1, CD68) in the *GFP-Grn*^{-/-} proteome across rAAV treatment groups. rAAV-mediated expression of either hGRN2, hGRN4, or hPGRN in *Grn*^{-/-} mice significantly decreased expression levels back towards wild-type levels of all nine proteins, indicating correction of abnormally elevated proteins (**Fig. 2.7A**). This analysis provides strong evidence that expression of an individual granulin in the *Grn*^{-/-} mouse brain can functionally

substitute for the full length PGRN protein.

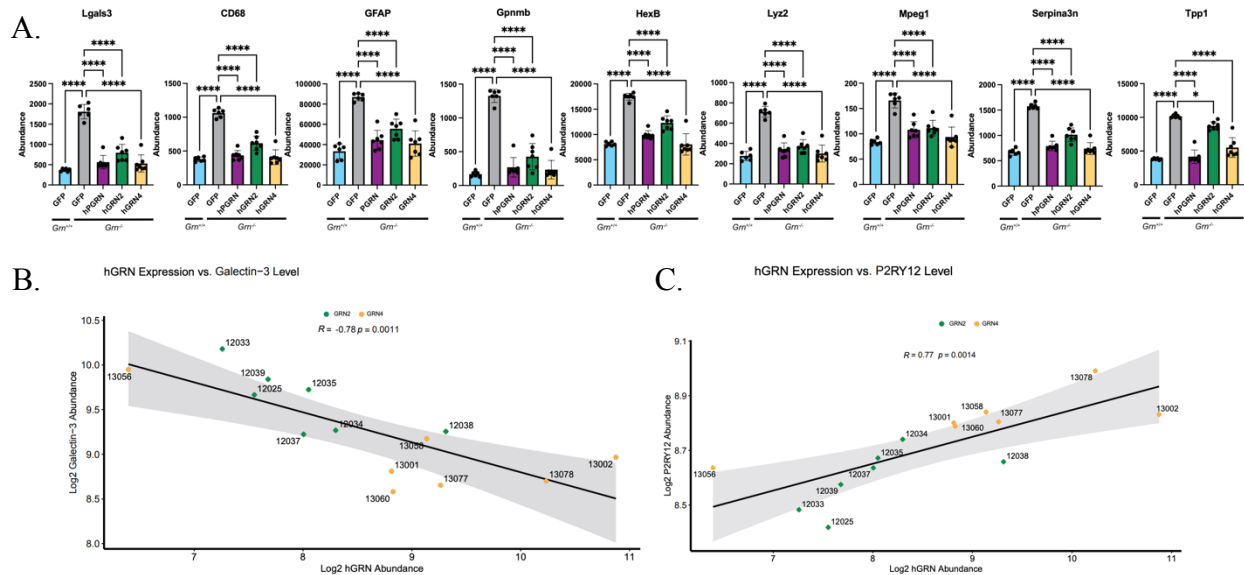


Figure 2.7: Granulins rescue dysregulated proteins in a dose dependent manner.

A) Bar plots comparing correction of elevated levels of *Lgals3*, *Cd68*, *Gfap*, *Gpnmb*, *Hexb*, *Lyz2*, *Mpeg1*, *Serpina3n*, and *Tpp1* in *Grn*^{-/-} mice injected with GFP, hGRN2, hGRN4, or hPGRN. Data (protein abundance measured using TMT-based proteomics) mean \pm SD. Significance was determined using a One-way ANOVA and corrected using Tukey's post-hoc analysis. $N=5-7$ mice/group. * $p < 0.05$, ** $p < 0.01$, *** $p < 0.001$, **** $p < 0.0001$. (B, C) Correlation comparing hGRN2 and hGRN4 expression with Galectin-3 (F) ($R=0.78$, $p=0.0011$) or P2RY12 (G) ($R=0.77$, $p=0.0014$).

Of note, elevated proteins in *Grn*^{-/-} mouse brains were not corrected as efficiently in hGRN2-injected groups compared to hGRN4 and hPGRN injected groups (e.g., *Tpp1*; **Fig. 2.7A**). One possible explanation for this result is that specific granulins are expressed at different levels between groups. To investigate this, we compared expression levels of hGRN2 and hGRN4 in the *Grn*^{-/-} thalamic proteomics data set by examining a tryptic fragment of the twin Strep-FLAG tag shared between both proteins, revealing that hGRN4 expression was ~ 2.5 fold higher than hGRN2 (**Supp. Fig. 3C**). We then asked whether the expression level of granulin-2 or granulin-4 correlated with phenotypic rescue. Notably, the abundance of hGRN2 and hGRN4 correlated with galectin-3 ($R = -0.78$; $p = 0.0011$) (**Fig. 2.7B**) and P2RY12 ($R = 0.77$, $p = 0.0014$) levels (**Fig. 2.7C**) in the *Grn*^{-/-}

^{-/-} thalamic proteome. Further, in individual mice higher levels of either hGRN2 or hGRN4 correlated with correction of altered protein levels, suggesting the decreased efficacy of hGRN2 is most likely due to lower expression levels and not function. Taken together, proteomic analysis of the thalamus of *Grn*^{-/-} mouse reveals that rAAV-mediated expression of a single granulin ameliorates widespread protein dysregulation caused by loss of PGRN.

2.6 Markers of Lysosomal Dysfunction are rescued by granulin expression across brain regions.

To validate and extend the proteomics data, we analyzed tissue from additional, separate cohorts of rAAV2/1-injected *Grn*^{+/+} and *Grn*^{-/-} mice that were processed for immunohistochemistry, immunoblot (western blot), or lipidomics (**Fig. 2.1B**). Because “lysosome” was the most significant GO term in the GFP-*Grn*^{-/-} thalamic proteome, we focused on two markers of lysosomal dysfunction, galectin-3 (LGALS3) and cathepsin Z (CatZ) (227) (**Fig. 2.8A**). Cathepsin Z is a unique lysosomal cysteine protease that is upregulated in LSDs and neurodegenerative diseases.(328-330) We performed IHC to examine the levels of cathepsin Z in hippocampal, thalamic, and cortical tissues of *Grn*^{-/-} mice injected with rAAV2/1 expressing GFP, hGRN2, hGRN4, and hPGRN (n=5; one section/mouse) (**Fig. 2.9A**). Quantification of IHC staining in the cortex, thalamus, and hippocampus was performed using CellProfiler (**Supp. Fig 4**) and revealed a significant increase in cathepsin Z signal in GFP-*Grn*^{-/-} mice across all regions examined (**Fig. 2.9B**). We found that the expression of hGRN2, hGRN4, and hPGRN corrected elevated levels of cathepsin Z in the cortex (**Fig. 2.9B**). In the thalamus and hippocampus only hGRN4 expression led to a statistically significant decrease in the level of cathepsin Z in these samples (**Fig. 2.9B**).

We then performed immunoblotting to provide a complementary measurement of

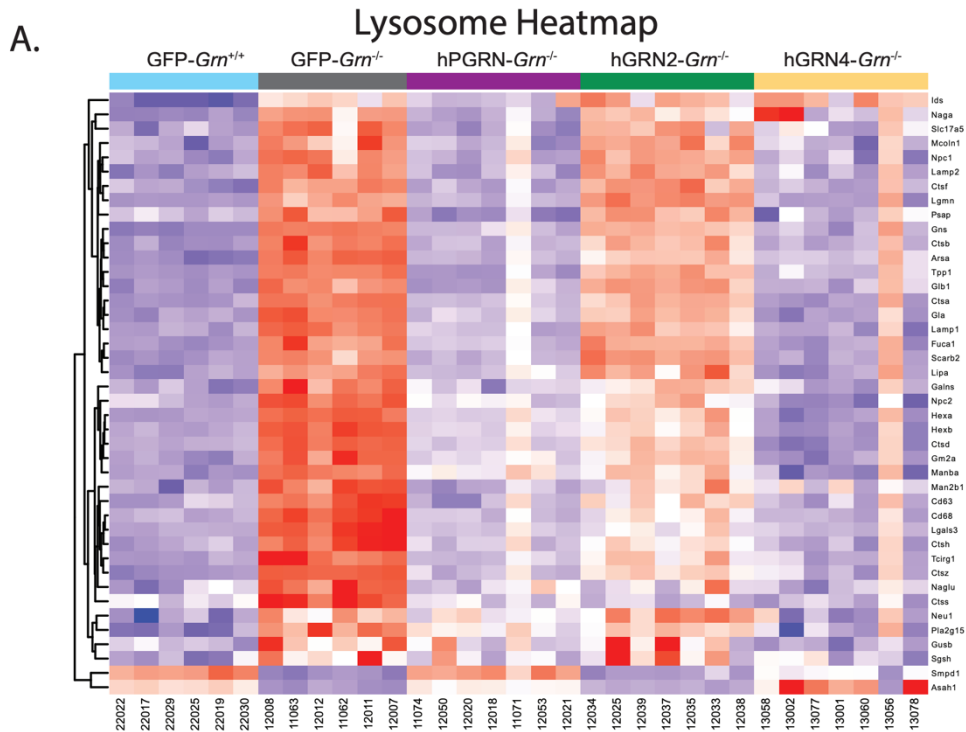


Figure 2.8: GRNs rescue altered lysosomal protein levels.

- A) Heatmap of differentially expressed (Log_2Z score transformed) lysosomal proteins from GO module (Keeg mmu04142) in GFP-*Grn*^{-/-} and GFP-*Grn*^{+/+} mice. 42 proteins are included (rows) across mice from all treatment groups (columns).

cathepsin Z, in hippocampal, thalamic, and cortical tissue samples from separate cohorts (**Fig. 2.10A**). Cathepsin Z was increased in the GFP-*Grn*^{-/-} mouse cortex, hippocampus, and thalamus compared to wild-type counterparts (**Fig. 2.10A, B-D**). In agreement with the proteomics analyses, cathepsin Z levels were normalized by expression of hGRN2, hGRN4, and hPGRN in the *Grn*^{-/-} thalamus (**Fig. 2.10C**). Cathepsin Z levels were also decreased in the cortex and hippocampus by hGRN4 and hPGRN, while hGRN2 treatment trended lower, but did not reach significance (**Fig. 2.10B, 10D**).

We also assessed levels of galectin-3 (LGALS3), a beta-galactoside binding lectin that is recruited to damaged lysosomes(331) to facilitate lysosomal repair (332). Immunostaining of 12-month-old GFP-*Grn*^{+/+}, GFP-*Grn*^{-/-}, hPGRN-*Grn*^{-/-}, hGRN2-*Grn*^{-/-}, and hGRN4-*Grn*^{-/-} mouse

coronal sections demonstrated that galectin-3 was increased in the thalamus and cortex of GFP-*Grn*^{-/-} mice (**Fig. 2.11A**). Similarly, to cathepsin Z, expression of hGRN2, hGRN4, and hPGRN corrected elevated galectin-3 in the thalamus compared to GFP-*Grn*^{+/+} mice (**Fig. 2.11B**).

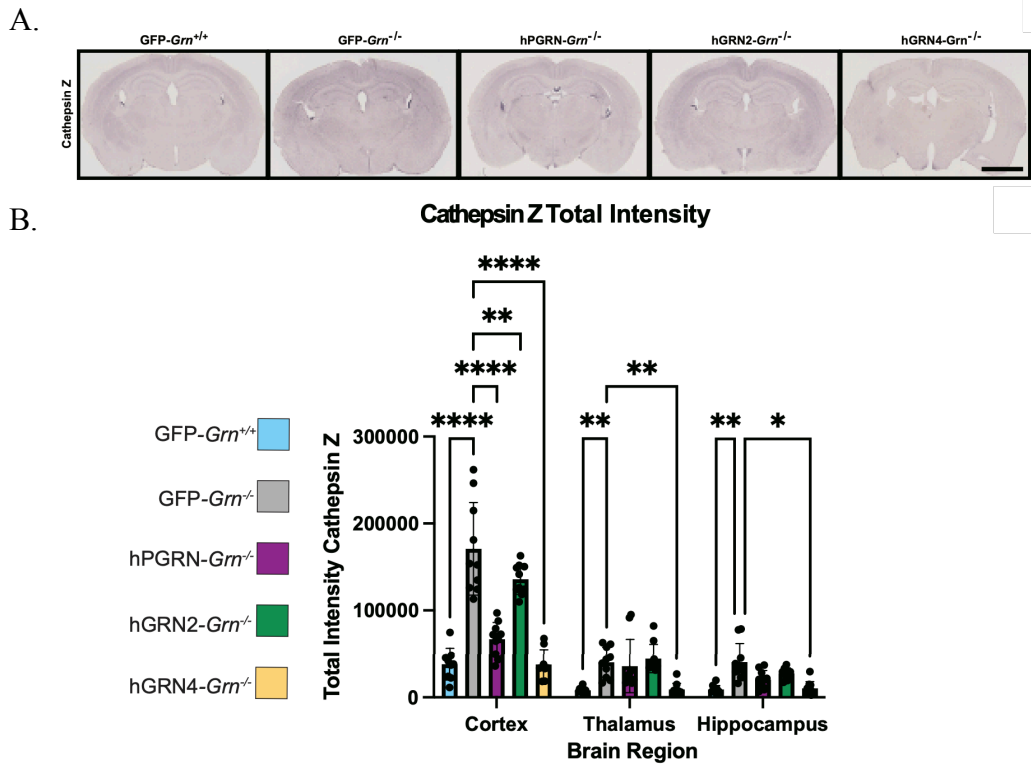


Figure 2.9: GRNs ameliorate levels of Cathepsin Z across brain regions measured by IHC.

- A) Representative images of cathepsin Z immunohistochemistry (IHC) staining of coronal sections of all rAAV injected groups (GFP, hPGRN, hGRN2, hGRN4).
- B) Quantification of cathepsin Z IHC signal in cortex, hippocampus, and thalamus. Data are mean \pm SD, significance determined with Two-Way ANOVA (two-way ANOVA *Region X Injection* $F(8, 133) = 17.37$) followed by Tukey's post-hoc analysis. $N=5$ mice/group. * $p < 0.05$, ** $p < 0.01$, *** $p < 0.001$, **** $p < 0.0001$

These results were further validated by using immunoblot to measure galectin-3 levels in lysates of the cortex, thalamus, and hippocampus tissue from a separate cohort of rAAV2/1 injected mice ($n=5$) (**Fig. 2.12A**). We confirmed that galectin-3 was upregulated in cortical, thalamic, and hippocampus tissue lysates of GFP-*Grn*^{-/-} mice compared to GFP-*Grn*^{+/+} (**Fig. 2.12A, B-D**). Importantly, rAAV-mediated expression of hGRN2, hGRN4, and hPGRN reduced

elevated galectin-3 expression in cortical and thalamic tissues (**Fig. 2.12B, C**). In hippocampal samples, hGRN4 and hPGRN significantly reduced elevated galectin-3 levels in *Grn*^{-/-} mice (**Fig. 2.12D**). Together, these findings broaden the context of our proteomics data using IHC and

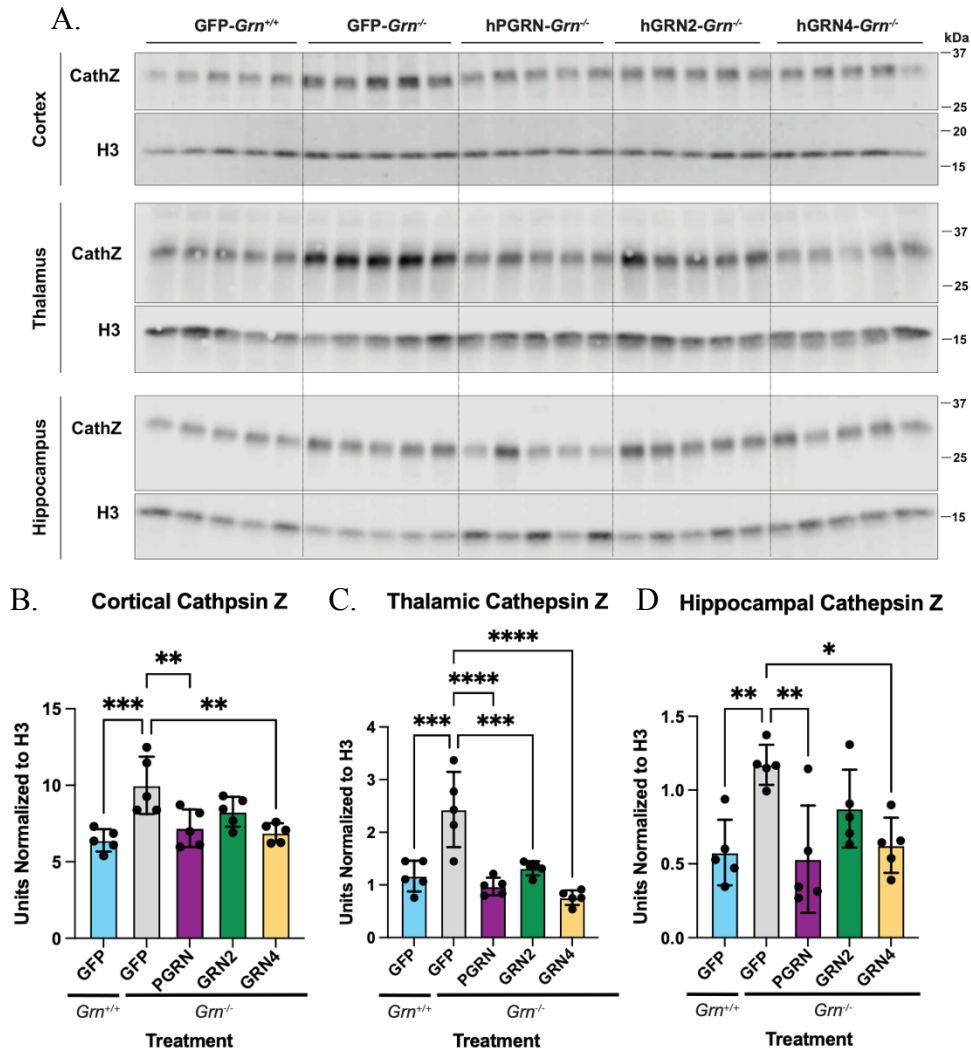


Figure 2.10: Granulins rescue elevated Cathepsin Z levels detected via immunoblot.

- A) Immunoblot for cathepsin Z in cortical, hippocampal, and thalamic brain lysates from all injection groups.
- B) Quantification of immunoblot of cortical cathepsin Z normalized to H3. Data are mean±SD and significance determined by One-Way ANOVA (Tukey's post-hoc analysis GFP-*Grn*^{-/-} vs GFP-*Grn*^{+/+} $p=0.0009$, GFP-*Grn*^{-/-} vs hPGRN-*Grn*^{-/-} $p=0.0095$, GFP-*Grn*^{-/-} vs hGRN2-*Grn*^{-/-} $p=ns$, GFP-*Grn*^{-/-} vs hGRN4-*Grn*^{-/-} $p<0.0038$).
- C) Quantification of immunoblot of thalamic cathepsin Z normalized to H3. Data are mean±SD and significance determined by One-Way ANOVA (Tukey's post-hoc analysis GFP-*Grn*^{-/-} vs GFP-*Grn*^{+/+} $p=0.0087$, GFP-*Grn*^{-/-} vs hPGRN-*Grn*^{-/-} $p=0.0046$, GFP-*Grn*^{-/-} vs hGRN2-*Grn*^{-/-} $p=ns$, GFP-*Grn*^{-/-} vs hGRN4-*Grn*^{-/-} $p<0.0175$).
- D) Quantification of immunoblot of hippocampal cathepsin Z normalized to H3. Data are mean±SD and significance determined by One-Way ANOVA (Tukey's post-hoc analysis GFP-*Grn*^{-/-} vs GFP-*Grn*^{+/+} $p=0.0002$, GFP-*Grn*^{-/-} vs hPGRN-*Grn*^{-/-} $p<0.0001$, GFP-*Grn*^{-/-} vs hGRN2-*Grn*^{-/-} $p=0.0008$, GFP-*Grn*^{-/-} vs hGRN4-*Grn*^{-/-} $p<0.0001$).

immunoblot to confirm that expression of individual granulins reduce elevated levels of galectin-3 back to wild-type levels in the cortex and thalamus of 12-month-old GFP-*Grn*^{-/-} mice.

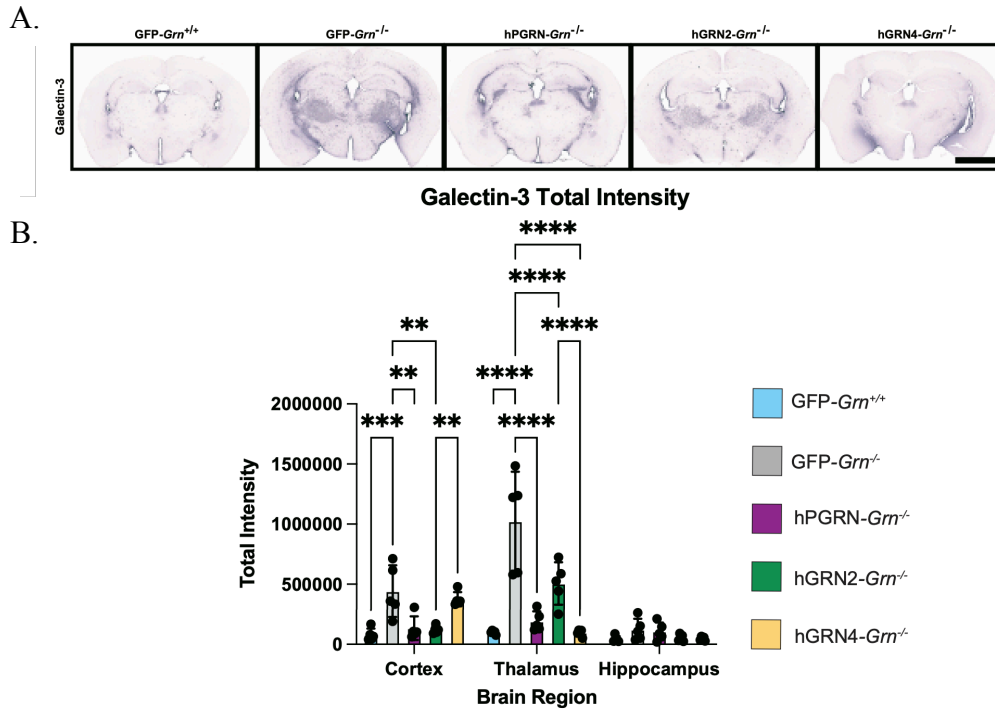


Figure 2.11: Granulins ameliorate elevated galectin 3 levels throughout the brain detected by IHC.

- A) Representative images of galectin-3 immunohistochemistry from coronal sections of all injection groups.
- B) Quantification of galectin-3 IHC signal in cortex, hippocampus, and thalamus. Data are mean±SD significance determined (two-way ANOVA $Region \times Injection$ $F(8, 60) = 11.95$). followed by Tukey's post-hoc analysis. $N=5$ mice/group. * $p < 0.05$, ** $p < 0.01$, *** $p < 0.001$, **** $p < 0.0001$.

In summary, we find that immunohistochemistry and immunoblot analysis confirm and extend our proteomics data, demonstrating that expression of hGRN2 or hGRN4 ameliorate elevated cathepsin Z and galectin-3 levels. These data provide additional evidence that a single granulin can functionally substitute for the activity of full-length PGRN.

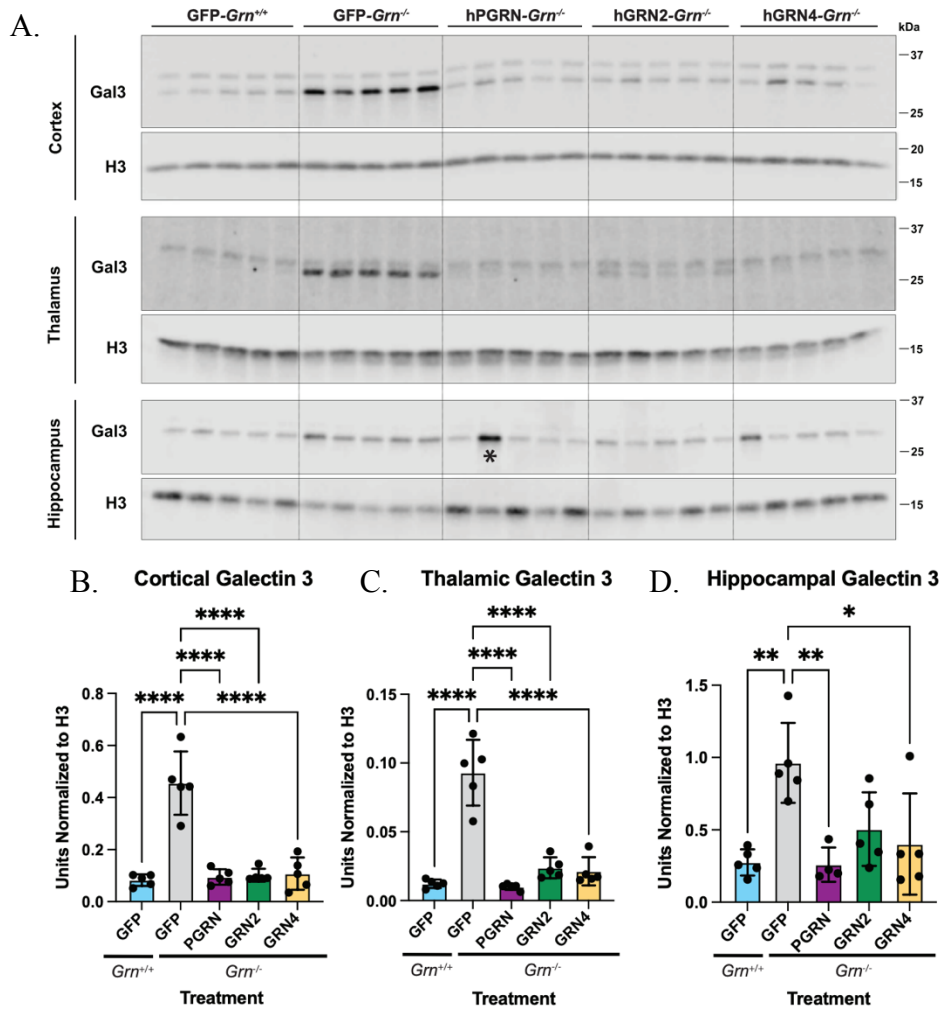


Figure 2.12: Granulins rescue elevated galectin-3 levels detected via immunoblot

- A) Immunoblot of galectin-3 in cortical, hippocampal, and thalamic brain lysates from all injection groups.
- B) Quantification of immunoblot of cortical galectin-3 normalized to H3. Data are mean±SD and significance determined by One-Way ANOVA (Tukey's post-hoc analysis GFP-Grn^{-/-} vs GFP-Grn^{+/+} $p < 0.0001$, GFP-Grn^{-/-} vs hPGRN-Grn^{-/-} $p < 0.0001$, GFP-Grn^{-/-} vs hGRN2-Grn^{-/-} $p < 0.0001$, GFP-Grn^{-/-} vs hGRN4-Grn^{-/-} $p < 0.0001$).
- C) Quantification of immunoblot of thalamic galectin-3 signal normalized to H3. Data are mean±SD and significance determined by One-Way ANOVA (Tukey's post-hoc analysis GFP-Grn^{-/-} vs GFP-Grn^{+/+} $p < 0.0001$, GFP-Grn^{-/-} vs hPGRN-Grn^{-/-} $p < 0.0001$, GFP-Grn^{-/-} vs hGRN2-Grn^{-/-} $p < 0.0001$, GFP-Grn^{-/-} vs hGRN4-Grn^{-/-} $p < 0.0001$).
- D) Quantification of immunoblot of hippocampal galectin-3 normalized to H3. Data are mean±SD and significance determined by One-Way ANOVA (Tukey's post-hoc analysis GFP-Grn^{-/-} vs GFP-Grn^{+/+} $p = 0.002$, GFP-Grn^{-/-} vs hPGRN-Grn^{-/-} $p = 0.0031$, GFP-Grn^{-/-} vs hGRN2-Grn^{-/-} $p = 0.053$, GFP-Grn^{-/-} vs hGRN4-Grn^{-/-} $p = 0.0132$).

2.7 Microglial activation and inflammatory markers are reduced by hGRNs

While neuronal cell death is a hallmark of PGRN deficiency, the *GRN* gene is also highly expressed in microglia.(333) Loss of PGRN in *Grn*^{-/-} mice causes inflammation, astrogliosis, and

microgliosis, which has been linked to synaptic loss and disease progression.(259, 334) In the *Grn*^{-/-} thalamic proteome, we find that many of the most dysregulated proteins are expressed by microglia including GPNMB, CD68, and P2RY12 (**Fig. 2.5A**). To examine this in more detail, we constructed a heatmap containing microglial activation markers found in the proteome of *Grn*^{+/+} and *Grn*^{-/-} injected cohorts (**Fig. 2.13A**).(335, 336) We find multiple markers of microglial activation including CD45 (PTPRC) and CD68 are upregulated in the GFP-*Grn*^{-/-} thalamus (**Fig. 2.13 B, D**). In addition, P2RY12, a marker of microglia homeostasis was down regulated in GFP-*Grn*^{-/-} mice (**Fig. 2.13C**). Based on proteomics analyses, the elevation of CD45 was reduced by expression of hGRN2, hGRN4, and hPGRN, while depressed P2RY12 levels were increased by hGRN4 and hPGRN (**Fig. 2.13B, C**).

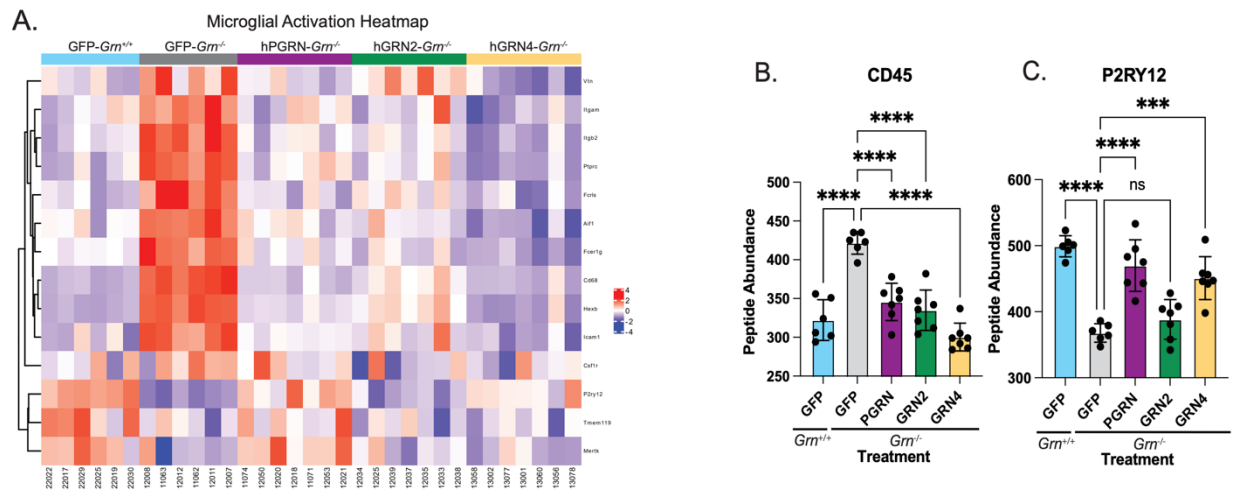


Figure 2.13: Granulins rescues signs of microglial activation in *Grn*^{-/-} mouse cortex.

- A) Heatmap of differentially expressed (Log_2Z score transformed) proteins associated with microglial activation and dysfunction(335-337) (rows) in all treatment groups in GFP-*Grn*^{-/-} compared to GFP-*Grn*^{+/+} (columns).
- B) Proteomics abundance of CD45 (PTPRC) across all treatment groups (One-way ANOVA; Tukey's post-hoc analysis GFP-*Grn*^{-/-} vs GFP-*Grn*^{+/+} $p < 0.0001$, GFP-*Grn*^{-/-} vs hPGRN-*Grn*^{-/-} $p < 0.0001$, GFP-*Grn*^{-/-} vs hGRN2-*Grn*^{-/-} $p < 0.0001$, GFP-*Grn*^{-/-} vs hGRN4-*Grn*^{-/-} $p < 0.0001$)
- C) Proteomics abundance of P2RY12 across all treatment groups. Data represented at mean \pm SD One Way ANOVA (Tukey's post-hoc analysis GFP-*Grn*^{-/-} vs GFP-*Grn*^{+/+} $p < 0.0001$, GFP-*Grn*^{-/-} vs hPGRN-*Grn*^{-/-} $p < 0.0001$, GFP-*Grn*^{-/-} vs hGRN2-*Grn*^{-/-} $p = ns$, GFP-*Grn*^{-/-} vs hGRN4-*Grn*^{-/-} $p = 0.0002$).

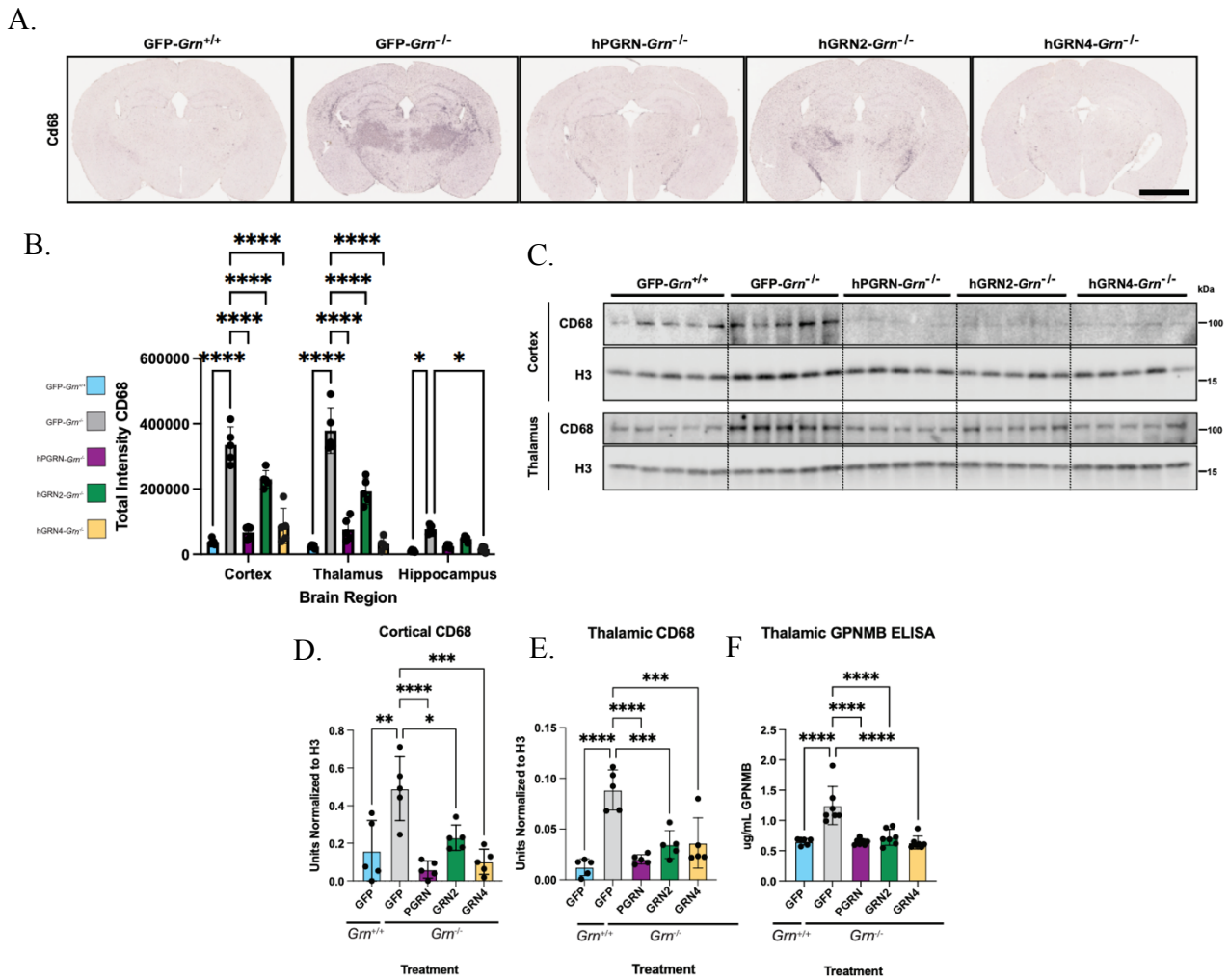


Figure 2.14: Granulins ameliorate elevated CD68 and GPNMB levels in *Grn*^{-/-} mice.

- A) Representative images of CD68 immunohistochemistry of 12-month-old mouse coronal brain sections including all injection groups.
- B) Quantification of CD68 immunohistochemistry regions of interest cortex, hippocampus and thalamic signals quantified by CellProfiler. Data represented as mean±SD, significance was determined (Two Way ANOVA_{Region X Injection} $F(8, 60) = 21.09$). Followed by Tukey's post-hoc analysis $N=5$ mice/group. * $p < 0.05$, ** $p < 0.01$, *** $p < 0.001$, **** $p < 0.0001$.
- C) Immunoblot of 12-month mouse cortical and thalamic brain tissue from all injection groups.
- D) Quantification of immunoblot of cortical CD68 signal normalized to H3. Data represented as mean±SD and significance determined by One-Way ANOVA (Tukey's post-hoc analysis GFP-*Grn*^{-/-} vs GFP-*Grn*^{+/+} $p=0.016$, GFP-*Grn*^{-/-} vs hPGRN-*Grn*^{-/-} $p<0.0001$, GFP-*Grn*^{-/-} vs hGRN2-*Grn*^{-/-} $p=0.0145$, GFP-*Grn*^{-/-} vs hGRN4-*Grn*^{-/-} $p=0.0003$)
- E) Quantification of immunoblot of thalamic CD68 signal normalized to H3. Data represented as mean±SD and significance determined by One-Way ANOVA (Tukey's post-hoc analysis GFP-*Grn*^{-/-} vs GFP-*Grn*^{+/+} $p<0.0001$, GFP-*Grn*^{-/-} vs hPGRN-*Grn*^{-/-} $p<0.0001$, GFP-*Grn*^{-/-} vs hGRN2-*Grn*^{-/-} $p=0.0003$, GFP-*Grn*^{-/-} vs hGRN4-*Grn*^{-/-} $p=0.0004$)
- F) Quantification of GPNMB levels in thalamic lysates measured using ELISA. Quantified data are mean±SD. Significance determined by one-way ANOVA (Tukey's post-hoc analysis GFP-*Grn*^{-/-} vs GFP-*Grn*^{+/+} $p<0.0001$, GFP-*Grn*^{-/-} vs hPGRN-*Grn*^{-/-} $p<0.0001$, GFP-*Grn*^{-/-} vs hGRN2-*Grn*^{-/-} $p<0.0001$, GFP-*Grn*^{-/-} vs hGRN4-*Grn*^{-/-} $p<0.0001$)

To expand our investigation to additional brain regions and validate proteomics, we examined expression levels of CD68 (CD68), a type I transmembrane glycoprotein commonly used as a microglial activation marker(338), using immunohistochemistry, and immunoblotting in additional cohorts of mice. Immunohistochemical staining for CD68 revealed robust and significant increases in CD68 in the cortex, hippocampus, and thalamus of GFP-*Grn*^{-/-} mice (**Fig. 2.14A, B**). Expression of hGRN4 in *Grn*^{-/-} mice lowered CD68 reactivity in all regions, while expression of hGRN2 significantly reduced levels in the thalamus and cortex, but not the hippocampus (**Fig. 2.14B**). Immunoblot of tissue lysates verified CD68 levels were increased in the cortex and thalamus of GFP-*Grn*^{-/-} mice compared to GFP-*Grn*^{+/+} mice, but below detection in the hippocampus (n=5; **Fig. 2.14C**). Similar to immunohistochemical analysis, rAAV expression of both hGRN2 and hGRN4 corrected elevated CD68 levels relative to GFP-*Grn*^{-/-} in the cortex (**Fig. 2.14D**) and in the thalamus (**Fig. 2.14E**).

Finally, we asked if expression of granulins corrected levels of glycoprotein non-metastatic melanoma protein B (GPNMB), the most elevated protein in the *Grn*^{-/-} brain thalamic proteome (**Fig. 2.5A**), which was decreased by the expression of hGRN2 and hGRN4 in the thalamic proteomics (**Fig. 2.7A**). GPNMB is a type-1 transmembrane glycoprotein that we discovered to be highly upregulated by PGRN deficient microglia.(227) The function of GPNMB in microglia is unknown, however GPNMB upregulation has been observed in activated damage-associated microglia(339) and functionally linked to lysosomal stress and lipid accumulation.(340, 341) We could not detect GPNMB via immunoblot, therefore, we quantified murine GPNMB levels in thalamic tissue lysates using a validated ELISA.(227) Using this approach, we found that expression of either hGRN2 or hGRN4 corrected elevated GPNMB levels to the same extent as hPGRN in *Grn*^{-/-} mice (**Fig. 2.14F**). In sum, proteomics and multiple orthogonal biochemical

measurements reveal that expression of hGRN2, hGRN4, and hPGRN, especially in the thalamus, decrease microglial activation in *Grn*^{-/-} mice.

2.8 Lysosomal lipid dysregulation is rescued by a single granulin.

The role of granulins in the lysosome is not fully understood. Previous studies identified lipid dysregulation in PGRN deficient animal models and FTD-*GRN* patient samples, suggesting lysosomal metabolism of lipids is impaired.(21, 224, 243, 342) In particular, *Grn*^{-/-} mice display decreased levels of bis(monoacylglycerol)phosphate (BMP), an atypical endo-lysosomal lipid, and increased levels of glucosylsphingosine (GlcSph), a substrate of glucocerebrosidase (GCase), which can be corrected by administration of exogenous full-length hPGRN.(238) Additionally, ganglioside levels increase in brain tissues from *Grn*^{-/-} mice and FTD-*GRN* patients (242), which may accumulate as secondary storage material, a phenomenon observed in many LSDs.(241, 343) To validate these observations and determine whether expression of a single granulin or full-length

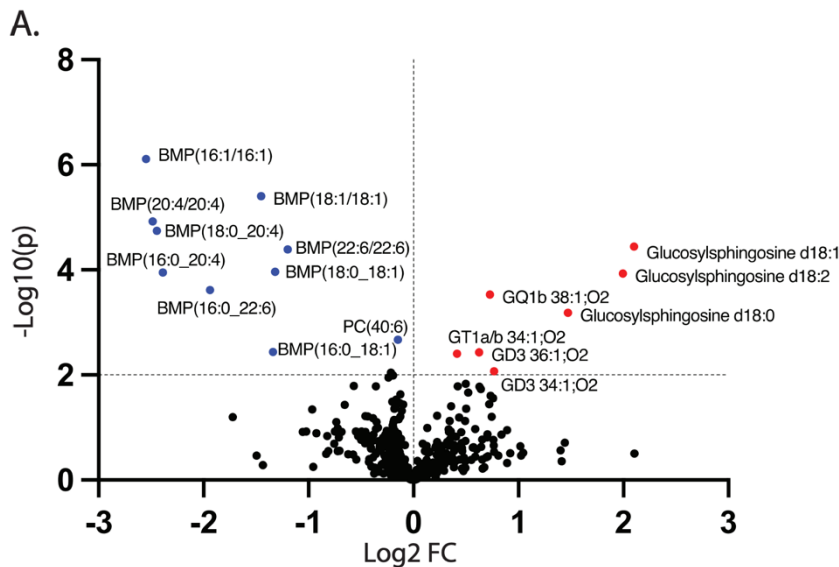


Figure 2.12: Loss of PGRN leads to dysregulation of lipids.

- A) Volcano plot of differential abundance of lipids and metabolites quantified in GFP-*Grn*^{-/-} and GFP-*Grn*^{+/+} mouse cortex. Lipids or metabolites upregulated in GFP-*Grn*^{-/-} (red) and downregulated in GFP-*Grn*^{-/-} (blue) are represented ($p < 0.1$).

hPGRN can correct them, we performed lipidomics and metabolomics analyses on the cortex of GFP-*Grn*^{+/+}, GFP-*Grn*^{-/-}, hPGRN-*Grn*^{-/-}, hGRN2-*Grn*^{-/-}, and hGrn4-*Grn*^{-/-} mice.

These studies confirmed a decrease in the levels of BMP species and an increase in the

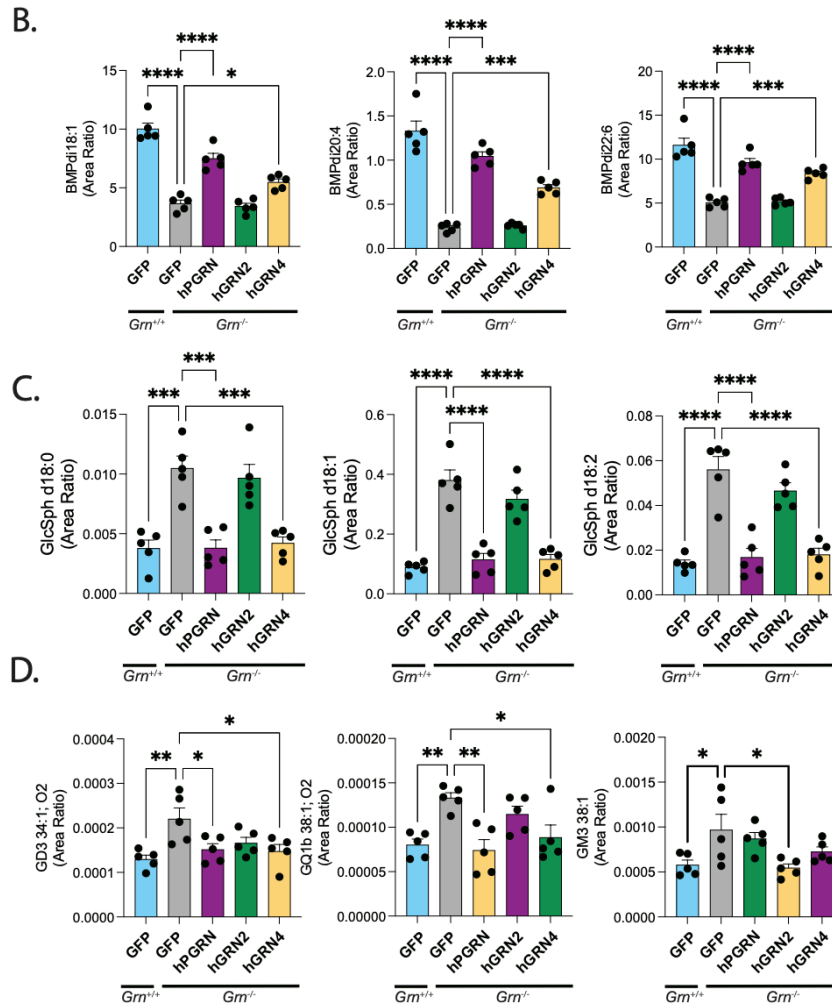


Figure 2.16: BMP, GlcSph, and Gangliosides are rescued by hGRN4.

- A) Quantification of differentially abundant BMP species. Data represented as mean±SD, significance was determined by One-way ANOVA with Tukey's post-hoc analysis. N=5-7 mice/group. * $p < 0.05$, ** $p < 0.01$, *** $p < 0.001$, **** $p < 0.0001$.
- B) Quantification of differentially abundant glucosylsphingosine species. Data represented as mean±SD, significance was determined by One-way ANOVA with Tukey's post-hoc analysis. N=5-7 mice/group. * $p < 0.05$, ** $p < 0.01$, *** $p < 0.001$, **** $p < 0.0001$.
- C) Quantification of differentially abundant gangliosides species. Data represented as mean±SD, significance was determined by One-way ANOVA with Tukey's post-hoc analysis. N=5-7 mice/group. * $p < 0.05$, ** $p < 0.01$, *** $p < 0.001$, **** $p < 0.0001$.

levels of GlcSph species in GFP-*Grn*^{-/-} mice compared with GFP-*Grn*^{+/+} mice (Fig. 2.15A). In addition, we observed smaller, but significant increases of several gangliosides in the GFP-*Grn*^{-/-}

mouse brain (**Fig. 2.15A**), similar to what has been previously reported.(242) AAV-mediated expression of hGRN4 and hPGRN in the *Grn*^{-/-} mouse brain, but not hGRN2, significantly increased all measured BMP species back towards levels found in GFP-*Grn*^{+/+} mice (**Fig. 2.16A**). Similarly, we found that both hGRN4 and hPGRN corrected the elevation of GlcSph (**Fig. 2.16B**) and gangliosides (**Fig. 2.16C**) in the GFP-*Grn*^{-/-} mouse brain. hGRN2 showed a slight but non-significant reduction in GlcSph and ganglioside levels as well. It is unclear why hGRN2 did not rescue BMP and gangliosides to the same extent as hGRN4 and hPGRN. This could be due to lower expression of hGRN2 (**Supp. Fig. 3C**), or that different granulins may have specific functions in lysosomal lipid metabolism. Overall, these results demonstrate that a single granulin can correct multiple lysosomal lipids that are dysregulated in the *Grn*^{-/-} mouse brain to the same extent as full-length hPGRN. Further research is required to understand the specific functions of different granulins on lysosomal lipid metabolism.

2.9 Lipofuscin accumulation in *Grn*^{-/-} brains is alleviated by expression of human granulins.

Auto fluorescent lipofuscin is a marker of lysosome dysfunction and is a neuropathologic feature of human FTD-*GRN* and *Grn*^{-/-} mouse brain tissue.(255, 256, 344) We set out to evaluate the extent and anatomical location of lipofuscin neuropathology in our rAAV-injected *Grn*^{-/-} mouse brain cohorts. We imaged whole coronal sections using Cy5 excitation and emission filters to capture autofluorescence in GFP-*Grn*^{+/+}, GFP-*Grn*^{-/-}, hPGRN-*Grn*^{-/-}, hGRN2-*Grn*^{-/-}, and hGRN4-*Grn*^{-/-} mice (n=5). Fluorescent signal in the cortex, hippocampus, and thalamic regions of all AAV injected mice was then quantified using CellProfiler (**Fig. 2.17A**). We observed a robust increase in lipofuscin in GFP-*Grn*^{-/-} animals compared with GFP-*Grn*^{+/+} in the thalamus

and hippocampal regions, but not the cortex (Fig. 2.17 A, B). Next, we found that expression of hGRN2, hGRN4, and hPGRN all decreased lipofuscin accumulation in the thalamus and hippocampus compared to GFP-*Grn*^{-/-} mice (Fig. 2.17 A, B). These data agree with our proteomic

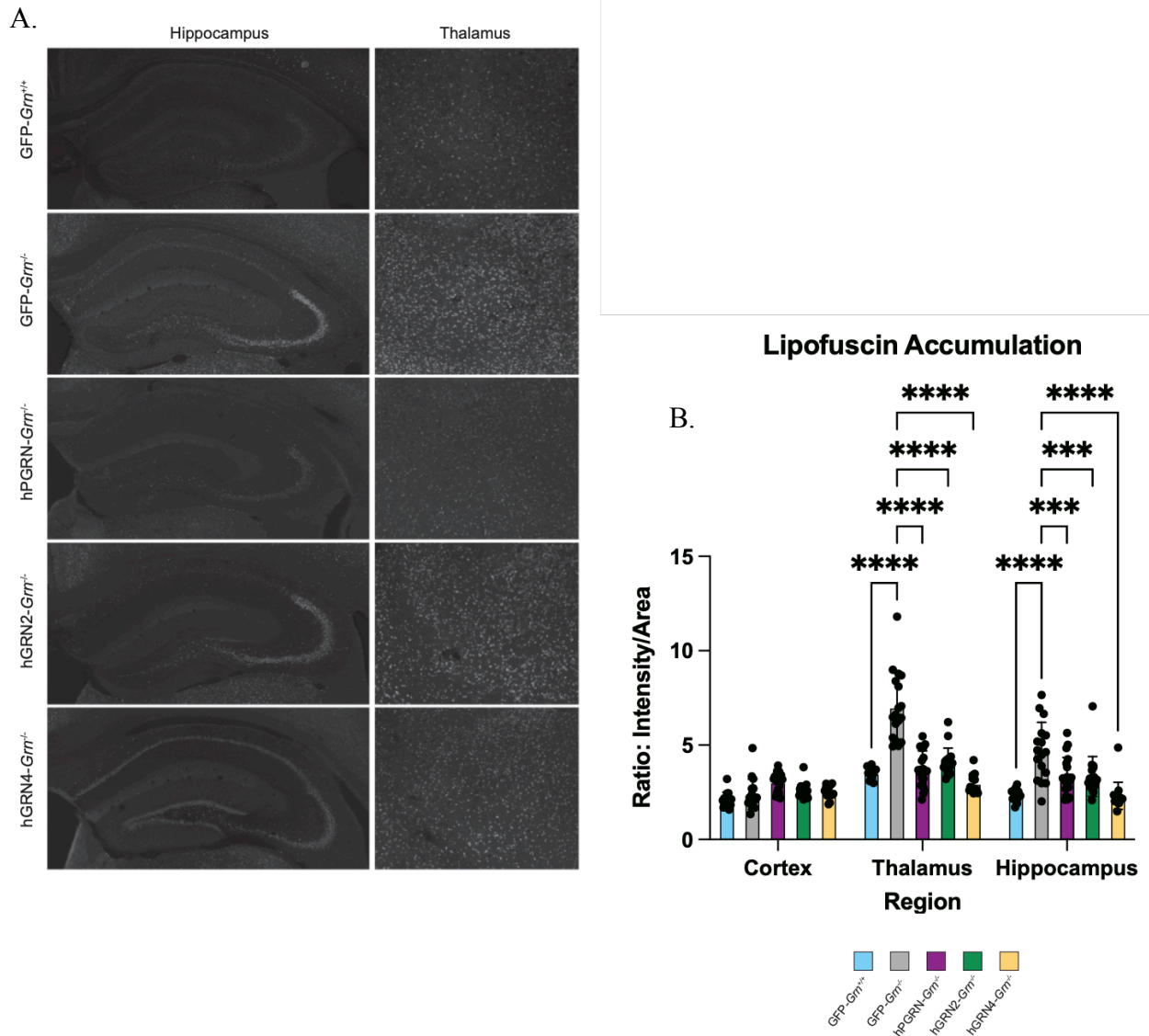


Figure 2.17: Granulins decrease levels of lipofuscin in *Grn*^{-/-} mice.

- A) Representative images of lipofuscin autofluorescence as detected in the Cy5 channel from hippocampal and thalamic regions of coronal sections from all injection groups presented in grayscale.
- B) Quantification of fluorescent lipofuscin signal from cortex, hippocampus, and thalamus across all injected groups. Images were quantified in CellProfiler, and total intensity signal was divided by area of region assessed. Data represented as mean±SD significance determined with Two-Way ANOVA (two-way ANOVA_{injectionXregion} $F_{(8, 246)} = 16.53$ $p < 0.0001$). Followed by Tukey's post-hoc analysis $N=5$ mice/group. * $p < 0.05$, ** $p < 0.01$, *** $p < 0.001$, **** $p < 0.0001$

and lipidomic analyses and provide additional evidence that individual granulins can ameliorate

widespread lysosomal dysregulation in *Grn*^{-/-} mice including accumulation of lipofuscin, which has been linked to neurotoxicity and neurodegeneration in LSDs.(255) This is the first report that a single granulin confers such broad beneficial effects in *Grn*^{-/-} mice and provides compelling evidence that individual granulins are bioactive and neuroprotective.

2.10 Behavioral Phenotypes

Previous studies have found behavioral differences in *Grn*^{-/-} mice including changes in impulsivity, anxiety, social, and well-being measures (345). These changes correlate with some of the most common early behavioral changes in FTD-*GRN* patients CITE. The expression of PGRN in the mPFC of adult mice was able to rescue changes in social dominance and nest building, but the ability of GRNs to confer a similar effect has not been assessed (244, 256). To address this gap, we completed a set of behavioral tests including nest building, nestlet shredding, and marble burying across all the injected mice.

First, we aimed to identify assays that showed a phenotypic difference between GFP-*Grn*^{+/+} and GFP-*Grn*^{-/-} mice in our cohort. We found that there was a difference in nest building (student's t-test p=0.0122) and nestlet shredding (Welch's t-test p=0.0071) between *Grn*^{+/+} and GFP-*Grn*^{-/-} mice, but not in mice's propensity to bury marbles (**Fig 2.18A-C**). *Grn*^{-/-} built nests of poorer quality (**Fig 2.18A**) and showed less nestlet shredding behavior than their *Grn*^{+/+} counterparts (**Fig 2.18B**). As nest building is an important survival skill for mice, the ability of a mouse to build a well-formed nest is considered a measure of well-being, that is often decreased in (346). Nestlet shredding is considered an anxiety-like behavior and less nestlet shredding is generally considered to be a sign of a lower anxiety-like state in mice (347). However, in light of a concomitant decrease in nestlet building ability it is possible that the lack of nestlet shredding could also be interpreted through the lens of behavior necessary for general well-being (348).

Similar to previous studies assessing behavioral outcomes in PGRN-*Grn*^{-/-} mice we found that the expression of PGRN was able to rescue nestlet shredding to a level not significantly

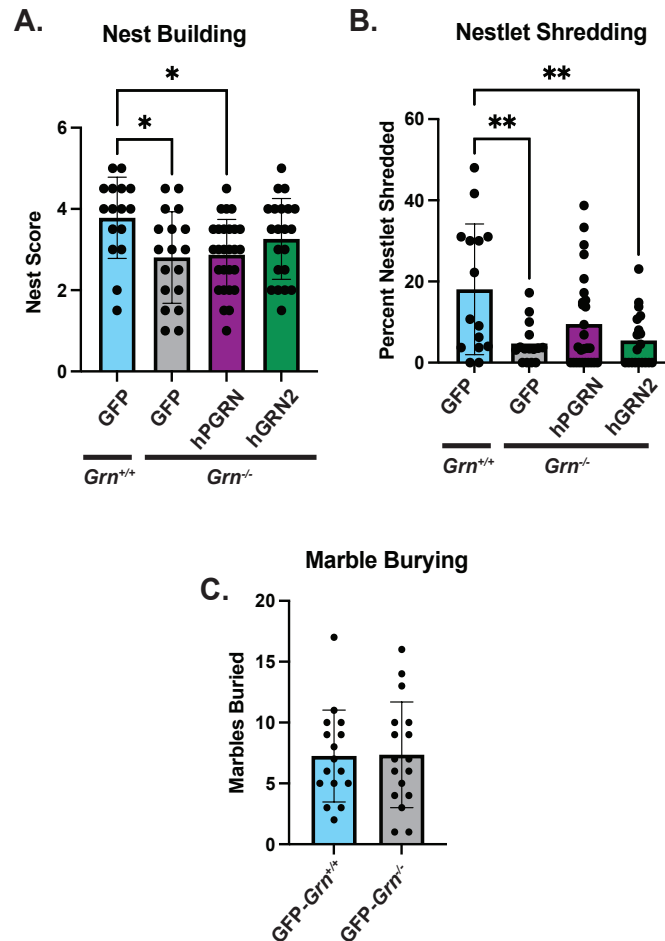


Figure 2.18: Behavioral Assessment Reveals that individual GRNs alleviate some dysregulated behavior in *Grn*^{-/-} mice.

- A) Quantification of nest building scores. Data represented as mean±SD, significance was determined by One-way ANOVA with Tukey's post-hoc analysis. N=18-23 mice/group. * $p < 0.05$, ** $p < 0.01$, *** $p < 0.001$, **** $p < 0.0001$.
- B) Percent of nestlet shredded quantified by weight. Data represented as mean±SD, significance was determined by One-way ANOVA with Tukey's post-hoc analysis. N=18-23 mice/group. * $p < 0.05$, ** $p < 0.01$, *** $p < 0.001$, **** $p < 0.0001$.
- C) Number of marbles buried. Data represented as mean±SD, significance was determined by Student's T-test N=18-20 mice/group. * $p < 0.05$, ** $p < 0.01$, *** $p < 0.001$, **** $p < 0.0001$.

different from *GFP-Grn*^{+/+} (Fig 2.6B). The nest building behavior was not improved by the expression of hPGRN, however, the expression of hGRN2 was able to ameliorate the loss of nest

building behavior in *Grn*^{-/-} mice (**Fig 2.6A**). In the context of our study only hGRN2-*Grn*^{-/-} were assessed using our set of behavioral tests. Interestingly the expression of hGRN2 did not affect level of nestlet shredding in *Grn*^{-/-} mice. The interpretation of these data is limited by the restriction of our testing to only hGRN2 mice which showed a subtler biochemical rescue phenotype compared to hGRN4 injected animals. Further, we were unable to recapitulate trends in PGRN rescue previously reported by other labs, suggesting that the sensitivity of our assay may not be optimal. Overall, these findings suggest that GRNs may be able to rescue behaviors effected by the loss of PGRN, but require additional investigation and more thorough behavioral profiling before more concrete conclusions can be reported.

2.11 Discussion

In this study, we find that delivery of an individual granulin using rAAV is equally efficacious as full-length hPGRN, correcting a variety of disease-linked neuropathology in *Grn*^{-/-} mice. Proteomic analyses of the *Grn*^{-/-} mouse thalamus at 12-months revealed wide-spread dysregulation of lysosomal hydrolases, lysosomal lipid metabolism, neuroinflammation, and proteostasis pathways, which can all be corrected by adding back hPGRN (~88 kDa) or a single granulin (~6k Da) subunit. This fills a critical gap in our knowledge of PGRN biology, strongly supporting the idea that individual granulins are the bioactive, functional components of PGRN. Moreover, our data suggest protein replacement with a single granulin may be a viable therapeutic approach in FTD caused by *GRN* mutations, which should be explored further.

Although it is well established that pathogenic *GRN* mutations decrease PGRN levels and ultimately cause neurodegeneration, the precise function of PGRN itself is still unclear. In general, the full-length PGRN protein has been thought to be directly neurotrophic, growth promoting, and anti-inflammatory. PGRN has been proposed to mediate these activities through binding and

activation of extracellular signaling receptors(225, 320), however this concept does not explain why complete lack of PGRN causes lysosome dysfunction and manifests as an LSD. Based on our discovery that PGRN is rapidly processed into individual granulins in the lysosome(349), we tested the idea that the cleaved granulins themselves are active.

This is an important conceptual advance, because, prior to this study, granulins were thought to have the opposite activity of PGRN, potentially promoting inflammation(193) and neurotoxicity(309) while impairing lysosomal function(281). In contradiction to these hypotheses, we find that long-term expression of two different granulins in *Grn*^{-/-} mouse brain reduced multiple markers of neuroinflammation and glial activation, ameliorated the accumulation of lipofuscin, and broadly corrected dysregulated lysosomal proteins and lipids. Additional substantiation of our data comes from a study which found that PTV:PGRN, a brain penetrant form of hPGRN, is efficacious for multiple weeks after dosing *Grn*^{-/-} mice, when PGRN has been completely cleared, suggesting that granulins made in the lysosome are stable and mediate prolonged efficacy(238). Taken together, these findings suggest granulins have a central role regulating lysosomal function, lysosomal lipid metabolism, and may hold therapeutic potential for multiple neurodegenerative diseases associated with lysosomal dysfunction.(160, 350, 351)

A limitation of our study is that we only examined the efficacy of two of the seven granulins in *Grn*^{-/-} mouse brains. We focused on hGRN2 and hGRN4 because they are 50% dissimilar, reported to have opposite function *in vitro*, and we were able to generate specific antibodies to assist experimental analysis. Considering this limitation, we found that rAAV-mediated expression of either hGRN2 or hGRN4 equally corrected major markers of lysosome dysfunction (galecin-3), microglial activation (Cd68, Gpnmb), and lipofuscin pathology in *Grn*^{-/-} mouse brains. However, in some cases, such as correction of BMP and GlcSph lipids, hGRN2 was not as efficacious as

hGRN4 or hPGRN. Proteomics quantification revealed that despite the injection of equivalent rAAV titers, hGRN2 was expressed at ~2.5-fold lower levels than hGRN4, raising the possibility that insufficient expression of hGRN2 limited efficacy in the *Grn*^{-/-} mouse brain. Alternatively, hGRN2 and hGRN4 may have different functions or binding partners in the lysosome explaining some of the observed differences. It is also possible that hGRN2 and hGRN4 may be differentially regulated or have different half-lives in the lysosome.(286) Nevertheless, the shared ability of hGRN2 and hGRN4 to rescue many pathologic phenotypes in *Grn*^{-/-} mice, strongly supports further investigation of the bioactivity of all granulins (1 to 7) *in vivo*.

The findings from our work have important implications for therapeutic development to treat FTD-*GRN* and other neurodegenerative diseases with PGRN deficiency. Multiple therapeutic strategies to increase PGRN levels in the CNS are being pursued for clinical development ranging from protein replacement(224), to gene therapy(264), and small molecule approaches.(352) One approach aims to increase PGRN by depleting sortilin (*SORT1*), a PGRN lysosomal trafficking receptor, with an antibody (AL001) that has advanced to a phase 3 clinical trial (NCT04374136).(318) Antibodies targeting the sortilin extracellular domain increase circulating levels of PGRN in mice(266) but decrease lysosomal granulins in iPSC-derived neurons.(353)

Our data raise a concern with this approach, because anti-sortilin antibodies likely raise extracellular PGRN by reducing trafficking to the lysosome, leading to decreased production of intracellular granulins, which we find are functional and prevent lysosome dysfunction caused by PGRN deficiency. On the other hand, PGRN can be trafficked to the lysosome through alternative receptor pathways by binding prosaposin(157, 294), which may reduce this concern, however it is unclear whether this occurs in the CNS following anti-sortilin treatment.(354) At a minimum, our data raise a cautionary note that both PGRN and intra-lysosomal granulin levels should be

measured when evaluating pre-clinical therapeutic approaches to treat PGRN deficiency in humans.

In conclusion, we find that neuronal expression of a single granulin can functionally substitute for the full length PGRN protein and correct a wide spectrum of disease-like phenotypes in *Grn*^{-/-} mice including lysosome dysfunction, gliosis, dysregulated metabolism of lipids (BMP, GlcSph and gangliosides) and accumulation of lipofuscin. These findings support the idea that PGRN serves as a precursor to bioactive granulins, which are made in the lysosome, and directly mediate lysosomal homeostasis and neuroprotection. Key questions remain including whether all granulins can equivalently rescue pathologic phenotypes caused by PGRN deficiency. Additionally, the precise molecular function of granulins inside the lysosome, or whether each granulin has a unique or overlapping activity has yet to be resolved. From a therapeutic perspective, due to their small size, granulins may have advantages for treating FTD-*GRN* by crossing the blood-barrier more readily than PGRN due to their small size, although this needs to be empirically tested. Furthermore, therapies that aim to raise PGRN levels need to consider the impact on granulin levels throughout the CNS. Finally, our data strongly suggest that focused attention on the function of granulins inside the endosomal-lysosomal pathway is necessary to understand how granulins mediate lysosomal protein and lipid homeostasis and prevent neurodegeneration in FTD-*GRN* and related neurodegenerative disorders.

2.12 Acknowledgements

We thank all the members of the Kukar lab, the Emory Center for Neurodegenerative Disease (CND), and the Emory Neuroscience (NS) graduate program for their support and helpful comments throughout this research project. We thank Dr. Shawn Ferguson (Yale) for the generous gift of HeLa *GRN*^{-/-} cells. We greatly appreciate the kind support of Dr. Yona Levites and Dr.

Todd E. Golde producing recombinant AAV. We thank Dr. Nicholas Seyfried, Duc Duong, and the Emory Proteomics core for excellent analytical services and technical expertise. Research reported in this publication was supported in part by the Emory Integrated Proteomics shared resource of Winship Cancer Institute of Emory University and NIH/NCI under award number P30CA138292. The content is solely the responsibility of the authors and does not necessarily represent the official views of the National Institutes of Health. This work was supported by the National Institutes of Health (NIH) National Institute of Neurological Disorders and Stroke (NINDS) grant R01NS105971, NIH National Institute of Aging (NIA) RF1AG079318 grant, a New Vision Research Investigator Award, the Alzheimer's Drug Discovery Foundation (ADDF) and the Association for Frontotemporal Degeneration (AFTD), the Bluefield Project to Cure Frontotemporal Dementia, the BrightFocus Foundation, a gift from Arkuda Therapeutics, and an Emory School of Medicine (SOM) Dean's Imagine, Innovate, and Impact (I³) Wow! Research Award Investigator grant. J.R. was supported by an NIH NINDS F31 Ruth L. Kirschstein National Research Service Award (NRSA) fellowship grant (F31NS117129).

2.13 Supplemental Figures

Supplemental Figures can be found in Appendix 4

2.14 Experimental models and subject details

Mouse Model and Neonatal rAAV injections.

The *Grn*^{-/-} mice used in this study were purchased from the Jackson Laboratory (B6(Cg)-Grntm1.1Aidi/, IMSR Cat# JAX:013175, RRID:IMSR_JAX:013175) and generated as previously described. Mice were bred and housed in the Department of Animal Resources at Emory University and all work was approved by the Institutional Animal Care and Use Committee (IACUC) and performed in accordance with the Guide for the Care and Use of Laboratory Animals

of the National Institutes of Health. Postnatal day 0 (P0) mouse pups (*GRN*^{+/+} or *GRN*^{-/-}) were injected with rAAV vectors.(325) Briefly, P0 pups were cryoanesthetized in a nest protected by aluminum foil placed on ice for 5 min. One microliter of rAAV was injected intracerebroventricularly (ICV) into both hemispheres using a 10 ml Hamilton syringe with a 30-gauge needle. The pups were then placed on a heating pad with their original nesting material for 3–5 min and returned to their mother for further recovery. Mice were not sexed before injection, males and females were injected.

2.15 Methods

Production of recombinant adeno-associated virus

Four purified recombinant adeno-associated virus vectors (rAAVs) for injection were produced by plasmid transfection with helper plasmids in HEK293T cells. Briefly, the coding sequence of twin-Strep-GFP (GFP), twin-Strep-V5 human progranulin (hPGRN), twin-Strep-FLAG-granulin-2 with linker region 3 (hGRN2) and twin-Strep-FLAG-granulin-4 with linker region 5 (hGRN4) were subcloned from a pcDNA3.1 expression plasmid into pAAV. hPGRN, hGRN2, and hGRN4 all contain the native hPGRN signal peptide at the N-terminus. The AAV vectors express hPGRN, hGRN2, hGRN4, or GFP under the control of the cytomegalovirus enhancer/chicken β -actin promoter, a woodchuck post-transcriptional regulatory element, and the bovine growth hormone, poly(A), and were generated by plasmid transfection with helper plasmids in HEK293T cells. Forty-eight hours after transfection, the cells were harvested and lysed in the presence of 0.5% sodium deoxycholate and 50 U/ml Benzonase (Sigma, St. Louis, MO) by freeze thawing, and the virus was isolated using a discontinuous iodixanol gradient and affinity purified on a HiTrap HQ column (Amersham Biosciences, Arlington Heights, IL). The genomic titer of each virus was determined by quantitative PCR.

Collection of Brain Tissue

Mice were sacrificed after 12 months and brains were processed in two downstream pathways. Brains from half of the individuals from each cohort were immediately dissected from the skull and frozen at -80C. Whole brains were later thawed on ice and cortical, hippocampal, and thalamic sections were bulk dissected from the brain and frozen immediately at -80C. Remaining animals were transcardially perfused using ice cold PBS then fixed in methanol-free 4% PFA before dissecting all brains and storing in 4% PFA for 24 hours before transferring samples to 30% sucrose, which was replaced at 24 and 48 hours. The final storage solution was 30% sucrose and 1% sodium azide. Fixed tissue was stored at 4C until it was prepared for sectioning. Brain sectioning was performed using a freezing microtome set to 40 μm . Brains were frozen in ground dry ice, then mounted with 30% sucrose onto the pre-frozen sectioning stage, where serial sections were collected from the entire brain and stored in 30% sucrose, 30% ethylene glycol and 1% sodium azide. Frozen hippocampal and cortical brain samples from 12-month-old *Grn*^{+/+} (n=27) and *Grn*^{-/-} (n=44) mice were allocated for further processing.

Thalamic Proteomics Sample Preparation

Each tissue sample was homogenized in 300 μL of 8 M urea/100 mM NaHPO₄, pH 8.5 with HALT protease and phosphatase inhibitor cocktail (Pierce) using a Bullet Blender (Next Advance) according to manufacturer protocols. Briefly, tissue lysis was transferred to a 1.5 mL Rino tube (Next Advance) with 350 mg stainless steel beads (0.9–2 mm in diameter) and blended for 5-minute intervals, two times, at 4°C. Protein supernatants were sonicated (Sonic Dismembrator, Fisher Scientific) three times for 5 seconds, with 15 second intervals of rest, at 30% amplitude to

disrupt nucleic acids, in 1.5 mL Eppendorf tubes. Protein concentration was determined by BCA method, and aliquots were frozen at -80°C . Protein homogenates (200 μg) were treated with 1 mM dithiothreitol (DTT) at 25°C for 30 minutes, followed by 5 mM iodoacetamide (IAA) at 25°C for 30 minutes in the dark. Proteins were digested with 1:25 (w/w) lysyl endopeptidase (Wako) at 25°C for overnight followed by another overnight digestion with 1:25 (w/w) trypsin (Pierce) at 25°C after dilution with 50 mM NH_4HCO_3 to a final concentration of 1 M urea. The resulting peptides were desalted on a Sep-Pak C18 column (Waters) and dried under vacuum. All samples were across 2 batches and labeled with an 18-plex Tandem Mass Tag (TMTPro) kit (ThermoFisher, Lot numbers: UK297033 and WI336758) according to manufacturer's protocol. Each TMT batch was desalted with 60 mg HLB columns (Waters) and dried via speed vacuum (Labconco). Dried samples were re-suspended in high pH loading buffer (0.07% vol/vol NH_4OH , 0.045% vol/vol FA, 2% vol/vol ACN) and loaded onto a Water's BEH column (2.1 mm x 150 mm with 1.7 μm particles). A Vanquish UPLC system (ThermoFisher Scientific) was used to carry out the fractionation. Solvent A consisted of 0.0175% (vol/vol) NH_4OH , 0.01125% (vol/vol) FA, and 2% (vol/vol) ACN; solvent B consisted of 0.0175% (vol/vol) NH_4OH , 0.01125% (vol/vol) FA, and 90% (vol/vol) ACN. The sample elution was performed over a 25 min gradient with a flow rate of 0.6 mL/min with a gradient from 0 to 50% solvent B. A total of 192 individual equal volume fractions were collected across the gradient. Fractions were concatenated to 96 fractions and dried to completeness using vacuum centrifugation. Dried peptide fractions were resuspended in 20 μl of peptide loading buffer (0.1% formic acid, 0.03% trifluoroacetic acid, 1% acetonitrile). Peptide mixtures (2 μl) were separated on a self-packed C18 (Dr. Maisch) fused silica column (15 cm \times 150 μm internal diameter) by a Dionex Ultimate rsLCnano and monitored on a Fusion Lumos mass spectrometer (ThermoFisher). Elution was performed over a 42 min gradient at a rate of 1250

nl/min with buffer B ranging from 1% to 99% (buffer A: 0.1% formic acid in water, buffer B: 0.1% formic in 80% acetonitrile). The mass spectrometer cycle was programmed to collect at the top speed for 3 s cycles. The MS scans (410-1600 m/z range, 400,000 AGC, 50 ms maximum ion time) were collected at a resolution of 60,000 at m/z 200 in profile mode. HCD MS/MS spectra (0.7 m/z isolation width, 35% collision energy, 125,000 AGC target, 86 ms maximum ion time) were collected in the Orbitrap at a resolution of 50000. Dynamic exclusion was set to exclude previous sequenced precursor ions for 20 s within a 10-ppm window. Precursor ions with +1 and +8 or higher charge states were excluded from sequencing.

Thalamic Proteomics Data Processing

All raw files were analyzed using the Proteome Discoverer Suite (v.2.4.1.15, ThermoFisher). MS/MS spectra were searched against the UniProtKB mouse proteome database (downloaded in August 2020 with 91417 total sequences) supplemented with 4 variant sequences (twin-Strep-GFP, hGRN2, hGRN4, and hPGRN). The Sequest HT search engine was used to search the RAW files, with search parameters specified as follows: fully tryptic specificity, maximum of two missed cleavages, minimum peptide length of six, fixed modifications for TMTPro tags on lysine residues and peptide N-termini (+304.207 Da) and carbamidomethylation of cysteine residues (+57.02146 Da), variable modifications for oxidation of methionine residues (+15.99492 Da), serine, threonine and tyrosine phosphorylation (+79.966 Da) and deamidation of asparagine and glutamine (+0.984 Da), precursor mass tolerance of 10 ppm and a fragment mass tolerance of 0.05 Da. Percolator was used to filter peptide spectral matches and peptides to an FDR <1%. Following spectral assignment, peptides were assembled into proteins and were further filtered

based on the combined probabilities of their constituent peptides to a final FDR of 1%. Peptides were grouped into proteins following strict parsimony principles.

Differential expression analysis

Differentially enriched or depleted proteins ($p \leq 0.05$) were identified by one-way ANOVA with post-hoc Tukey HSD test comparing five groups: GFP-Grn^{+/+}, GFP-Grn^{-/-}, PGRN-Grn^{-/-}, GRN2-Grn^{-/-}, GRN4-Grn^{-/-} mice. Differential expression of proteins was visualized with volcano plots generated using the ggplot2(355) package in Microsoft R Open v3.4.2. Significantly differentially expressed proteins were determined by both having a $p \leq 0.05$ and a fold change difference of greater than $\log_2(1.25)$ or less than $-\log_2(1.20)$ (a minimum 1.2-fold change).

Proteomics Analysis and Visualization

Differential Expression data from comparisons GFP-Grn^{+/+} vs GFP-Grn^{-/-}, GFP-Grn^{-/-} vs hPGRN-Grn^{-/-}, GFP-Grn^{-/-} vs hGRN2-Grn^{-/-}, and GFP-Grn^{-/-} versus hGRN4-Grn^{-/-} including adjusted p values, and abundance values were imported into Quickomics, an R-shiny powered proteomics analysis and visualization tool.(356) GIS internal standards were removed from the data set and Heatmaps were created filtering proteins from the GFP-Grn^{+/+} vs GFP-Grn^{-/-} comparison with an adjusted p-value of < 0.05 and a fold change value of at least 1.2 or 20%. Clustering was performed grouping proteins by the similarity across the sample ID using a k-means approach. Other visualizations created in Quickomics include 2-Way DEG plots and PCA visualizations. Additional PCA analysis was undertaken in R using the PCAtools package.(357)

Gene ontology (GO)

Genes IDs identified from proteins determined to be differentially abundant (adjusted p-value 0.05, FC 1.2) between GFP-Grn^{+/+}, GFP-Grn^{-/-} mice were input into the Metascape Gene Ontology Analysis tool (<https://metascape.org>).⁽³⁵⁸⁾ Express Analysis was conducted and the top 50 Ontology Terms were collected.

Lipidomics and Metabolomics

Sample preparation for lipidomics and metabolomics analyses.

During tissue collection, the cortex was dissected, weighed, and flash frozen. Each frozen cortex was pulverized into a homogenous powder, and roughly 30 mg of each cortex powder sample was used to extract lipids. Methanol spiked with internal standards (see LCMS methods below) was added to each sample and homogenized with FastPrep-24TM 5G bead beating grinder and lysis system using Lysing Matrix D tubes with CoolPrepTM adapter (MP Biomedicals) for 40 seconds at a speed of 6 m/s. The methanol fraction was then isolated via centrifugation (20 minutes at 4°C, 14,000 x g), followed by transfer of supernatant to a 96 well plate. After a 1 h incubation at 20°C followed by an additional centrifugation (20 minutes, 4,000 x g at 4°C), methanol was transferred to glass vials for LCMS analysis.

Lipidomics analysis.

Lipid analyses were performed by liquid chromatography on an ExionLC (Sciex) coupled with electrospray mass spectrometry TripleQuad 7500 (Sciex). For each analysis, 1 µL of the sample was injected on a Premier BEH C18 1.7 µm, 2.1×100 mm column (Waters) using a flow rate of 0.25 mL/min at 55°C. For positive ionization mode, mobile phase A consisted of 60/40 (vol/vol)

acetonitrile/water with 10 mM ammonium formate + 0.1% formic acid; mobile phase B consisted of 90/10 (vol/vol) isopropyl alcohol/acetonitrile with 10 mM ammonium formate + 0.1% formic acid. For negative ionization mode, mobile phase A consisted of 60/40 (vol/vol) acetonitrile/water with 10 mM ammonium acetate; mobile phase B consisted of 90/10 (vol/vol) isopropyl alcohol/acetonitrile with 10 mM ammonium acetate. The gradient was programmed as follows: 0.0-8.0 min from 45% B to 99% B, 8.0-9.0 min at 99% B, 9.0-9.1 min to 45% B, and 9.1-10.0 min at 45% B. Electrospray ionization was performed in positive or negative ion mode. We applied the following settings: curtain gas at 40 psi (negative mode) and curtain gas at 40 psi (positive mode); collision gas was set at 9; ion spray voltage at 2000 V (positive mode) or -2000 V (negative mode); temperature at 250°C (positive mode) or 450°C (negative mode); ion source Gas 1 at 40 psi; ion source Gas 2 at 70 psi; entrance potential at 10 V (positive mode) or -10 V (negative mode); and collision cell exit potential at 15 V (positive mode) or -15 V (negative mode). Data acquisition was performed in multiple reaction monitoring mode (MRM) with the collision energy (CE) values reported in **Supplementary Tables 2.1 and 2.2**. Area ratios of endogenous lipids and surrogate internal standards were quantified using SCIEX OS 3.1 (Sciex).

Metabolomics analysis.

Metabolites analyses were performed by liquid chromatography on an ExionLC (Sciex) coupled with electrospray mass spectrometry TripleQuad 7500 (Sciex). For each analysis, 1 μ L of the sample was injected on a Premier BEH amide 1.7 μ m, 2.1 \times 150 mm column (Waters) using a flow rate of 0.40 mL/min at 40°C. Mobile phase A consisted of water with 10 mM ammonium formate + 0.1% formic acid. Mobile phase B consisted of acetonitrile with 0.1% formic acid. The gradient was programmed as follows: 0.0–1.0 min at 95% B; 1.0–7.0 min to 50% B; 7.0–7.1 min to 95% B; and 7.1–10.0 min at 95% B. Electrospray ionization was performed in positive ion mode. We

applied the following settings: curtain gas at 40 psi; collision gas was set at 9; ion spray voltage at 1600 V; the temperature at 350°C; ion source Gas 1 at 30 psi; ion source Gas 2 at 50 psi; entrance potential at 10 V; and collision cell exit potential at 10 V. Data acquisition was performed in MRM mode with the CE values reported in **Supp. Table 3**. Area ratios of endogenous metabolites and surrogate internal standards (**Supp. Table 3**) were quantified using SCIEX OS 3.1 (Sciex).

Analysis of glucosyl- and galactosyl-sphingolipids.

Glucosyl- and galactosyl-sphingolipids analyses were performed by liquid chromatography ExionLC coupled to electrospray mass spectrometry TQ7500. For each analysis, 1 μ L of sample was injected on a HALO HILIC 2.0 μ m, 3.0 \times 150 mm column (Advanced Materials Technology) using a flow rate of 0.48mL/min at 45°C. Mobile phase A consisted of 92.5/5/2.5 (vol/vol/vol) acetonitrile/isopropanol/water with 5 mM ammonium formate and 0.5% formic acid. Mobile phase B consisted of 92.5/5/2.5 (vol/vol/vol) acetonitrile/isopropanol/water with 5 mM ammonium formate and 0.5% formic acid. The gradient was programmed as follows: 0.0–2 min at 0% B, 2.1 min at 5% B, 4.5 min at 15% B, hold to 6.0 min at 15% B, up to 100% B at 6.1 min and hold to 7.0 min, drop back to 0% B at 7.1 min and hold to 8.5 min. Electrospray ionization was performed in positive ion mode. We applied the following settings: curtain gas at 40 psi; collision gas was set at 9 psi; ion spray voltage at 2250 V; temperature at 450°C; ion source Gas 1 at 40 psi; ion source Gas 2 at 70 psi; entrance potential at 10 V; and collision cell exit potential at 15 V. Area ratios of endogenous glucosyl- or galactosyl-sphingolipids and surrogate internal standards (Table 4) were quantified using SCIEX OS 3.1 (Sciex).

Immunohistochemistry

Paraformaldehyde fixed coronal tissue sections from each group of rAAV-injected mice were stained with the StrepTagII C23.21 antibody or cell type markers (neurons (NeuN), microglia (IBA-1), astrocytes (GFAP)) using previously published procedures. The full list of antibodies is listed in the key resources table. For this procedure, 40 μ m coronal brain sections were processed using a free-floating method. For StrepTagII and CD68 antibodies, antigen retrieval with Citrate buffer pH 6.0 (30min) was performed for epitope retrieval. Sections were rinsed three times in phosphate-buffered saline containing 0.3% Triton-X100 (PBST) (0.1M Phosphate buffer, pH 7.4, 0.137 M NaCl, 0.3% Triton-X100) and reacted in PBST containing 1% hydrogen peroxide (30 min) to remove endogenous peroxidase activity, rinsed three times in PBST, blocked with 2.5% normal horse serum, and then incubated in optimal dilutions of antibody overnight with shaking at room temperature (RT). Sections were then rinsed three times, incubated in biotinylated anti-species immunoglobulin (Vector Laboratories) at 1:1000 for 2 hours at room temperature, rinsed three times and then incubated with avidin-biotin-peroxidase complex (ABC) (Vector Laboratories). Localization of bound antibody was visualized using avidin-biotin horseradish peroxidase (HRP) enzyme complex histochemistry and nickel ammonium sulfate-enhanced diaminobenzidine-HCl (100 μ g/ml) (TCI Chemicals, Tokyo, Japan) as a substrate to produce a dark purple reaction product. Sections were then mounted on microscope slides and coverslipped with permanent mounting agent.

For detection of the twin-Strep tag on constructs, the StrepTagII C23.21 antibody was visualized using the Mouse on Mouse ImmPress HRP Polymer kit (Vector Laboratories) according to the manufacturer's protocol. To Quantify IHC signal cortical, thalamic, and hippocampal regions were

cropped from a whole coronal section image. Brain regions of interest analyzed using an automated pipeline created using CellProfiler (www.cellprofiler.org)(4) for quantification.

Fluorescent immunohistochemistry

Double-color fluorescent immunohistochemistry was carried out to verify cellular co-localization of PGRN-expressing cells in hPGRN-*Grn*^{-/-} mice with cellular antigenic markers such as neuronal marker (NeuN), microglial marker (Iba-1), and astrocyte marker (Gfap). Tissue sections were incubated with optimal dilutions of antibodies at 4 degrees overnight with shaking. After three washes (10 min each) in PBST, sections were incubated with optimal concentrations of fluorescent-labeled secondary antibodies. Bound primary antibodies were detected with Alexa Fluor 488-donkey anti-goat IgG, and Cy3-donkey anti-rabbit IgG. After three washes, sections were mounted, coverslipped with Immuno-mount fluorescent mounting media (Thermo Fisher) and imaged using Lecia DMI 8 microscope with a DFC9000 GT camera and system software (LAS X Life Science microscope software).

Cell Culture

HeLa *GRN*^{-/-} cells were a gift from Dr. Shawn Ferguson (Yale) and generated using CRISPR as described.(137) HeLa wild-type or *GRN*^{-/-} cells were cultured in DMEM medium plus 10% fetal bovine serum (FBS) and 1% Pen/Strep and maintained at 37 °C with 5% CO₂. 24 hours before collection DMEM media was replaced with OptiMEM media (Gibco).

HeLa Lysis and Media Collection

Cells were suspended in MES buffer (50mM MES pH6.5, 1% Triton, 150mM NaCl, 1XHALT PPI) 5uL for every 1mg cell pellet. Cells were then lysed on ice for 10 mins briefly vortexing every 3 minutes. Lysates were then spun at 600xg for 10 minutes and supernatant was collected. Conditioned media was collected from culture dish and spun at 500xg for 10 minutes to remove any cell debris.

Flash Frozen Mouse Brain Sample Processing for Immunoblot

To prepare samples for the immunoblot analysis of proteins, a novel protocol was developed in which approximately 40 mg of mouse hippocampal tissue from each sample was placed in a solution of PBS with added HALT phosphatase protease inhibitor (PPI) at a dilution of 1:2 (weight to volume). The PPI was diluted into the 1xPBS at 1:100. In the PBS + PPI solution, the sample was cut into smaller pieces with mini scissors. Once cut into smaller pieces, the sample is ready for further homogenization.

A bead lysis kit was used for the homogenization of these small, soft hippocampal samples. The samples were cut into pieces and still in the PBS + PPI solution were pipetted into 1.5 mL RINO screw-tap tubes (Next Advance) prefilled with zirconium oxide beads. Tubes were placed into the Bullet Blender (Next Advance) for homogenization.

Once homogenized, the solution was diluted 1:5 in RIPA lysis buffer supplemented with 1x HALT protease and phosphatase inhibitor. After 15 minutes, the solution was sonicated (30A; 2 seconds on; 8 seconds of rest; 10 seconds total sonication time/sample). After sonication, the solution was spun down in a centrifuge at 20,000xRCF at 4C for 10 minutes. Protein concentration was measured with the bicinchoninic acid (BCA) assay, samples were frozen in aliquots at -80C.

Immunoblot

SDS/PAGE and immunoblotting of HeLa cell lysates, cell media, and mouse brain lysates were performed as described.(25, 359, 360) Mouse brain running samples were prepared for immunoblot in 1X Laemmli loading buffer with 20 mM tris(2-carboxyethyl)phosphine (TCEP)) followed by denaturation at 70 degrees C for 15 minutes. For immunoblotting, protein samples were first separated on Bio-Rad TGX 4-20% 26-well gels at 100 V and transferred to a 0.2-micron nitrocellulose membrane using the Bio-Rad Trans-blot Turbo system. BulletBlock (Nacalai) for 30 minutes at room temperature membranes were incubated overnight at 4C with primary antibodies (STAR MATERIALS). Membranes were probed with anti-Histone H3 or anti-Beta tubulin antibodies and imaged on the Odyssey Fc (LI-COR), to normalize protein abundance between samples.

For hGRN2 and hGRN4 protein samples were separated using 4-20% BisTris gels run using MES buffer (Genscript) at 100V to resolve bands. Transfers were completed using Bio-Rad Trans-blot Turbo to a 0.2-micron nitrocellulose membrane, then blocked with Fish Serum Blocking Buffer (ThermoFisher) for 60 minutes at room temperature. Membranes were then incubated with primary antibodies (1ug/mL) overnight at 4C. All primary antibodies were diluted to a final concentration of 50% glycerol for long term storage at -20C. Near-infrared fluorescent secondary antibodies (diluted in TBST) or HRP-conjugated (diluted in 0.5% milk in TBST) antibodies (STAR Materials) were incubated for 1 hour at room temperature. For HRP visualization, blots were incubated in WesternSure PREMIUM Chemiluminescent Substrate (LI-COR) for 5 min before imaging. Near infrared or chemiluminescent blots were imaged using Odyssey Fc (LI-COR) and analyzed by Image Studio software 5.2 (LI-COR).

Alignment and Percent Identity

Granulin 1-7 amino acid sequences were accessed from Uniprot Human: P28799 (Table 5). Sequences were aligned using the msa R package with ClustalOmega.(361) Alignments were visualized and consensus sequence calculated using ggmsa.(362) Percent Identity of amino acids was calculated from the ClustalOmega hGRN alignment using Bio3D.(363-365)

Granulin	UniProt Accession Number
hGRN1	PRO_0000012695
hGRN2	PRO_0000012696
hGRN3	PRO_0000012697
hGRN4	PRO_0000012698
hGRN5	PRO_0000012699
hGRN6	PRO_0000012700
hGRN7	PRO_0000012701

Marble Burying

The assay was carried out a previously described (366). Briefly, mice were moved from their home cage to a fresh cage with 2 inches of bedding. 20 Marbles were placed in a 5x4 grid atop fresh bedding. Mice were given 30 minutes in the new environment to bury marbles. Mice were removed and images were taken at multiple aspects. Marbles buried were quantified day of assay, 3 days after assay, and 2 months after assay then averaged.

Nestlet Shredding

In line with previously described protocols (367), mice were placed in individual novel cages with a fresh nestlet that was pre-weighed. After one hour the remaining solid nestlet was removed and weighed. The percentage of nestlet shredded by weight was recorded.

Nest Building

Mice were singly housed in a novel cage overnight starting at 6pm with a fresh nestlet. In the morning at 9am mice were removed and returned to their home cage and nests were scored according to previously published criteria (368). Nest quality was scored day of assay, and from images taken day of 3 days after assay, and 2 months after assay then averaged.

Diagrams

All diagrams and representative figures were made using BioRender (biorender.com).

Statistics

Proteomics, lipidomics, and metabolomics: LC/MS data was Log₂ transformed and ANOVAs for the following comparisons were performed (GFP-*Grn*^{-/-} and GFP-*Grn*^{+/+}) (GFP-*Grn*^{-/-} and hPGRN-*Grn*^{-/-}) (GFP-*Grn*^{-/-} and hGRN2-*Grn*^{-/-}) (GFP-*Grn*^{-/-} and hGRN4-*Grn*^{-/-}) p-values were adjusted using the Benjamini-Hochberg method. Abundance of individual proteins of interest were analyzed using One-Way ANOVA followed by Tukey's post-hoc analysis. Variance was assessed using the Brown-Forsythe test, p=0.05 and the normality of GFP *Grn*^{-/-} and GFP-*Grn*^{+/+} samples was determined using the Shapiro-Wilk test p=0.05. PCA confidence intervals were analyzed using the PCAtools R package alpha set to 95%. The area ratios of endogenous lipids, metabolites, and surrogate internal standards were quantified using SCIEX OS 3.1. Statistical analysis of

significance for lipid and metabolite levels in samples was determined by One-way ANOVA with Tukey's post-hoc analysis. * $p < 0.05$, ** $p < 0.01$, *** $p < 0.001$, **** $p < 0.0001$. (GFP-*Grn*^{-/-} and GFP-*Grn*^{+/+}) (GFP-*Grn*^{-/-} and hPGRN-*Grn*^{-/-}) (GFP-*Grn*^{-/-} and hGRN2-*Grn*^{-/-}) (GFP-*Grn*^{-/-} and hGRN4-*Grn*^{-/-}) comparisons are visualized in figures.

Immunohistochemistry and Lipofuscin: IHC image quantification was performed single brain sections from 5 animals per group (N=5). Normality of GFP *Grn*^{-/-} and GFP-*Grn*^{+/+} samples was assessed using Shapiro-Wilk test $p=0.05$ and variance was assessed using Brown-Forsythe test $p=0.05$. Comparisons were conducted using Two-way ANOVA, one factor being brain region and the second being AAV treatment group. A full effect model was fitted and Tukey's post-hoc analysis was completed comparing treatments groups to all other treatment groups within brain region.

Western Blot and ELISA Quantification: All blots were run using 5 individual animals per group (N=5) and normalized values were analyzed using One-Way ANOVA followed by Tukey's post-hoc analysis. Variance and normality were assessed in the same manner as immunohistochemistry experiments. All regions were assessed independently. The hippocampal galectin-3 outlier was identified using Grubbs test $p= 0.0001$. ELISA data was analyzed using One-Way ANOVA followed by Tukey's post-hoc test.

Mouse Behavior: Groups were assessed for outliers using ROUTs outlier test set to remove definitive outliers $Q=0.2\%$. Outliers were identified in the nestlet shredding test and removed from consideration. Nestlet, and Nest Building tests were assessed using One-Way ANOVA followed by Tukey's post hoc test. Marble Burying scores were assessed using Student's T test.

Visualization: All bar charts were produced in PRISM version 9 and heatmaps were made using Quickomics.(356)

3 Chapter 3: HeLa cells Recapitulate Phenotypes of Lipid Dysregulation after loss of PGRN

3.1 Introduction

Lysosomes are membrane enclosed organelles that degrade a variety of macromolecules and were first described by Christian de Duve in 1955 (369). Lysosomes have a single lipid bilayer, which contains over 100 membrane proteins, enclosing an acidic lumen that hosts 50 or more lysosomal hydrolases (370). Lysosomes are critically involved in the degradation and recycling of intracellular and extracellular material including lipids, proteins, nucleic acids, and carbohydrates. Historically, lysosomes were viewed as static organelles that represented the endpoint of degradation following endocytosis or phagocytosis. In fact, lysosomes are dynamic, highly regulated, and can vary in their pH (371), sub-cellular location (372), and morphology (373). Moreover, our understanding of lysosomes has expanded from an organelle that degrades molecules to a multifunctional compartment that plays critical roles in cellular signaling, metabolism, membrane repair, homeostasis, and the immune response (253, 374).

Under normal physiological conditions, the lysosome participates in the degradation and recycling of numerous macromolecules and organelles throughout the cell (375). However, dysfunction of components of the lysosomal system is deleterious and causes a variety of fatal diseases including lysosomal storage diseases (LSD). Lysosomes are found in all eukaryotic cells (376) and with this widespread dysfunction LSDs are a clinically heterogeneous group of diseases (377). Clinical presentations include cardiac (378), immune (379), musculoskeletal (380), and central nervous system (CNS) manifestations (381) among others. The CNS is particularly

vulnerable to lysosome dysfunction, causing impairment of neuronal and glial function, which ultimately leads to neurodegeneration.

Lysosomal dysfunction is a key pathological feature observed in FTD-*GRN* patients. Neurons and microglia in the frontal cortex brain tissue have increased lipofuscin deposits, a diagnostic feature of many LSDs including CLN11 a disease caused by the complete loss of PGRN (344, 382). Enlarged endosomes and autophagic vesicles, signs of dysfunctional endo-lysosomal flux, occur in primary cell cultures and frontal cortical neurons of FTD (90, 383). Further, a lipidomic analysis found evidence that lysosomal degradation of triacylglycerides (TAGs) was impaired in human FTD brain tissue (21). These phenotypes suggest that impaired lysosomal function underpins FTD etiology. However, deep knowledge of lysosomal mechanisms that drive pathology and lead to disease are not well understood. Further without an understanding of the underlying biology of FTD, developing treatments will be more difficult.

To gain insight into the mechanisms driving disease models of PGRN deficiency have been studied. These models include *in vivo* animal models such as mice (22, 254, 261), zebrafish (384, 385), and *C. elegans* (309, 386). While some of these models recapitulate phenotypes associated with loss of PGRN in human patients, all miss important pathological aspects of human cases. Mechanistic studies can be difficult, costly, and prolonged, when employing rodent models, and models like *C. elegans* are phylogenetically distant from humans and may not produce results that are generalizable to humans or mammals. Yet, they serve an important role in the development of PGRN targeting therapeutics and understanding the role of PGRN systemically.

In addition to *in vivo* models groups have leveraged *in vitro* iPSC cell lines (265, 387), and primary cell cultures from mice and rats (286, 387, 388) to further understand the role PGRN plays in the cell. These lines have the benefit of reproducing some of the phenotypes not observed

in rodents, in the case of iPSCs (389). Or in the case of primary cells, may retain more characteristics of morphology and function like neurotransmitter receptors expression when compared to immortalized cells (390). However, there are limitations to the tractability of these systems as well, as resources like iPSCs and primary cells are more difficult to access, and have more limited life spans, and lower material yield (391). To further understand the role of PGRN in the lysosome consistent high yield, phylogenetically similar, models will be useful to screen a number of proposed mechanisms.

For this reason, we have set out to characterize a *GRN*^{-/-} HeLa cell line for the investigation of PGRN's biological mechanisms as well as establishing a baseline for screening potential interventions with both full length PGRN and individual GRNs. Based off of known phenotypes across models of PGRN deficiency previously reported (389, 392, 393) we predicted that *GRN*^{-/-} HeLa cells would display lysosomal dysfunction and lipid dysregulation. Here we report that *GRN*^{-/-} HeLa cells have disrupted lysosomal protease maturation and activity, alongside a decrease of BMP lipids and an accumulation of neutral lipids. Taken together, these findings show that *GRN*^{-/-} HeLa cells recapitulate some of the known phenotypes of PGRN deficiency across biological models and human patients and suggest that they can serve as an efficacious model for the assessment of future PGRN targeting interventions.

3.2 Confirming that HeLa *GRN*^{-/-} cell line is PGRN deficient

The HeLa cells were a generous gift to the Kukar lab by Dr. Shawn Ferguson. Cells were edited using CRISPR Cas-9 (137) to produce a *GRN*^{-/-} genotype and made no detectable *GRN* mRNA (137). Before we characterized differences between the *GRN*^{-/-} and *GRN*^{+/+} HeLa cells, we used immunoblotting (goat anti-hPGRN; R&D #AF2420) to confirm that the PGRN protein expression was ablated (**Fig 3.1A**).

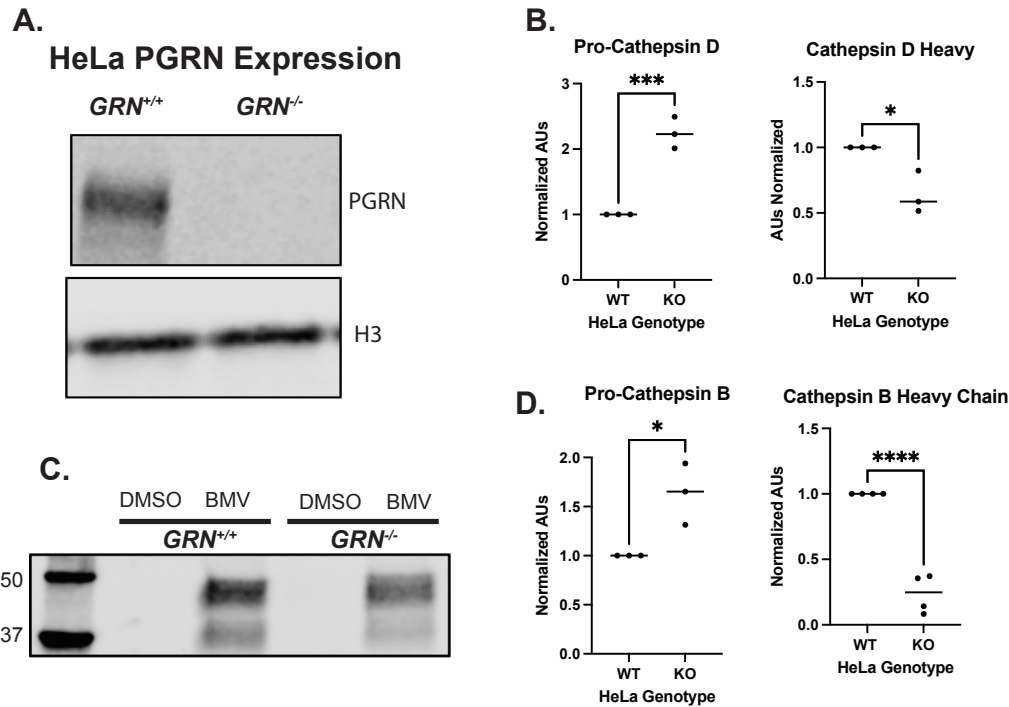


Figure 3.1: Cathepsin Processing and cysteine cathepsin activity are dysregulated in GRN^{-/-} HeLa cells.

- A) Immunoblot of GRN^{+/+} and GRN^{-/-} HeLa cell RIPA lysates. Acetylated histone protein 3 as a loading control.
- B) Cathepsin D protein levels from HeLa lysates. Bands detected by immunoblot were quantified individually, 50kDa precursor band and the 35kDa heavy cleaved unit of the processed protein. Totals were normalized to H3 levels and GRN^{-/-} is reported as a ratio to the GRN^{+/+} passaged matched replicates. Student's T Test * $p < 0.05$, ** $p < 0.01$, *** $p < 0.001$, **** $p < 0.0001$.
- C) Cysteine cathepsin activity measured by BMV-109. Signal Quantified by immunoblot normalized to H3 and reported as a ratio to the DMSO control. Student's T Test * $p < 0.05$, ** $p < 0.01$, *** $p < 0.001$, **** $p < 0.0001$.
- D) Cathepsin B protein levels from HeLa lysates. Bands detected by immunoblot were quantified individually, 50kDa precursor band and the 35kDa heavy cleaved unit of the processed protein. Totals were normalized to H3 levels and GRN^{-/-} is reported as a ratio to the GRN^{+/+} passaged matched replicates. Student's T Test * $p < 0.05$, ** $p < 0.01$, *** $p < 0.001$, **** $p < 0.0001$.

3.3 Characterizing Levels of lysosomal Proteins in GRN^{-/-} HeLas

Previous work characterizing cell models of PGRN deficiency, such as MEFs, found increased levels of lysosomal genes particularly those targeted by TFEB like cathepsin D and cathepsin Z (394). Further HeLa cells that have had PGRN transiently downregulated also show an increase in levels of cathepsin (249). Importantly increases in these proteins are seen in both murine and human derived PGRN deficiency models (227, 229) and in human FTD-GRN patient

derived iPSCs (19), suggesting that the mechanisms underlying increases in these proteins are conserved across models.

We first assessed whether the loss of PGRN lead to an increase in lysosomal cathepsins in HeLa cells. We found that aspartyl protease Cathepsin D and serine protease Cathepsin B were both dysregulated by the loss of PGRN (**Fig 3.1B,D**). Cathepsins are synthesized as inactive (immature) pro-cathepsins and are proteolytically processed to form active (mature) cathepsins by the cleavage of an N-terminal signaling peptide (395, 396). Studies have shown that when autophagy is impaired the immature form of lysosomal cathepsins accumulate (397). when assessing the levels of mature and processed protein, we detected an accumulation of the immature form of the proteases and a significant decrease in the level of the mature lower molecular weight protein (**Fig. 3.1B,D**). This suggests that the processing of both CatD and CatB are defective in *GRN*^{-/-} HeLa cells. Because the dysregulation of CatB and CatD has been associated with dysregulated levels of serine protease Cathepsin L, we sought out to assess levels of Cathepsin L in *GRN*^{-/-} and *GRN*^{+/+} HeLa cells. Unlike the previous cathepsins we were unable to detect differences in Cathepsin L levels. This is an interesting finding as CatL has been identified as an enzyme that cleaves full length PGRN in GRNs (26).

The processing of Cathepsin D to it mature form is dependent of Cathepsin B and Cathepsin L activity (398), and the inhibition of CatB and CatL leads to an accumulation of immature serine and aspartyl cathepsins (397), including Cathepsin D (398). Further the loss of CatD activity has been shown to result in the accumulation of Cathepsin B and Cathepsin L (399). Therefore, it is possible that the loss of cathepsin activity is the cause of the increased abundance of the observed cathepsin proteases.

3.4 Activity of Cysteine Cathepsins are dysregulated in *GRN*^{-/-} HeLa cells

Cathepsins are the most abundant lysosomal proteases, and therefore, are responsible for a majority of the degradation that takes place in the compartment (400). While alterations in the activity and abundance of lysosomal cathepsins have been observed as part of the normal aging process (401), there is evidence of dysregulation of lysosomal cathepsins in several neurodegenerative diseases (401-403). Loss of PGRN down regulates activity of cathepsin hydrolases in several models (19, 228, 404). While we identified cathepsin abundance as a feature of *GRN*^{-/-} HeLa cells, we next aimed to determine whether the activity of the lysosomal cathepsins possibly underlying the differences in cathepsin processing.

There are 15 known cathepsins and they are classified based on their catabolic mechanism into serine, cysteine, and aspartyl (or aspartic) cathepsins (405). There are several ways that cathepsin activity can be detected generally along the lines of the catabolic mechanism. This includes substrate-based assays as well as activity-based probes (ABP) (406, 407). activity-based probes are small molecule reporters of enzymatic activity that are designed to covalently and irreversibly attach to the active-site of the target enzyme in a mechanism dependent manner (407). BMV-109 is an ABP that detects that activity of cysteine cathepsins like CatB. BMV-109 belongs to a subset of ABPs known as qABPs, which are constitutively fluorescently quenched, but upon binding to an active cathepsin the mechanism removes the quencher group resulting in a detectable fluorescent signal which can be detected by cell imaging, or immunoblot (408). Importantly BMV-109 signal has been shown to be decreased in *Grn*^{-/-} mouse microglia (404).

We conducted immunoblotting to detect BMV-109 fluorescent signal and found a reduction in fluorescent signal in the *GRN*^{-/-} cells compared to the *GRN*^{+/+} cells (**Fig 3.1C**). This suggests that the overall activity of cysteine cathepsins is reduced by the loss of PGRN compared to *GRN*^{+/+}. Though this activity cannot be attributed directly to CatB, it does indicate that the

dysregulation of cathepsin abundance is concomitant with a disruption in protease activity. It is also possible that other cysteine cathepsins such as CatL which were not significantly different in abundance could have altered levels of activity as indicated by a reduced BMV-109 signal. Importantly, this result does not reflect on the activity level of CatD which is an aspartyl protease, for which an activity-based probe is not available at this time. Overall, this evidence further suggests that the lysosomal activity of *GRN*^{-/-} is dysfunctional, and it is a plausible mechanism underlying the dysregulation in cathepsin processing observed in this cell line.

3.5 Levels of LMP proteins and Lysosomal Membrane Integrity

The activity of the lysosome is determined by the levels of two classes of proteins, first lysosomal hydrolases, which we found to be dysregulated, and lysosomal membrane proteins (LMPs). LMPs are highly glycosylated proteins that are part of the barrier between the lysosomal lumen and the cytosol (409). As such they fulfill organizational tasks between the lysosome and the cytosol, such as lysosomal acidification, fusion of lysosomes with endosomes, phagosomes or the plasma membrane, and transportation of degradation products (410). Underscoring their importance in lysosomal function, the loss of LMP proteins leads to several lysosomal storage disorders including NCL subtypes CLN3 and CLN7 (411, 412). In addition to loss of LMP proteins leading to LSD, increases in LMP proteins have been implicated as a biomarker for poor cancer and COPD outcomes (413, 414). As dysregulation of LMPs is a marker of lysosomal dysfunction, we set out to determine whether LMPs were affected in *GRN*^{-/-} HeLa cells.

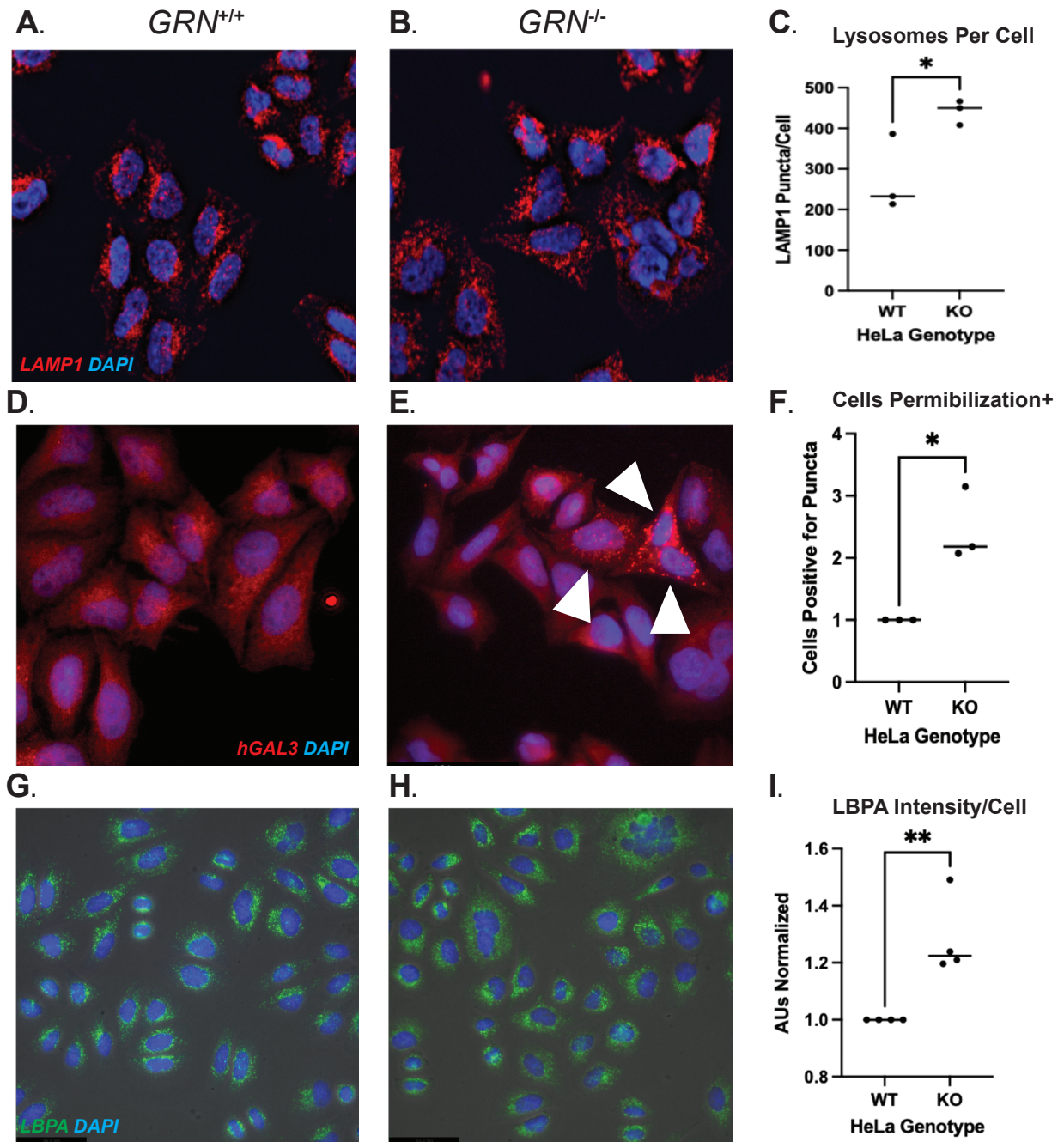


Figure 3.2: Lysosomal membranes shows signs of damage and dysregulated protein composition after the loss of PGRN

A-B) Representative images of HeLa cells probed for LAMP1 and counterstained with DAPI.

C) Quantification of LAMP1 signal / cell. Cell area and puncta identified and overlaid in CellProfiler (4). Statistical comparison Student's T Test.

D-E) Representative images of HeLa cells probed for hGAL3 counterstained with DAPI.

F) Quantification of cells with punctate hGAL3 signal assessed over 3 replicated passages of cells. Student's T-test

G-H) Representative images of HeLa cells stained for LBPA and counterstained with DAPI.

I) Quantification of intensity of LBPA signal/cell quantified using CellProfiler. Signal is reported as a ratio calculated between matched passages.

LAMP-1 and LAMP-2 are the two most abundant LMPs representing about 50% of all

proteins on lysosomes and late endosomes (415). LAMP proteins are involved in chaperone mediated autophagy, class II antigen degradation (416), and lysosomal exocytosis (417). *GRN*^{-/-} HeLa cells display an increased amount of LAMP1 positive vesicles per cell in comparison to *GRN*^{+/+} (**Fig 3.2A-C**), suggesting that there is an upregulation in lysosomal membrane abundance, and potentially, biogenesis that could account for the upregulation of LAMP1. In addition to LAMP1 we find that there is an increase in the level of LBPA a component of endo-lysosomes is also increased in *GRN*^{-/-} cells, extending the dysregulation more generally to the endo-lysosomal pathway. The upregulation of lysosomal biogenesis takes place in response to nutrient imbalance, lysosomal stress, pathogen infections, ER stress, and exercise to regulate organismal homeostasis (250, 418). It has also been shown that endosome-lysosome repair mechanisms are upregulated before lysophagy in a response to lysosomal dysfunction and damage (419). This could lead to an increase in LMPs including LAMP1 and LBPA.

To determine whether the lysosomal membranes of *GRN*^{-/-} HeLa displayed signs of damage we used Galectin-3 as a marker of lysosomal membrane permeability. Although we did not see an overall change in the levels of Galectin-3 proteins (**Fig 3.2D-E**) lysosomal damage leads to a translocation of Galectin-3 from a diffuse cytosolic distribution to a concentration localization at the lysosomal membrane (331, 332). Therefore, while the overall level of Galectin-3 may stay similar, the localization may vary and signal dysfunction. Using ICC *GRN*^{-/-} and *GRN*^{+/+} were stained for galectin-3. We found that *GRN*^{-/-} cells had increased numbers of positive puncta per cell compared to *GRN*^{+/+} cells (**Fig 3.2F**). Of note, this assay was carried out under endogenous cell culture conditions. This contrasts with other protocols that recommend inducing lysosomal membrane damage using reagents such as LLOMe (331). Taken together these data suggest that

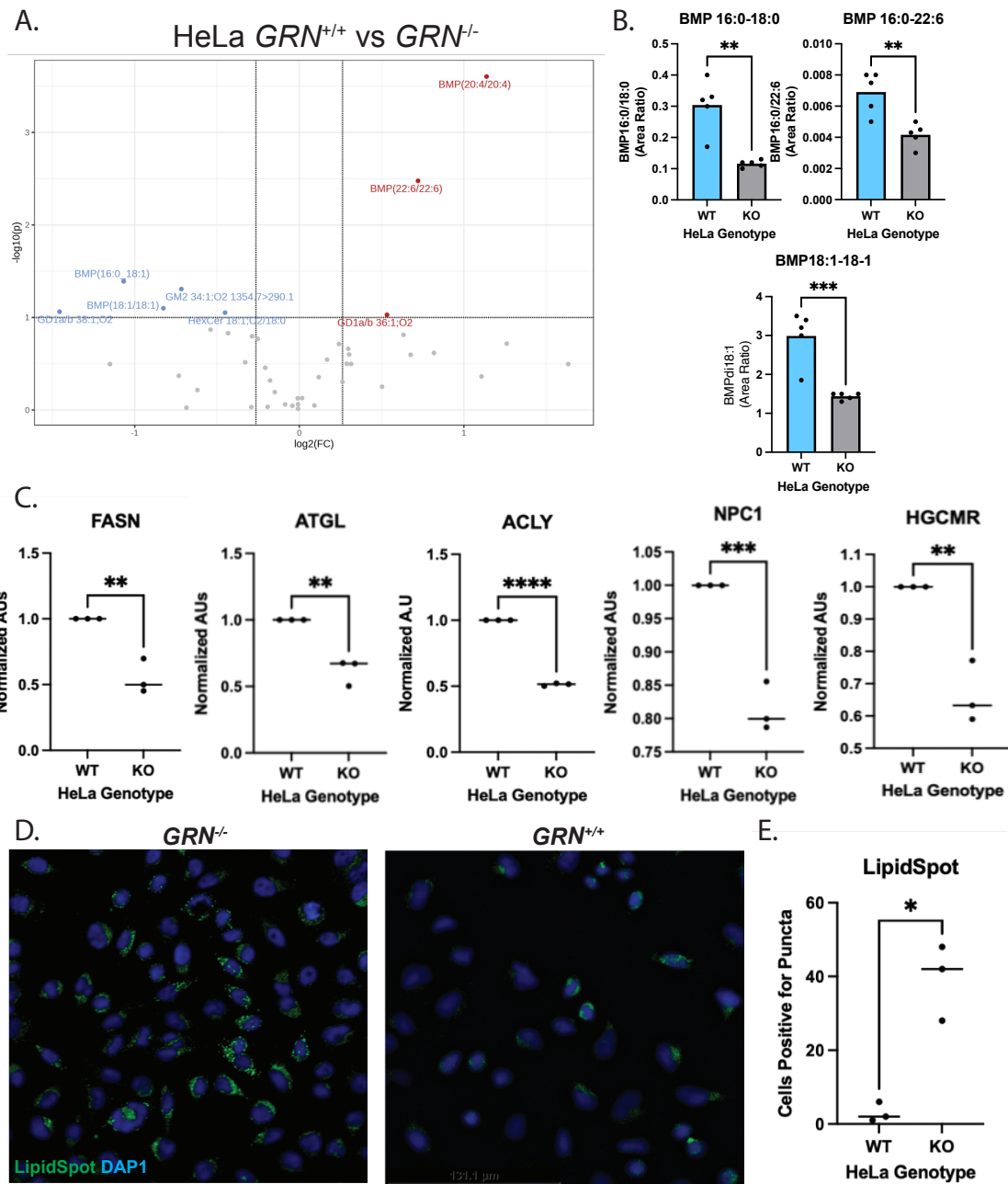


Figure 3.3: $GRN^{-/-}$ HeLa cells display dysregulated lipid phenotypes that recapitulate other models of PGRN deficiency

- Volcano plot comparing the abundance of 48 lipid species between $GRN^{-/-}$ and $GRN^{+/+}$ HeLa cells.
- T-tests assessing the levels of specific BMP levels detected as differentially abundant in the volcano plot.
- Assessments of protein levels of enzymes involved in lipid synthesis between $GRN^{-/-}$ and $GRN^{+/+}$ cells. Significance determined by Student's T-test.
- Representative images of LipidSpot signal from HeLa cells
- Quantification of cells positive for lipid spot signal in a single image field from 3 replicate passages. Assessed with Student's T-Test.

the lysosomal membranes in $GRN^{-/-}$ are dysregulated and damaged. The change in lysosomal

membrane composition could have far reaching effects as LMPs are crucial for the organization and signaling of the lysosome.

3.6 Lipid Dysregulation is a characteristic of *GRN*^{-/-} HeLa cells

The lysosome is a key regulator of cellular metabolism and are involved in both nutrient sensing, lipid degradation, and lipid trafficking within the cell (239, 420). Loss of hydrolytic or lysosomal transport ability due to impairment of lysosomal hydrolases and LMPs causes the accumulation of macromolecules within the lysosome including lipid species (421). Macromolecule accumulation is well documented in LSDs, in fact, these disorders can be further classified by the predominant macromolecule that accumulates (377). As lysosomal dysfunction deteriorates, material can be seen accumulating in CNL patient tissues in the form of the storage material known as lipofuscin (219). Increased Lipofuscinosis is a hallmark of both NCL11 and FTD-*GRN* (344), and altered lipid levels a more recently become an appreciated phenotype in PGRN deficiency (224). Particularly, increases in sphingolipids, gangliosides, and triglycerides, and decreases in bis(monoacylglycero) phosphate (BMP) (21, 238, 242).

First lipidomic analysis was conducted using both *GRN*^{-/-} and *GRN*^{+/+} cells to detect 48 species including BMPs, TAGs/DAGs, and gangliosides based on phenotypes previously reported. This assessment detected a dysregulation of BMP species in particular (**Fig 3.3 A,B**). Interestingly when assessing individual species, we find that there are species that are both increased and decreased by the loss of PGRN (**Fig 3.3A**). This differs from previous findings which report decreases in BMP species (238, 242). However, this may align with our previous observation that LBPA, another name for the family of BMP species was increased in *GRN*^{-/-} cells (**Fig 3.2G-I**). Reconciling these findings, the LBPA levels were assessed using a pan-BMP antibody, while lipidomic mass spectrometry allows for more precise identification and quantification of specific species. It is possible that while all BMP species are collectively upregulated, while key BMP

species are down-regulated, this has been previously observed in a fibroblast models of LSDs where overall levels of BMP were not statistically different than controls, but polyunsaturated BMP 22:6/22:6 was decreased (422).

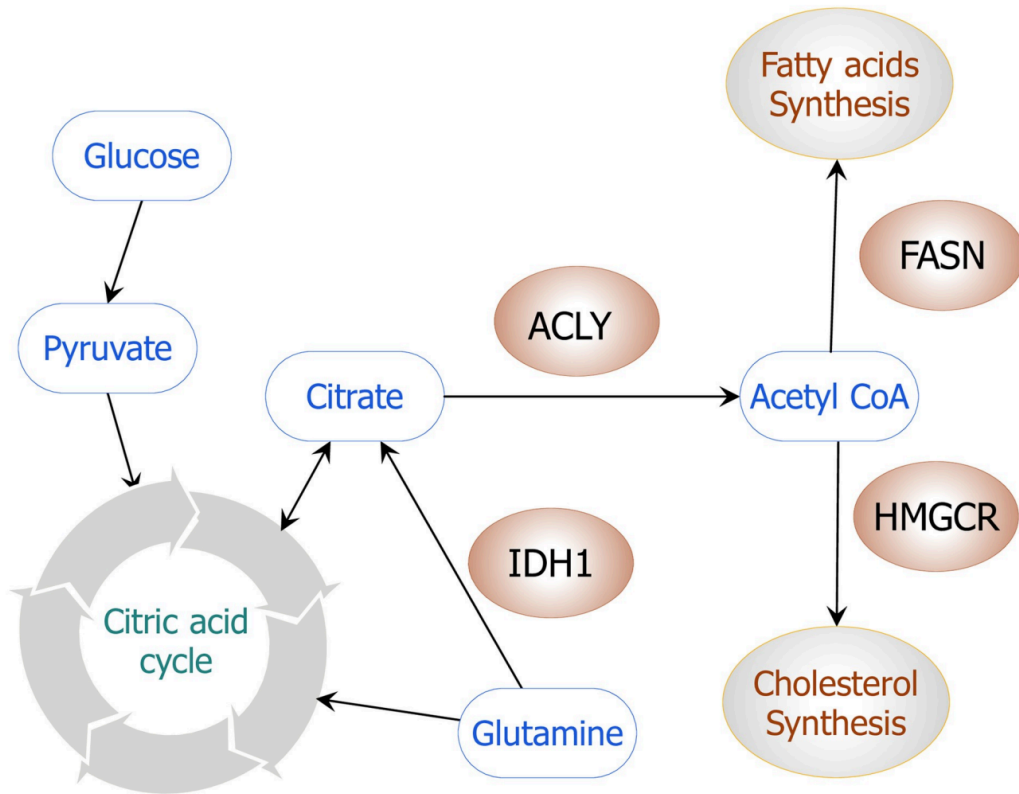


Figure 3.4: Neutral Lipid Synthesis Pathways

A) Diagram from Ghimire et al. 2021 (1) highlighting the connections of proteins ACLY, HMGCR, FASN.

To further explore phenotypes of lipid dysregulation we used the cell dye LipidSpot which labels lipid droplets containing neutral lipid species within the cell. Lipid droplets are ubiquitous membrane-less organelles that participate in fat storage and interact with lysosomes during the process of lipid regulation (423, 424). They store neutral lipids including cholesteryl esters (CE), and fatty acids like triacylglycerols (TAGs) and diacylglycerols (DAGs) (425). Dysregulation of lipid droplets has been characterized as part of the aging process, and during neurodegeneration

(426). PGRN has been identified as a genetic regulator of lipid droplet formation and lipid droplets are enriched in microglia from *Grn*^{-/-} mice (245). We find that *GRN*^{-/-} HeLa cells have increased lipid droplet counts compared to *GRN*^{+/+} cells, which do not display appreciable levels of LipidSpot signal endogenously (**Fig 3.3 D,E**). This indicates that lipid metabolism in these cells is altered, and the storage of neutral lipid species has increased.

In addition to the observation of upregulated lipid droplets, we also assessed the protein level of several enzymes involved in neutral lipid synthesis. We found decreases in enzymes involved in both cholesterol metabolism (NPC1, HGCMR) and fatty acid synthesis (FASN, ATGL) (**Fig 3.3C**). ATP citrate lyase (ACLY) produces acetyl-Co-A and lies upstream of both the FASN driven fatty acid synthesis and HGCMR driven cholesterol synthesis pathways (**Fig 3.4**). They are regulated by the sterol regulatory element binding protein SREBP1 which is activated when cholesterol is scarce (427). Therefore, it is possible that these hydrolysis pathways are downregulation in response to the accumulation of neutral lipids observed in *GRN*^{-/-} HeLa cells.

These proteins individually have been found to be implicated in LSDs and neurodegenerative conditions. ACLY is implicated in many cellular processes but decreases have been associated with lipid accumulation in both cancers, and CLN3 (428, 429). Downstream of ACLY FASN and ATGL which are involved in fatty acid synthesis and regulation (430). In particular, adipose triglyceride lipase (ATGL) is the rate-limiting enzyme for LD-associated TAG hydrolysis, and activation of ATGL is the first step of lipolysis which is a key mechanism required for effective phagocytosis (431). Another pathway downstream of ACLY is *de novo* cholesterol synthesis including HGCMR and NPC1. Interestingly, mutations in NPC1 cause a neurodegenerative lysosomal storage disorder Niemann-Pick type C disease (432). The encoded protein is involved in cholesterol recycling from late endosomes and lysosomes (433), and

interference in this pathway causes the accumulation of both cholesterol and other lipid species (434). Interestingly lipidomic analysis of MEF cells found up regulation of cholesterol and TAGs in *Grn*^{-/-} cells and an accumulation of TAGs in *Grn*^{-/-} mouse brains (21).

Across our methods of assessment *GRN*^{-/-} HeLa cells recapitulate findings from other models of PGRN deficiency characterized by a loss of BMP and an accumulation of fatty acid proteins. Taken together these data show that *GRN*^{-/-} HeLa cells have dysregulated lipid phenotypes possibly as a consequence of altered lysosomal function.

3.7 Discussion

Establishing tractable *in vitro* models for the use of understanding basic mechanisms underlying the development of neurodegenerative diseases has led to advancements in understanding relevant pathways and the development of novel treatments. Immortalized cells have the practical benefit of being fast growing, robustly replicating, genetically homogenous models that can be easily cultured and modified using techniques like CRISPR Cas-9. Two of the most commonly used immortalized human cell lines are HeLa cells and HEK 293 cells. Unfortunately, HEK cells contain several duplications of chromosome 17, and thus are challenging to genetically target the PGRN gene which lies on this chromosome. Therefore, it is advantageous that a *GRN*^{-/-} HeLa cell line has been previously produced by the lab of Dr. Ferguson, however, phenotypic characterization of these cells has never been widely reported. The aim of this study was to assess phenotypes observed in other models of *GRN* deficiency to evaluate the impact of the loss of PGRN on HeLa cells. We report that the loss of PGRN leads to dysregulated levels of lysosomal proteases, both in protein abundance and activity level, as well as lipid accumulation and perturbation of the biosynthetic pathways of neutral lipids. These findings are in concordance with the observations for both human patients, murine models, and other *in vitro* studies, and suggests that the basic pathways disturbed by the loss of PGRN in human patients could be studied

in HeLa cells. Further, by thoroughly characterizing the impact of the loss of PGRN these identified phenotypes can be used as markers for amelioration in future intervention studies.

The concomitant dysregulation of proteins in the lipid biosynthesis pathway with the accumulation of the associated lipids is a previously unreported finding. It is possible that the downregulation of these proteins is an adaptive response by the cell in a cholesterol rich environment. The accumulation of neutral lipids, measured by lipid droplets, possibly includes cholesterol species. This is particularly interesting in combination with the downregulation of BMP. BMP is known to be an important factor in sorting cholesterol in cellular membranes (435), and the efflux of cholesterol out of internal membranes (436). If BMP levels are decreased, this could impact these sorting and collection functions, leading to an accumulation of cholesterol in the lysosome. This is the proposed mechanism in a model of NPC1 (422).

While it is possible that the downregulation of ACLY is a consequence of increased lipid droplet accumulation. ACLY is important for the synthesis and bioavailability of acetyl-Co-A a molecule that plays an important role in many aspects of cellular metabolism and nucleic acid regulation including synthesis of fatty acids and cholesterol (437) acetylation of proteins including histones (438). Acetyl-CoA is also a precursor for the neurotransmitter acetylcholine, and dysregulation in this pathway is implicated in death of cholinergic neurons and neurodegenerative diseases (439). This could suggest that lipid dysregulation is just one aspect of further metabolic disruption caused by the loss of PGRN. To elucidate this direct measurement of acetyl-CoA should be performed.

Lipid droplets, which accumulate in *GRN*^{-/-} HeLa cells, are themselves bioactive organelles within the cell. The increased flux of lipid droplets could have regulatory effects in lipid signaling (440), membrane composition (441), and energy substrates (426, 442), possibly further impacting

cellular metabolism and function. Future studies should explore other markers of metabolic health including mitochondrial function. In *Grn*^{-/-} mice, particularly in microglia the accumulation of lipid droplets is associated with differential cytokine release and transcriptomic changes in ROS production and lysosomes related genes (245). While this data does suggest that the loss of PGRN leads to lysosomal dysfunction, and subsequent accumulation of lipid droplets, the mechanism is unclear. As the brain is the second most lipid rich organ in the body (443), further understanding how dysregulated lipid synthesis pathways and differential lipidomes are present will shed light on to the etiology of PGRN deficiency disorders and their impact on the brain.

GRN^{-/-} cells present with disease relevant phenotypes that can serve as appropriate read outs for evaluating potential disease modifying modifications. We have recently shown that individual GRNs have the ability to rescue signs of dysfunction caused by the loss of PGRN in *Grn*^{-/-} mice (237). However, the mechanism through which GRNs confer their protective effect in the absence of PGRN was directly investigable within the design on the *in vivo* experiment. These characterized HeLa cells can be used to either over express GRNs via transfection, stably express GRNs via transduction, or treated with purified recombinant GRNs. These approaches will not only provide insight into the biology of GRNs, but can also be utilized to test additional GRN based therapies not included in our initial study (237).

While we find that this cell line is a good candidate model system for understanding the impact of PGRN loss of lipid dysregulation and lysosomal dysfunction, it is important to acknowledge that working with HeLa cells requires ethical consideration as to the history of the line. The progenitors of modern HeLa cells were collected at John's Hopkins from cervical cancer patient Henrietta Lacks in 1951 a working-class African-American woman living near Baltimore. The cells were collected without her or her family's knowledge or consent, and unfortunately

Lacks died shortly after the cells were collected at the age of 31 (444). Johns Hopkins was the one of Henrietta's only options for treatment, as it was one of the few institutions that would accept African-American patients. Though the university has been clear in asserting that the doctor, George Gey, who collected the cells nor the university have ever directly benefited financially from the cell line, we must consider the tenant of informed consent were breached in this case (445). Henrietta's identity was revealed in the 1970s after the discovery of widespread contamination of other cell lines lead researchers to contact Henrietta's family members for DNA samples to act as controls (446). Although HeLa cells are still available for purchase from cell repositories, neither Henrietta nor the Lack family has never been compensated for the resource even in the years since their identity was revealed.

This cell line was the first to be successfully cultured, and has been critical for the discovery of many biological advancements of this century and the last including the development of the polio vaccine, *in vitro* fertilization (447), and recently in the fight against COVID-19 (448). Many people have inarguably benefitted from discoveries made using HeLa cells and HeLa cells continue to be used in research programs today. While some groups have advocated for the removal of HeLa cells from biological research, members of Henrietta's family have expressed they wish for the cells to be continued to aid the discovery of medical technology, and most importantly for the contribution of their mother, cousin, and grandmother, to be acknowledged and appreciated (444). Therefore, all researchers utilizing HeLa cells need to share the story of Henrietta Lacks. These cells will continue to be an important tool for understanding the biology of the human body, however, the unethical circumstances of their origin must be reiterated in any literature using them.

Overall, these HeLa cells display robust and reproducible phenotypes that are relevant to other models of PGRN deficiency. These cells will be a good platform to further investigate the biochemical role of GRNs. HeLa cells are very amenable to transfection, transduction, and exogenous recombinant protein application all of which are approaches that can be targeted to study each individual GRN in isolation. Findings will help to complement ongoing *in vivo* work in deepening our understanding of the role of GRNs and PGRN in the lysosome.

3.8 Methods

Cell Culture

HeLa *GRN*^{-/-} cells were a gift from Dr. Shawn Ferguson (Yale) and generated using CRISPR as described.(137) HeLa wild-type or *GRN*^{-/-} cells were cultured in DMEM medium plus 10% fetal bovine serum (FBS) and 1% Pen/Strep and maintained at 37 °C with 5% CO₂. 24 hours before collection DMEM media was replaced with OptiMEM media (Gibco).

HeLa Lysis and Media Collection

Cells were suspended in MES buffer (50mM MES pH6.5, 1% Triton, 150mM NaCl, 1XHALT PPI) 5uL for every 1mg cell pellet. Cells were then lysed on ice for 10 mins briefly vortexing every 3 minutes. Lysates were then spun at 600xg for 10 minutes and supernatant was collected. Conditioned media was collected from culture dish and spun at 500xg for 10 minutes to remove any cell debris.

Immunoblot

SDS/PAGE and immunoblotting of HeLa cell lysates were performed as described.(25, 359, 360) Mouse brain running samples were prepared for immunoblot in 1X Laemmli loading

buffer with 20 mM tris(2-carboxyethyl)phosphine (TCEP)) followed by denaturation at 70 degrees C for 15 minutes. For immunoblotting, protein samples were first separated on Bio-Rad TGX 4-20% 26-well gels at 100 V and transferred to a 0.2-micron nitrocellulose membrane using the Bio-Rad Trans-blot Turbo system. BulletBlock (Nacalai) for 30 minutes at room temperature membranes were incubated overnight at 4C with primary antibodies (STAR MATERIALS). Membranes were probed with anti-Histone H3 or anti-Beta tubulin antibodies and imaged on the Odyssey Fc (LI-COR), to normalize protein abundance between samples.

BMV-109 Assay

Cells from both genotypes were plated in 6 well dishes 300,000 cells/well. After 24 hours 1mL of cell media was removed and 2mM BMV (calculated for total culture volume of 1.8mL) was suspended in 1mL conditioned media. An equal volume of DMSO was added to controls. Cells were incubated for 2 hours after which media was aspirated and cells were washed 2X with PBS. Cells were scraped and spun @500xg before being lysed with BMV buffer (50mM Citrate buffer pH 5.5, 25mM CHAPS, 0.1% Triton) added mL * 5X weight of the collected pellet. Cells were lysed at RT for 2 mins, on ice for 10 mins, then pipette with a p200 20 times. Lysate was spun in the rotar bucket 600xg for 10 mins. Lysate protein was then used in immunoblot procedures as previously described. Blot was imaged after transfer without blocking.

Immunofluorescent Staining

Add an acid-washed, sterile glass cover slip to each well of 6-well dish then coated with polylysine solution 0.01% 5 minutes at RT. Coverslips were then washed with PBS X2, after which fresh media was added. HeLa cells at a seeding density of $\sim 2.5 \times 10^5$ cells/ml in 2 ml of growth

medium in six-well dishes containing poly-lysine-treated glass cover slips. Cells were about 80% at 24 hours.

Media was removed and washed with PBS. 4% paraformaldehyde/PBS was added and incubate 20 minutes at 4 C (place dish in refrigerator). Afterwards PFA was removed and fixative and gently wash cells 2 times with 2 ml PBS. After fixation cells can be stored at 4C or proceed to immo-detection

Cells were Blocked with ICC Buffer (10% FBS+.05% Saponin in PBS) at RT for 30 min. Cells were then Incubated with the antibody against target of interest (see materials table) in ICC blocking buffer at RT for 2 h. Afterward, coverslips were washed the cells at least three times with PBS for 10 mins. Next coverslips were incubated for 30 min with the fluorophore conjugated secondary antibodies in ICC buffer. After washing 3X with PBS for 10 mins coverslips were mounted to slides using DAPI Prolong Gold (Invitrogen) and dried overnight before imaging.

LipidSpot Assay

Cells were added to glass coverslips in 24 well dishes 50,000 cells/ well. When cells reached 70-80% confluence coverslips were permeabilized with 4% PFA for 20 mins at 4C and rinsed 2X with PBS from storage in fridge. LipidSpot488 (Biotium) was made up fresh and diluted 1:1000 in PBS. LipidSpot treatment was applied to cells at RT and incubated not rocking for 30 mins. LipidSpot was then removed and coverslips briefly wash with PBS x2. Coverslips were mounted with Abcam mounting media with Fluoroshield. (abcam) and dried for 3 hours before imaging. Slides were imaged as soon as possible as signal deteriorates after 24 hours.

Puncta Quantification

Puncta detected in immunofluorescent staining of LAMP1 and LBPA staining analyzed using an automated pipeline created using CellProfiler (www.cellprofiler.org)(4) for quantification.

Sample preparation for lipidomics and metabolomics analyses.

HeLa cells were collected at 80% confluency and pelleted at 600xg. 30 mg of pellet was collected and frozen to be used to extract lipids. Methanol spiked with internal standards was added to each sample and homogenized with FastPrep-24™ 5G bead beating grinder and lysis system using Lysing Matrix D tubes with CoolPrep™ adapter (MP Biomedicals) for 40 seconds at a speed of 6 m/s. The methanol fraction was then isolated via centrifugation (20 minutes at 4°C, 14,000 x g), followed by transfer of supernatant to a 96 well plate. After a 1 h incubation at 20°C followed by an additional centrifugation (20 minutes, 4,000 x g at 4°C), methanol was transferred to glass vials for LCMS analysis.

3.9 Lipidomics analysis.

Lipid analyses were performed by liquid chromatography on an ExionLC (Sciex) coupled with electrospray mass spectrometry TripleQuad 7500 (Sciex). For each analysis, 1 µL of the sample was injected on a Premier BEH C18 1.7 µm, 2.1×100 mm column (Waters) using a flow rate of 0.25 mL/min at 55°C. For positive ionization mode, mobile phase A consisted of 60/40 (vol/vol) acetonitrile/water with 10 mM ammonium formate + 0.1% formic acid; mobile phase B consisted of 90/10 (vol/vol) isopropyl alcohol/acetonitrile with 10 mM ammonium formate + 0.1% formic acid. For negative ionization mode, mobile phase A consisted of 60/40 (vol/vol) acetonitrile/water with 10 mM ammonium acetate; mobile phase B consisted of 90/10 (vol/vol) isopropyl alcohol/acetonitrile with 10 mM ammonium acetate. The gradient was programmed as follows:

0.0-8.0 min from 45% B to 99% B, 8.0-9.0 min at 99% B, 9.0-9.1 min to 45% B, and 9.1-10.0 min at 45% B. Electrospray ionization was performed in positive or negative ion mode. We applied the following settings: curtain gas at 40 psi (negative mode) and curtain gas at 40 psi (positive mode); collision gas was set at 9; ion spray voltage at 2000 V (positive mode) or -2000 V (negative mode); temperature at 250°C (positive mode) or 450°C (negative mode); ion source Gas 1 at 40 psi; ion source Gas 2 at 70 psi; entrance potential at 10 V (positive mode) or -10 V (negative mode); and collision cell exit potential at 15 V (positive mode) or -15 V (negative mode). Data acquisition was performed in multiple reaction monitoring mode (MRM) with the collision energy (CE) values reported in **Supplementary Tables 2.1 and 2.2**. Area ratios of endogenous lipids and surrogate internal standards were quantified using SCIEX OS 3.1 (Sciex).

4 Discussion and Future Directions

4.1 Summary of Findings:

As reviewed in Chapter 1, loss of the secreted glycoprotein PGRN causes FTD and CLN11. Both diseases are characterized by lysosomal dysfunction, the accumulation of lipofuscin, and cognitive decline (315, 344). These clinical presentations have led to the identification of PGRN as a protein important for lysosomal function, however, how the loss of PGRN leads to dysfunction, and cell death remains unclear. Work by the Kukar lab and others, has shown that PGRN is trafficked to the lysosome where it is processed into its 7.5 constitutive GRN subunits. Like PGRN, GRNs are decreased in *GRN*-FTD patient brains. However, it was unclear whether the loss of PGRN or GRNs lead to lysosomal dysfunction. In the work described here, I aimed to investigate whether GRNs confer the homeostatic role of PGRN in the lysosome. In this final chapter I briefly summarize the findings presented in chapters 2 and 3. I propose how these findings build upon the existing body of literature to inform a new working model for the role of GRNs in the lysosome. Finally, I identify future directions relevant for the continuation and expansion of our understanding of the biological role of GRNs in homeostasis and disease.

4.2 Shared phenotypes between models:

The work presented here compares phenotypes of *in vitro* and *in vivo* models of PGRN deficiency. In *Grn*^{-/-} mice we characterized novel datasets of thalamic proteomics, cortical lipidomics, and biochemical assessment throughout the brains of 12-month old mice injected with either negative control GFP, positive control PGRN, GRN2, or GRN4. We found that at 12 months of age *Grn*^{-/-} mice exhibit dysregulated lysosomal protein levels, increased lipofuscin, and the accumulation of lipid species including glucosylsphingosines, and gangliosides. We also found that *Grn*^{-/-} mice have increased microglial activation and upregulation of neuroinflammatory

markers. Finally, we find that levels of the atypical phospholipid, BMP, are decreased. These phenotypes could all be driven by lysosomal dysfunction and are often observed in models of lysosomal storage diseases, as well as other neurodegenerative diseases known to involve impaired lysosomal function.

In chapter 3 we also observe an increase in lysosomal proteases, particularly the precursor forms of cathepsins in *GRN*^{-/-} HeLa cells. Further, we see the accumulation of lipid species, in this model the detected species were neutral lipids in lipid droplets. Finally, similar to *Grn*^{-/-} mice we see a decrease in BMP levels after the loss of PGRN in HeLa cells. Identifying phenotypes across different models including dysregulation in lysosomal proteases, accumulation of several lipids, accompanied by the downregulation of BMP in *GRN*^{-/-} HeLa cells and *Grn*^{-/-} mice indicate that these may be conserved functions of GRNs and PGRN. These similarities not only provide insight into the biological role of the proteins but confirm that *GRN*^{-/-} HeLa cells provide an exciting platform to investigate the molecular processes GRNs and PGRN influence in the lysosome.

4.3 GRNs are beneficial proteins in the lysosome

Chapter 2 addresses a longstanding question in the field of PGRN biology, assessing whether the expression of an individual GRN subunit is sufficient to ameliorate disease-like pathology in *Grn*^{-/-} mice. Previous studies had suggested that increases in GRNs were pro-inflammatory and neurotoxic, however, work conducted in our lab produced evidence suggesting that the administration of individual GRNs could be beneficial. I hypothesized that if GRNs are conferring the function of PGRN in the lysosome, then the expression of a single GRN subunit may be able to rescue the phenotypes of dysfunction we identified in our GFP-*Grn*^{-/-} mice.

In this dissertation work I find that *Grn*^{-/-} mice have a disrupted proteome that can be rescued by the expression of in hGRN2 and hGRN4. Multiple lysosomal proteins, including cathepsins, lysosomal transporters, and lysosomal membrane proteins are increased by loss of

PGRN and ameliorated after GRNs are added back. The expression of hGRN2 and hGRN4 are also able decrease markers of neuroinflammation including proteins associated with microglial activation and complement proteins. Importantly, lipofuscin, the lysosomal storage material characteristic of FTD-GRN and NCL11 patients, is also decreased. hGRN4 also reduces disease associated dysregulation in lipids including the accumulation of GlcSph, and gangliosides and the decrease of BMPs.

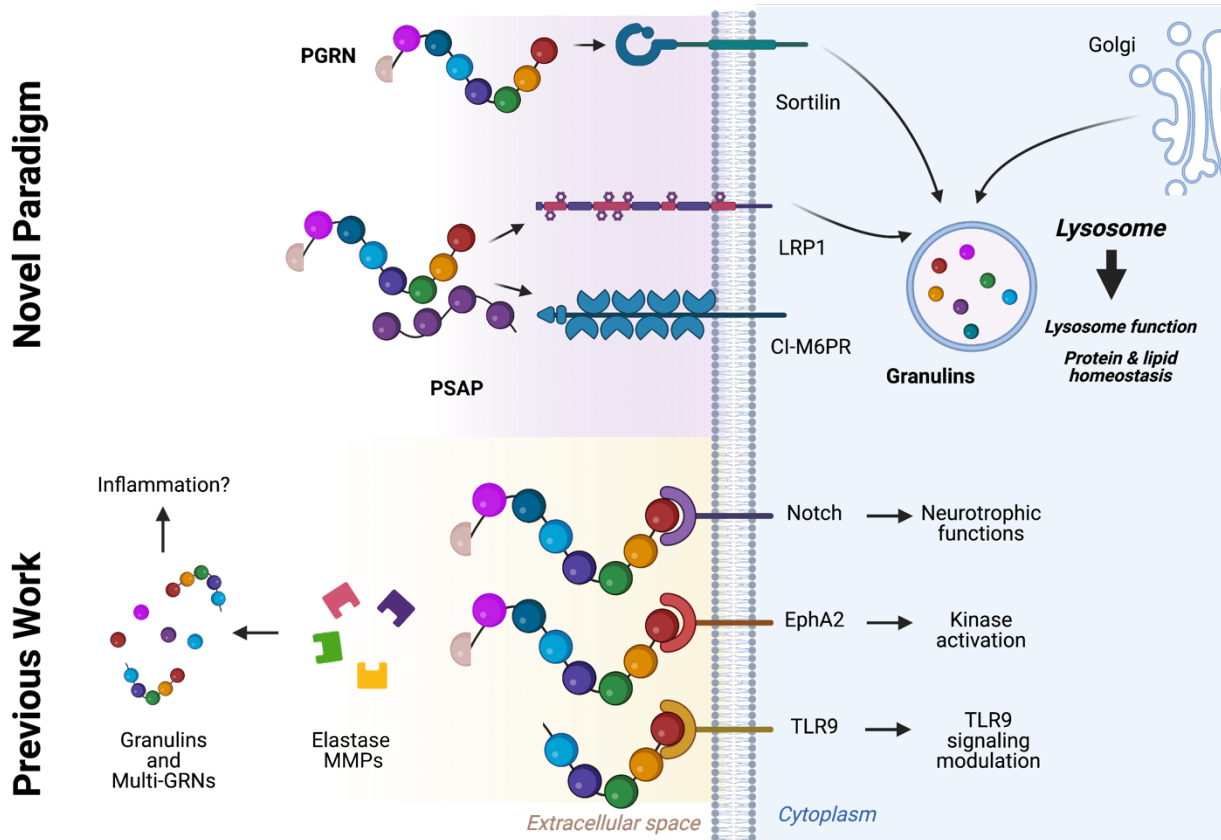
These findings suggest that GRNs are not primarily neurotoxic as previously postulated, and identifies potential functional pathways GRNs may be involved in to maintain a healthy cell. While the precise function of the GRNs in the lysosome remains unknown, the findings presented here suggest that further investigation is necessary and identifies an immortalized cell line as a potential model system. Together they support a paradigm shift in the way we understand the role of PGRN and GRNs in lysosomal function.

4.4 A New Model of GRN Function

These findings shed light on a novel intracellular function for granulins. The molecular mechanisms granulins participate in are not well understood, as granulins are difficult to study individually. Some studies have proposed that individual granulins serve an opposing function to full length progranulin and may be pro-inflammatory, detrimental to survival, and that their expression could lead to an exacerbation of disease-like phenotypes (309, 449, 450). It has also been suggested that increased levels of granulins could contribute to disease etiology (281). If this was the case, we would expect that the increased expression of individual granulins would lead to increased disease-like phenotypes in our *Grn*^{-/-} mice, which we did not observe. Further, when we probed our proteomic data for signs of microglial activation we found that the expression of granulins decrease of multiple markers of microglial activation and disease-associated microglia in a similar degree to full length hPGRN. Lastly, levels of proteins associated with cytokine

signaling were also ameliorated by the expression of granulins including C1qa, C1qc, C1qc, C4b (Appendix 1). This suggests that the expression of granulins in a progranulin deficient mouse is anti-inflammatory and neuroprotective.

Figure 4.1: Granulins are Beneficial and function in the lysosome



In addition, we found that treatment with granulins broadly rescued lysosomal dysfunction and lipofuscin accumulation. The expression of granulins decreased levels of lysosomal hydrolases, markers of lysosomal membrane damage, and reduced the accumulation of the LSD storage material, lipofuscin. Proteomic comparison between hPGRN-*Grn*^{-/-} and hGRN4-*Grn*^{-/-} indicates that there no differentially regulated proteins out of the over 9000 detected (Appendix 2). While there are several differentially regulated proteins when comparing hGRN4 and hPGRN injected mice to hGRN2, these comparisons are more difficult to interpret as the expression level of hGRN2 was much lower than hGRN4 and resulted in less efficient rescue of disease related

phenotypes. Overall, these data coupled with the knowledge that granulins are localized to the lysosome (280) provide preliminary evidence that granulins mediate the activity of PGRN at the site of the lysosome through similar pathways when expressed adequately (Fig 4.1), yet further study is necessary investigate this hypothesis in detail.

This finding is significant for two reasons. Firstly, it suggests that granulin subunits are beneficial *in vivo*, potentially through the same pathways attributed to PGRN. This contrasts with previous theories that granulins may act in an opposing fashion to progranulin (451). It builds up a growing body of literature reporting beneficial roles for granulins including enhancing survival of motor neurons in culture (11), inducing neuronal outgrowth and branching (155), enhancing neuron survival and axon growth (164, 299) and protecting retinal photoreceptor cell degeneration (300) and informs our understanding of how PGRN carries out its cellular functions. Secondly, it is of therapeutic interest, as delivering 7 kDa granulin subunits to the brain may be more feasible than full length PGRN and could also lead to fewer off target effects than replacement, or expression of the entire protein.

4.5 Role of GRNs in Lipid Metabolism:

4.5.1 BMP

The accumulation of lipids is a conserved phenotype across models of PGRN deficiency. This phenotype is a characteristic of lysosomal storage disorders, including NCLs as lipids are a component of lipofuscin, and several of the identified NCL genes are known to play a role in lipid regulation (452). Further, recent studies have drawn links between the primary mechanisms driving lysosomal storage disorders and neurodegeneration as many genes associated with LSDs are known risk factors in neurodegenerative processes. The data discussed in chapter 2 and 3 define that the accumulation of lipids such as glycosylsphingosines, gangliosides, and neutral lipids are accompanied by a decrease in BMP, an atypical phospholipid. These replicated phenotypes

suggest that GRNs may play a role in the regulation of lipid metabolism similar to many other proteins in the NCL and LSD field.

While *in vitro* studies had identified lipid dysregulation as a consequence of PGRN deficiency as early as 2017 (21), recent reports suggest that the concomitant reduction in species of an endo-lysosomal specific lipid species (BMP) were recently reported by several groups (238, 242), and replicated by the work presented in this dissertation. While accumulation of phospholipids is observed in other LSDs, the co-occurrence of decreased BMP is unique. Lysosomal storage diseases are generally characterized by the accumulation of BMPs (422, 453, 454). Although reductions in polyunsaturated species like BMP 22:6 have been previously reported in LSD patient derived fibroblasts (422).

A recent study, Laqtom *et al*, assessed the contents of isolated lysosomes from a model of CLN3 and revealed a similar pattern of phospholipid accumulation and BMP reduction (455) we observed in *Grn*^{-/-} mice. The model proposed in this study asserts that the accumulation of glycerophospholipids including GPG, GPI, GPE, GPC, as well as the intermediate lysosomal species LPGs, leads to a decrease in BMPs. BMP is a structural isomer of phosphatidylglycerol (PG) and it is proposed that BMP is synthesized from PG (456). Therefore, this model asserts that an accumulation of precursor glycerophospholipids leads to a decrease in BMP. Although, these pathways are still an active area of investigation (2, 457). In our dataset, we did not detect overall increases in glycerophospholipids, however, in an independent data set, we did detect an increase in cardiolipins, also known as diphosphatidylglycerol (Appendix 3). Cardiolipins are a product of PG as well indicating that dysregulation in the glycerophospholipids exists in *Grn*^{-/-} mice (458).

Although we did not detect many differences in whole tissue, the previous Laqtom *et al*. study did not detect phospholipid changes at the whole tissue level. However after lysosomal

isolation differences in the accumulation of lyso-phospholipids and glycerophosphodiester were detected (455). Taken together, this data suggests that although we do not observe accumulation of glycerophospholipids at the whole tissue level in *Grn*^{-/-} mice that does not exclude the possibility that a similar mechanism could underlie the accumulation of lipids, and the downregulation of BMP in models of CLN3 and PGRN deficiency. In this proposed model the reduction of various BMPs are a consequence of the accumulation of precursor lipid species in the lysosome and their subsequent unavailability for the synthesis of BMP.

The loss of BMP could have a critical effect on efficient lysosome to function. Lipid composition of the lysosomal membrane is an important factor that modulates the degradation pathways carried out in the lysosome. BMP is of particular interest when considering the lysosomal membrane because of its unique status as a negatively charged lipid species. While BMP is not present in the limiting membrane of the lysosome, it is an anionic lipid species localized to the inner leaflet of the acidic compartments where it assists as a docking site and cofactor for many lysosomal proteins (459). This unique biochemistry is essential for the function of lysosomal hydrolases such as ASM, lysosomal phospholipase A2 (LPLA2), and SAPs (460). These are proteins that we have identified as upregulated in *Grn*^{-/-} mouse brains (chapter 2) which could be interpreted as an adaptive response to compensate for downregulated activity. Therefore, the loss of BMP could be a mechanistic link between the possible primary accumulation of phospholipids and the secondary accumulation of other lipid species and secondary effect on other lysosomal functions.

While it is unclear how the loss of PGRN leads to phospholipid dysregulation, it is possible that GRNs play a role in stabilizing, activating, or chaperoning a protein involved in the synthesis of BMPs. GBA is not the only lysosomal hydrolase that PGRN interacts with, in a recent study phospholipase sPLA2-IIA levels are regulated by PGRN in the extracellular space (461). Though this particular phospholipase is secreted, the PLA2 enzyme group includes lysosomal phospholipase (PLA2G15) which is upregulated in PGRN deficiency and rescued by PGRN and

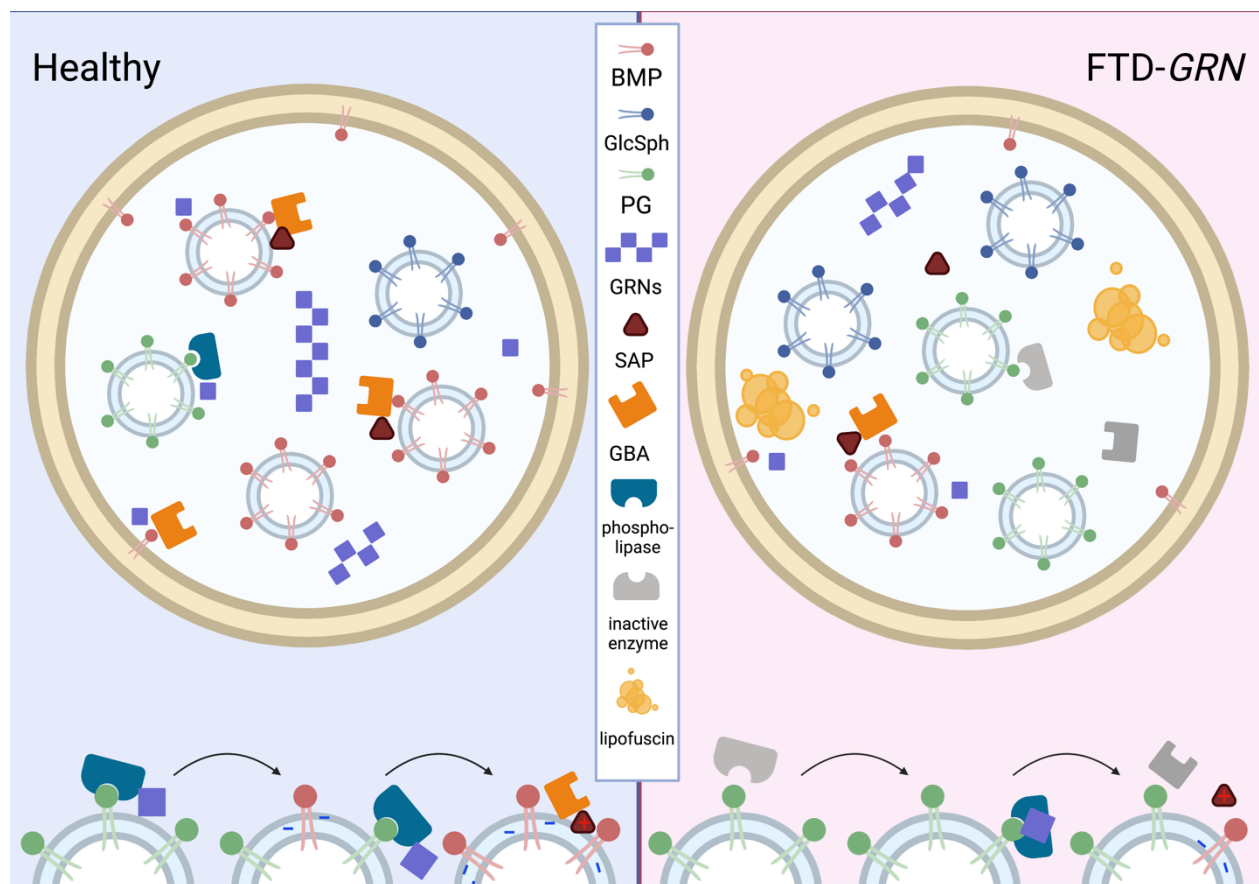


Figure 4.2: GRNs function to regulate lipid metabolism in the lysosome.

hGRN4. Interestingly a recent study asserts that PLA2G15 is sufficient to convert phosphatidylglycerol to lyso-phosphatidylglycerol (LPG) and that modulating PLA2G15 levels impacts BMP levels (462). It is possible that GRNs serve as an activator or co-factor in PLA2G15

activity, and the loss of GRNs lead to a downregulation of PLA2G15 activity. This dysregulation in processing could lead to a reduction in the availability of LPG a BMP precursor species, and less BMP synthesis. Previous work by Logan et al. found that BMP can be produced by *Grn*^{-/-} cells when phosphatidylglycerol is added (238). This evidence could support the model that BMP levels are reduced because of a reduction in precursor species availability, but further research focusing on the activity levels of lysosomal phospholipases in models of PGRN deficiency could provide insight into this possibility.

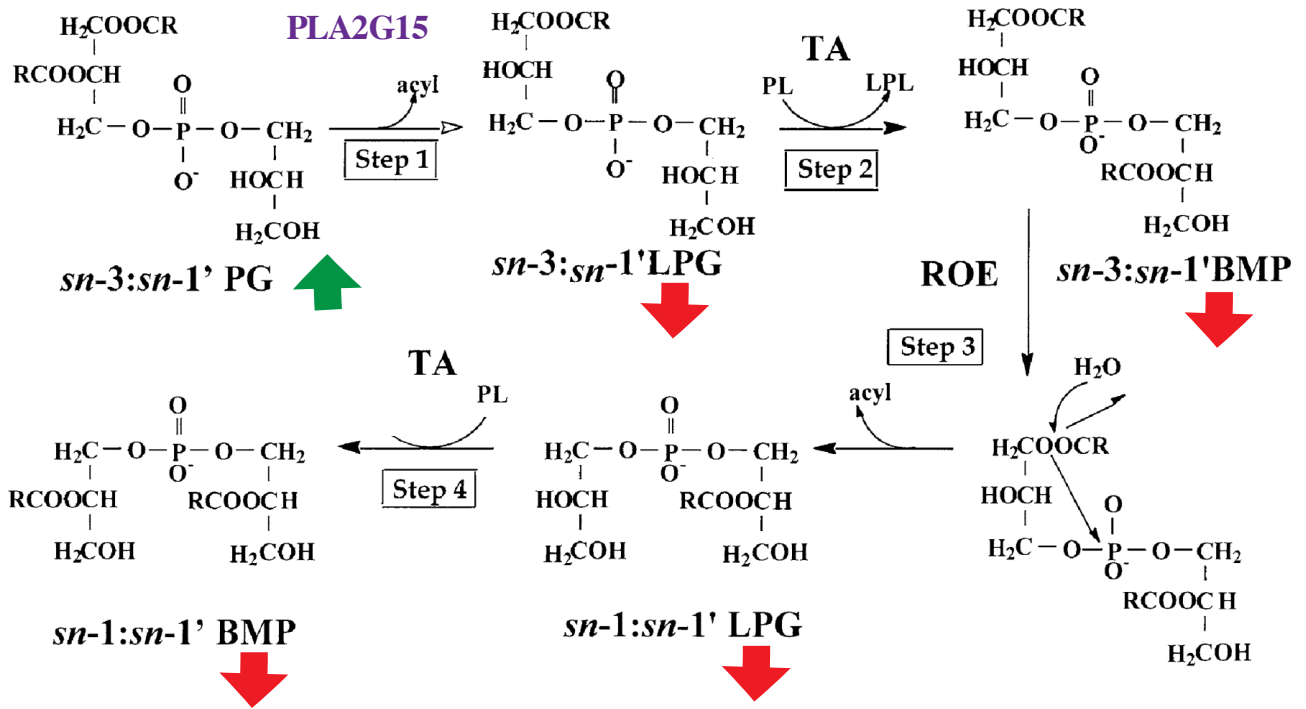


Figure 4.3: Proposed Mechanism of PGRNs impact of BMP synthesis

Adapted from (2). Proposed biosynthesis pathway of BMP (5). The first step in the conversion of phosphatidylglycerol (PG) to BMP is the hydrolysis of PG by a lysosomal phospholipase A₂, in the lysosome this could be PLA2G15, to form 1-acyl-*sn-1'* LPG. In the second step, *sn-3:sn-1'* LPG is acylated on the head group glycerol, the enzyme is unknown and abbreviated TA. The next step proposed is the reorientation of the phosphoryl ester unknown enzyme abbreviated ROE. The final step is a second transacylation to incorporate an acyl chain into the original backbone *sn-1:sn-1'* LPG. If PGRN is involved in the activity of PLA2G15, then loss of PGRN could impact the conversion of PG to LPG leading to a decrease in downstream lipid species.

BMP associated pathways are also seen to be dysregulated in PGRN deficiency. Levels of cholesterol abundance in the internal lysosomal membranes are required for the degradation of glycosphingolipids and are found to be important for the activity of helper proteins like SAPs (322, 463). Interestingly in HeLa cells, we find an increase in neutral lipids, and a decrease in BMPs suggesting that the environment for glycosphingolipid degradation is not ideal. Dysregulating of PLA2G15 and BMP levels is concomitant with dysregulation of cholesterol in HeLa cells (462), but this has not been investigated in the context of PGRN deficiency. Though we do see lipid dysregulation in our *GRN*^{-/-} HeLa cells as the accumulation of LipidSpot positive puncta, LipidSpot dye is a marker of lipid droplets and is not specific to a class of neutral lipids. Further, though increased accumulation of lipid droplets is observed it is not clear whether levels of lysosomal levels of lipid cholesterol are perturbed. Adapted from Gallala *et al*, 2011

In chapter 2 we report that the expression of hGRN4 elevates levels of BMP downregulated by the loss of PGRN in *Grn*^{-/-} mice. In light of this work, I propose that GRNs play a similar role to saposins acting as a cofactor to facilitate the catabolism or transport of lysophospholipids in the glycerophospholipid family. This dysregulation of glycerophospholipids interferes with the production of BMP species (Fig 4.3) causing a biochemical disruption of the lysosomal limiting membrane. This disruption of lysosomal membrane and leaflet composition causes a downstream downregulation in lysosomal catabolic capacity and phenotypes associated with lysosomal storage disorders (Fig 4.2). Further mechanistic studies will be necessary to evaluate this potential function of GRNs both *in vitro* and *in vivo*.

4.5.2 Glucosylsphingosines

The cortical lipidomics reported in chapter 2 detail an increase in glucosylsphingosines (GlcSph) in *Grn*^{-/-} mice, and recently GlcSph was found to be increased in FTD-*GRN* patient

plasma (342). GlcSph is an amphipathic compound that can react with GBA to produce glucosylsphingosine, though in models of decreased GBA activity it has been reported that acid ceramidase may catabolize glucosylceramide to GlcSph. These two enzymes are of interest, as they have been identified in our data presented here and by others to be downregulated in either abundance (ASAH1) or activity (GBA) in *Grn*^{-/-} mice. GlcSph is known to be neurotoxic (464), and accumulates in lysosomal storage diseases Niemann Pick-Type C and Gaucher Disease (465), as well as cases of Parkinson's disease with GBA mutations (466, 467). Interestingly GlcSph only accumulates in cases of Gaucher's with neuropathic presentations, suggesting that the accumulation of GlcSph may be directly related to neuronal degeneration in Gaucher Disease (468). Further GlcSph has been mechanistically tied to neurotoxic processes including promoting the aggregation of alpha synuclein (469), modulating inflammatory responses (470), and plasma levels of GlcSph d18:1 have been found to increase overtime in FTD-*GRN* variant carriers. The accumulation of GlcSph may track with the increase in pathological dysregulation in FTD-*GRN* patients, though longitudinal studies following participants for a longer period of time are necessary.

The accumulation of GlcSph may also have a direct effect on lysosomal function. GlcSph plays a role in regulating calcium homeostasis (471) and, Ca²⁺ has been found to be decreased in the lysosomes of Niemann Pick Type C patients with accumulation of GlcSph (472). Interestingly, proteins associated with the GO term "Calcium Ion Binding" are significantly increased in GFP-*Grn*^{-/-} mice compared to GFP-*Grn*^{+/+} mice. In NPC1 models, decreases in lysosomal Ca²⁺ lead to dysregulation of calcium binding proteins and deficits in endocytosis and endo-lysosomal function (472). Though it is unclear whether calcium storage in the lysosome is dysregulated by the loss of

PGRN, the accumulation of glucosylsphingosine suggests that this may be a consequence and should be investigated moving forward.

The accumulation of GlcSph in *Grn*^{-/-} mice could be driven by the downregulation of GBA activity, which can be ameliorated by the administration of hGRN4, suggesting that the accumulation may be due to the loss of GRNs. GBA is a lysosomal hydrolase known to be modulated by PGRN (20), and it is also important for the processing of GlcSph species. Simon et al. suggests that GRNs may stabilize BMPs at the lysosomal limiting membrane. Increased BMP turnover interferes with the ability of proteins like SAPs to recruit GBA to the lysosomal membrane leading to decreased activity and substrate accumulation (224). Therefore, as the increase in GlcSph can be tied to the activity of GBA, GlcSph could be classified as a secondary storage material in PGRN deficiency. Further, the neurotoxic effects of GlcSph in other models of LSDs and neurodegenerative disorders suggests that GlcSph could also be driving neurodegenerative phenotypes in cases of PGRN deficiency. The accumulation of GlcSph reveals another aspect of GRNs potential role as a regulator of lipid metabolism and homeostasis, and the crucial role lipids play in lysosomal and cellular homeostasis. However, further experimentation and investigation is necessary to understand whether findings from other neurodegenerative and lysosomal diseases are mechanistically relevant in models of FTD-*GRN*.

While it remains unclear why the loss of PGRN leads to dysregulation of lipid levels, data presented here suggests that differential regulation of lysosomal proteins that control levels of lysophospholipids is a common theme underlying variation observed across models of PGRN deficiency. I have proposed a mechanism for these perturbations including the loss of GRNs as stabilizing proteins for phospholipid degradation which directly leads to a decrease in BMP by interfering with the availability of BMP synthesis substrates, and indirectly as the consequences

of decreased BMP localization with the lysosomal inner leaflet disrupts the activity of lysosomal hydrolases causing an accumulation of toxic lipid species like glucosylsphingosine.

4.6 The roles of individual GRNs, interchangeable, or divergent?

We find compelling evidence that GRN2 and GRN4 are beneficial when expressed in *Grn*^{-/-} mice. However, a limitation of this study is that we did not test all the GRNs. While these findings shed light on pathways of particular interest for further investigation, conclusions necessitate the exploration of the roles of the additional granulins.

The ability of hGRN2 and hGRN4 to ameliorate increased proteins levels were not equivalent. This may be a consequence of unequal expression of the constructs in the injected GFP-*Grn*^{-/-} mice as the levels of LGALS3, and CD68 correlate with the level of expression in these cohorts, with mice expressing higher levels of granulins exhibiting the largest rescue in these proteins. This suggests that the GRNs assessed here, and additional GRN subunits have redundant functions. However, it is also possible that the individual granulins could have independent roles leading to their divergent ability to rescue our measured phenotypes.

While not much is currently known about the individual roles of the granulin subunits, there have been studies that have found diverging structural and biological properties as discussed in chapter 1. Structurally, each GRN amino acid sequence differs between 70% and 40% from the other GRNs. There are also differences in both the three-dimensional structure and post-translational modifications among the individual granulins, though the potential implications of these remain unclear. Biochemically GRN4 has been shown to either induce cell growth or inhibit cell proliferation in different cell lines, while GRN3 and GRN2 presented with inhibitory or antagonistic effects to granulin 4 (28, 31, 148, 301). GRN5 and GRN7 have also been shown to have neurotrophic properties in hippocampal neurons (10), although this observation may also be

neuronal type specific as motor neurons and cortical neurons, granulin 7 but not granulin 5 had an effect (298). While these findings underline a number of outstanding questions regarding the functions of GRN, they do suggest that there may be some differences between GRNs.

In addition to differences in function, the localization or distribution of the GRNs could vary between cell types, brain region, or tissue, similar to findings about the distribution of cathepsins (473, 474) and saposins (475). A recent study has suggested that GRN4 in particular was localized to neurons. This difference in endogenous localization could underlie the difference in the ability of GRN4 and GRN2 to ameliorate disease-associated phenotypes in the neurons of *Grn*^{-/-} mice. This raises the possibility that while GRNs may play redundant functions in the cell, all GRNs may not be equally present in each cell therefore the function may be attributed to individual GRNs in a specific or independent manner. This hypothesis remains untested and future investigations will be required to assess the distribution of GRNs across tissues.

It is also possible to model the function of individual GRNs similar to the saposins (SAPs) that make up PSAP, PGRN's trafficking partner. Levels of PSAP are critical for sphingolipid metabolism in the endolysosomal pathway as discussed above. As sphingolipid degradation proceeds, the length of the sugar headgroup inevitably shrinks in size, thereby becoming less accessible to water-soluble glycosidases. To overcome this physicochemical obstacle and to bring sphingolipids and their respective enzymes in close proximity, mammals possess four saposins (SAPA-D) (476) which function as activator proteins and assist in the function of lysosomal hydrolases. Though the individual SAPs share a high level of structural homology, they participate in different aspects of sphingolipid degradation evidenced by the various species that accumulate after the loss of a single subunit. SAPA activates galactosylceramide b-galactosidase (GALC) (477) and loss of this activator leads to a late onset form of Krabbe's Disease (477, 478). SACP

which activates GBA (479), and loss of this activator leads to Gaucher's disease (480). SAPD is the most abundant SAP and promotes the hydrolysis of substrates by acid ceramidase (ASAH1) (481). Loss of ASAH1 function leads to Farber Disease, however human patients with SAPD mutations present with Gaucher Disease (482). There are also some functions that are replicated by subunits, like SAPB which is seen as a non-specific activator protein and assists in the degradation of several species (483), and has overlapping activation profiles the final saposin GM2-AP (484), and SAPC and SAPA which are necessary components to activate the degradation of GalCer by galactosylceramidase (485).

The structure of the saposins are divergent even though they share homology (486, 487). It is possible that the GRNs could play a similar role in the lysosome, as discussed previously, as that the divergence of the subunits could follow a similar pattern, however, further investigation is required to support this model. In particular, newly developed tools to detect individual hGRNs and mGRNs (286) will enable the characterization of GRN distribution and cell type localization, and the assessment of proposed cellular functions *in vitro*.

4.7 Reconciling findings that GRNs are beneficial with previous findings

While the data presented here suggests that GRNs are beneficial and have a role in lipid metabolism, previous work has suggested GRNs are pro-inflammatory, cytokine-like molecules. The scope of the work presented here does not preclude some GRNs or multi-GRNs could have functions as modulators of inflammation.

As noted in chapter 1, until recently, most work understanding the role of PGRN and GRNs focused on protein that was extracellular. The localization of multifunctional proteins is known to influence the pathways they participate in, therefore, the localization of the GRNs could be a key variable in determining the “inflammatory” propensity of the proteins. For example, cathepsins

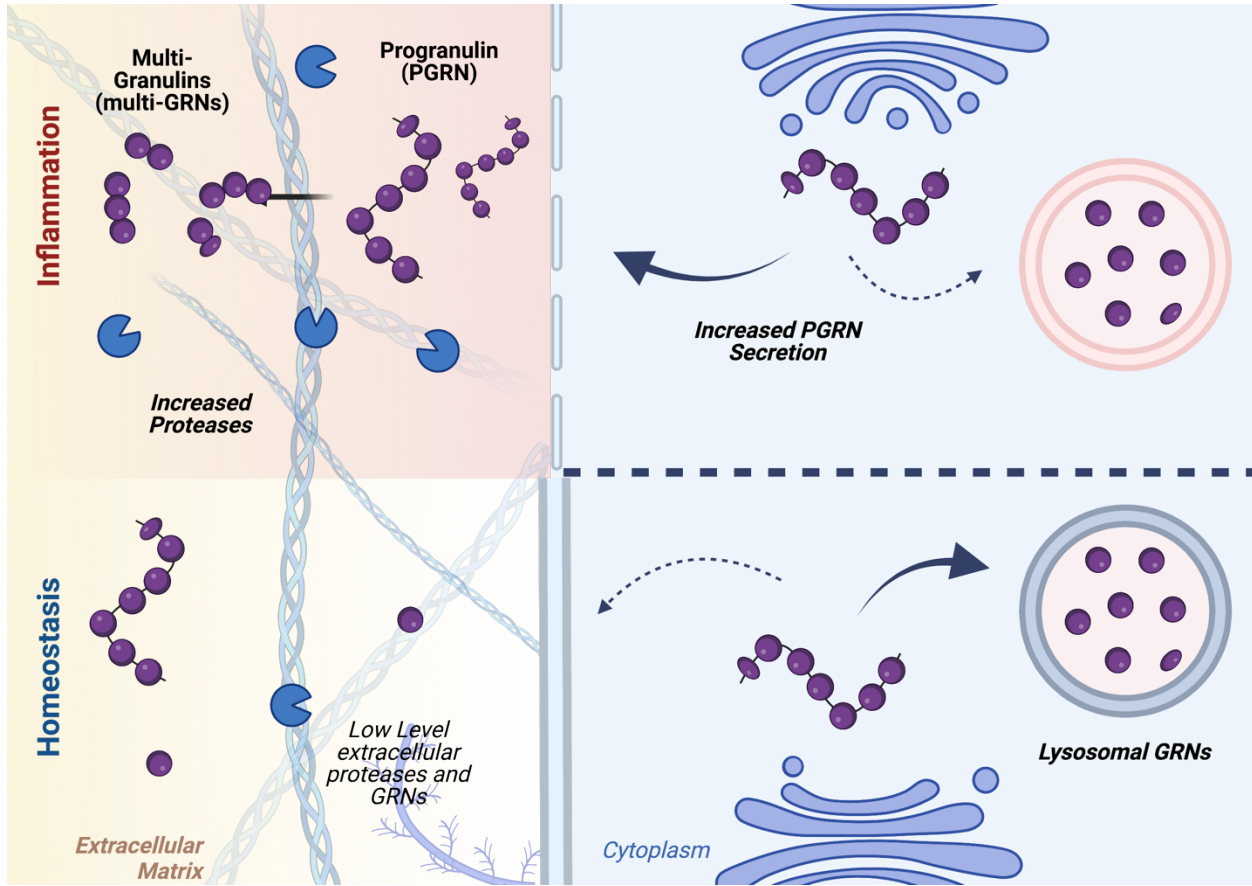


Figure 4.4: Localization of GRNs determines inflammatory profiles

are known lysosomal proteins that are necessary for correct lysosomal function. However, secreted cathepsins are known to be pro-inflammatory (488), and induce neuronal apoptosis (489). Extracellular cathepsins participate in functions such as host-defense after infection, and have an adaptive role (490). However, increased extracellular cathepsins have been associated with neurodegeneration (491, 492), and mis-localized lysosomal proteins are a known sign of lysosomal

membrane permeability (493). It is possible that, similarly to cathepsins, GRNs may be secreted from the endo-lysosomal pathway after damage or infection. Therefore, in the extra-cellular space GRNs might be pro-inflammatory.

It was confirmed that the AAV-hGRN constructs are secreted by HeLa cells *in vitro* suggesting that they are also secreted *in vivo* (Supplementary Fig2). These findings suggest that these GRNs are not pro-inflammatory even when secreted, as the hGRN2-*Grn*^{-/-} and hGRN4-*Grn*^{-/-} mice have reduced inflammation. Interestingly, a multiGRN fragment was found to be upregulated in rat brain after ischemic injury (450). Further, after the inhibition of PGRN cleavage by neutrophil elastase inflammatory cytokine release was decreased. Neutrophil elastase (NE) is a serine protease secreted from neutrophils during the inflammatory response (494). Therefore, PGRN would most likely encounter this protease in the extracellular space after neutrophil activation, and infiltration across the BBB as neutrophils are present in low levels in the brain (495). It is possible that the pro-inflammatory multi-GRN detected and inhibited by the reduction of NE activity is unique to the extracellular space and could be structurally different than the GRNs produced in the lysosome. Since proteases like NE and other neutrophil proteases like protease-3 known to cleave PGRN are produced by peripheral immune cells, the presence of their cleavage products in the brain could be a sign of BBB breakdown or peripheral immune infiltration (495, 496). Thus, the presence of these multiGRNs may be inflammatory because of unique cleavage patterns or products found in the extracellular space after the BBB is compromised.

There are several mechanisms through which extracellular multiGRNs could be pro-inflammatory, including binding through extracellular receptors, or through proteolytic roles. Building off of the model of extracellular cathepsins it is known that cathepsins in the extracellular space, cleave the extracellular domains of cell surface receptors (490), process and activate

chemokines (497, 498), and remodel the extracellular matrix (499) which can alter inflammatory signaling pathways. Recently extracellular cathepsin Z was found to signal through $\alpha 5$ integrin to promote the generation of IL-1 β in THP-1 cells (500). These findings suggest that multiGRN fragments could function in the inflammatory pathway in a similar manner, however further study will be required to investigate these mechanisms.

Overall, while the work presented here does not suggest that GRNs are primarily pro-inflammatory, that does not exclude them from being inflammatory signals in specific contexts. I suggest a mechanism through which extracellular multiGRNs may be pro-inflammatory while GRNs localized to the endo-lysosomal pathway are beneficial (Fig 4.3). The localization of PGRN/GRNs and its cleavage by multiple proteases with their own pattern of localization, are important variables to consider and further study is required to measure levels of extracellular PGRN and GRNs, and to assess levels of peripheral immune cell invasion in PGRN deficient brains to determine whether this paradigm is supported.

4.8 Autonomous vs. Non-cell Autonomous Benefits of GRN expression

In the work described in chapter 2 I expressed hPGRN and hGRN constructs using as adeno-associated virus delivered in P0 mouse pups, a model of somatic brain transgenesis (SBT) (324). Previous studies have delivered AAV mediated PGRN to mice at different time points (adults, aged) and several groups have used various approaches including different viral vectors including AAV serotype 9 which targets both neurons and glial cells (270, 501).

Our experimental design focused on expression of hPGRN and hGRNs in neuronal cell types via our neonatal intracerebroventricular injection scheme using rAAV1. We chose this strategy as previous studies transducing neurons with full length PGRN had proven ameliorative

while approaches using other serotypes target neurons and glia more broadly, or ependymal cells resulted in T-cell mediated toxicity (270). However, it is well known that PGRN is highly expressed in microglia (132, 502), therefore it is important to understand if focused neuronal delivery of GRNs is effective in ameliorating glial and inflammatory phenotypes. rAAV1 expression of GRNs does not directly deliver protein to glial cell types, however, this intervention did ameliorate glial activation and inflammatory phenotypes described in chapter 2. This modulation of disease-associated phenotypes could be modulated through cell autonomous or non-cell autonomous mechanisms.

The non-cell autonomous mechanism of GRNs in non-neuronal cell types is driven by PGRN's status as a secreted protein (503). PGRN can be taken up from the extracellular space trafficking either directly or indirectly with extracellular receptors including sortilin, lipoprotein receptor-related protein 1, mannose 6 phosphate receptor, and Notch1 among others described in chapter 1 (157, 222, 504). Importantly, we find that our GRN constructs expressed *in vitro* are also secreted. It is possible that the effects of rAAV1 expressed GRNs on glial phenotypes may be mediated by secreted protein and taken up by glial cells where they confer their ameliorative effects in a non-cell autonomous manner. In cell specific BV2 studies the loss of PGRN in microglia has been found to increase the formation of lipid droplets which are associated with increased cytokine release and other pro-inflammatory profiles *in vivo* (245), therefore PGRN uptake to these cells may decrease the level of inflammatory cytokines released downregulating neuroinflammatory pathways. In addition to cell specific phenotypes, several cell-type specific mechanisms for the regulation of PGRN have been described such as that PGRN in microglial cells is regulated by Nemo-like kinase but not neurons (505). Taken together this suggesting that there may be cell specific roles or pathways that PGRN or GRNs participate in these cell types.

This theory would align with observations that loss of PGRN in one cell type, either selective depletion of PGRN from microglial cells (345, 506), or conditional neuronal knockout (507), were not able to induce disease-like phenotypes in *Grn*^{-/-} mice, suggesting that expression of PGRN in one cell type is able to compensate for selective loss in another. However, these findings are difficult to interpret in mice since heterozygous loss of PGRN does not lead to discernable phenotypes until very late in life. Because of this it is possible that the selective depletion is not sufficient to induce pathology in mice regardless of the cell type targeted. A recent study using iPSC derived organoids found that *GRN*^{-/-} iPSC astrocytes drove TDP-43 pathology when matched with *GRN*^{+/+} iPSC cortical neurons (508). To investigate the relationship between microglia and neurons with and without PGRN further cell specific characterization of PGRN related phenotypes could be paired with similar iPSC derived organoids to understand the cell type specific effects of PGRN loss in a human derived model.

It is also possible that cell autonomous effects could also convey these effects. A cell autonomous mechanism could be mediated by the beneficial role of GRNs in neurons decreasing the levels of damaged and degenerating neurons. With fewer dysfunctional neurons fewer microglial cells may be activated in response reducing the levels of lysosomal dysfunction and inflammatory upregulation observed in the absence of PGRN. This paradigm has been observed previously in other neurodegenerative disorders where delivering protein to neurons AAV1 serotype ameliorates inflammatory phenotypes (509). This has also been observed previously in AAV1 delivery of full length PGRN, which was replicated in chapter 2 (256, 269). Neurons secrete a number of factors that influence the state of microglial activation (510), and microglia are activated in the case of neuronal damage (511). By modulating the state of neurons in *Grn*^{-/-} mice changes in secreted signals can lead to a decrease in activated microglia. Understanding the

role of GRNs in a cell-autonomous and non-cell autonomous or cross correctional mechanisms further experiments are required keeping in mind that both mechanisms could be at work simultaneously for neuronally expressed GRNs to confer a beneficial effect in both neuronal and glial cell types.

Future Directions

4.9 Therapeutic Role of GRNs, Outstanding Questions and Future pre-clinical studies.

One major impact of the work described here relates to the ability for GRNs to be considered as a potential therapeutic approach for diseases impacted by the loss of PGRN. While there are several benefits to considering GRNs as a therapeutic intervention, further assessment is needed.

4.9.1 Time of administration

The AAV delivery of GRNs described in chapter 2 takes advantage of the neonatal P0 mouse pups to achieve widespread transduction of neurons throughout the brain with little inflammatory reaction. The paradigm of early GRN replacement allows for expression of the protein throughout life and, the timing of AAV administration is an important variable that can determine the extent of viral vector transduction (324). Further, this scenario is not likely to be replicated in humans as FTD and CLN11 patients become symptomatic in adulthood so understanding the ability of GRNs clinical benefit when administered at later timepoints is required. To investigate the translatability of AAV GRN replacement-based interventions future pre-clinical assessments can deliver AAV1-GRNs to adult *Grn*^{-/-} mice similar to previous studies which delivered AAV-PGRN to 8-month old mice and assessed phenotypes at 12 months (256). In adult mice the injection strategy should be re-assessed, as after P2 the expression pattern of ventricularly injected rAAV1 shifts to primarily transduce ependymal cells (512). For this reason,

stereotaxic injections into the parenchyma are likely to yield a more favorable expression pattern (256, 513). Following the protocols described by Arrant *et. al* rAAV1/2 packaged GRNs could be delivered via stereotaxic injection to the prefrontal cortex of 8-month old *Grn*^{-/-} mice. At 12 months tissues can be collected and disease-like phenotypes can be assessed. It is possible that expression of GRNs using rAAV1/2 will be effective in ameliorating disease-like phenotypes in *Grn*^{-/-} mice. However, if this is not the case additional methods to deliver GRNs can be explored.

4.9.2 Peripheral administration

The evidence presented here builds upon those studies isolating individual subunits of the PGRN protein that can successfully be expressed throughout the brain throughout the lifetime of a mouse. One of the major challenges in PGRN based therapies is introducing PGRN to the brain through the blood brain barrier. The possibility of delivering 6 kDa granulin subunits instead of full length PGRN, may allow for additional delivery routes to be explored. Previous work has demonstrated that coupling PGRN an engineered Fc domain that binds to the human transferrin receptor allows it to be trafficked across the blood brain barrier (BBB) and increases CNS penetrance. This allows the protein to enter the brain and rescue CNS disease-like phenotypes in *Grn*^{-/-} mice (238). A recent study administered a recombinant purified His tagged PGRN derived peptide termed ND7 and included the final 98 amino acids encompassing the L7+GRN7+L8 c-terminal region of PGRN to a mouse model of Gaucher's Disease (514). Protein was delivered intraperitoneal injection (IP), and although the brain penetrance of the protein was only assessed via the His tag, this suggests that recombinant individual GRNs may be able to cross the BBB.

Future studies could use a similar approach and deliver recombinant GRNs 1-7 IP to *Grn*^{-/-} mice. Protein constructs can be expressed using HEK Expi293 cells, a suspension cell line that is optimal for expressing proteins that require post-translational modifications like PGRN and GRNs. Proteins can be coupled to a double STREP tag to enable purification using STREP-XT

purification columns. After treatment brains and peripheral organs including liver and spleen can be assessed for the expression of individual GRN expression using antibodies currently under development by the Kukar lab (unpublished). If the individual GRNs are able to penetrate the BBB I would expect that the brain tissues would be immunoreactive to the individual GRN antibodies, in the case that the individual antibodies are not successful, the twin STREP tag can also be leveraged for detection in tissue. Immunodetection can be performed via immunohistochemical staining, ELISA, or immunoblot as *Grn*^{-/-} mice produce no endogenous GRNs any protein detected in the brain would be due to GRNs from the periphery trafficking to the brain. In the case that the individual GRNs are not detected in the brain further studies could be conducted attempting to identify the receptor the GRN7 fragment travels across the BBB, it is possible that the process is dependent on the binding domains found in the L8 region associated with GRN7. If this is the case, the binding domain could be engineered to the other GRNs, or another approach to deliver GRNs could be considered.

In addition to delivering recombinant GRNs peripherally new developments in AAV technology now allow for the peripheral injection of AAV vectors that can cross the BBB and transduce neurons (515, 516). The engineered capsid AAV-PHP.N transduces NeuN⁺ neurons efficiently after IV retro-orbital injection (516). In an effort to explore the ability for GRNs to be delivered peripherally individual human GRNs can be packaged into AAV-PHP.N capsids, delivered retro-orbitally to *Grn*^{-/-} mice, and allowed to express for 3-4 weeks. A similar procedure as the one described to evaluate the ability of recombinant GRNs to cross the BBB can be employed to determine the efficacy of AAV-PHP.N GRNs. If the transduction of GRNs proves successful, additional variables of interest like age of intervention, discussed above, could be integrated into the paradigm.

There are translational limitations with this method. Firstly, the PHP.B family of AAV capsids was developed in a screen on C57/BL6 mice, and there are differences in transduction efficiency in mice from other genetic backgrounds (517). In addition to variation between strains, PHP.B based AAV capsid do not transduce non-human primates (NHP), and therefore would not be a viable clinical approach for human patients (518). This is because the PHP.B capsid depends on the murine specific receptor LY6A to cross the BBB (519, 520). Screening patient relevant models like iPSC cell lines is currently underway to identify AAV capsids that can be translate to NHP and human patients (521). This limitation is not present in the recombinant protein delivery strategy but does offer cell type specificity in the production of the protein. While the impact of these variables is unclear, the benefit of assessing the efficacy of administering GRNs peripherally will have pre-clinical benefit. PGRN was first identified as a cell growth factor and positive regulator of cancerous cells (30), therefore the ability to confer ameliorating effects delivering specific GRN subunits, to specific cell types could reduce the likelihood of negative side effects due to the actions of full length extracellular PGRN. Understanding these aspects of GRN replacement informs the targeting of potential treatments and could potentially inform translational assessments for human patients.

4.9.3 Limitations of PGRN Deficient Mouse Models

A limitation of these studies is that mouse models of PGRN do not precisely recapitulate the pathology of human FTD-*GRN* patients or NCL11 patients. Firstly, as *Grn*^{+/-} mice do not present with many consistent biochemical disease-related phenotypes at 12 months as phenotypes are much milder than *Grn*^{-/-} mice (244). However, studies have reported differences in social behavior assays compared to *Grn*^{+/+} mice suggesting that there are some underlying perturbations caused by the partial loss of PGRN and GRNs (257, 262). The mechanism driving the differences in divergent phenotypes between humans and mice after loss of PGRN is unclear. It is known that

mice have higher endogenous levels of secreted PGRN, up to 5 times higher than what is observed in healthy human controls (135). This raises the possibility that there is a threshold level of PGRN that is required for homeostatic lysosomal function, and while a 50% reduction in protein from the endogenous levels in humans is sufficient to cause dysfunction, a 50% reduction in mice does not reach a pathological threshold. This difference in gene dose related phenotypic presentation compounds with the lack of general TDP-43 accumulation in *Grn*^{-/-} mice.

While some studies have detected increases in phospho-TDP-43 in aged *Grn*^{-/-} mice (202, 522), inclusions of TDP-43 are only observed in neurons of specific brain regions in mice aged about 2 years (260, 334, 522). These findings highlight another important difference in rodent models, which is that the lifespan of these model animals is a few years, while pathology in human patients requires decades to develop. It is possible that this time span is not sufficient for some of the pathological characteristics of FTD-*GRN* and CLN11 to be robustly detectable. If this is the case, *Grn*^{-/-} mice could be considered an early-stage disease model. These findings highlight limitations of *Grn*^{-/-} mice as a pre-clinical model of FTD-*GRN*. Future studies need to take species specific biology into account when considering the best models to investigate potential therapeutic interventions as well as mechanisms of action related to chosen interventions.

4.9.4 Patient Derived iPSC lines as a platform for assessing therapeutic potential of GRNs.

To address limitations of mouse models, iPSC models can be used to assess the therapeutic potential of individual GRNs in a patient derived model. The first FTD-*GRN* patient derived *GRN*^{+/-} iPSC neurons and microglia were produced in 2012, and since that time several lines encompassing several pathogenic mutations have been isolated (393). These cell lines have around a 50% reduction in PGRN mRNA (389). Human patient cortical neurons derived from these stem cells recapitulate several of the pathological characteristics of human patients including TDP-43

mis-localization and increased phosphorylation (19, 389), and lysosomal dysfunction (19). Similarly, *GRN*^{-/-} iPSC cortical neurons derived from a CLN11 patient displayed increased lysosomal volume, increased phosphorylated TDP-43 and cytoplasmic mislocalization of TDP-43 after 100 days of culturing (392). Unlike mouse models, the gene dose effect of PGRN is preserved in iPSC cortical neurons, as a partial loss of PGRN leads to dysregulation. iPSC cortical neurons also recapitulate phenotypes that are not consistently observed in *Grn*^{-/-} mice including TDP-43 pathology.

The ability of GRNs to ameliorate pathologies such as TDP-43 inclusions could be assessed in iPSC derived cortical neurons using AAV to transduce the expression of an individual GRN. In these conditions I would expect that the replacement of a single GRN would be able to correct mis-localized TDP-43, and the decrease in levels of LAMP1 and lipofuscin. Using iPSC models to gain insight into the ability of GRNs to clear TDP-43 is important, as it is not a phenotype accessible in mouse model of FTD-*GRN* but is the primary protein inclusion in human patients. As seen in other neurodegenerative diseases, clearing pathological inclusions is considered an important readout of efficacy. In addition to evaluating the potential application of GRNs as a therapeutic intervention, similar experimental paradigms can be leveraged to understand the mechanisms that drive the beneficial effects observed after the addition of GRNs in models of PGRN deficiency.

4.10 Investigating Proposed mechanisms for GRNs

iPSC derived microglia and neurons are an exciting platform to examine the mechanisms of GRN function. Many of the outstanding questions regarding the role of GRNs require experimentation *in vitro*. Patient derived iPSC lines provide a method to model PGRN deficient human neurons and microglia from the same background which cannot be achieved in other immortalized cell lines. Further, as PGRN is known to be differentially regulated in cancers, there

are potential adaptations and differences in baseline PGRN in immortalized cell lines that could interfere with the interpretation of GRN function.

In the current work we assess 2 of the 7 total GRNs. While we find that both hGRN2 and hGRN4 ameliorate phenotypes of disease, it is unclear whether all GRNs would rescue in an interchangeable manner. The expression of each GRN could be pursued in a *Grn*^{-/-} mouse, however, conducting such a screen could be done in iPSC cell lines, which have well defined phenotypes as previously described. This approach also has the advantage of reducing the number of animals required in the research program. iPSC cortical neurons can be transduced using AAVs (521). Using this strategy, we can transduce each individual GRN to *GRN*^{-/-} and *GRN*^{+/-} cortical neurons. Assessments of characteristic disease-like phenotypes can be completed. These can include those approaches used in the murine *in vivo* experiments described in chapter 2 including immunocytochemistry, immunoblot and -omics based assessments. This approach has the added benefit of being able to include both *GRN*^{+/-} and *GRN*^{-/-} cells. While work delivering full length PGRN to FTD-*GRN* iPSC derived cortical would suggest a similar effect would be achieved (523), there is the possibility that the additional of individual GRNs may identify variations, particularly if there are divergences in GRN function. Similarly, it is possible that each GRN has a similar effect in the mice after 12 months of expression, however, without insight into the precise function GRNs serve in the lysosome, attributing rescue to the same underlying mechanism cannot be achieved.

In this case iPSCs can also address outstanding questions, as delineating mechanistic pathways is more tractable. For example, recent work indicates that traditional markers of lysosomal compartments including LAMP1/2 and LysoTracker may identify a more heterogeneous collection of compartments (524), including degradative and non-degradative compartments.

Considering this, activity-based probes, like BMV-109 described in chapter 3, can be used to assess lysosomal hydrolase activity via cytochemistry or immunoblot, rather than the distribution of membrane proteins. These assays can be affected by fixation, and therefore, are well suited to live cell approaches using iPSCs. Other live based cell techniques can be applied to better understand the role of GRNs in the lysosome include the DQ-BSA assay to investigate the autophagic capacity of the neurons (525), pH markers such as BiDL (526) or OregonGreen (527) to determine the acidity of lysosomal compartments in the presence of individual GRNs, which can be measured together with intra-lysosomal calcium levels with the aid of probes (528). A more nuanced understanding of the role of GRNs in the lysosome will contribute to the overall understanding of their biology and could shed light on any differences in their function through their effect on lysosomal phenotypes.

4.11 Isolation of Lysosomes for PGRN deficient iPSCs

Recent technical advances have allowed for a genetically specific immunoprecipitation of lysosomes via a TMEM192-3XHA tag (Lyso-IP) (529). Isolation of lysosomes can detect differences in the proteomic and metabolomic composition, that are not characterized at the whole cell, or whole tissue level (455, 530). This is a significant advance, since we do detect differences at the whole cell and whole tissue level of some lipid species like phosphatidylglycerol, but a more focused approach could elucidate any changes in the specific lysosomal compartment.

Lipidomic analysis on isolated lysosomes from *GRN*^{-/-}, *GRN*^{F/+} and control iPSC cortical neurons will be important in understanding the significance of BMP reduction after the loss of PGRN. It would be possible to delineate whether the loss of BMP is due to a reduction in the lyso-lipid precursor species that give rise to BMPs. If lyso-phosphatidylglycerol or other glycoposphodiester are increased this could indicate that BMP synthesis is impeded by the loss

of PGRN. This could indicate that GRNs act in the lysosome in a function similar to CLN3 and facilitate the transit of these lipids from the lysosome. It is also possible that changes in phosphatidylglycerol metabolism could impact BMP levels as the specific increase in 22:6/22:6-PG has been found to lead to selective decreases in BMP levels (453). This presents another potential mechanism of action for GRNs which could be assessed through lipidomic assessment of PGRN deficient lysosomes.

In addition to lipidomics, further mechanistic insight can be gained from the assessment of metabolic composition of the lysosome. For example, the lysosome is an important storage compartment for calcium within the cell (531), and lysosomal calcium levels are known to be decreased across LSDs and neurodegenerative disorders (532). While there are several mechanisms that contribute to this, the accumulation of sphingosines is known to inhibit lysosomal calcium storage. Assessing the intra-lysosomal level of calcium could inform a mechanism of dysfunction in PGRN deficient systems, particularly the CNS where calcium serves specialized roles (533).

Employing a strategy to add back individual GRNs via AAV or recombinant protein, the ability of each subunit to impact the dysregulation of lipids, as well as changes in lysosomal protein levels and of any identified live cell assays. These panels will serve multiple functions. Firstly, it will help to describe the function of GRNs in the lysosome. Secondly, it will assist in identifying any divergent functions between GRN subunits. Particularly if multiple cell types are leveraged, as it is possible that individual GRNs may have cell type specific roles. This focused dataset may help to elucidate whether there are any specific differences in the roles individual GRNs may play in the lysosome, independent of the end point of disease-like phenotype rescue *in vivo*.

4.12 Exploring Cell Type Specific Effects

The majority of studies have focused on delivering PGRN, and in this study GRNs, to neurons. However, PGRN is most highly expressed in microglia in the CNS. Microglia are particularly involved in phagocytosis and clearance of extracellular debris, and damaged cells and due to this specialized role in the brain, may have a more complex regulation of lysosomal components (258). Further, microglia have been found to be particularly vulnerable to lysosomal accumulation in *Grn*^{-/-} mice (522). A benefit of using iPSC lines is the ability to generate hiPSC microglia (534). These cells can be assessed for lysosomal function as well as inflammatory profiles like cytokine release panels (535), and phagocytosis assays (536). While it is likely that the loss of PGRN leads to similar changes in lysosomal function across cell types, it is possible that microglial cells may be more sensitive as they have higher levels of PGRN therefore more severe phenotypes may be discernable, especially in *GRN*^{-/+} cells. Therefore, in addition to comparisons between genotypes, data produced from hiPSC microglia can be compared to derived cortical neurons to isolate differences in lysosomal composition between cell types using techniques like Lyso-IP, and the consequences of the loss of PGRN and the introduction of individual GRNs on those processes.

4.13 Understanding Inflammatory Roles of GRNs

As previously discussed, the localization and regulation of GRNs could allow GRNs to be both beneficial to the homeostatic function of the lysosome and proinflammatory in the extracellular space. However, further experimentation is needed to understand this possibility. Using either hiPSC microglia or an immortalized cell line such as BV2 cells, for which *GRN*^{-/-} lines are available (537). In the experimental design described we assessed 2 of 7 GRNs, to account for the additional GRNs recombinant protein of hGRN1-7 can be added to media of wildtype cells. After an incubation period, media and cell lysates can be assessed for cytokine release and regulation of inflammatory proteins compared to cells treated with base media. This design, however, may not

account for specific cleavage that may occur extracellularly. To account for this PGRN can be incubated with proteases like NE before being added to media for supplementation. The previous AAV mouse experiments focus on adding back GRNs to a system with no endogenous expression. It is possible that overabundance of extracellular GRNs or multiGRNs leads to inflammation that does not occur when increasing GRN levels in a PGRN deficient system. To assess this GRNs and multiGRNs can also be added to *GRN^{+/+}* lines.

While the localization of GRN *in vivo* cannot be controlled in the same manner. It is possible to question whether the addition and over-expression of GRNs is pro-inflammatory. To assess this *in vitro* the previously described GRN treatments could be replicated in *GRN^{+/+}* cell lines. *In vivo* GRNs can be expressed in a similar paradigm to chapter 2 in *Grn^{+/+}* mice. These mice can then be assessed for signs of inflammation including markers found to be ameliorated in chapter 2 like CD68 and CD45. Further, cytokine analysis can be completed on whole tissue using tools like the MesoScale Discovery Platform (535). These assessments could shed light on the function and regulation of GRNs, and could provide insight into the consequences of overexpressed GRNs which could inform potential clinical applications.

4.14 Closing Remarks

The work presented here answers a critical outstanding question in the field of PGRN biology, and strongly supports the hypothesis put forth in chapter 1, that granulins are the active components of the precursor protein PGRN in the lysosome and are beneficial for lysosomal function. In chapter 2 I found that granulins can rescue dysfunction caused by the loss of PGRN. In chapter 3 conserved dysfunction caused by the loss of PGRN and GRNs was described in an immortalized human cell line. Taken together these data lead to the conclusion that GRNs are bioactive subunits of PGRN, which serves as a precursor protein. Loss of GRNs leads to conserved phenotypes, and that role of the processed GRNs are beneficial both *in vitro* and *in vivo*. This finding has major implications

for the development of therapeutics for diseases involving PGRN loss, as new approaches targeting GRNs as clinical targets, or biomarkers should be investigated. Further, this work informs our understanding of how PGRN confers its effects intracellularly through its potential ability to mediate lipid metabolism. However, future steps in understanding diseases driven by the loss of PGRN is complicated by the limitation that the function of individual GRNs remains unclear. The work presented here necessitates investigation of individual GRNs in the lysosome. The experiments proposed here are a starting point for the elucidation that will enable the field to understand the role of GRNs, which are proteins critical for brain health, but have eluded functional understanding for decades.

5 References

1. Ghimire S, Kim J. PEG3 controls lipogenesis through ACLY. *PLoS One*. 2021;16(5):e0252354. Epub 2021/05/29. doi: 10.1371/journal.pone.0252354. PubMed PMID: 34048454; PMCID: PMC8162686.
2. Gallala HD, Sandhoff K. Biological function of the cellular lipid BMP-BMP as a key activator for cholesterol sorting and membrane digestion. *Neurochem Res*. 2011;36(9):1594-600. Epub 2010/12/08. doi: 10.1007/s11064-010-0337-6. PubMed PMID: 21136156.
3. Hrabal R, Chen Z, James S, Bennett HP, Ni F. The hairpin stack fold, a novel protein architecture for a new family of protein growth factors. *Nat Struct Biol*. 1996;3(9):747-52. Epub 1996/09/01. doi: 10.1038/nsb0996-747. PubMed PMID: 8784346.
4. Lamprecht MR, Sabatini DM, Carpenter AE. CellProfiler: free, versatile software for automated biological image analysis. *Biotechniques*. 2007;42(1):71-5. Epub 2007/02/03. doi: 10.2144/000112257. PubMed PMID: 17269487.
5. Heravi J, Waite M. Transacylase formation of bis(monoacylglycerol)phosphate. *Biochim Biophys Acta*. 1999;1437(3):277-86. Epub 1999/04/02. doi: 10.1016/s1388-1981(99)00021-9. PubMed PMID: 10101262.
6. Bang J, Spina S, Miller BL. Frontotemporal dementia. *Lancet*. 2015;386(10004):1672-82. doi: 10.1016/S0140-6736(15)00461-4. PubMed PMID: 26595641.
7. Gass J, Prudencio M, Stetler C, Petrucelli L. Progranulin: an emerging target for FTLD therapies. *Brain Res*. 2012;1462:118-28. Epub 2012/02/18. doi: 10.1016/j.brainres.2012.01.047. PubMed PMID: 22338605; PMCID: PMC3647886.
8. Meeter LHH, Patzke H, Loewen G, Dopfer EGP, Pijnenburg YAL, van Minkelen R, van Swieten JC. Progranulin Levels in Plasma and Cerebrospinal Fluid in Granulin Mutation Carriers. *Dement Geriatr Cogn Dis Extra*. 2016;6(2):330-40. doi: 10.1159/000447738. PubMed PMID: 27703466.
9. Ahmed Z, Mackenzie IRA, Hutton ML, Dickson DW. Progranulin in frontotemporal lobar degeneration and neuroinflammation. *Journal of Neuroinflammation*. 2007;4(1):7. doi: 10.1186/1742-2094-4-7.
10. Gass J, Lee WC, Cook C, Finch N, Stetler C, Jansen-West K, Lewis J, Link CD, Rademakers R, Nykjaer A, Petrucelli L. Progranulin regulates neuronal outgrowth independent of sortilin. *Mol Neurodegener*. 2012;7:33-. doi: 10.1186/1750-1326-7-33. PubMed PMID: 22781549.
11. Van Damme P, Van Hoecke A, Lambrechts D, Vanacker P, Bogaert E, van Swieten J, Carmeliet P, Van Den Bosch L, Robberecht W. Progranulin functions as a neurotrophic factor to regulate neurite outgrowth and enhance neuronal survival. *Journal of Cell Biology*. 2008;181(1):37-41. doi: 10.1083/jcb.200712039.
12. Bossù P, Salani F, Alberici A, Archetti S, Bellelli G, Galimberti D, Scarpini E, Spalletta G, Caltagirone C, Padovani A, Borroni B. Loss of function mutations in the progranulin gene are related to pro-inflammatory cytokine dysregulation in frontotemporal lobar degeneration patients. *Journal of Neuroinflammation*. 2011;8(1):65. doi: 10.1186/1742-2094-8-65.

13. Martens LH, Zhang J, Barmada SJ, Zhou P, Kamiya S, Sun B, Min S-W, Gan L, Finkbeiner S, Huang EJ, Farese RV, Jr. Progranulin deficiency promotes neuroinflammation and neuron loss following toxin-induced injury. *The Journal of Clinical Investigation*. 2012;122(11):3955-9. doi: 10.1172/JCI63113.
14. Almeida MR, Macário MC, Ramos L, Baldeiras I, Ribeiro MH, Santana I. Portuguese family with the co-occurrence of frontotemporal lobar degeneration and neuronal ceroid lipofuscinosis phenotypes due to progranulin gene mutation. *Neurobiology of Aging*. 2016;41:200.e1-e5. doi: <https://doi.org/10.1016/j.neurobiolaging.2016.02.019>.
15. Canafoglia L, Morbin M, Scafoli V, Pareyson D, D'Incerti L, Fugnanesi V, Tagliavini F, Berkovic SF, Franceschetti S. Recurrent generalized seizures, visual loss, and palinopsia as phenotypic features of neuronal ceroid lipofuscinosis due to progranulin gene mutation. *Epilepsia*. 2014;55(6):e56-e9. doi: 10.1111/epi.12632.
16. Huin V, Barbier M, Bottani A, Lobrinus JA, Clot F, Lamari F, Chat L, Rucheton B, Fluchère F, Auvin S, Myers P, Gelot A, Camuzat A, Caillaud C, Journéa L, Forlani S, Saracino D, Duyckaerts C, Brice A, Durr A, Le Ber I. Homozygous GRN mutations: new phenotypes and new insights into pathological and molecular mechanisms. *Brain*. 2020;143(1):303-19. doi: 10.1093/brain/awz377.
17. Gotzl JK, Mori K, Damme M, Fellerer K, Tahirovic S, Kleinberger G, Janssens J, van der Zee J, Lang CM, Kremmer E, Martin JJ, Engelborghs S, Kretzschmar HA, Arzberger T, Van Broeckhoven C, Haass C, Capell A. Common pathobiochemical hallmarks of progranulin-associated frontotemporal lobar degeneration and neuronal ceroid lipofuscinosis. *Acta Neuropathol*. 2014;127(6):845-60. Epub 2014/03/13. doi: 10.1007/s00401-014-1262-6. PubMed PMID: 24619111.
18. Jian J, Tian QY, Hettinghouse A, Zhao S, Liu H, Wei J, Grunig G, Zhang W, Setchell KDR, Sun Y, Overkleeft HS, Chan GL, Liu CJ. Progranulin Recruits HSP70 to beta-Glucocerebrosidase and Is Therapeutic Against Gaucher Disease. *EBioMedicine*. 2016;13:212-24. Epub 2016/10/30. doi: 10.1016/j.ebiom.2016.10.010. PubMed PMID: 27789271; PMCID: PMC5264254.
19. Valdez C, Wong YC, Schwake M, Bu G, Wszolek ZK, Krainc D. Progranulin-mediated deficiency of cathepsin D results in FTD and NCL-like phenotypes in neurons derived from FTD patients. *Hum Mol Genet*. 2017;26(24):4861-72. Epub 2017/10/17. doi: 10.1093/hmg/ddx364. PubMed PMID: 29036611; PMCID: PMC5886207.
20. Zhou X, Paushter DH, Pagan MD, Kim D, Nunez Santos M, Lieberman RL, Overkleeft HS, Sun Y, Smolka MB, Hu F. Progranulin deficiency leads to reduced glucocerebrosidase activity. *PLoS One*. 2019;14(7):e0212382. Epub 2019/07/11. doi: 10.1371/journal.pone.0212382. PubMed PMID: 31291241; PMCID: PMC6619604.
21. Evers BM, Rodriguez-Navas C, Tesla RJ, Prange-Kiel J, Wasser CR, Yoo KS, McDonald J, Cenik B, Ravenscroft TA, Plattner F, Rademakers R, Yu G, White CL, 3rd, Herz J. Lipidomic and Transcriptomic Basis of Lysosomal Dysfunction in Progranulin Deficiency. *Cell Rep*. 2017;20(11):2565-74. Epub 2017/09/14. doi: 10.1016/j.celrep.2017.08.056. PubMed PMID: 28903038; PMCID: PMC5757843.
22. Wils H, Kleinberger G, Pereson S, Janssens J, Capell A, Van Dam D, Cuijt I, Joris G, De Deyn PP, Haass C, Van Broeckhoven C, Kumar-Singh S. Cellular ageing, increased mortality and FTLD-TDP-associated neuropathology in progranulin knockout mice. *The Journal of Pathology*. 2012;228(1):67-76. doi: 10.1002/path.4043.

23. Mole SE, Schulz A, Haltia M. Chapter 4 - The neuronal ceroid-lipofuscinoses (Batten disease). In: Rosenberg RN, Pascual JM, editors. *Rosenberg's Molecular and Genetic Basis of Neurological and Psychiatric Disease (Sixth Edition)*: Academic Press; 2020. p. 53-71.
24. Cárcel-Trullols J, Kovács AD, Pearce DA. Cell biology of the NCL proteins: What they do and don't do. *Biochim Biophys Acta*. 2015;1852(10 Pt B):2242-55. Epub 2015/05/13. doi: 10.1016/j.bbadis.2015.04.027. PubMed PMID: 25962910.
25. Holler CJ, Taylor G, Deng Q, Kukar T. Intracellular Proteolysis of Progranulin Generates Stable, Lysosomal Granulins that Are Haploinsufficient in Patients with Frontotemporal Dementia Caused by *GRN* Mutations. *eneuro*. 2017;4(4):ENEURO.0100-17.2017. doi: 10.1523/eneuro.0100-17.2017.
26. Lee CW, Stankowski JN, Chew J, Cook CN, Lam Y-W, Almeida S, Carlomagno Y, Lau K-F, Prudencio M, Gao F-B, Bogyo M, Dickson DW, Petrucelli L. The lysosomal protein cathepsin L is a progranulin protease. *Mol Neurodegener*. 2017;12(1):55. doi: 10.1186/s13024-017-0196-6.
27. Bateman A, Belcourt D, Bennett H, Lazure C, Solomon S. Granulins, a novel class of peptide from leukocytes. *Biochemical and Biophysical Research Communications*. 1990;173(3):1161-8. doi: [https://doi.org/10.1016/S0006-291X\(05\)80908-8](https://doi.org/10.1016/S0006-291X(05)80908-8).
28. Shoyab M, McDonald VL, Byles C, Todaro GJ, Plowman GD. Epithelins 1 and 2: isolation and characterization of two cysteine-rich growth-modulating proteins. *Proc Natl Acad Sci U S A*. 1990;87(20):7912-6. Epub 1990/10/01. doi: 10.1073/pnas.87.20.7912. PubMed PMID: 2236009; PMCID: PMC54861.
29. Anakwe O, Gerton GL. Acrosome biogenesis begins during meiosis: evidence from the synthesis and distribution of an acrosomal glycoprotein, acrogranin, during guinea pig spermatogenesis. *Biology of reproduction*. 1989;42(2):317-28.
30. He Z, Bateman A. Progranulin (granulin-epithelin precursor, PC-cell-derived growth factor, acrogranin) mediates tissue repair and tumorigenesis. *Journal of Molecular Medicine*. 2003;81(10):600-12. doi: 10.1007/s00109-003-0474-3.
31. Tolkmachev D, Malik S, Vinogradova A, Wang P, Chen Z, Xu P, Bennett HPJ, Bateman A, Ni F. Structure dissection of human progranulin identifies well-folded granulin/epithelin modules with unique functional activities. *Protein Sci*. 2008;17(4):711-24. doi: 10.1110/ps.073295308. PubMed PMID: 18359860.
32. Pick A. Über die Beziehungen der senilen Hirnatrophie zur Aphasie. *Prag Med Wchenschr*. 1892;17:165-7.
33. Pick A. Zur Symptomatologie der linksseitigen Schläfenlappenatrophie. *European Neurology*. 1904;16(4):378-88.
34. Pick A. umschriebene stärkere Hirnatrophie (gemischte Apraxie)'. *Monatsschrift für Psychiatrie und Neurologie*. 1906;19:97.
35. Pick A, Girling D, Marková I. Senile hirnatrophie als grundlage von Herderscheinungen1995.
36. Alzheimer A. Über eigenartige Krankheitsfalle des späteren Alters. *Psychiatr Nervenkr Z Gesamte Neurol Psychiatr*. 1911;4:356-85.
37. Gans A. Betrachtungen über Art und Ausbreitung des krankhaften Prozesses in einem Fall von Pickscher Atrophie des Stirnhirns. *Z Neurol*. 1923;80:10-28.
38. Onari K, Spatz H. Anatomische beiträge zur lehre von der pickschen umschriebenen grosshirnrinden-atrophie („picksche krankheit“). *Arbeiten aus der Deutschen Forschungsanstalt für Psychiatrie in München (Kaiser-Wilhelm-Institut)*. 1926:546-87.

39. Schneider C. Über Picksche Krankheit. pp. 230–252. *European Neurology*. 1927;65(1):230-52.
40. Schneider C. Weitere beiträge zur lehre von der pickschen krankheit. *Zeitschrift für die gesamte Neurologie und Psychiatrie*. 1929;120(1):340-84.
41. Constantinidis J, Richard J, Tissot R. Pick's disease. Histological and clinical correlations. *Eur Neurol*. 1974;11(4):208-17. Epub 1974/01/01. doi: 10.1159/000114320. PubMed PMID: 4137107.
42. Gustafson L. Frontal lobe degeneration of non-Alzheimer type. II. Clinical picture and differential diagnosis. *Arch Gerontol Geriatr*. 1987;6(3):209-23. Epub 1987/09/01. doi: 10.1016/0167-4943(87)90022-7. PubMed PMID: 3689054.
43. Brun A. Frontal lobe degeneration of non-Alzheimer type. I. Neuropathology. *Arch Gerontol Geriatr*. 1987;6(3):193-208. Epub 1987/09/01. doi: 10.1016/0167-4943(87)90021-5. PubMed PMID: 3689053.
44. Neary D, Snowden JS, Northen B, Goulding P. Dementia of frontal lobe type. *J Neurol Neurosurg Psychiatry*. 1988;51(3):353-61. Epub 1988/03/01. doi: 10.1136/jnnp.51.3.353. PubMed PMID: 3258902; PMCID: PMC1032860.
45. Clinical and neuropathological criteria for frontotemporal dementia. The Lund and Manchester Groups. *J Neurol Neurosurg Psychiatry*. 1994;57(4):416-8. Epub 1994/04/01. doi: 10.1136/jnnp.57.4.416. PubMed PMID: 8163988; PMCID: PMC1072868.
46. Neary D, Snowden JS, Mann DM. Classification and description of frontotemporal dementias. *Ann N Y Acad Sci*. 2000;920:46-51. Epub 2001/02/24. doi: 10.1111/j.1749-6632.2000.tb06904.x. PubMed PMID: 11193176.
47. Cairns NJ, Bigio EH, Mackenzie IR, Neumann M, Lee VM-Y, Hatanpaa KJ, White CL, Schneider JA, Grinberg LT, Halliday G. Neuropathologic diagnostic and nosologic criteria for frontotemporal lobar degeneration: consensus of the Consortium for Frontotemporal Lobar Degeneration. *Acta Neuropathol*. 2007;114:5-22.
48. Bott NT, Radke A, Stephens ML, Kramer JH. Frontotemporal dementia: diagnosis, deficits and management. *Neurodegener Dis Manag*. 2014;4(6):439-54. Epub 2014/12/23. doi: 10.2217/nmt.14.34. PubMed PMID: 25531687; PMCID: PMC4824317.
49. Roy ARK, Datta S, Hardy E, Sturm VE, Kramer JH, Seeley WW, Rankin KP, Rosen HJ, Miller BL, Perry DC. Behavioural subphenotypes and their anatomic correlates in neurodegenerative disease. *Brain Commun*. 2023;5(2):fcad038. Epub 2023/03/14. doi: 10.1093/braincomms/fcad038. PubMed PMID: 36910420; PMCID: PMC9999361.
50. Schubert S, Leyton CE, Hodges JR, Piguet O. Longitudinal Memory Profiles in Behavioral-Variant Frontotemporal Dementia and Alzheimer's Disease. *J Alzheimers Dis*. 2016;51(3):775-82. Epub 2016/02/19. doi: 10.3233/jad-150802. PubMed PMID: 26890749.
51. Johnson JK, Diehl J, Mendez MF, Neuhaus J, Shapira JS, Forman M, Chute DJ, Roberson ED, Pace-Savitsky C, Neumann M, Chow TW, Rosen HJ, Forstl H, Kurz A, Miller BL. Frontotemporal lobar degeneration: demographic characteristics of 353 patients. *Arch Neurol*. 2005;62(6):925-30. Epub 2005/06/16. doi: 10.1001/archneur.62.6.925. PubMed PMID: 15956163.
52. Rascovsky K, Hodges JR, Knopman D, Mendez MF, Kramer JH, Neuhaus J, van Swieten JC, Seelaar H, Dopper EG, Onyike CU, Hillis AE, Josephs KA, Boeve BF, Kertesz A, Seeley WW, Rankin KP, Johnson JK, Gorno-Tempini ML, Rosen H, Prioleau-Latham CE, Lee A, Kipps CM, Lillo P, Piguet O, Rohrer JD, Rossor MN, Warren JD, Fox NC, Galasko D, Salmon DP, Black SE, Mesulam M, Weintraub S, Dickerson BC, Diehl-Schmid J, Pasquier F, Deramecourt V, Lebert

- F, Pijnenburg Y, Chow TW, Manes F, Grafman J, Cappa SF, Freedman M, Grossman M, Miller BL. Sensitivity of revised diagnostic criteria for the behavioural variant of frontotemporal dementia. *Brain*. 2011;134(Pt 9):2456-77. Epub 2011/08/04. doi: 10.1093/brain/awr179. PubMed PMID: 21810890; PMCID: PMC3170532.
53. Gregory CA, Serra-Mestres J, Hodges JR. Early diagnosis of the frontal variant of frontotemporal dementia: how sensitive are standard neuroimaging and neuropsychologic tests? *Neuropsychiatry Neuropsychol Behav Neurol*. 1999;12(2):128-35. Epub 1999/05/01. PubMed PMID: 10223261.
54. Woolley JD, Khan BK, Murthy NK, Miller BL, Rankin KP. The diagnostic challenge of psychiatric symptoms in neurodegenerative disease: rates of and risk factors for prior psychiatric diagnosis in patients with early neurodegenerative disease. *J Clin Psychiatry*. 2011;72(2):126-33. Epub 2011/03/09. doi: 10.4088/JCP.10m06382oli. PubMed PMID: 21382304; PMCID: PMC3076589.
55. Rabinovici GD, Seeley WW, Kim EJ, Gorno-Tempini ML, Rascovsky K, Pagliaro TA, Allison SC, Halabi C, Kramer JH, Johnson JK, Weiner MW, Forman MS, Trojanowski JQ, Dearmond SJ, Miller BL, Rosen HJ. Distinct MRI atrophy patterns in autopsy-proven Alzheimer's disease and frontotemporal lobar degeneration. *Am J Alzheimers Dis Other Demen*. 2007;22(6):474-88. Epub 2008/01/02. doi: 10.1177/1533317507308779. PubMed PMID: 18166607; PMCID: PMC2443731.
56. Chan D, Anderson V, Pijnenburg Y, Whitwell J, Barnes J, Scahill R, Stevens JM, Barkhof F, Scheltens P, Rossor MN, Fox NC. The clinical profile of right temporal lobe atrophy. *Brain*. 2009;132(Pt 5):1287-98. Epub 2009/03/20. doi: 10.1093/brain/awp037. PubMed PMID: 19297506.
57. Henry ML, Wilson SM, Ogar JM, Sidhu MS, Rankin KP, Cattaruzza T, Miller BL, Gorno-Tempini ML, Seeley WW. Neuropsychological, behavioral, and anatomical evolution in right temporal variant frontotemporal dementia: a longitudinal and post-mortem single case analysis. *Neurocase*. 2014;20(1):100-9. Epub 2012/11/23. doi: 10.1080/13554794.2012.732089. PubMed PMID: 23171151; PMCID: PMC3775867.
58. Mesulam MM. Slowly progressive aphasia without generalized dementia. *Ann Neurol*. 1982;11(6):592-8. Epub 1982/06/01. doi: 10.1002/ana.410110607. PubMed PMID: 7114808.
59. Gorno-Tempini ML, Hillis AE, Weintraub S, Kertesz A, Mendez M, Cappa SF, Ogar JM, Rohrer JD, Black S, Boeve BF, Manes F, Dronkers NF, Vandenberghe R, Rascovsky K, Patterson K, Miller BL, Knopman DS, Hodges JR, Mesulam MM, Grossman M. Classification of primary progressive aphasia and its variants. *Neurology*. 2011;76(11):1006-14. Epub 2011/02/18. doi: 10.1212/WNL.0b013e31821103e6. PubMed PMID: 21325651; PMCID: PMC3059138.
60. Mesulam MM. Primary progressive aphasia. *Ann Neurol*. 2001;49(4):425-32. Epub 2001/04/20. PubMed PMID: 11310619.
61. Coyle-Gilchrist IT, Dick KM, Patterson K, Vázquez Rodríguez P, Wehmann E, Wilcox A, Lansdall CJ, Dawson KE, Wiggins J, Mead S, Brayne C, Rowe JB. Prevalence, characteristics, and survival of frontotemporal lobar degeneration syndromes. *Neurology*. 2016;86(18):1736-43. Epub 2016/04/03. doi: 10.1212/wnl.0000000000002638. PubMed PMID: 27037234; PMCID: PMC4854589.
62. Julie S, PJ G, Neary D. Semantic dementia: a form of circumscribed cerebral atrophy. *Behavioural Neurology*. 1989;2(3):167-82.
63. Grossman M, Mickanin J, Onishi K, Hughes E, D'Esposito M, Ding XS, Alavi A, Reivich M. Progressive Nonfluent Aphasia: Language, Cognitive, and PET Measures Contrasted with

- Probable Alzheimer's Disease. *J Cogn Neurosci*. 1996;8(2):135-54. Epub 1996/04/01. doi: 10.1162/jocn.1996.8.2.135. PubMed PMID: 23971420.
64. Gorno-Tempini ML, Dronkers NF, Rankin KP, Ogar JM, Phengrasamy L, Rosen HJ, Johnson JK, Weiner MW, Miller BL. Cognition and anatomy in three variants of primary progressive aphasia. *Ann Neurol*. 2004;55(3):335-46. Epub 2004/03/03. doi: 10.1002/ana.10825. PubMed PMID: 14991811; PMCID: PMC2362399.
65. Kertesz A, Jesso S, Harciarek M, Blair M, McMonagle P. What is semantic dementia?: a cohort study of diagnostic features and clinical boundaries. *Arch Neurol*. 2010;67(4):483-9. Epub 2010/04/14. doi: 10.1001/archneurol.2010.55. PubMed PMID: 20385916.
66. Snowden JS, Harris JM, Thompson JC, Kobylecki C, Jones M, Richardson AM, Neary D. Semantic dementia and the left and right temporal lobes. *Cortex*. 2018;107:188-203. Epub 2017/09/28. doi: 10.1016/j.cortex.2017.08.024. PubMed PMID: 28947063.
67. Ogar JM, Dronkers NF, Brambati SM, Miller BL, Gorno-Tempini ML. Progressive nonfluent aphasia and its characteristic motor speech deficits. *Alzheimer Disease & Associated Disorders*. 2007;21(4):S23-S30.
68. Hillis AE, Oh S, Ken L. Deterioration of naming nouns versus verbs in primary progressive aphasia. *Annals of Neurology: Official Journal of the American Neurological Association and the Child Neurology Society*. 2004;55(2):268-75.
69. Broe M, Hodges J, Schofield E, Shepherd C, Kril J, Halliday G. Staging disease severity in pathologically confirmed cases of frontotemporal dementia. *Neurology*. 2003;60(6):1005-11.
70. Mackenzie IRA, Neumann M, Bigio EH, Cairns NJ, Alafuzoff I, Kril J, Kovacs GG, Ghetti B, Halliday G, Holm IE, Ince PG, Kamphorst W, Revesz T, Rozemuller AJM, Kumar-Singh S, Akiyama H, Baborie A, Spina S, Dickson DW, Trojanowski JQ, Mann DMA. Nomenclature and nosology for neuropathologic subtypes of frontotemporal lobar degeneration: an update. *Acta Neuropathol*. 2010;119(1):1-4. doi: 10.1007/s00401-009-0612-2.
71. Holm IE, Isaacs AM, Mackenzie IR. Absence of FUS-immunoreactive pathology in frontotemporal dementia linked to chromosome 3 (FTD-3) caused by mutation in the CHMP2B gene. *Acta Neuropathol*. 2009;118(5):719-20. Epub 2009/10/22. doi: 10.1007/s00401-009-0593-1. PubMed PMID: 19844732.
72. Neumann M, Mackenzie IRA. Review: Neuropathology of non-tau frontotemporal lobar degeneration. *Neuropathol Appl Neurobiol*. 2019;45(1):19-40. doi: <https://doi.org/10.1111/nan.12526>.
73. Rohrer JD, Lashley T, Schott JM, Warren JE, Mead S, Isaacs AM, Beck J, Hardy J, De Silva R, Warrington E. Clinical and neuroanatomical signatures of tissue pathology in frontotemporal lobar degeneration. *Brain*. 2011;134(9):2565-81.
74. Josephs KA, Hodges JR, Snowden JS, Mackenzie IR, Neumann M, Mann DM, Dickson DW. Neuropathological background of phenotypical variability in frontotemporal dementia. *Acta Neuropathol*. 2011;122:137-53.
75. Mackenzie IRA, Neumann M. Molecular neuropathology of frontotemporal dementia: insights into disease mechanisms from postmortem studies. *Journal of Neurochemistry*. 2016;138(S1):54-70. doi: <https://doi.org/10.1111/jnc.13588>.
76. Murphy DB, Johnson KA, Borisy GG. Role of tubulin-associated proteins in microtubule nucleation and elongation. *Journal of Molecular Biology*. 1977;117(1):33-52. doi: [https://doi.org/10.1016/0022-2836\(77\)90021-3](https://doi.org/10.1016/0022-2836(77)90021-3).

77. Lee G, Leegers CJ. Tau and tauopathies. *Prog Mol Biol Transl Sci.* 2012;107:263-93. Epub 2012/04/10. doi: 10.1016/b978-0-12-385883-2.00004-7. PubMed PMID: 22482453; PMCID: PMC3614411.
78. Lee VM, Goedert M, Trojanowski JQ. Neurodegenerative tauopathies. *Annu Rev Neurosci.* 2001;24:1121-59. Epub 2001/08/25. doi: 10.1146/annurev.neuro.24.1.1121. PubMed PMID: 11520930.
79. Halliday G, Bigio EH, Cairns NJ, Neumann M, Mackenzie IRA, Mann DMA. Mechanisms of disease in frontotemporal lobar degeneration: gain of function versus loss of function effects. *Acta Neuropathol.* 2012;124(3):373-82. doi: 10.1007/s00401-012-1030-4.
80. Shi J, Shaw CL, Du Plessis D, Richardson AMT, Bailey KL, Julien C, Stopford C, Thompson J, Varma A, Craufurd D, Tian J, Pickering-Brown S, Neary D, Snowden JS, Mann DMA. Histopathological changes underlying frontotemporal lobar degeneration with clinicopathological correlation. *Acta Neuropathol.* 2005;110(5):501-12. doi: 10.1007/s00401-005-1079-4.
81. Bahia VS, Takada LT, Deramecourt V. Neuropathology of frontotemporal lobar degeneration: a review. *Dement Neuropsychol.* 2013;7(1):19-26. doi: 10.1590/S1980-57642013DN70100004. PubMed PMID: 29213815.
82. Neumann M, Lee EB, Mackenzie IR. Frontotemporal Lobar Degeneration TDP-43-Immunoreactive Pathological Subtypes: Clinical and Mechanistic Significance. *Adv Exp Med Biol.* 2021;1281:201-17. Epub 2021/01/13. doi: 10.1007/978-3-030-51140-1_13. PubMed PMID: 33433877; PMCID: PMC8183578.
83. Gao J, Wang L, Huntley ML, Perry G, Wang X. Pathomechanisms of TDP-43 in neurodegeneration. *J Neurochem.* 2018. Epub 2018/02/28. doi: 10.1111/jnc.14327. PubMed PMID: 29486049; PMCID: PMC6110993.
84. Ou SH, Wu F, Harrich D, García-Martínez LF, Gaynor RB. Cloning and characterization of a novel cellular protein, TDP-43, that binds to human immunodeficiency virus type 1 TAR DNA sequence motifs. *J Virol.* 1995;69(6):3584-96. Epub 1995/06/01. doi: 10.1128/jvi.69.6.3584-3596.1995. PubMed PMID: 7745706; PMCID: PMC189073.
85. Prasad A, Bharathi V, Sivalingam V, Girdhar A, Patel BK. Molecular Mechanisms of TDP-43 Misfolding and Pathology in Amyotrophic Lateral Sclerosis. *Front Mol Neurosci.* 2019;12:25. Epub 2019/03/07. doi: 10.3389/fnmol.2019.00025. PubMed PMID: 30837838; PMCID: PMC6382748.
86. Mackenzie IR, Neumann M, Baborie A, Sampathu DM, Du Plessis D, Jaros E, Perry RH, Trojanowski JQ, Mann DM, Lee VM. A harmonized classification system for FTLTDP pathology. *Acta Neuropathol.* 2011;122(1):111-3. Epub 2011/06/07. doi: 10.1007/s00401-011-0845-8. PubMed PMID: 21644037; PMCID: PMC3285143.
87. Burrell JR, Halliday GM, Kril JJ, Ittner LM, Götz J, Kiernan MC, Hodges JR. The frontotemporal dementia-motor neuron disease continuum. *Lancet.* 2016;388(10047):919-31. Epub 2016/03/19. doi: 10.1016/s0140-6736(16)00737-6. PubMed PMID: 26987909.
88. Tan RH, Ke YD, Ittner LM, Halliday GM. ALS/FTLD: experimental models and reality. *Acta Neuropathol.* 2017;133(2):177-96. Epub 2017/01/07. doi: 10.1007/s00401-016-1666-6. PubMed PMID: 28058507.
89. Van Mossevelde S, Engelborghs S, van der Zee J, Van Broeckhoven C. Genotype-phenotype links in frontotemporal lobar degeneration. *Nat Rev Neurol.* 2018;14(6):363-78. Epub 2018/05/20. doi: 10.1038/s41582-018-0009-8. PubMed PMID: 29777184.

90. Urwin H, Authier A, Nielsen JE, Metcalf D, Powell C, Froud K, Malcolm DS, Holm I, Johannsen P, Brown J, Fisher EM, van der Zee J, Bruyland M, Consortium FR, Van Broeckhoven C, Collinge J, Brandner S, Futter C, Isaacs AM. Disruption of endocytic trafficking in frontotemporal dementia with CHMP2B mutations. *Hum Mol Genet.* 2010;19(11):2228-38. Epub 2010/03/13. doi: 10.1093/hmg/ddq100. PubMed PMID: 20223751; PMCID: PMC2865375.
91. Neumann M, Valori CF, Ansorge O, Kretzschmar HA, Munoz DG, Kusaka H, Yokota O, Ishihara K, Ang LC, Bilbao JM, Mackenzie IR. Transportin 1 accumulates specifically with FET proteins but no other transportin cargos in FTLD-FUS and is absent in FUS inclusions in ALS with FUS mutations. *Acta Neuropathol.* 2012;124(5):705-16. Epub 2012/07/31. doi: 10.1007/s00401-012-1020-6. PubMed PMID: 22842875.
92. Andersson MK, Ståhlberg A, Arvidsson Y, Olofsson A, Semb H, Stenman G, Nilsson O, Aman P. The multifunctional FUS, EWS and TAF15 proto-oncoproteins show cell type-specific expression patterns and involvement in cell spreading and stress response. *BMC Cell Biol.* 2008;9:37. Epub 2008/07/16. doi: 10.1186/1471-2121-9-37. PubMed PMID: 18620564; PMCID: PMC2478660.
93. Schwartz JC, Cech TR, Parker RR. Biochemical Properties and Biological Functions of FET Proteins. *Annu Rev Biochem.* 2015;84:355-79. Epub 2014/12/11. doi: 10.1146/annurev-biochem-060614-034325. PubMed PMID: 25494299; PMCID: PMC9188303.
94. Pottier C, Ravenscroft TA, Sanchez-Contreras M, Rademakers R. Genetics of FTLD: overview and what else we can expect from genetic studies. *Journal of Neurochemistry.* 2016;138(S1):32-53. doi: 10.1111/jnc.13622.
95. Mackenzie IR, Foti D, Woulfe J, Hurwitz TA. Atypical frontotemporal lobar degeneration with ubiquitin-positive, TDP-43-negative neuronal inclusions. *Brain.* 2008;131(Pt 5):1282-93. Epub 2008/03/26. doi: 10.1093/brain/awn061. PubMed PMID: 18362096.
96. Mann DMA, Snowden JS. Frontotemporal lobar degeneration: Pathogenesis, pathology and pathways to phenotype. *Brain Pathol.* 2017;27(6):723-36. Epub 2017/01/19. doi: 10.1111/bpa.12486. PubMed PMID: 28100023; PMCID: PMC8029341.
97. Munoz DG, Neumann M, Kusaka H, Yokota O, Ishihara K, Terada S, Kuroda S, Mackenzie IR. FUS pathology in basophilic inclusion body disease. *Acta Neuropathol.* 2009;118(5):617-27. Epub 2009/10/16. doi: 10.1007/s00401-009-0598-9. PubMed PMID: 19830439.
98. Cairns NJ, Grossman M, Arnold SE, Burn DJ, Jaros E, Perry RH, Duyckaerts C, Stankoff B, Pillon B, Skullerud K, Cruz-Sanchez FF, Bigio EH, Mackenzie IR, Gearing M, Juncos JL, Glass JD, Yokoo H, Nakazato Y, Mosaheb S, Thorpe JR, Uryu K, Lee VM, Trojanowski JQ. Clinical and neuropathologic variation in neuronal intermediate filament inclusion disease. *Neurology.* 2004;63(8):1376-84. Epub 2004/10/27. doi: 10.1212/01.wnl.0000139809.16817.dd. PubMed PMID: 15505152; PMCID: PMC3516854.
99. Neumann M, Roeber S, Kretzschmar HA, Rademakers R, Baker M, Mackenzie IR. Abundant FUS-immunoreactive pathology in neuronal intermediate filament inclusion disease. *Acta Neuropathol.* 2009;118(5):605-16. Epub 2009/08/12. doi: 10.1007/s00401-009-0581-5. PubMed PMID: 19669651; PMCID: PMC2864784.
100. Mackenzie IR, Munoz DG, Kusaka H, Yokota O, Ishihara K, Roeber S, Kretzschmar HA, Cairns NJ, Neumann M. Distinct pathological subtypes of FTLD-FUS. *Acta Neuropathol.* 2011;121(2):207-18. Epub 2010/11/06. doi: 10.1007/s00401-010-0764-0. PubMed PMID: 21052700.

101. Richter H. Eine besondere art von stirnhirnschwund mit verblödung. *Zeitschrift für die gesamte Neurologie und Psychiatrie: Originalien*. 1918:127-60.
102. Rohrer JD, Guerreiro R, Vandrovcova J, Uphill J, Reiman D, Beck J, Isaacs AM, Authier A, Ferrari R, Fox NC, Mackenzie IR, Warren JD, de Silva R, Holton J, Revesz T, Hardy J, Mead S, Rossor MN. The heritability and genetics of frontotemporal lobar degeneration. *Neurology*. 2009;73(18):1451-6. Epub 2009/11/04. doi: 10.1212/WNL.0b013e3181bf997a. PubMed PMID: 19884572; PMCID: PMC2779007.
103. Wood EM, Falcone D, Suh E, Irwin DJ, Chen-Plotkin AS, Lee EB, Xie SX, Van Deerlin VM, Grossman M. Development and validation of pedigree classification criteria for frontotemporal lobar degeneration. *JAMA Neurol*. 2013;70(11):1411-7. Epub 2013/10/02. doi: 10.1001/jamaneurol.2013.3956. PubMed PMID: 24081456; PMCID: PMC3906581.
104. Cacace R, Slegers K, Van Broeckhoven C. Molecular genetics of early-onset Alzheimer's disease revisited. *Alzheimers Dement*. 2016;12(6):733-48. Epub 2016/03/27. doi: 10.1016/j.jalz.2016.01.012. PubMed PMID: 27016693.
105. Borroni B, Alberici A, Archetti S, Magnani E, Di Luca M, Padovani A. New insights into biological markers of frontotemporal lobar degeneration spectrum. *Curr Med Chem*. 2010;17(10):1002-9. Epub 2010/02/17. doi: 10.2174/092986710790820651. PubMed PMID: 20156164.
106. Sieben A, Van Langenhove T, Engelborghs S, Martin JJ, Boon P, Cras P, De Deyn PP, Santens P, Van Broeckhoven C, Cruts M. The genetics and neuropathology of frontotemporal lobar degeneration. *Acta Neuropathol*. 2012;124(3):353-72. Epub 2012/08/15. doi: 10.1007/s00401-012-1029-x. PubMed PMID: 22890575; PMCID: PMC3422616.
107. Cruts M, Van Broeckhoven C. Data Mining: Applying the AD&FTD Mutation Database to Progranulin. *Methods in molecular biology (Clifton, NJ)*. 2018;1806:81-92. Epub 2018/06/30. doi: 10.1007/978-1-4939-8559-3_6. PubMed PMID: 29956270.
108. Le Ber I, Camuzat A, Berger E, Hannequin D, Laquerrière A, Golfier V, Seilhean D, Viennet G, Couratier P, Verpillat P, Heath S, Camu W, Martinaud O, Lacomblez L, Vercelletto M, Salachas F, Sellal F, Didic M, Thomas-Anterion C, Puel M, Michel BF, Besse C, Duyckaerts C, Meininger V, Campion D, Dubois B, Brice A. Chromosome 9p-linked families with frontotemporal dementia associated with motor neuron disease. *Neurology*. 2009;72(19):1669-76. Epub 2009/05/13. doi: 10.1212/WNL.0b013e3181a55f1c. PubMed PMID: 19433740.
109. Valdmanis PN, Dupre N, Bouchard JP, Camu W, Salachas F, Meininger V, Strong M, Rouleau GA. Three families with amyotrophic lateral sclerosis and frontotemporal dementia with evidence of linkage to chromosome 9p. *Arch Neurol*. 2007;64(2):240-5. Epub 2007/02/14. doi: 10.1001/archneur.64.2.240. PubMed PMID: 17296840.
110. Vance C, Al-Chalabi A, Ruddy D, Smith BN, Hu X, Sreedharan J, Siddique T, Schelhaas HJ, Kusters B, Troost D, Baas F, de Jong V, Shaw CE. Familial amyotrophic lateral sclerosis with frontotemporal dementia is linked to a locus on chromosome 9p13.2-21.3. *Brain*. 2006;129(Pt 4):868-76. Epub 2006/02/24. doi: 10.1093/brain/awl030. PubMed PMID: 16495328.
111. DeJesus-Hernandez M, Mackenzie IR, Boeve BF, Boxer AL, Baker M, Rutherford NJ, Nicholson AM, Finch NA, Flynn H, Adamson J, Kouri N, Wojtas A, Sengdy P, Hsiung GY, Karydas A, Seeley WW, Josephs KA, Coppola G, Geschwind DH, Wszolek ZK, Feldman H, Knopman DS, Petersen RC, Miller BL, Dickson DW, Boylan KB, Graff-Radford NR, Rademakers R. Expanded GGGGCC hexanucleotide repeat in noncoding region of C9ORF72 causes chromosome 9p-linked FTD and ALS. *Neuron*. 2011;72(2):245-56. Epub 2011/09/29. doi: 10.1016/j.neuron.2011.09.011. PubMed PMID: 21944778; PMCID: PMC3202986.

112. Renton AE, Majounie E, Waite A, Simón-Sánchez J, Rollinson S, Gibbs JR, Schymick JC, Laaksovirta H, van Swieten JC, Myllykangas L, Kalimo H, Paetau A, Abramzon Y, Remes AM, Kaganovich A, Scholz SW, Duckworth J, Ding J, Harmer DW, Hernandez DG, Johnson JO, Mok K, Ryten M, Trabzuni D, Guerreiro RJ, Orrell RW, Neal J, Murray A, Pearson J, Jansen IE, Sondervan D, Seelaar H, Blake D, Young K, Halliwell N, Callister JB, Toulson G, Richardson A, Gerhard A, Snowden J, Mann D, Neary D, Nalls MA, Peuralinna T, Jansson L, Isoviita VM, Kaivorinne AL, Hölttä-Vuori M, Ikonen E, Sulkava R, Benatar M, Wu J, Chiò A, Restagno G, Borghero G, Sabatelli M, Heckerman D, Rogaeva E, Zinman L, Rothstein JD, Sendtner M, Drepper C, Eichler EE, Alkan C, Abdullaev Z, Pack SD, Dutra A, Pak E, Hardy J, Singleton A, Williams NM, Heutink P, Pickering-Brown S, Morris HR, Tienari PJ, Traynor BJ. A hexanucleotide repeat expansion in C9ORF72 is the cause of chromosome 9p21-linked ALS-FTD. *Neuron*. 2011;72(2):257-68. Epub 2011/09/29. doi: 10.1016/j.neuron.2011.09.010. PubMed PMID: 21944779; PMCID: PMC3200438.
113. Rademakers R, Neumann M, Mackenzie IR. Advances in understanding the molecular basis of frontotemporal dementia. *Nat Rev Neurol*. 2012;8(8):423-34. Epub 2012/06/27. doi: 10.1038/nrneurol.2012.117. PubMed PMID: 22732773; PMCID: PMC3629543.
114. Majounie E, Renton AE, Mok K, Dopper EG, Waite A, Rollinson S, Chiò A, Restagno G, Nicolaou N, Simon-Sanchez J, van Swieten JC, Abramzon Y, Johnson JO, Sendtner M, Pamphelet R, Orrell RW, Mead S, Sidle KC, Houlden H, Rohrer JD, Morrison KE, Pall H, Talbot K, Ansorge O, Hernandez DG, Arepalli S, Sabatelli M, Mora G, Corbo M, Giannini F, Calvo A, Englund E, Borghero G, Floris GL, Remes AM, Laaksovirta H, McCluskey L, Trojanowski JQ, Van Deerlin VM, Schellenberg GD, Nalls MA, Drory VE, Lu CS, Yeh TH, Ishiura H, Takahashi Y, Tsuji S, Le Ber I, Brice A, Drepper C, Williams N, Kirby J, Shaw P, Hardy J, Tienari PJ, Heutink P, Morris HR, Pickering-Brown S, Traynor BJ. Frequency of the C9orf72 hexanucleotide repeat expansion in patients with amyotrophic lateral sclerosis and frontotemporal dementia: a cross-sectional study. *Lancet Neurol*. 2012;11(4):323-30. Epub 2012/03/13. doi: 10.1016/s1474-4422(12)70043-1. PubMed PMID: 22406228; PMCID: PMC3322422.
115. Taylor JP, Brown RH, Jr., Cleveland DW. Decoding ALS: from genes to mechanism. *Nature*. 2016;539(7628):197-206. Epub 2016/11/11. doi: 10.1038/nature20413. PubMed PMID: 27830784; PMCID: PMC5585017.
116. Balendra R, Isaacs AM. C9orf72-mediated ALS and FTD: multiple pathways to disease. *Nat Rev Neurol*. 2018;14(9):544-58. Epub 2018/08/19. doi: 10.1038/s41582-018-0047-2. PubMed PMID: 30120348; PMCID: PMC6417666.
117. Haeusler AR, Donnelly CJ, Rothstein JD. The expanding biology of the C9orf72 nucleotide repeat expansion in neurodegenerative disease. *Nat Rev Neurosci*. 2016;17(6):383-95. Epub 2016/05/07. doi: 10.1038/nrn.2016.38. PubMed PMID: 27150398; PMCID: PMC7376590.
118. Dobson-Stone C, Hallupp M, Bartley L, Shepherd CE, Halliday GM, Schofield PR, Hodges JR, Kwok JB. C9ORF72 repeat expansion in clinical and neuropathologic frontotemporal dementia cohorts. *Neurology*. 2012;79(10):995-1001. Epub 2012/08/10. doi: 10.1212/WNL.0b013e3182684634. PubMed PMID: 22875086; PMCID: PMC3430710.
119. Snowden JS, Adams J, Harris J, Thompson JC, Rollinson S, Richardson A, Jones M, Neary D, Mann DM, Pickering-Brown S. Distinct clinical and pathological phenotypes in frontotemporal dementia associated with MAPT, PGRN and C9orf72 mutations. *Amyotrophic Lateral Sclerosis and Frontotemporal Degeneration*. 2015;16(7-8):497-505.

120. Poorkaj P, Bird TD, Wijsman E, Nemens E, Garruto RM, Anderson L, Andreadis A, Wiederholt WC, Raskind M, Schellenberg GD. Tau is a candidate gene for chromosome 17 frontotemporal dementia. *Annals of Neurology*. 1998;43(6):815-25. doi: 10.1002/ana.410430617.
121. Hutton M, Lendon CL, Rizzu P, Baker M, Froelich S, Houlden H, Pickering-Brown S, Chakraverty S, Isaacs A, Grover A, Hackett J, Adamson J, Lincoln S, Dickson D, Davies P, Petersen RC, Stevens M, de Graaff E, Wauters E, van Baren J, Hillebrand M, Joosse M, Kwon JM, Nowotny P, Che LK, Norton J, Morris JC, Reed LA, Trojanowski J, Basun H, Lannfelt L, Neystat M, Fahn S, Dark F, Tannenberg T, Dodd PR, Hayward N, Kwok JBJ, Schofield PR, Andreadis A, Snowden J, Craufurd D, Neary D, Owen F, Oostra BA, Hardy J, Goate A, van Swieten J, Mann D, Lynch T, Heutink P. Association of missense and 5'-splice-site mutations in tau with the inherited dementia FTDP-17. *Nature*. 1998;393(6686):702-5. doi: 10.1038/31508.
122. Spillantini MG, Murrell JR, Goedert M, Farlow MR, Klug A, Ghetti B. Mutation in the tau gene in familial multiple system tauopathy with presenile dementia. *Proc Natl Acad Sci U S A*. 1998;95(13):7737-41. doi: 10.1073/pnas.95.13.7737. PubMed PMID: 9636220.
123. Rohrer JD, Warren JD. Phenotypic signatures of genetic frontotemporal dementia. *Current Opinion in Neurology*. 2011;24(6):542-9. doi: 10.1097/WCO.0b013e32834cd442. PubMed PMID: 00019052-201112000-00005.
124. Greaves CV, Rohrer JD. An update on genetic frontotemporal dementia. *Journal of Neurology*. 2019;266(8):2075-86. doi: 10.1007/s00415-019-09363-4.
125. Ghetti B, Oblak AL, Boeve BF, Johnson KA, Dickerson BC, Goedert M. Invited review: Frontotemporal dementia caused by microtubule-associated protein tau gene (MAPT) mutations: a chameleon for neuropathology and neuroimaging. *Neuropathol Appl Neurobiol*. 2015;41(1):24-46. Epub 2015/01/06. doi: 10.1111/nan.12213. PubMed PMID: 25556536; PMCID: PMC4329416.
126. Rademakers R, Cruts M, Van Broeckhoven C. The role of tau (MAPT) in frontotemporal dementia and related tauopathies. *Human mutation*. 2004;24(4):277-95.
127. LeBoeuf AC, Levy SF, Gaylord M, Bhattacharya A, Singh AK, Jordan MA, Wilson L, Feinstein SC. FTDP-17 mutations in Tau alter the regulation of microtubule dynamics: an "alternative core" model for normal and pathological Tau action. *The Journal of biological chemistry*. 2008;283(52):36406-15. Epub 2008/10/21. doi: 10.1074/jbc.M803519200. PubMed PMID: 18940799.
128. Espay AJ, Litvan I. Parkinsonism and frontotemporal dementia: the clinical overlap. *Journal of Molecular Neuroscience*. 2011;45:343-9.
129. Boeve BF, Hutton M. Refining frontotemporal dementia with parkinsonism linked to chromosome 17: introducing FTDP-17 (MAPT) and FTDP-17 (PGRN). *Arch Neurol*. 2008;65(4):460-4.
130. Neumann M, Sampathu DM, Kwong LK, Truax AC, Micsenyi MC, Chou TT, Bruce J, Schuck T, Grossman M, Clark CM, McCluskey LF, Miller BL, Masliah E, Mackenzie IR, Feldman H, Feiden W, Kretschmar HA, Trojanowski JQ, Lee VM. Ubiquitinated TDP-43 in frontotemporal lobar degeneration and amyotrophic lateral sclerosis. *Science*. 2006;314(5796):130-3. Epub 2006/10/07. doi: 10.1126/science.1134108. PubMed PMID: 17023659.
131. Arai T, Hasegawa M, Akiyama H, Ikeda K, Nonaka T, Mori H, Mann D, Tsuchiya K, Yoshida M, Hashizume Y, Oda T. TDP-43 is a component of ubiquitin-positive tau-negative inclusions in frontotemporal lobar degeneration and amyotrophic lateral sclerosis. *Biochem*

Biophys Res Commun. 2006;351(3):602-11. Epub 2006/11/07. doi: 10.1016/j.bbrc.2006.10.093. PubMed PMID: 17084815.

132. Baker M, Mackenzie IR, Pickering-Brown SM, Gass J, Rademakers R, Lindholm C, Snowden J, Adamson J, Sadovnick AD, Rollinson S, Cannon A, Dwosh E, Neary D, Melquist S, Richardson A, Dickson D, Berger Z, Eriksen J, Robinson T, Zehr C, Dickey CA, Crook R, McGowan E, Mann D, Boeve B, Feldman H, Hutton M. Mutations in progranulin cause tau-negative frontotemporal dementia linked to chromosome 17. *Nature*. 2006;442(7105):916-9. doi: 10.1038/nature05016.

133. Cruts M, Gijselinck I, van der Zee J, Engelborghs S, Wils H, Pirici D, Rademakers R, Vandenberghe R, Dermaut B, Martin J-J, van Duijn C, Peeters K, Sciot R, Santens P, De Pooter T, Mattheijssens M, Van den Broeck M, Cuijt I, Vennekens KI, De Deyn PP, Kumar-Singh S, Van Broeckhoven C. Null mutations in progranulin cause ubiquitin-positive frontotemporal dementia linked to chromosome 17q21. *Nature*. 2006;442(7105):920-4. doi: 10.1038/nature05017.

134. Gass J, Cannon A, Mackenzie IR, Boeve B, Baker M, Adamson J, Crook R, Melquist S, Kuntz K, Petersen R, Josephs K, Pickering-Brown SM, Graff-Radford N, Uitti R, Dickson D, Wszolek Z, Gonzalez J, Beach TG, Bigio E, Johnson N, Weintraub S, Mesulam M, White CL, 3rd, Woodruff B, Caselli R, Hsiung GY, Feldman H, Knopman D, Hutton M, Rademakers R. Mutations in progranulin are a major cause of ubiquitin-positive frontotemporal lobar degeneration. *Hum Mol Genet*. 2006;15(20):2988-3001. Epub 2006/09/05. doi: 10.1093/hmg/ddl241. PubMed PMID: 16950801.

135. Finch N, Baker M, Crook R, Swanson K, Kuntz K, Surtees R, Bisceglia G, Rovelet-Lecrux A, Boeve B, Petersen RC, Dickson DW, Younkin SG, Deramecourt V, Crook J, Graff-Radford NR, Rademakers R. Plasma progranulin levels predict progranulin mutation status in frontotemporal dementia patients and asymptomatic family members. *Brain*. 2009;132(Pt 3):583-91. Epub 2009/01/23. doi: 10.1093/brain/awn352. PubMed PMID: 19158106; PMCID: PMC2664450.

136. De Riz M, Galimberti D, Fenoglio C, Piccio LM, Scalabrini D, Venturelli E, Pietroboni A, Piola M, Naismith RT, Parks BJ, Fumagalli G, Bresolin N, Cross AH, Scarpini E. Cerebrospinal fluid progranulin levels in patients with different multiple sclerosis subtypes. *Neurosci Lett*. 2010;469(2):234-6. Epub 2009/12/08. doi: 10.1016/j.neulet.2009.12.002. PubMed PMID: 19963041; PMCID: PMC2893414.

137. Nguyen AD, Nguyen TA, Zhang J, Devireddy S, Zhou P, Karydas AM, Xu X, Miller BL, Rigo F, Ferguson SM, Huang EJ, Walther TC, Farese RV. Murine knockin model for progranulin-deficient frontotemporal dementia with nonsense-mediated mRNA decay. *Proceedings of the National Academy of Sciences*. 2018;115(12):E2849-E58. doi: 10.1073/pnas.1722344115.

138. Yu CE, Bird TD, Bekris LM, Montine TJ, Leverenz JB, Steinbart E, Galloway NM, Feldman H, Woltjer R, Miller CA, Wood EM, Grossman M, McCluskey L, Clark CM, Neumann M, Danek A, Galasko DR, Arnold SE, Chen-Plotkin A, Karydas A, Miller BL, Trojanowski JQ, Lee VM, Schellenberg GD, Van Deerlin VM. The spectrum of mutations in progranulin: a collaborative study screening 545 cases of neurodegeneration. *Arch Neurol*. 2010;67(2):161-70. Epub 2010/02/10. doi: 10.1001/archneurol.2009.328. PubMed PMID: 20142524; PMCID: PMC2901991.

139. Huey ED, Grafman J, Wassermann EM, Pietrini P, Tierney MC, Ghetti B, Spina S, Baker M, Hutton M, Elder JW, Berger SL, Heflin KA, Hardy J, Momeni P. Characteristics of frontotemporal dementia patients with a Progranulin mutation. *Ann Neurol*. 2006;60(3):374-80. Epub 2006/09/20. doi: 10.1002/ana.20969. PubMed PMID: 16983677; PMCID: PMC2987739.

140. Le Ber I, van der Zee J, Hannequin D, Gijselinck I, Campion D, Puel M, Laquerrière A, De Pooter T, Camuzat A, Van den Broeck M, Dubois B, Sellal F, Lacomblez L, Vercelletto M, Thomas-Antérion C, Michel BF, Golfier V, Didic M, Salachas F, Duyckaerts C, Cruts M, Verpillat P, Van Broeckhoven C, Brice A. Progranulin null mutations in both sporadic and familial frontotemporal dementia. *Hum Mutat.* 2007;28(9):846-55. Epub 2007/04/17. doi: 10.1002/humu.20520. PubMed PMID: 17436289.
141. van Swieten JC, Heutink P. Mutations in progranulin (GRN) within the spectrum of clinical and pathological phenotypes of frontotemporal dementia. *Lancet Neurol.* 2008;7(10):965-74. Epub 2008/09/06. doi: 10.1016/s1474-4422(08)70194-7. PubMed PMID: 18771956.
142. Xu HM, Tan L, Wan Y, Tan MS, Zhang W, Zheng ZJ, Kong LL, Wang ZX, Jiang T, Tan L, Yu JT. PGRN Is Associated with Late-Onset Alzheimer's Disease: a Case-Control Replication Study and Meta-analysis. *Mol Neurobiol.* 2017;54(2):1187-95. Epub 2016/01/29. doi: 10.1007/s12035-016-9698-4. PubMed PMID: 26820675.
143. Sheng J, Su L, Xu Z, Chen G. Progranulin polymorphism rs5848 is associated with increased risk of Alzheimer's disease. *Gene.* 2014;542(2):141-5. Epub 2014/04/01. doi: 10.1016/j.gene.2014.03.041. PubMed PMID: 24680777.
144. Chang KH, Chen CM, Chen YC, Hsiao YC, Huang CC, Kuo HC, Hsu HC, Lee-Chen GJ, Wu YR. Association between GRN rs5848 polymorphism and Parkinson's disease in Taiwanese population. *PLoS One.* 2013;8(1):e54448. Epub 2013/01/24. doi: 10.1371/journal.pone.0054448. PubMed PMID: 23342160; PMCID: PMC3546937.
145. Chen Y, Li S, Su L, Sheng J, Lv W, Chen G, Xu Z. Association of progranulin polymorphism rs5848 with neurodegenerative diseases: a meta-analysis. *J Neurol.* 2015;262(4):814-22. Epub 2015/01/13. doi: 10.1007/s00415-014-7630-2. PubMed PMID: 25578179.
146. Zhou J, Gao G, Crabb JW, Serrero G. Purification of an autocrine growth factor homologous with mouse epithelin precursor from a highly tumorigenic cell line. *J Biol Chem.* 1993;268(15):10863-9. Epub 1993/05/25. PubMed PMID: 8496151.
147. Baba T, Hoff HB, 3rd, Nemoto H, Lee H, Orth J, Arai Y, Gerton GL. Acrogranin, an acrosomal cysteine-rich glycoprotein, is the precursor of the growth-modulating peptides, granulins, and epithelins, and is expressed in somatic as well as male germ cells. *Mol Reprod Dev.* 1993;34(3):233-43. Epub 1993/03/01. doi: 10.1002/mrd.1080340302. PubMed PMID: 8471244.
148. Plowman GD, Green JM, Neubauer MG, Buckley SD, McDonald VL, Todaro GJ, Shoyab M. The epithelin precursor encodes two proteins with opposing activities on epithelial cell growth. *J Biol Chem.* 1992;267(18):13073-8. Epub 1992/06/25. PubMed PMID: 1618805.
149. Xu SQ, Tang D, Chamberlain S, Pronk G, Masiarz FR, Kaur S, Prisco M, Zanocco-Marani T, Baserga R. The granulin/epithelin precursor abrogates the requirement for the insulin-like growth factor 1 receptor for growth in vitro. *J Biol Chem.* 1998;273(32):20078-83. Epub 1998/08/01. doi: 10.1074/jbc.273.32.20078. PubMed PMID: 9685348.
150. Parnell PG, Wunderlich J, Carter B, Halper J. Transforming growth factor e: amino acid analysis and partial amino acid sequence. *Growth Factors.* 1992;7(1):65-72. Epub 1992/01/01. doi: 10.3109/08977199209023938. PubMed PMID: 1503782.
151. Eichinger L, Pachebat JA, Glöckner G, Rajandream MA, Sucgang R, Berriman M, Song J, Olsen R, Szafranski K, Xu Q, Tunggal B, Kummerfeld S, Madera M, Konfortov BA, Rivero F, Bankier AT, Lehmann R, Hamlin N, Davies R, Gaudet P, Fey P, Pilcher K, Chen G, Saunders D, Sodergren E, Davis P, Kerhornou A, Nie X, Hall N, Anjard C, Hemphill L, Bason N, Farbrother P, Desany B, Just E, Morio T, Rost R, Churcher C, Cooper J, Haydock S, van Driessche N, Cronin

- A, Goodhead I, Muzny D, Mourier T, Pain A, Lu M, Harper D, Lindsay R, Hauser H, James K, Quiles M, Madan Babu M, Saito T, Buchrieser C, Wardroper A, Felder M, Thangavelu M, Johnson D, Knights A, Loulseged H, Mungall K, Oliver K, Price C, Quail MA, Urushihara H, Hernandez J, Rabbinowitsch E, Steffen D, Sanders M, Ma J, Kohara Y, Sharp S, Simmonds M, Spiegler S, Tivey A, Sugano S, White B, Walker D, Woodward J, Winckler T, Tanaka Y, Shaulsky G, Schleicher M, Weinstock G, Rosenthal A, Cox EC, Chisholm RL, Gibbs R, Loomis WF, Platzer M, Kay RR, Williams J, Dear PH, Noegel AA, Barrell B, Kuspa A. The genome of the social amoeba *Dictyostelium discoideum*. *Nature*. 2005;435(7038):43-57. Epub 2005/05/06. doi: 10.1038/nature03481. PubMed PMID: 15875012; PMCID: PMC1352341.
152. Cadieux B, Chitramuthu BP, Baranowski D, Bennett HP. The zebrafish progranulin gene family and antisense transcripts. *BMC Genomics*. 2005;6:156. Epub 2005/11/10. doi: 10.1186/1471-2164-6-156. PubMed PMID: 16277664; PMCID: PMC1310530.
153. Palfree RG, Bennett HP, Bateman A. The Evolution of the Secreted Regulatory Protein Progranulin. *PLoS One*. 2015;10(8):e0133749. Epub 2015/08/08. doi: 10.1371/journal.pone.0133749. PubMed PMID: 26248158; PMCID: PMC4527844.
154. Lee MJ, Chen TF, Cheng TW, Chiu MJ. rs5848 variant of progranulin gene is a risk of Alzheimer's disease in the Taiwanese population. *Neurodegener Dis*. 2011;8(4):216-20. Epub 2011/01/08. doi: 10.1159/000322538. PubMed PMID: 21212639.
155. Reho P, Koga S, Shah Z, Chia R, Rademakers R, Dalgard CL, Boeve BF, Beach TG, Dickson DW, Ross OA, Scholz SW. GRN Mutations Are Associated with Lewy Body Dementia. *Mov Disord*. 2022;37(9):1943-8. Epub 2022/07/11. doi: 10.1002/mds.29144. PubMed PMID: 35810449; PMCID: PMC9474656.
156. Dugan AJ, Nelson PT, Katsumata Y, Shade LMP, Boehme KL, Teylan MA, Cykowski MD, Mukherjee S, Kauwe JSK, Hohman TJ, Schneider JA, Fardo DW. Analysis of genes (TMEM106B, GRN, ABCC9, KCNMB2, and APOE) implicated in risk for LATE-NC and hippocampal sclerosis provides pathogenetic insights: a retrospective genetic association study. *Acta Neuropathol Commun*. 2021;9(1):152. Epub 2021/09/17. doi: 10.1186/s40478-021-01250-2. PubMed PMID: 34526147; PMCID: PMC8442328.
157. Zhou X, Sun L, Bastos de Oliveira F, Qi X, Brown WJ, Smolka MB, Sun Y, Hu F. Prosaposin facilitates sortilin-independent lysosomal trafficking of progranulin. *The Journal of cell biology*. 2015;210(6):991-1002. doi: 10.1083/jcb.201502029. PubMed PMID: 26370502.
158. Daniel R, He Z, Carmichael KP, Halper J, Bateman A. Cellular localization of gene expression for progranulin. *J Histochem Cytochem*. 2000;48(7):999-1009. Epub 2000/06/17. doi: 10.1177/002215540004800713. PubMed PMID: 10858277.
159. Toh H, Chitramuthu BP, Bennett HP, Bateman A. Structure, function, and mechanism of progranulin; the brain and beyond. *J Mol Neurosci*. 2011;45(3):538-48. Epub 2011/06/22. doi: 10.1007/s12031-011-9569-4. PubMed PMID: 21691802.
160. Root J, Merino P, Nuckols A, Johnson M, Kukar T. Lysosome dysfunction as a cause of neurodegenerative diseases: Lessons from frontotemporal dementia and amyotrophic lateral sclerosis. *Neurobiology of Disease*. 2021;154:105360. doi: <https://doi.org/10.1016/j.nbd.2021.105360>.
161. Díaz-Cueto L, Gerton GL. The influence of growth factors on the development of preimplantation mammalian embryos. *Arch Med Res*. 2001;32(6):619-26. Epub 2001/12/26. doi: 10.1016/s0188-4409(01)00326-5. PubMed PMID: 11750739.
162. Qin J, Díaz-Cueto L, Schwarze JE, Takahashi Y, Imai M, Isuzugawa K, Yamamoto S, Chang KT, Gerton GL, Imakawa K. Effects of progranulin on blastocyst hatching and subsequent

- adhesion and outgrowth in the mouse. *Biol Reprod.* 2005;73(3):434-42. Epub 2005/05/20. doi: 10.1095/biolreprod.105.040030. PubMed PMID: 15901638.
163. Daniel R, Daniels E, He Z, Bateman A. Progranulin (acrogranin/PC cell-derived growth factor/granulin-epithelin precursor) is expressed in the placenta, epidermis, microvasculature, and brain during murine development. *Dev Dyn.* 2003;227(4):593-9. Epub 2003/07/31. doi: 10.1002/dvdy.10341. PubMed PMID: 12889069.
164. Hyung S, Im SK, Lee BY, Shin J, Park JC, Lee C, Suh JF, Hur EM. Dedifferentiated Schwann cells secrete progranulin that enhances the survival and axon growth of motor neurons. *Glia.* 2019;67(2):360-75. Epub 2018/11/18. doi: 10.1002/glia.23547. PubMed PMID: 30444070.
165. Egashira Y, Suzuki Y, Azuma Y, Takagi T, Mishiro K, Sugitani S, Tsuruma K, Shimazawa M, Yoshimura S, Kashimata M, Iwama T, Hara H. The growth factor progranulin attenuates neuronal injury induced by cerebral ischemia-reperfusion through the suppression of neutrophil recruitment. *Journal of Neuroinflammation.* 2013;10(1):884. doi: 10.1186/1742-2094-10-105.
166. Cheung PFY, Cheung ST. Methods to Analyze the Role of Progranulin (PGRN/GEP) on Cancer Stem Cell Features. *Methods in molecular biology (Clifton, NJ).* 2018;1806:145-53. Epub 2018/06/30. doi: 10.1007/978-1-4939-8559-3_11. PubMed PMID: 29956275.
167. Yang D, Wang LL, Dong TT, Shen YH, Guo XS, Liu CY, Liu J, Zhang P, Li J, Sun YP. Progranulin promotes colorectal cancer proliferation and angiogenesis through TNFR2/Akt and ERK signaling pathways. *Am J Cancer Res.* 2015;5(10):3085-97. Epub 2015/12/23. PubMed PMID: 26693061; PMCID: PMC4656732.
168. Diaz-Cueto L, Arechavaleta-Velasco F, Diaz-Arizaga A, Dominguez-Lopez P, Robles-Flores M. PKC signaling is involved in the regulation of progranulin (acrogranin/PC-cell-derived growth factor/granulin-epithelin precursor) protein expression in human ovarian cancer cell lines. *Int J Gynecol Cancer.* 2012;22(6):945-50. Epub 2012/06/06. doi: 10.1097/IGC.0b013e318253499c. PubMed PMID: 22665040.
169. Tanimoto R, Morcavallo A, Terracciano M, Xu SQ, Stefanello M, Buraschi S, Lu KG, Bagley DH, Gomella LG, Scotlandi K, Belfiore A, Iozzo RV, Morrione A. Sortilin regulates progranulin action in castration-resistant prostate cancer cells. *Endocrinology.* 2015;156(1):58-70. Epub 2014/11/05. doi: 10.1210/en.2014-1590. PubMed PMID: 25365768; PMCID: PMC4272403.
170. Zhou C, Huang Y, Wu J, Wei Y, Chen X, Lin Z, Nie S. A narrative review of multiple mechanisms of progranulin in cancer: a potential target for anti-cancer therapy. *Translational Cancer Research.* 2021;10(9):4207-16.
171. Arechavaleta-Velasco F, Perez-Juarez CE, Gerton GL, Diaz-Cueto L. Progranulin and its biological effects in cancer. *Med Oncol.* 2017;34(12):194. Epub 2017/11/09. doi: 10.1007/s12032-017-1054-7. PubMed PMID: 29116422; PMCID: PMC5810362.
172. Tanimoto R, Lu KG, Xu SQ, Buraschi S, Belfiore A, Iozzo RV, Morrione A. Mechanisms of Progranulin Action and Regulation in Genitourinary Cancers. *Front Endocrinol (Lausanne).* 2016;7:100. Epub 2016/08/12. doi: 10.3389/fendo.2016.00100. PubMed PMID: 27512385; PMCID: PMC4961702.
173. Monami G, Gonzalez EM, Hellman M, Gomella LG, Baffa R, Iozzo RV, Morrione A. Proepithelin promotes migration and invasion of 5637 bladder cancer cells through the activation of ERK1/2 and the formation of a paxillin/FAK/ERK complex. *Cancer Res.* 2006;66(14):7103-10. Epub 2006/07/20. doi: 10.1158/0008-5472.Can-06-0633. PubMed PMID: 16849556.
174. Chen XY, Li JS, Liang QP, He DZ, Zhao J. Expression of PC cell-derived growth factor and vascular endothelial growth factor in esophageal squamous cell carcinoma and their

clinicopathologic significance. *Chin Med J (Engl)*. 2008;121(10):881-6. Epub 2008/08/19. PubMed PMID: 18706200.

175. Tangkeangsirisin W, Serrero G. PC cell-derived growth factor (PCDGF/GP88, progranulin) stimulates migration, invasiveness and VEGF expression in breast cancer cells. *Carcinogenesis*. 2004;25(9):1587-92. Epub 2004/05/01. doi: 10.1093/carcin/bgh171. PubMed PMID: 15117809.

176. Tangkeangsirisin W, Hayashi J, Serrero G. PC cell-derived growth factor mediates tamoxifen resistance and promotes tumor growth of human breast cancer cells. *Cancer Res*. 2004;64(5):1737-43. Epub 2004/03/05. doi: 10.1158/0008-5472.can-03-2364. PubMed PMID: 14996734.

177. Bandey I, Chiou SH, Huang AP, Tsai JC, Tu PH. Progranulin promotes Temozolomide resistance of glioblastoma by orchestrating DNA repair and tumor stemness. *Oncogene*. 2015;34(14):1853-64. Epub 2014/05/06. doi: 10.1038/onc.2014.92. PubMed PMID: 24793792.

178. Cheung PF, Yip CW, Wong NC, Fong DY, Ng LW, Wan AM, Wong CK, Cheung TT, Ng IO, Poon RT, Fan ST, Cheung ST. Granulin-epithelin precursor renders hepatocellular carcinoma cells resistant to natural killer cytotoxicity. *Cancer Immunol Res*. 2014;2(12):1209-19. Epub 2014/10/16. doi: 10.1158/2326-6066.Cir-14-0096. PubMed PMID: 25315249.

179. Han JJ, Yu M, Houston N, Steinberg SM, Kohn EC. Progranulin is a potential prognostic biomarker in advanced epithelial ovarian cancers. *Gynecol Oncol*. 2011;120(1):5-10. Epub 2010/10/19. doi: 10.1016/j.ygyno.2010.09.006. PubMed PMID: 20950846; PMCID: PMC2997933.

180. Carlson AM, Maurer MJ, Goergen KM, Kalli KR, Erskine CL, Behrens MD, Knutson KL, Block MS. Utility of progranulin and serum leukocyte protease inhibitor as diagnostic and prognostic biomarkers in ovarian cancer. *Cancer Epidemiol Biomarkers Prev*. 2013;22(10):1730-5. Epub 2013/07/24. doi: 10.1158/1055-9965.Epi-12-1368. PubMed PMID: 23878295; PMCID: PMC3839679.

181. Tkaczuk KR, Yue B, Zhan M, Tait N, Yarlagadda L, Dai H, Serrero G. Increased Circulating Level of the Survival Factor GP88 (Progranulin) in the Serum of Breast Cancer Patients When Compared to Healthy Subjects. *Breast Cancer (Auckl)*. 2011;5:155-62. Epub 2011/07/28. doi: 10.4137/bcbr.S7224. PubMed PMID: 21792312; PMCID: PMC3140268.

182. Wang M, Li G, Yin J, Lin T, Zhang J. Progranulin overexpression predicts overall survival in patients with glioblastoma. *Med Oncol*. 2012;29(4):2423-31. Epub 2011/12/14. doi: 10.1007/s12032-011-0131-6. PubMed PMID: 22161130.

183. Yoo HJ, Hwang SY, Hong HC, Choi HY, Yang SJ, Choi DS, Baik SH, Blüher M, Youn B-S, Choi KM. Implication of progranulin and C1q/TNF-related protein-3 (CTRP3) on inflammation and atherosclerosis in subjects with or without metabolic syndrome. *PloS one*. 2013;8(2):e55744.

184. Youn B-S, Bang S-I, Kloting N, Park JW, Lee N, Oh J-E, Pi K-B, Lee TH, Ruschke K, Fasshauer M. Serum progranulin concentrations may be associated with macrophage infiltration into omental adipose tissue. *Diabetes*. 2009;58(3):627-36.

185. Richter J, Focke D, Ebert T, Kovacs P, Bachmann A, Lössner U, Kralisch S, Kratzsch J, Beige J, Anders M. Serum levels of the adipokine progranulin depend on renal function. *Diabetes care*. 2013;36(2):410-4.

186. Vercellino M, Grifoni S, Romagnolo A, Masera S, Mattioda A, Trebini C, Chiavazza C, Caligiana L, Capello E, Mancardi GL, Giobbe D, Mutani R, Giordana MT, Cavalla P. Progranulin expression in brain tissue and cerebrospinal fluid levels in multiple sclerosis. *Mult Scler*.

- 2011;17(10):1194-201. Epub 2011/05/27. doi: 10.1177/1352458511406164. PubMed PMID: 21613335.
187. Chen J, Li S, Shi J, Zhang L, Li J, Chen S, Wu C, Shen B. Serum progranulin unrelated with Breg cell levels, but elevated in RA patients, reflecting high disease activity. *Rheumatol Int*. 2016;36(3):359-64. Epub 2015/10/16. doi: 10.1007/s00296-015-3372-4. PubMed PMID: 26462672.
188. Pogonowska M, Poniatowski Ł A, Wawrzyniak A, Królikowska K, Kalicki B. The role of progranulin (PGRN) in the modulation of anti-inflammatory response in asthma. *Cent Eur J Immunol*. 2019;44(1):97-101. Epub 2019/05/23. doi: 10.5114/ceji.2019.83267. PubMed PMID: 31114443; PMCID: PMC6526594.
189. Hughes CE, Nibbs RJB. A guide to chemokines and their receptors. *Febs j*. 2018;285(16):2944-71. Epub 2018/04/11. doi: 10.1111/febs.14466. PubMed PMID: 29637711; PMCID: PMC6120486.
190. Kojima Y, Ono K, Inoue K, Takagi Y, Kikuta K, Nishimura M, Yoshida Y, Nakashima Y, Matsumae H, Furukawa Y, Mikuni N, Nobuyoshi M, Kimura T, Kita T, Tanaka M. Progranulin expression in advanced human atherosclerotic plaque. *Atherosclerosis*. 2009;206(1):102-8. Epub 2009/03/27. doi: 10.1016/j.atherosclerosis.2009.02.017. PubMed PMID: 19321167.
191. Wang S, Wei J, Fan Y, Ding H, Tian H, Zhou X, Cheng L. Progranulin is positively associated with intervertebral disc degeneration by interaction with IL-10 and IL-17 through TNF pathways. *Inflammation*. 2018;41:1852-63.
192. Kessenbrock K, Fröhlich L, Sixt M, Lämmermann T, Pfister H, Bateman A, Belaouaj A, Ring J, Ollert M, Fässler R, Jenne DE. Proteinase 3 and neutrophil elastase enhance inflammation in mice by inactivating antiinflammatory progranulin. *The Journal of Clinical Investigation*. 2008;118(7):2438-47. doi: 10.1172/JCI34694.
193. Zhu J, Nathan C, Jin W, Sim D, Ashcroft GS, Wahl SM, Lacomis L, Erdjument-Bromage H, Tempst P, Wright CD, Ding A. Conversion of Proepithelin to Epithelins: Roles of SLPI and Elastase in Host Defense and Wound Repair. *Cell*. 2002;111(6):867-78. doi: 10.1016/S0092-8674(02)01141-8.
194. Mundra JJ, Jian J, Bhagat P, Liu CJ. Progranulin inhibits expression and release of chemokines CXCL9 and CXCL10 in a TNFR1 dependent manner. *Sci Rep*. 2016;6:21115. Epub 2016/02/20. doi: 10.1038/srep21115. PubMed PMID: 26892362; PMCID: PMC4759551.
195. Tian Q, Zhao Y, Mundra JJ, Gonzalez-Gugel E, Jian J, Uddin SM, Liu C. Three TNFR-binding domains of PGRN act independently in inhibition of TNF-alpha binding and activity. *Front Biosci (Landmark Ed)*. 2014;19(7):1176-85. Epub 2014/06/05. doi: 10.2741/4274. PubMed PMID: 24896343; PMCID: PMC4410860.
196. Tian Q, Zhao S, Liu C. A solid-phase assay for studying direct binding of progranulin to TNFR and progranulin antagonism of TNF/TNFR interactions. *Methods in molecular biology (Clifton, NJ)*. 2014;1155:163-72. Epub 2014/05/03. doi: 10.1007/978-1-4939-0669-7_14. PubMed PMID: 24788181; PMCID: PMC4406480.
197. Liu CJ, Bosch X. Progranulin: a growth factor, a novel TNFR ligand and a drug target. *Pharmacol Ther*. 2012;133(1):124-32. Epub 2011/10/20. doi: 10.1016/j.pharmthera.2011.10.003. PubMed PMID: 22008260; PMCID: PMC4429904.
198. Etemadi N, Webb A, Bankovacki A, Silke J, Nachbur U. Progranulin does not inhibit TNF and lymphotoxin- α signalling through TNF receptor 1. *Immunol Cell Biol*. 2013;91(10):661-4. Epub 2013/10/09. doi: 10.1038/icb.2013.53. PubMed PMID: 24100384.

199. Chen X, Chang J, Deng Q, Xu J, Nguyen TA, Martens LH, Cenik B, Taylor G, Hudson KF, Chung J, Yu K, Yu P, Herz J, Farese RV, Jr., Kukar T, Tansey MG. Progranulin does not bind tumor necrosis factor (TNF) receptors and is not a direct regulator of TNF-dependent signaling or bioactivity in immune or neuronal cells. *J Neurosci*. 2013;33(21):9202-13. Epub 2013/05/24. doi: 10.1523/jneurosci.5336-12.2013. PubMed PMID: 23699531; PMCID: PMC3707136.
200. Wang BC, Liu H, Talwar A, Jian J. New discovery rarely runs smooth: an update on progranulin/TNFR interactions. *Protein & Cell*. 2015;6(11):792-803. doi: 10.1007/s13238-015-0213-x.
201. Kawase R, Ohama T, Matsuyama A, Matsuwaki T, Okada T, Yamashita T, Yuasa-Kawase M, Nakaoka H, Nakatani K, Inagaki M. Deletion of progranulin exacerbates atherosclerosis in ApoE knockout mice. *Cardiovascular research*. 2013;100(1):125-33.
202. Yin F, Banerjee R, Thomas B, Zhou P, Qian L, Jia T, Ma X, Ma Y, Iadecola C, Beal MF, Nathan C, Ding A. Exaggerated inflammation, impaired host defense, and neuropathology in progranulin-deficient mice. *J Exp Med*. 2010;207(1):117-28. Epub 2009/12/21. doi: 10.1084/jem.20091568. PubMed PMID: 20026663.
203. Lan YJ, Sam NB, Cheng MH, Pan HF, Gao J. Progranulin as a Potential Therapeutic Target in Immune-Mediated Diseases. *J Inflamm Res*. 2021;14:6543-56. Epub 2021/12/14. doi: 10.2147/jir.S339254. PubMed PMID: 34898994; PMCID: PMC8655512.
204. Ren Y, Zhao H, Yin C, Lan X, Wu L, Du X, Griffiths HR, Gao D. Adipokines, Hepatokines and Myokines: Focus on Their Role and Molecular Mechanisms in Adipose Tissue Inflammation. *Front Endocrinol (Lausanne)*. 2022;13:873699. Epub 2022/08/02. doi: 10.3389/fendo.2022.873699. PubMed PMID: 35909571; PMCID: PMC9329830.
205. Schmid A, Hochberg A, Kreiß AF, Gehl J, Patz M, Thomalla M, Hanses F, Karrasch T, Schäffler A. Role of progranulin in adipose tissue innate immunity. *Cytokine*. 2020;125:154796. Epub 2019/08/28. doi: 10.1016/j.cyto.2019.154796. PubMed PMID: 31454754.
206. Matsubara T, Mita A, Minami K, Hosooka T, Kitazawa S, Takahashi K, Tamori Y, Yokoi N, Watanabe M, Matsuo E, Nishimura O, Seino S. PGRN is a key adipokine mediating high fat diet-induced insulin resistance and obesity through IL-6 in adipose tissue. *Cell Metab*. 2012;15(1):38-50. Epub 2012/01/10. doi: 10.1016/j.cmet.2011.12.002. PubMed PMID: 22225875.
207. Qu H, Deng H, Hu Z. Plasma progranulin concentrations are increased in patients with type 2 diabetes and obesity and correlated with insulin resistance. *Mediators Inflamm*. 2013;2013:360190. Epub 2013/03/12. doi: 10.1155/2013/360190. PubMed PMID: 23476101; PMCID: PMC3588183.
208. Li H, Zhou B, Xu L, Liu J, Zang W, Wu S, Sun H. Circulating PGRN is significantly associated with systemic insulin sensitivity and autophagic activity in metabolic syndrome. *Endocrinology*. 2014;155(9):3493-507. Epub 2014/06/28. doi: 10.1210/en.2014-1058. PubMed PMID: 24971611.
209. Kim HK, Shin MS, Youn BS, Namkoong C, Gil SY, Kang GM, Yu JH, Kim MS. Involvement of progranulin in hypothalamic glucose sensing and feeding regulation. *Endocrinology*. 2011;152(12):4672-82. Epub 2011/09/22. doi: 10.1210/en.2011-1221. PubMed PMID: 21933869.
210. Smith KR, Damiano J, Franceschetti S, Carpenter S, Canafoglia L, Morbin M, Rossi G, Pareyson D, Mole SE, Staropoli JF, Sims KB, Lewis J, Lin W-L, Dickson DW, Dahl H-H, Bahlo M, Berkovic SF. Strikingly different clinicopathological phenotypes determined by progranulin-

- mutation dosage. *Am J Hum Genet.* 2012;90(6):1102-7. Epub 2012/05/17. doi: 10.1016/j.ajhg.2012.04.021. PubMed PMID: 22608501.
211. Radke J, Stenzel W, Goebel HH. Human NCL Neuropathology. *Biochimica et Biophysica Acta (BBA) - Molecular Basis of Disease.* 2015;1852(10, Part B):2262-6. doi: <https://doi.org/10.1016/j.bbadis.2015.05.007>.
212. Anderson GW, Goebel HH, Simonati A. Human pathology in NCL. *Biochimica et Biophysica Acta (BBA)-Molecular Basis of Disease.* 2013;1832(11):1807-26.
213. Mukherjee AB, Appu AP, Sadhukhan T, Casey S, Mondal A, Zhang Z, Bagh MB. Emerging new roles of the lysosome and neuronal ceroid lipofuscinoses. *Mol Neurodegener.* 2019;14(1):4. doi: 10.1186/s13024-018-0300-6.
214. Isik E, Yilmaz S, Atik T, Aktan G, Onay H, Gokben S, Ozkinay F. The utility of whole exome sequencing for identification of the molecular etiology in autosomal recessive developmental and epileptic encephalopathies. *Neurol Sci.* 2020;41(12):3729-39. Epub 2020/07/25. doi: 10.1007/s10072-020-04619-8. PubMed PMID: 32705489.
215. Kamate M, Detroja M, Hattiholi V. Neuronal ceroid lipofuscinosis type-11 in an adolescent. *Brain and Development.* 2019;41(6):542-5. doi: <https://doi.org/10.1016/j.braindev.2019.03.004>.
216. Faber I, Prota JR, Martinez AR, Lopes-Cendes I, França MCJ. A new phenotype associated with homozygous GRN mutations: complicated spastic paraplegia. *Eur J Neurol.* 2017;24(1):e3-e4. Epub 2016/12/22. doi: 10.1111/ene.13194. PubMed PMID: 28000352.
217. Neuray C, Sultan T, Alvi JR, Franca MC, Jr., Assmann B, Wagner M, Canafoglia L, Franceschetti S, Rossi G, Santana I, Macario MC, Almeida MR, Kamate M, Parikh S, Elloumi HZ, Murphy D, Efthymiou S, Maroofian R, Houlden H. Early-onset phenotype of bi-allelic GRN mutations. *Brain.* 2021;144(2):e22-e. doi: 10.1093/brain/awaa414.
218. Mole SE, Anderson G, Band HA, Berkovic SF, Cooper JD, Kleine Holthaus S-M, McKay TR, Medina DL, Rahim AA, Schulz A, Smith AJ. Clinical challenges and future therapeutic approaches for neuronal ceroid lipofuscinosis. *The Lancet Neurology.* 2019;18(1):107-16. doi: [https://doi.org/10.1016/S1474-4422\(18\)30368-5](https://doi.org/10.1016/S1474-4422(18)30368-5).
219. Mole SE, Cotman SL. Genetics of the neuronal ceroid lipofuscinoses (Batten disease). *Biochimica et Biophysica Acta (BBA)-Molecular Basis of Disease.* 2015;1852(10):2237-41.
220. Ward ME, Taubes A, Chen R, Miller BL, Sephton CF, Gelfand JM, Minami S, Boscardin J, Martens LH, Seeley WW, Yu G, Herz J, Filiano AJ, Arrant AE, Roberson ED, Kraft TW, Farese RV, Jr., Green A, Gan L. Early retinal neurodegeneration and impaired Ran-mediated nuclear import of TDP-43 in progranulin-deficient FTLD. *J Exp Med.* 2014;211(10):1937-45. Epub 2014/08/27. doi: 10.1084/jem.20140214. PubMed PMID: 25155018; PMCID: PMC4172214.
221. Ward ME, Chen R, Huang HY, Ludwig C, Telpoukhovskaia M, Taubes A, Boudin H, Minami SS, Reichert M, Albrecht P, Gelfand JM, Cruz-Herranz A, Cordano C, Alavi MV, Leslie S, Seeley WW, Miller BL, Bigio E, Mesulam MM, Bogyo MS, Mackenzie IR, Staropoli JF, Cotman SL, Huang EJ, Gan L, Green AJ. Individuals with progranulin haploinsufficiency exhibit features of neuronal ceroid lipofuscinosis. *Sci Transl Med.* 2017;9(385). Epub 2017/04/14. doi: 10.1126/scitranslmed.aah5642. PubMed PMID: 28404863; PMCID: PMC5526610.
222. Hu F, Padukkavidana T, Vægter CB, Brady OA, Zheng Y, Mackenzie IR, Feldman HH, Nykjaer A, Strittmatter SM. Sortilin-Mediated Endocytosis Determines Levels of the Frontotemporal Dementia Protein, Progranulin. *Neuron.* 2010;68(4):654-67. doi: <https://doi.org/10.1016/j.neuron.2010.09.034>.

223. Naphade SB, Kigerl KA, Jakeman LB, Kostyk SK, Popovich PG, Kuret J. Progranulin expression is upregulated after spinal contusion in mice. *Acta Neuropathol.* 2010;119(1):123-33. Epub 2009/12/01. doi: 10.1007/s00401-009-0616-y. PubMed PMID: 19946692; PMCID: PMC4290888.
224. Simon MJ, Logan T, DeVos SL, Di Paolo G. Lysosomal functions of progranulin and implications for treatment of frontotemporal dementia. *Trends Cell Biol.* 2023. doi: 10.1016/j.tcb.2022.09.006.
225. Zhou X, Kukar T, Rademakers R. Lysosomal Dysfunction and Other Pathomechanisms in FTL D: Evidence from Progranulin Genetics and Biology. *Adv Exp Med Biol.* 2021;1281:219-42. Epub 2021/01/13. doi: 10.1007/978-3-030-51140-1_14. PubMed PMID: 33433878; PMCID: PMC8672701.
226. Paushter DH, Du H, Feng T, Hu F. The lysosomal function of progranulin, a guardian against neurodegeneration. *Acta Neuropathol.* 2018;136(1):1-17. Epub 2018/05/11. doi: 10.1007/s00401-018-1861-8. PubMed PMID: 29744576; PMCID: PMC6117207.
227. Huang M, Modeste E, Dammer E, Merino P, Taylor G, Duong DM, Deng Q, Holler CJ, Gearing M, Dickson D, Seyfried NT, Kukar T. Network analysis of the progranulin-deficient mouse brain proteome reveals pathogenic mechanisms shared in human frontotemporal dementia caused by GRN mutations. *Acta Neuropathologica Communications.* 2020;8(1):163. doi: 10.1186/s40478-020-01037-x.
228. Zhou X, Paushter DH, Feng T, Pardon CM, Mendoza CS, Hu F. Regulation of cathepsin D activity by the FTL D protein progranulin. *Acta Neuropathol.* 2017;134(1):151-3. Epub 2017/05/12. doi: 10.1007/s00401-017-1719-5. PubMed PMID: 28493053; PMCID: PMC5568051.
229. Beel S, Moisse M, Damme M, De Muyenck L, Robberecht W, Van Den Bosch L, Saftig P, Van Damme P. Progranulin functions as a cathepsin D chaperone to stimulate axonal outgrowth in vivo. *Hum Mol Genet.* 2017;26(15):2850-63. Epub 2017/04/30. doi: 10.1093/hmg/ddx162. PubMed PMID: 28453791; PMCID: PMC5886064.
230. Siintola E, Partanen S, Strömme P, Haapanen A, Haltia M, Maehlen J, Lehesjoki AE, Tyynelä J. Cathepsin D deficiency underlies congenital human neuronal ceroid-lipofuscinosis. *Brain.* 2006;129(Pt 6):1438-45. Epub 2006/05/04. doi: 10.1093/brain/aw1107. PubMed PMID: 16670177.
231. Arrant AE, Roth JR, Boyle NR, Kashyap SN, Hoffmann MQ, Murchison CF, Ramos EM, Nana AL, Spina S, Grinberg LT, Miller BL, Seeley WW, Roberson ED. Impaired β -glucocerebrosidase activity and processing in frontotemporal dementia due to progranulin mutations. *Acta Neuropathol Commun.* 2019;7(1):218. Epub 2019/12/25. doi: 10.1186/s40478-019-0872-6. PubMed PMID: 31870439; PMCID: PMC6929503.
232. Valdez C, Ysselstein D, Young TJ, Zheng J, Krainc D. Progranulin mutations result in impaired processing of prosaposin and reduced glucocerebrosidase activity. *Hum Mol Genet.* 2020;29(5):716-26. Epub 2019/10/11. doi: 10.1093/hmg/ddz229. PubMed PMID: 31600775; PMCID: PMC7104673.
233. Chen Y, Jian J, Hettinghouse A, Zhao X, Satchell KDR, Sun Y, Liu CJ. Progranulin associates with hexosaminidase A and ameliorates GM2 ganglioside accumulation and lysosomal storage in Tay-Sachs disease. *J Mol Med (Berl).* 2018;96(12):1359-73. Epub 2018/10/21. doi: 10.1007/s00109-018-1703-0. PubMed PMID: 30341570; PMCID: PMC6240367.
234. Beutler E, Demina A, Gelbart T. Glucocerebrosidase mutations in Gaucher disease. *Mol Med.* 1994;1(1):82-92. Epub 1994/11/01. PubMed PMID: 8790604; PMCID: PMC2229932.

235. Ferreira CR, Gahl WA. Lysosomal storage diseases. *Translational Science of Rare Diseases*. 2017;2:1-71. doi: 10.3233/TRD-160005.
236. Schulze H, Sandhoff K. Sphingolipids and lysosomal pathologies. *Biochim Biophys Acta*. 2014;1841(5):799-810. Epub 2013/11/05. doi: 10.1016/j.bbalip.2013.10.015. PubMed PMID: 24184515.
237. Root J, Mendsaikhan A, Nandy S, Taylor G, Wang M, Troiano Araujo L, Merino P, Ryu D, Holler C, Thompson BM, Astarita G, Blain J, Kukar T. Granulins rescue inflammation, lysosome dysfunction, and neuropathology in a mouse model of progranulin deficiency. *bioRxiv*. 2023. Epub 2023/05/03. doi: 10.1101/2023.04.17.536004. PubMed PMID: 37131734; PMCID: PMC10153205 of Arkuda Therapeutics. Patent pending related to this work entitled “Methods to treat neurodegeneration with granulins” to C.H., G.T., T.K. All authors declare that they have no conflicts of interest with the contents of this article.
238. Logan T, Simon MJ, Rana A, Cherf GM, Srivastava A, Davis SS, Low RLY, Chiu CL, Fang M, Huang F, Bhalla A, Llapashtica C, Prorok R, Pizzo ME, Calvert MEK, Sun EW, Hsiao-Nakamoto J, Rajendra Y, Lexa KW, Srivastava DB, van Lengerich B, Wang J, Robles-Colmenares Y, Kim DJ, Duque J, Lenser M, Ear TK, Nguyen H, Chau R, Tsogtbaatar B, Ravi R, Skuja LL, Solanoy H, Rosen HJ, Boeve BF, Boxer AL, Heuer HW, Dennis MS, Kariolis MS, Monroe KM, Przybyla L, Sanchez PE, Meisner R, Diaz D, Henne KR, Watts RJ, Henry AG, Gunasekaran K, Astarita G, Suh JH, Lewcock JW, DeVos SL, Di Paolo G. Rescue of a lysosomal storage disorder caused by Grn loss of function with a brain penetrant progranulin biologic. *Cell*. 2021;184(18):4651-68.e25. Epub 2021/08/28. doi: 10.1016/j.cell.2021.08.002. PubMed PMID: 34450028; PMCID: PMC8489356.
239. Thelen AM, Zoncu R. Emerging Roles for the Lysosome in Lipid Metabolism. *Trends Cell Biol*. 2017;27(11):833-50. doi: <https://doi.org/10.1016/j.tcb.2017.07.006>.
240. Jaishy B, Abel ED. Lipids, lysosomes, and autophagy. *Journal of Lipid Research*. 2016;57(9):1619-35. doi: <https://doi.org/10.1194/jlr.R067520>.
241. Breiden B, Sandhoff K. Lysosomal glycosphingolipid storage diseases. *Annual review of biochemistry*. 2019;88:461-85.
242. Boland S, Swarup S, Ambaw YA, Malia PC, Richards RC, Fischer AW, Singh S, Aggarwal G, Spina S, Nana AL, Grinberg LT, Seeley WW, Surma MA, Klose C, Paulo JA, Nguyen AD, Harper JW, Walther TC, Farese RV, Jr. Deficiency of the frontotemporal dementia gene GRN results in gangliosidosis. *Nat Commun*. 2022;13(1):5924. Epub 2022/10/08. doi: 10.1038/s41467-022-33500-9. PubMed PMID: 36207292; PMCID: PMC9546883 Inc. and a founding scientific board member of Interline Therapeutics Inc. R.V.F. serves gratis on the board of the Bluefield Project to Cure FTD. T.C.W. is a founder and scientific advisory board chair of Antora Bio Inc. The remaining authors declare no competing interests.
243. Marian OC, Teo JD, Lee JY, Song H, Kwok JB, Landin-Romero R, Halliday G, Don AS. Disrupted myelin lipid metabolism differentiates frontotemporal dementia caused by GRN and C9orf72 gene mutations. *Acta Neuropathologica Communications*. 2023;11(1):52. doi: 10.1186/s40478-023-01544-7.
244. Arrant AE, Filiano AJ, Unger DE, Young AH, Roberson ED. Restoring neuronal progranulin reverses deficits in a mouse model of frontotemporal dementia. *Brain*. 2017;140(5):1447-65. Epub 2017/04/06. doi: 10.1093/brain/awx060. PubMed PMID: 28379303; PMCID: PMC5965303.
245. Marschallinger J, Iram T, Zardeneta M, Lee SE, Lehallier B, Haney MS, Pluvinage JV, Mathur V, Hahn O, Morgens DW, Kim J, Tevini J, Felder TK, Wolinski H, Bertozzi CR, Bassik

- MC, Aigner L, Wyss-Coray T. Lipid-droplet-accumulating microglia represent a dysfunctional and proinflammatory state in the aging brain. *Nat Neurosci.* 2020. Epub 2020/01/22. doi: 10.1038/s41593-019-0566-1. PubMed PMID: 31959936.
246. Papadopoulos C, Kravic B, Meyer H. Repair or Lysophagy: Dealing with Damaged Lysosomes. *J Mol Biol.* 2020;432(1):231-9. Epub 2019/08/27. doi: 10.1016/j.jmb.2019.08.010. PubMed PMID: 31449799.
247. Wang F, Gómez-Sintes R, Boya P. Lysosomal membrane permeabilization and cell death. *Traffic.* 2018;19(12):918-31. Epub 2018/08/21. doi: 10.1111/tra.12613. PubMed PMID: 30125440.
248. Boya P, Kroemer G. Lysosomal membrane permeabilization in cell death. *Oncogene.* 2008;27(50):6434-51. Epub 2008/10/29. doi: 10.1038/onc.2008.310. PubMed PMID: 18955971.
249. Tanaka Y, Suzuki G, Matsuwaki T, Hosokawa M, Serrano G, Beach TG, Yamanouchi K, Hasegawa M, Nishihara M. Progranulin regulates lysosomal function and biogenesis through acidification of lysosomes. *Human Molecular Genetics.* 2017;26(5):969-88. doi: 10.1093/hmg/ddx011.
250. Settembre C, Di Malta C, Polito VA, Garcia Arencibia M, Vetrini F, Erdin S, Erdin SU, Huynh T, Medina D, Colella P, Sardiello M, Rubinsztein DC, Ballabio A. TFEB links autophagy to lysosomal biogenesis. *Science.* 2011;332(6036):1429-33. Epub 2011/05/28. doi: 10.1126/science.1204592. PubMed PMID: 21617040; PMCID: PMC3638014.
251. Tanaka Y, Matsuwaki T, Yamanouchi K, Nishihara M. Increased lysosomal biogenesis in activated microglia and exacerbated neuronal damage after traumatic brain injury in progranulin-deficient mice. *Neuroscience.* 2013;250:8-19. doi: <https://doi.org/10.1016/j.neuroscience.2013.06.049>.
252. Belcastro V, Siciliano V, Gregoret F, Mithbaokar P, Dharmalingam G, Berlingieri S, Iorio F, Oliva G, Polishchuck R, Brunetti-Pierri N, di Bernardo D. Transcriptional gene network inference from a massive dataset elucidates transcriptome organization and gene function. *Nucleic Acids Res.* 2011;39(20):8677-88. Epub 2011/07/26. doi: 10.1093/nar/gkr593. PubMed PMID: 21785136; PMCID: PMC3203605.
253. Settembre C, Fraldi A, Medina DL, Ballabio A. Signals from the lysosome: a control centre for cellular clearance and energy metabolism. *Nature Reviews Molecular Cell Biology.* 2013;14(5):283-96. doi: 10.1038/nrm3565.
254. Yin F, Dumont M, Banerjee R, Ma Y, Li H, Lin MT, Beal MF, Nathan C, Thomas B, Ding A. Behavioral deficits and progressive neuropathology in progranulin-deficient mice: a mouse model of frontotemporal dementia. *FASEB J.* 2010;24(12):4639-47. Epub 2010/07/28. doi: 10.1096/fj.10-161471. PubMed PMID: 20667979.
255. Ahmed Z, Sheng H, Xu Y-F, Lin W-L, Innes AE, Gass J, Yu X, Wuertzer CA, Hou H, Chiba S, Yamanouchi K, Leissring M, Petrucelli L, Nishihara M, Hutton ML, McGowan E, Dickson DW, Lewis J. Accelerated lipofuscinosis and ubiquitination in granulin knockout mice suggest a role for progranulin in successful aging. *Am J Pathol.* 2010;177(1):311-24. Epub 2010/06/03. doi: 10.2353/ajpath.2010.090915. PubMed PMID: 20522652.
256. Arrant AE, Onyilo VC, Unger DE, Roberson ED. Progranulin Gene Therapy Improves Lysosomal Dysfunction and Microglial Pathology Associated with Frontotemporal Dementia and Neuronal Ceroid Lipofuscinosis. *J Neurosci.* 2018;38(9):2341-58. Epub 2018/01/29. doi: 10.1523/JNEUROSCI.3081-17.2018. PubMed PMID: 29378861.
257. Filiano AJ, Martens LH, Young AH, Warmus BA, Zhou P, Diaz-Ramirez G, Jiao J, Zhang Z, Huang EJ, Gao F-B, Farese RV, Jr., Roberson ED. Dissociation of frontotemporal dementia-

related deficits and neuroinflammation in progranulin haploinsufficient mice. *J Neurosci*. 2013;33(12):5352-61. doi: 10.1523/JNEUROSCI.6103-11.2013. PubMed PMID: 23516300.

258. Götzl JK, Colombo A-V, Fellerer K, Reifschneider A, Werner G, Tahirovic S, Haass C, Capell A. Early lysosomal maturation deficits in microglia triggers enhanced lysosomal activity in other brain cells of progranulin knockout mice. *Mol Neurodegener*. 2018;13(1):48-. doi: 10.1186/s13024-018-0281-5. PubMed PMID: 30180904.

259. Lui H, Zhang J, Makinson SR, Cahill MK, Kelley KW, Huang H-Y, Shang Y, Oldham MC, Martens LH, Gao F, Coppola G, Sloan SA, Hsieh CL, Kim CC, Bigio EH, Weintraub S, Mesulam M-M, Rademakers R, Mackenzie IR, Seeley WW, Karydas A, Miller BL, Borroni B, Ghidoni R, Farese RV, Jr., Paz JT, Barres BA, Huang EJ. Progranulin Deficiency Promotes Circuit-Specific Synaptic Pruning by Microglia via Complement Activation. *Cell*. 2016;165(4):921-35. Epub 2016/04/21. doi: 10.1016/j.cell.2016.04.001. PubMed PMID: 27114033.

260. Tanaka Y, Chambers JK, Matsuwaki T, Yamanouchi K, Nishihara M. Possible involvement of lysosomal dysfunction in pathological changes of the brain in aged progranulin-deficient mice. *Acta Neuropathol Commun*. 2014;2:78. Epub 2014/07/16. doi: 10.1186/s40478-014-0078-x. PubMed PMID: 25022663; PMCID: PMC4149276.

261. Ghoshal N, Dearborn JT, Wozniak DF, Cairns NJ. Core features of frontotemporal dementia recapitulated in progranulin knockout mice. *Neurobiology of Disease*. 2012;45(1):395-408. doi: <https://doi.org/10.1016/j.nbd.2011.08.029>.

262. Seeley WW. Anterior insula degeneration in frontotemporal dementia. *Brain Struct Funct*. 2010;214(5-6):465-75. Epub 2010/06/01. doi: 10.1007/s00429-010-0263-z. PubMed PMID: 20512369; PMCID: PMC2886907.

263. Arrant AE, Filiano AJ, Warmus BA, Hall AM, Roberson ED. Progranulin haploinsufficiency causes biphasic social dominance abnormalities in the tube test. *Genes Brain Behav*. 2016;15(6):588-603. doi: 10.1111/gbb.12300. PubMed PMID: 27213486.

264. Kashyap SN, Boyle NR, Roberson ED. Preclinical Interventions in Mouse Models of Frontotemporal Dementia Due to Progranulin Mutations. *Neurotherapeutics*. 2023. doi: 10.1007/s13311-023-01348-6.

265. Almeida S, Zhang Z, Coppola G, Mao W, Futai K, Karydas A, Geschwind MD, Tartaglia MC, Gao F, Gianni D, Sena-Esteves M, Geschwind DH, Miller BL, Farese RV, Jr., Gao FB. Induced pluripotent stem cell models of progranulin-deficient frontotemporal dementia uncover specific reversible neuronal defects. *Cell Rep*. 2012;2(4):789-98. Epub 2012/10/16. doi: 10.1016/j.celrep.2012.09.007. PubMed PMID: 23063362; PMCID: PMC3532907.

266. Miyakawa S, Sakuma H, Warude D, Asanuma S, Arimura N, Yoshihara T, Tavares D, Hata A, Ida K, Hori Y, Okuzono Y, Yamamoto S, Iida K, Shimizu H, Kondo S, Sato S. Anti-sortilin1 Antibody Up-Regulates Progranulin via Sortilin1 Down-Regulation. *Front Neurosci*. 2020;14:586107. Epub 2021/01/02. doi: 10.3389/fnins.2020.586107. PubMed PMID: 33384578; PMCID: PMC7770147.

267. Aggarwal G, Banerjee S, Jones SA, Pavlack M, Benchaar Y, Bélanger J, Sévigny M, Smith DM, Niehoff ML, de Vera IMS, Petkau TL, Leavitt BR, Ling K, Jafar-nejad P, Rigo F, Morley JE, Farr SA, Dutchak PA, Sephton CF, Nguyen AD. Antisense oligonucleotides targeting miR-29b binding site increase translation of progranulin protein: potential therapeutic strategy for progranulin-deficient frontotemporal dementia. *Alzheimer's & Dementia*. 2022;18(S10):e067828. doi: <https://doi.org/10.1002/alz.067828>.

268. Frew J, Baradaran-Heravi A, Balgi AD, Wu X, Yan TD, Arns S, Shidmoossavee FS, Tan J, Jaquith JB, Jansen-West KR, Lynn FC, Gao FB, Petrucelli L, Feldman HH, Mackenzie IR, Roberge M, Nygaard HB. Premature termination codon readthrough upregulates progranulin expression and improves lysosomal function in preclinical models of GRN deficiency. *Mol Neurodegener.* 2020;15(1):21. Epub 2020/03/18. doi: 10.1186/s13024-020-00369-5. PubMed PMID: 32178712; PMCID: PMC7075020.
269. Hinderer C, Miller R, Dyer C, Johansson J, Bell P, Buza E, Wilson JM. Adeno-associated virus serotype 1-based gene therapy for FTD caused by GRN mutations. *Ann Clin Transl Neurol.* 2020;7(10):1843-53. Epub 2020/09/17. doi: 10.1002/acn3.51165. PubMed PMID: 32937039; PMCID: PMC7545603 he holds equity in Surmount Bio; he also has a sponsored research agreement with Ultragenyx, Biogen, Janssen, Precision Biosciences, Moderna Inc., Scout Bio, Passage Bio, Amicus Therapeutics, and Surmount Bio which are licensees of Penn technology. JMW is an inventor on patents that have been licensed to various biopharmaceutical companies and for which he may receive payments. C. Hinderer is an inventor on patents licensed to biopharmaceutical companies and holds equity in Scout Bio.
270. Amado DA, Rieders JM, Diatta F, Hernandez-Con P, Singer A, Mak JT, Zhang J, Lancaster E, Davidson BL, Chen-Plotkin AS. AAV-Mediated Progranulin Delivery to a Mouse Model of Progranulin Deficiency Causes T Cell-Mediated Toxicity. *Mol Ther.* 2018. Epub 2018/12/19. doi: 10.1016/j.ymthe.2018.11.013. PubMed PMID: 30559071.
271. Fischell JM, Fishman PS. A Multifaceted Approach to Optimizing AAV Delivery to the Brain for the Treatment of Neurodegenerative Diseases. *Front Neurosci.* 2021;15:747726. Epub 2021/10/12. doi: 10.3389/fnins.2021.747726. PubMed PMID: 34630029; PMCID: PMC8497810.
272. Bhopatkar AA, Uversky VN, Rangachari V. Disorder and cysteines in proteins: A design for orchestration of conformational see-saw and modulatory functions. *Prog Mol Biol Transl Sci.* 2020;174:331-73. Epub 2020/08/24. doi: 10.1016/bs.pmbts.2020.06.001. PubMed PMID: 32828470; PMCID: PMC8048112.
273. Wiedemann C, Kumar A, Lang A, Ohlenschläger O. Cysteines and Disulfide Bonds as Structure-Forming Units: Insights From Different Domains of Life and the Potential for Characterization by NMR. *Front Chem.* 2020;8:280. Epub 2020/05/12. doi: 10.3389/fchem.2020.00280. PubMed PMID: 32391319; PMCID: PMC7191308.
274. Postic G, Gracy J, Périn C, Chiche L, Gelly JC. KNOTTIN: the database of inhibitor cystine knot scaffold after 10 years, toward a systematic structure modeling. *Nucleic Acids Res.* 2018;46(D1):D454-d8. Epub 2017/11/15. doi: 10.1093/nar/gkx1084. PubMed PMID: 29136213; PMCID: PMC5753296.
275. Ghag G, Wolf LM, Reed RG, Van Der Munnik NP, Mundoma C, Moss MA, Rangachari V. Fully reduced granulin-B is intrinsically disordered and displays concentration-dependent dynamics. *Protein Eng Des Sel.* 2016;29(5):177-86. Epub 2016/03/10. doi: 10.1093/protein/gzw005. PubMed PMID: 26957645; PMCID: PMC4830411.
276. Cenik B, Sephton CF, Kutluk Cenik B, Herz J, Yu G. Progranulin: a proteolytically processed protein at the crossroads of inflammation and neurodegeneration. *The Journal of biological chemistry.* 2012;287(39):32298-306. Epub 2012/08/02. doi: 10.1074/jbc.R112.399170. PubMed PMID: 22859297.
277. Mohan S, Sampognaro PJ, Argouarch AR, Maynard JC, Welch M, Patwardhan A, Courtney EC, Zhang J, Mason A, Li KH, Huang EJ, Seeley WW, Miller BL, Burlingame A, Jacobson MP, Kao AW. Processing of progranulin into granulins involves multiple lysosomal

- proteases and is affected in frontotemporal lobar degeneration. *Mol Neurodegener.* 2021;16(1):51. doi: 10.1186/s13024-021-00472-1.
278. Dastpeyman M, Smout MJ, Wilson D, Loukas A, Daly NL. Folding of granulin domains. *Peptide Science.* 2018;110(3):e24062. doi: <https://doi.org/10.1002/pep2.24062>.
279. Ghag G, Holler CJ, Taylor G, Kukar TL, Uversky VN, Rangachari V. Disulfide bonds and disorder in granulin-3: An unusual handshake between structural stability and plasticity. *Protein Sci.* 2017;26(9):1759-72. Epub 2017/06/14. doi: 10.1002/pro.3212. PubMed PMID: 28608407; PMCID: PMC5563133.
280. Holler CJ, Taylor G, Deng Q, Kukar T. Intracellular Proteolysis of Progranulin Generates Stable, Lysosomal Granulins that Are Haploinsufficient in Patients with Frontotemporal Dementia Caused by GRN Mutations. *eNeuro.* 2017;4(4). Epub 2017/08/23. doi: 10.1523/ENEURO.0100-17.2017. PubMed PMID: 28828399; PMCID: PMC5562298.
281. Butler VJ, Gao F, Corrales CI, Cortopassi WA, Caballero B, Vohra M, Ashrafi K, Cuervo AM, Jacobson MP, Coppola G, Kao AW. Age- and stress-associated *C. elegans* granulins impair lysosomal function and induce a compensatory HLH-30/TFEB transcriptional response. *PLoS Genet.* 2019;15(8):e1008295. Epub 2019/08/10. doi: 10.1371/journal.pgen.1008295. PubMed PMID: 31398187; PMCID: PMC6703691 following competing interests: M.P.J. is a consultant to and shareholder of Schrodinger LLC, which licenses software used in this work.
282. Butler VJ, Cortopassi WA, Gururaj S, Wang AL, Pierce OM, Jacobson MP, Kao AW. Multi-Granulin Domain Peptides Bind to Pro-Cathepsin D and Stimulate Its Enzymatic Activity More Effectively Than Progranulin in Vitro. *Biochemistry.* 2019;58(23):2670-4. Epub 2019/05/18. doi: 10.1021/acs.biochem.9b00275. PubMed PMID: 31099551; PMCID: PMC6666309.
283. Russell ST, Warshel A. Calculations of electrostatic energies in proteins. The energetics of ionized groups in bovine pancreatic trypsin inhibitor. *J Mol Biol.* 1985;185(2):389-404. Epub 1985/09/20. doi: 10.1016/0022-2836(85)90411-5. PubMed PMID: 2414450.
284. Bateman A, Bennett HP. Granulins: the structure and function of an emerging family of growth factors. *J Endocrinol.* 1998;158(2):145-51. Epub 1998/10/15. doi: 10.1677/joe.0.1580145. PubMed PMID: 9771457.
285. Songsrirote K, Li Z, Ashford D, Bateman A, Thomas-Oates J. Development and application of mass spectrometric methods for the analysis of progranulin N-glycosylation. *Journal of proteomics.* 2010;73(8):1479-90.
286. Zhang T, Du H, Santos MN, Wu X, Pagan MD, Trigiani LJ, Nishimura N, Reinheckel T, Hu F. Differential regulation of progranulin derived granulin peptides. *Mol Neurodegener.* 2022;17(1):15. doi: 10.1186/s13024-021-00513-9.
287. Schedin-Weiss S, Winblad B, Tjernberg LO. The role of protein glycosylation in Alzheimer disease. *The FEBS Journal.* 2014;281(1):46-62. doi: <https://doi.org/10.1111/febs.12590>.
288. Hoque M, Mathews MB, Pe'ery T. Progranulin (granulin/epithelin precursor) and its constituent granulin repeats repress transcription from cellular promoters. *J Cell Physiol.* 2010;223(1):224-33. Epub 2010/01/08. doi: 10.1002/jcp.22031. PubMed PMID: 20054825; PMCID: PMC2904068.
289. Suh H-S, Choi N, Tarassishin L, Lee SC. Regulation of Progranulin Expression in Human Microglia and Proteolysis of Progranulin by Matrix Metalloproteinase-12 (MMP-12). *PLOS ONE.* 2012;7(4):e35115. doi: 10.1371/journal.pone.0035115.

290. Butler GS, Dean RA, Tam EM, Overall CM. Pharmacoproteomics of a metalloproteinase hydroxamate inhibitor in breast cancer cells: dynamics of membrane type 1 matrix metalloproteinase-mediated membrane protein shedding. *Mol Cell Biol.* 2008;28(15):4896-914. Epub 2008/05/29. doi: 10.1128/mcb.01775-07. PubMed PMID: 18505826; PMCID: PMC2493375.
291. Bai XH, Wang DW, Kong L, Zhang Y, Luan Y, Kobayashi T, Kronenberg HM, Yu XP, Liu CJ. ADAMTS-7, a direct target of PTHrP, adversely regulates endochondral bone growth by associating with and inactivating GEP growth factor. *Mol Cell Biol.* 2009;29(15):4201-19. Epub 2009/06/03. doi: 10.1128/mcb.00056-09. PubMed PMID: 19487464; PMCID: PMC2715794.
292. Zhou X, Paushter DH, Feng T, Sun L, Reinheckel T, Hu F. Lysosomal processing of progranulin. *Mol Neurodegener.* 2017;12(1):62. Epub 2017/08/25. doi: 10.1186/s13024-017-0205-9. PubMed PMID: 28835281; PMCID: PMC5569495.
293. Zhang Y, Sloan SA, Clarke LE, Caneda C, Plaza CA, Blumenthal PD, Vogel H, Steinberg GK, Edwards MS, Li G, Duncan JA, 3rd, Cheshier SH, Shuer LM, Chang EF, Grant GA, Gephart MG, Barres BA. Purification and Characterization of Progenitor and Mature Human Astrocytes Reveals Transcriptional and Functional Differences with Mouse. *Neuron.* 2016;89(1):37-53. Epub 2015/12/22. doi: 10.1016/j.neuron.2015.11.013. PubMed PMID: 26687838; PMCID: PMC4707064.
294. Du H, Zhou X, Feng T, Hu F. Regulation of lysosomal trafficking of progranulin by sortilin and prosaposin. *Brain Commun.* 2022;4(1):fcab310. Epub 2022/02/17. doi: 10.1093/braincomms/fcab310. PubMed PMID: 35169707; PMCID: PMC8833632.
295. Dall E, Brandstetter H. Structure and function of legumain in health and disease. *Biochimie.* 2016;122:126-50. Epub 2015/09/26. doi: 10.1016/j.biochi.2015.09.022. PubMed PMID: 26403494.
296. Okura H, Yamashita S, Ohama T, Saga A, Yamamoto-Kakuta A, Hamada Y, Sougawa N, Ohyama R, Sawa Y, Matsuyama A. HDL/apolipoprotein A-I binds to macrophage-derived progranulin and suppresses its conversion into proinflammatory granulins. *J Atheroscler Thromb.* 2010;17(6):568-77. Epub 2010/03/11. doi: 10.5551/jat.3921. PubMed PMID: 20215705.
297. Zheng Y, Brady OA, Meng PS, Mao Y, Hu F. C-terminus of progranulin interacts with the beta-propeller region of sortilin to regulate progranulin trafficking. *PLoS One.* 2011;6(6):e21023. Epub 2011/06/24. doi: 10.1371/journal.pone.0021023. PubMed PMID: 21698296; PMCID: PMC3115958.
298. De Muynck L, Herdewyn S, Beel S, Scheveneels W, Van Den Bosch L, Robberecht W, Van Damme P. The neurotrophic properties of progranulin depend on the granulin E domain but do not require sortilin binding. *Neurobiol Aging.* 2013;34(11):2541-7. Epub 2013/05/28. doi: 10.1016/j.neurobiolaging.2013.04.022. PubMed PMID: 23706646.
299. Wang J, Van Damme P, Cruchaga C, Gitcho MA, Vidal JM, Seijo-Martínez M, Wang L, Wu JY, Robberecht W, Goate A. Pathogenic cysteine mutations affect progranulin function and production of mature granulins. *J Neurochem.* 2010;112(5):1305-15. Epub 2009/12/24. doi: 10.1111/j.1471-4159.2009.06546.x. PubMed PMID: 20028451; PMCID: PMC2819556.
300. Tanaka M, Kuse Y, Nakamura S, Hara H, Shimazawa M. Potential effects of progranulin and granulins against retinal photoreceptor cell degeneration. *Mol Vis.* 2019;25:902-11. Epub 2020/02/07. PubMed PMID: 32025182; PMCID: PMC6982430.
301. Culouscou JM, Carlton GW, Shoyab M. Biochemical analysis of the epithelin receptor. *J Biol Chem.* 1993;268(14):10458-62. Epub 1993/05/15. PubMed PMID: 8387520.

302. Liao LM, Lallone RL, Seitz RS, Buznikov A, Gregg JP, Kornblum HI, Nelson SF, Bronstein JM. Identification of a human glioma-associated growth factor gene, granulin, using differential immuno-absorption. *Cancer research*. 2000;60(5):1353-60.
303. Hoque M, Young TM, Lee CG, Serrero G, Mathews MB, Pe'ery T. The growth factor granulin interacts with cyclin T1 and modulates P-TEFb-dependent transcription. *Mol Cell Biol*. 2003;23(5):1688-702. Epub 2003/02/18. doi: 10.1128/mcb.23.5.1688-1702.2003. PubMed PMID: 12588988; PMCID: PMC151712.
304. Hoque M, Tian B, Mathews MB, Pe'ery T. Granulin and Granulin Repeats Interact with the TatP-TEFb Complex and Inhibit Tat Transactivation *. *Journal of Biological Chemistry*. 2005;280(14):13648-57. doi: 10.1074/jbc.M409575200.
305. Trinh DP, Brown KM, Jeang KT. Epithelin/granulin growth factors: extracellular cofactors for HIV-1 and HIV-2 Tat proteins. *Biochem Biophys Res Commun*. 1999;256(2):299-306. Epub 1999/03/18. doi: 10.1006/bbrc.1999.0317. PubMed PMID: 10079180.
306. Santos MN, Paushter DH, Zhang T, Wu X, Feng T, Lou J, Du H, Becker SM, Fragoza R, Yu H. Progranulin-derived granulin E and lysosome membrane protein CD68 interact to reciprocally regulate their protein homeostasis. *Journal of Biological Chemistry*. 2022;298(9).
307. Raden D, Hildebrandt S, Xu P, Bell E, Doyle FJ, 3rd, Robinson AS. Analysis of cellular response to protein overexpression. *Syst Biol (Stevenage)*. 2005;152(4):285-9. Epub 2006/09/22. doi: 10.1049/ip-syb:20050048. PubMed PMID: 16986272.
308. Tanudji M, Hevi S, Chuck SL. Improperly folded green fluorescent protein is secreted via a non-classical pathway. *J Cell Sci*. 2002;115(Pt 19):3849-57. Epub 2002/09/18. doi: 10.1242/jcs.00047. PubMed PMID: 12235295.
309. Salazar DA, Butler VJ, Argouarch AR, Hsu T-Y, Mason A, Nakamura A, McCurdy H, Cox D, Ng R, Pan G, Seeley WW, Miller BL, Kao AW. The Progranulin Cleavage Products, Granulins, Exacerbate TDP-43 Toxicity and Increase TDP-43 Levels. *The Journal of Neuroscience*. 2015;35(25):9315-28. doi: 10.1523/jneurosci.4808-14.2015.
310. Xu D, Suenaga N, Edelmann MJ, Fridman R, Muschel RJ, Kessler BM. Novel MMP-9 substrates in cancer cells revealed by a label-free quantitative proteomics approach. *Mol Cell Proteomics*. 2008;7(11):2215-28. Epub 2008/07/04. doi: 10.1074/mcp.M800095-MCP200. PubMed PMID: 18596065; PMCID: PMC2577209.
311. Ungurs MJ, Sinden NJ, Stockley RA. Progranulin is a substrate for neutrophil-elastase and proteinase-3 in the airway and its concentration correlates with mediators of airway inflammation in COPD. *Am J Physiol Lung Cell Mol Physiol*. 2014;306(1):L80-7. Epub 2013/11/05. doi: 10.1152/ajplung.00221.2013. PubMed PMID: 24186875.
312. Park B, Buti L, Lee S, Matsuwaki T, Spooner E, Brinkmann MM, Nishihara M, Ploegh HL. Granulin is a soluble cofactor for toll-like receptor 9 signaling. *Immunity*. 2011;34(4):505-13. Epub 2011/04/19. doi: 10.1016/j.immuni.2011.01.018. PubMed PMID: 21497117.
313. Yee CM, Zak AJ, Hill BD, Wen F. The Coming Age of Insect Cells for Manufacturing and Development of Protein Therapeutics. *Ind Eng Chem Res*. 2018;57(31):10061-70. Epub 2019/03/20. doi: 10.1021/acs.iecr.8b00985. PubMed PMID: 30886455; PMCID: PMC6420222.
314. Hervas-Stubbs S, Rueda P, Lopez L, Leclerc C. Insect baculoviruses strongly potentiate adaptive immune responses by inducing type I IFN. *J Immunol*. 2007;178(4):2361-9. Epub 2007/02/06. doi: 10.4049/jimmunol.178.4.2361. PubMed PMID: 17277142.
315. Townley RA, Boeve BF, Benarroch EE. Progranulin: Functions and neurologic correlations. *Neurology*. 2018;90(3):118-25. Epub 2017/12/22. doi: 10.1212/wnl.0000000000004840. PubMed PMID: 29263224; PMCID: PMC5772162.

316. van der Zee J, Le Ber I, Maurer-Stroh S, Engelborghs S, Gijssels I, Camuzat A, Brouwers N, Vandenberghe R, Slegers K, Hannequin D, Dermaut B, Schymkowitz J, Campion D, Santens P, Martin JJ, Lacomblez L, De Pooter T, Peeters K, Mattheijssens M, Verdelletto M, Van den Broeck M, Cruts M, De Deyn PP, Rousseau F, Brice A, Van Broeckhoven C. Mutations other than null mutations producing a pathogenic loss of progranulin in frontotemporal dementia. *Hum Mutat.* 2007;28(4):416. Epub 2007/03/09. doi: 10.1002/humu.9484. PubMed PMID: 17345602.
317. Katsumata Y, Shade LM, Hohman TJ, Schneider JA, Bennett DA, Farfel JM, Kukull WA, Fardo DW, Nelson PT. Multiple gene variants linked to Alzheimer's-type clinical dementia via GWAS are also associated with non-Alzheimer's neuropathologic entities. *Neurobiol Dis.* 2022;174:105880. Epub 2022/10/04. doi: 10.1016/j.nbd.2022.105880. PubMed PMID: 36191742; PMCID: PMC9641973.
318. Rhinn H, Tatton N, McCaughey S, Kurnellas M, Rosenthal A. Progranulin as a therapeutic target in neurodegenerative diseases. *Trends Pharmacol Sci.* 2022;43(8):641-52. Epub 2022/01/19. doi: 10.1016/j.tips.2021.11.015. PubMed PMID: 35039149.
319. Uhlén M, Fagerberg L, Hallström BM, Lindskog C, Oksvold P, Mardinoglu A, Sivertsson Å, Kampf C, Sjöstedt E, Asplund A, Olsson I, Edlund K, Lundberg E, Navani S, Szigartyo CA, Odeberg J, Djureinovic D, Takanen JO, Hober S, Alm T, Edqvist PH, Berling H, Tegel H, Mulder J, Rockberg J, Nilsson P, Schwenk JM, Hamsten M, von Feilitzen K, Forsberg M, Persson L, Johansson F, Zwahlen M, von Heijne G, Nielsen J, Pontén F. Proteomics. Tissue-based map of the human proteome. *Science.* 2015;347(6220):1260419. Epub 2015/01/24. doi: 10.1126/science.1260419. PubMed PMID: 25613900.
320. Neill T, Buraschi S, Goyal A, Sharpe C, Natkanski E, Schaefer L, Morrione A, Iozzo RV. EphA2 is a functional receptor for the growth factor progranulin. *J Cell Biol.* 2016;215(5):687-703. Epub 2016/12/03. doi: 10.1083/jcb.201603079. PubMed PMID: 27903606; PMCID: PMC5146997.
321. Lang I, Füllsack S, Wajant H. Lack of Evidence for a Direct Interaction of Progranulin and Tumor Necrosis Factor Receptor-1 and Tumor Necrosis Factor Receptor-2 From Cellular Binding Studies. *Front Immunol.* 2018;9:793. Epub 2018/05/10. doi: 10.3389/fimmu.2018.00793. PubMed PMID: 29740434; PMCID: PMC5925078.
322. Darmoise A, Maschmeyer P, Winau F. The immunological functions of saposins. *Adv Immunol.* 2010;105:25-62. Epub 2010/06/01. doi: 10.1016/s0065-2776(10)05002-9. PubMed PMID: 20510729; PMCID: PMC4030616.
323. Verbeeck C, Deng Q, DeJesus-Hernandez M, Taylor G, Ceballos-Diaz C, Kocerha J, Golde T, Das P, Rademakers R, Dickson DW, Kukar T. Expression of Fused in sarcoma mutations in mice recapitulates the neuropathology of FUS proteinopathies and provides insight into disease pathogenesis. *Mol Neurodegener.* 2012;7. doi: Artn 53 10.1186/1750-1326-7-53. PubMed PMID: WOS:000312651200001.
324. Chakrabarty P, Rosario A, Cruz P, Siemienski Z, Ceballos-Diaz C, Crosby K, Jansen K, Borchelt D, Kim J-Y, Jankowsky J, Levites Y. Capsid Serotype and Timing of Injection Determines AAV Transduction in the Neonatal Mice Brain. *PloS one.* 2013;8:e67680. doi: 10.1371/journal.pone.0067680.
325. Kim JY, Grunke SD, Levites Y, Golde TE, Jankowsky JL. Intracerebroventricular viral injection of the neonatal mouse brain for persistent and widespread neuronal transduction. *J Vis Exp.* 2014(91):51863. Epub 2014/10/07. doi: 10.3791/51863. PubMed PMID: 25286085; PMCID: PMC4199253.

326. Bocchetta M, Gordon E, Cardoso MJ, Modat M, Ourselin S, Warren JD, Rohrer JD. Thalamic atrophy in frontotemporal dementia - Not just a C9orf72 problem. *Neuroimage Clin.* 2018;18:675-81. Epub 2018/06/08. doi: 10.1016/j.nicl.2018.02.019. PubMed PMID: 29876259; PMCID: PMC5988457.
327. Bocchetta M, Todd EG, Peakman G, Cash DM, Convery RS, Russell LL, Thomas DL, Eugenio Iglesias J, van Swieten JC, Jiskoot LC, Seelaar H, Borroni B, Galimberti D, Sanchez-Valle R, Laforce R, Moreno F, Synofzik M, Graff C, Masellis M, Carmela Tartaglia M, Rowe JB, Vandenberghe R, Finger E, Tagliavini F, de Mendonça A, Santana I, Butler CR, Ducharme S, Gerhard A, Danek A, Levin J, Otto M, Sorbi S, Le Ber I, Pasquier F, Rohrer JD. Differential early subcortical involvement in genetic FTD within the GENFI cohort. *Neuroimage Clin.* 2021;30:102646. Epub 2021/04/26. doi: 10.1016/j.nicl.2021.102646. PubMed PMID: 33895632; PMCID: PMC8099608.
328. Allan ERO, Campden RI, Ewanchuk BW, Taylor P, Balce DR, McKenna NT, Greene CJ, Warren AL, Reinheckel T, Yates RM. A role for cathepsin Z in neuroinflammation provides mechanistic support for an epigenetic risk factor in multiple sclerosis. *J Neuroinflammation.* 2017;14(1):103. Epub 2017/05/11. doi: 10.1186/s12974-017-0874-x. PubMed PMID: 28486971; PMCID: PMC5424360.
329. Brandenstein L, Schweizer M, Sedlacik J, Fiehler J, Storch S. Lysosomal dysfunction and impaired autophagy in a novel mouse model deficient for the lysosomal membrane protein Cln7. *Hum Mol Genet.* 2016;25(4):777-91. Epub 2015/12/19. doi: 10.1093/hmg/ddv615. PubMed PMID: 26681805.
330. Thygesen C, Ilkjær L, Kempf SJ, Hemdrup AL, von Linstow CU, Babcock AA, Darvesh S, Larsen MR, Finsen B. Diverse Protein Profiles in CNS Myeloid Cells and CNS Tissue From Lipopolysaccharide- and Vehicle-Injected APP(SWE)/PS1(Δ E9) Transgenic Mice Implicate Cathepsin Z in Alzheimer's Disease. *Front Cell Neurosci.* 2018;12:397. Epub 2018/11/22. doi: 10.3389/fncel.2018.00397. PubMed PMID: 30459560; PMCID: PMC6232379.
331. Aits S, Krickler J, Liu B, Ellegaard AM, Hämälistö S, Tvingsholm S, Corcelle-Termeau E, Høgh S, Farkas T, Holm Jonassen A, Gromova I, Mortensen M, Jäättelä M. Sensitive detection of lysosomal membrane permeabilization by lysosomal galectin puncta assay. *Autophagy.* 2015;11(8):1408-24. Epub 2015/06/27. doi: 10.1080/15548627.2015.1063871. PubMed PMID: 26114578; PMCID: PMC4590643.
332. Jia J, Claude-Taupin A, Gu Y, Choi SW, Peters R, Bissa B, Mudd MH, Allers L, Pallikkuth S, Lidke KA, Salemi M, Phinney B, Mari M, Reggiori F, Deretic V. Galectin-3 Coordinates a Cellular System for Lysosomal Repair and Removal. *Dev Cell.* 2020;52(1):69-87.e8. Epub 2019/12/10. doi: 10.1016/j.devcel.2019.10.025. PubMed PMID: 31813797; PMCID: PMC6997950.
333. Petkau TL, Neal SJ, Orban PC, MacDonald JL, Hill AM, Lu G, Feldman HH, Mackenzie IRA, Leavitt BR. Progranulin expression in the developing and adult murine brain. *Journal of Comparative Neurology.* 2010;518(19):3931-47. doi: 10.1002/cne.22430.
334. Zhang J, Velmshch D, Hashimoto K, Huang YH, Hofmann JW, Shi X, Chen J, Leidal AM, Dishart JG, Cahill MK, Kelley KW, Liddel SA, Seeley WW, Miller BL, Walther TC, Farese RV, Jr., Taylor JP, Ullian EM, Huang B, Debnath J, Wittmann T, Kriegstein AR, Huang EJ. Neurotoxic microglia promote TDP-43 proteinopathy in progranulin deficiency. *Nature.* 2020;588(7838):459-65. Epub 2020/09/01. doi: 10.1038/s41586-020-2709-7. PubMed PMID: 32866962; PMCID: PMC7746606.

335. Galloway DA, Phillips AEM, Owen DRJ, Moore CS. Phagocytosis in the Brain: Homeostasis and Disease. *Frontiers in Immunology*. 2019;10. doi: 10.3389/fimmu.2019.00790.
336. Hopperton KE, Mohammad D, Trépanier MO, Giuliano V, Bazinet RP. Markers of microglia in post-mortem brain samples from patients with Alzheimer's disease: a systematic review. *Mol Psychiatry*. 2018;23(2):177-98. doi: 10.1038/mp.2017.246.
337. Jurga AM, Paleczna M, Kuter KZ. Overview of General and Discriminating Markers of Differential Microglia Phenotypes. *Front Cell Neurosci*. 2020;14. doi: 10.3389/fncel.2020.00198.
338. Holness C, Simmons D. Molecular cloning of CD68, a human macrophage marker related to lysosomal glycoproteins. *Blood*. 1993;81(6):1607-13. doi: 10.1182/blood.V81.6.1607.1607.
339. Hüttenrauch M, Ogorek I, Klafki H, Otto M, Stadelmann C, Weggen S, Wiltfang J, Wirths O. Glycoprotein NMB: a novel Alzheimer's disease associated marker expressed in a subset of activated microglia. *Acta Neuropathol Commun*. 2018;6(1):108. Epub 2018/10/21. doi: 10.1186/s40478-018-0612-3. PubMed PMID: 30340518; PMCID: PMC6194687.
340. Moloney EB, Moskites A, Ferrari EJ, Isacson O, Hallett PJ. The glycoprotein GPNMB is selectively elevated in the substantia nigra of Parkinson's disease patients and increases after lysosomal stress. *Neurobiol Dis*. 2018;120:1-11. Epub 2018/08/28. doi: 10.1016/j.nbd.2018.08.013. PubMed PMID: 30149180; PMCID: PMC6748034.
341. Gabriel TL, Tol MJ, Ottenhof R, van Roomen C, Aten J, Claessen N, Hooibrink B, de Weijer B, Serlie MJ, Argmann C, van Elsenburg L, Aerts JM, van Eijk M. Lysosomal stress in obese adipose tissue macrophages contributes to MITF-dependent Gpnmb induction. *Diabetes*. 2014;63(10):3310-23. Epub 2014/05/03. doi: 10.2337/db13-1720. PubMed PMID: 24789918.
342. Khrouf W, Saracino D, Rucheton B, Houot M, Clot F, Rinaldi D, Vitor J, Huynh M, Heng E, Schlemmer D, Pasquier F, Deramecourt V, Auriacombe S, Azuar C, Levy R, Bombois S, Boutoleau-Brétonnière C, Pariente J, Didic M, Wallon D, Fluchère F, Auvin S, Younes IB, Nadjar Y, Brice A, Dubois B, Bonnefont-Rousselot D, Le Ber I, Lamari F. Plasma lysosphingolipids in GRN-related diseases: Monitoring lysosomal dysfunction to track disease progression. *Neurobiol Dis*. 2023;181:106108. Epub 2023/04/02. doi: 10.1016/j.nbd.2023.106108. PubMed PMID: 37003407.
343. Prinetti A, Prioni S, Chiricozzi E, Schuchman EH, Chigorno V, Sonnino S. Secondary alterations of sphingolipid metabolism in lysosomal storage diseases. *Neurochem Res*. 2011;36(9):1654-68. Epub 2011/01/06. doi: 10.1007/s11064-010-0380-3. PubMed PMID: 21207141.
344. Ward ME, Chen R, Huang H-Y, Ludwig C, Telpoukhovskaia M, Taubes A, Boudin H, Minami SS, Reichert M, Albrecht P, Gelfand JM, Cruz-Herranz A, Cordano C, Alavi MV, Leslie S, Seeley WW, Miller BL, Bigio E, Mesulam M-M, Bogyo MS, Mackenzie IR, Staropoli JF, Cotman SL, Huang EJ, Gan L, Green AJ. Individuals with progranulin haploinsufficiency exhibit features of neuronal ceroid lipofuscinosis. *Science Translational Medicine*. 2017;9(385):eaah5642. doi: 10.1126/scitranslmed.aah5642.
345. Arrant AE, Filiano AJ, Patel AR, Hoffmann MQ, Boyle NR, Kashyap SN, Onyilo VC, Young AH, Roberson ED. Reduction of microglial progranulin does not exacerbate pathology or behavioral deficits in neuronal progranulin-insufficient mice. *Neurobiology of disease*. 2019;124:152-62. Epub 2018/11/15. doi: 10.1016/j.nbd.2018.11.011. PubMed PMID: 30448285.
346. Gaskill BN, Karas AZ, Garner JP, Pritchett-Corning KR. Nest building as an indicator of health and welfare in laboratory mice. *Journal of visualized experiments: JoVE*. 2013(82).
347. Angoa-Perez M, Kane MJ, Briggs DI, Francescutti DM, Kuhn DM. Marble burying and nestlet shredding as tests of repetitive, compulsive-like behaviors in mice. *J Vis Exp*.

2013(82):50978. Epub 2014/01/17. doi: 10.3791/50978. PubMed PMID: 24429507; PMCID: PMC4108161.

348. Dorninger F, Zeitler G, Berger J. Nestlet Shredding and Nest Building Tests to Assess Features of Psychiatric Disorders in Mice. *Bio Protoc.* 2020;10(24). Epub 2021/01/22. doi: 10.21769/BioProtoc.3863. PubMed PMID: 33473360; PMCID: PMC7116606.

349. Holler C, Taylor G, T K, editors. Production, detection, and characterization of progranulin (PGRN) and granulins 10th International Conference on Frontotemporal Dementias; 2016; Munich Germany: Journal of Neurochemistry.

350. Zhang L, Sheng R, Qin Z. The lysosome and neurodegenerative diseases. *Acta Biochim Biophys Sin (Shanghai).* 2009;41(6):437-45. Epub 2009/06/06. doi: 10.1093/abbs/gmp031. PubMed PMID: 19499146.

351. Lie PPY, Nixon RA. Lysosome trafficking and signaling in health and neurodegenerative diseases. *Neurobiol Dis.* 2019;122:94-105. Epub 2018/06/03. doi: 10.1016/j.nbd.2018.05.015. PubMed PMID: 29859318; PMCID: PMC6381838.

352. Peng X, Lanter JC, A YPC, Brand MA, Wozniak MK, Hoekman S, Longin O, Regeling H, Zonneveld W, R PLB, Koenig G, Hurst RS, Blain JF, Burnett DA. Discovery of oxazoline enhancers of cellular progranulin release. *Bioorg Med Chem Lett.* 2023;80:129048. Epub 2022/11/12. doi: 10.1016/j.bmcl.2022.129048. PubMed PMID: 36368496.

353. Blain J-F, Chen AYP, Brand MA, Lanter JC, Holler CJ, Brendel JK, Koenig G, Burnett DA, Hurst RS. A Novel In Vivo-Active Small Molecule Inducer of Progranulin for the Treatment of Frontotemporal Dementia. *Alzheimer's & Dementia.* 2022;18(S10):e061924. doi: <https://doi.org/10.1002/alz.061924>.

354. Canuel M, Libin Y, Morales CR. The interactomics of sortilin: an ancient lysosomal receptor evolving new functions. *Histol Histopathol.* 2009;24(4):481-92. Epub 2009/02/19. doi: 10.14670/hh-24.481. PubMed PMID: 19224451.

355. Wickham H. *ggplot2: Elegant Graphics for Data Analysis*: Springer International Publishing; 2016.

356. Gao B, Zhu J, Negi S, Zhang X, Gyoneva S, Casey F, Wei R, Zhang B. Quickomics: exploring omics data in an intuitive, interactive and informative manner. *Bioinformatics.* 2021;37(20):3670-2. doi: 10.1093/bioinformatics/btab255.

357. Blighe K, Brown A-L, Carey V, Hooiveld G, Lun A. PCAtools: Everything Principal Components Analysis R package version 2.10.0 ed2022. p. Principal Component Analysis (PCA) is a very powerful technique that has wide applicability in data science, bioinformatics, and further afield. It was initially developed to analyse large volumes of data in order to tease out the differences/relationships between the logical entities being analysed. It extracts the fundamental structure of the data without the need to build any model to represent it. This 'summary' of the data is arrived at through a process of reduction that can transform the large number of variables into a lesser number that are uncorrelated (i.e. the 'principal components'), while at the same time being capable of easy interpretation on the original data. PCAtools provides functions for data exploration via PCA, and allows the user to generate publication-ready figures. PCA is performed via BiocSingular - users can also identify optimal number of principal components via different metrics, such as elbow method and Horn's parallel analysis, which has relevance for data reduction in single-cell RNA-seq (scRNA-seq) and high dimensional mass cytometry data.

358. Zhou Y, Zhou B, Pache L, Chang M, Khodabakhshi AH, Tanaseichuk O, Benner C, Chanda SK. Metascape provides a biologist-oriented resource for the analysis of systems-level

- datasets. *Nat Commun.* 2019;10(1):1523. Epub 2019/04/05. doi: 10.1038/s41467-019-09234-6. PubMed PMID: 30944313; PMCID: PMC6447622.
359. Johnson MA, Nuckols TA, Merino P, Bagchi P, Nandy S, Root J, Taylor G, Seyfried NT, Kukar T. Proximity-based labeling reveals DNA damage-induced phosphorylation of fused in sarcoma (FUS) causes distinct changes in the FUS protein interactome. *J Biol Chem.* 2022;298(8):102135. Epub 2022/06/17. doi: 10.1016/j.jbc.2022.102135. PubMed PMID: 35709984; PMCID: PMC9372748.
360. Johnson MA, Deng Q, Taylor G, McEachin ZT, Chan AWS, Root J, Bassell GJ, Kukar T. Divergent FUS phosphorylation in primate and mouse cells following double-strand DNA damage. *Neurobiol Dis.* 2020;146:105085. Epub 2020/09/21. doi: 10.1016/j.nbd.2020.105085. PubMed PMID: 32950644; PMCID: PMC8064403.
361. Bodenhofer U, Bonatesta E, Horejš-Kainrath C, Hochreiter S. msa: an R package for multiple sequence alignment. *Bioinformatics.* 2015;31(24):3997-9. doi: 10.1093/bioinformatics/btv494.
362. Zhou L, Feng T, Xu S, Gao F, Lam TT, Wang Q, Wu T, Huang H, Zhan L, Li L, Guan Y, Dai Z, Yu G. ggmsa: a visual exploration tool for multiple sequence alignment and associated data. *Briefings in Bioinformatics.* 2022;23(4). doi: 10.1093/bib/bbac222.
363. Grant BJ, Rodrigues APC, ElSawy KM, McCammon JA, Caves LSD. Bio3d: an R package for the comparative analysis of protein structures. *Bioinformatics.* 2006;22(21):2695-6. doi: 10.1093/bioinformatics/btl461.
364. Trifinopoulos J, Nguyen L-T, von Haeseler A, Minh BQ. W-IQ-TREE: a fast online phylogenetic tool for maximum likelihood analysis. *Nucleic Acids Res.* 2016;44(W1):W232-W5. doi: 10.1093/nar/gkw256.
365. Kalyanamorthy S, Minh BQ, Wong TKF, von Haeseler A, Jermini LS. ModelFinder: fast model selection for accurate phylogenetic estimates. *Nature Methods.* 2017;14(6):587-9. doi: 10.1038/nmeth.4285.
366. Nicolas LB, Kolb Y, Prinssen EP. A combined marble burying-locomotor activity test in mice: a practical screening test with sensitivity to different classes of anxiolytics and antidepressants. *Eur J Pharmacol.* 2006;547(1-3):106-15. Epub 2006/08/29. doi: 10.1016/j.ejphar.2006.07.015. PubMed PMID: 16934246.
367. Lustberg D, Iannitelli AF, Tillage RP, Pruitt M, Liles LC, Weinschenker D. Central norepinephrine transmission is required for stress-induced repetitive behavior in two rodent models of obsessive-compulsive disorder. *Psychopharmacology.* 2020;237(7):1973-87. doi: 10.1007/s00213-020-05512-0.
368. Deacon R. Assessing burrowing, nest construction, and hoarding in mice. *J Vis Exp.* 2012(59):e2607. Epub 2012/01/20. doi: 10.3791/2607. PubMed PMID: 22258546; PMCID: PMC3369766.
369. de Duve C. The lysosome turns fifty. *Nat Cell Biol.* 2005;7(9):847-9. doi: 10.1038/ncb0905-847.
370. Braulke T, Bonifacino JS. Sorting of lysosomal proteins. *Biochimica et Biophysica Acta (BBA) - Molecular Cell Research.* 2009;1793(4):605-14. doi: <https://doi.org/10.1016/j.bbamcr.2008.10.016>.
371. Johnson JO, Mandrioli J, Benatar M, Abramzon Y, Van Deerlin VM, Trojanowski JQ, Gibbs JR, Brunetti M, Gronka S, Wu J, Ding J, McCluskey L, Martinez-Lage M, Falcone D, Hernandez DG, Arepalli S, Chong S, Schymick JC, Rothstein J, Landi F, Wang YD, Calvo A, Mora G, Sabatelli M, Monsurrò MR, Battistini S, Salvi F, Spataro R, Sola P, Borghero G, Galassi

- G, Scholz SW, Taylor JP, Restagno G, Chiò A, Traynor BJ. Exome sequencing reveals VCP mutations as a cause of familial ALS. *Neuron*. 2010;68(5):857-64. Epub 2010/12/15. doi: 10.1016/j.neuron.2010.11.036. PubMed PMID: 21145000; PMCID: PMC3032425.
372. Li X, Rydzewski N, Hider A, Zhang X, Yang J, Wang W, Gao Q, Cheng X, Xu H. A molecular mechanism to regulate lysosome motility for lysosome positioning and tubulation. *Nat Cell Biol*. 2016;18(4):404-17. Epub 2016/03/08. doi: 10.1038/ncb3324. PubMed PMID: 26950892; PMCID: PMC4871318.
373. Saric A, Hipolito VE, Kay JG, Canton J, Antonescu CN, Botelho RJ. mTOR controls lysosome tubulation and antigen presentation in macrophages and dendritic cells. *Mol Biol Cell*. 2016;27(2):321-33. Epub 2015/11/20. doi: 10.1091/mbc.E15-05-0272. PubMed PMID: 26582390; PMCID: PMC4713134.
374. Xu H, Ren D. Lysosomal physiology. *Annual review of physiology*. 2015;77:57-80. doi: 10.1146/annurev-physiol-021014-071649. PubMed PMID: 25668017.
375. Martinez-Vicente M, Sovak G, Cuervo AM. Protein degradation and aging. *Exp Gerontol*. 2005;40(8-9):622-33. Epub 2005/08/30. doi: 10.1016/j.exger.2005.07.005. PubMed PMID: 16125351.
376. Lim C-Y, Zoncu R. The lysosome as a command-and-control center for cellular metabolism. *The Journal of cell biology*. 2016;214(6):653-64. doi: 10.1083/jcb.201607005. PubMed PMID: 27621362.
377. Platt FM, d'Azzo A, Davidson BL, Neufeld EF, Tiffit CJ. Lysosomal storage diseases. *Nature Reviews Disease Primers*. 2018;4(1):27. doi: 10.1038/s41572-018-0025-4.
378. Nair V, Belanger EC, Veinot JP. Lysosomal storage disorders affecting the heart: a review. *Cardiovasc Pathol*. 2019;39:12-24. Epub 2018/12/31. doi: 10.1016/j.carpath.2018.11.002. PubMed PMID: 30594732.
379. Rigante D, Cipolla C, Basile U, Gulli F, Savastano MC. Overview of immune abnormalities in lysosomal storage disorders. *Immunol Lett*. 2017;188:79-85. Epub 2017/07/09. doi: 10.1016/j.imlet.2017.07.004. PubMed PMID: 28687233.
380. Aldenhoven M, Sakkars RJB, Boelens J, Koning TJd, Wulffraat NM. Musculoskeletal manifestations of lysosomal storage disorders. *Annals of the Rheumatic Diseases*. 2009;68(11):1659. doi: 10.1136/ard.2008.095315.
381. Prada CE, Grabowski GA. Neuronopathic lysosomal storage diseases: clinical and pathologic findings. *Developmental disabilities research reviews*. 2013;17(3):226-46.
382. Clayton EL, Mizielińska S, Edgar JR, Nielsen TT, Marshall S, Norona FE, Robbins M, Damirji H, Holm IE, Johannsen P. Frontotemporal dementia caused by CHMP2B mutation is characterised by neuronal lysosomal storage pathology. *Acta Neuropathol*. 2015;130:511-23.
383. Tresse E, Salomons FA, Vesa J, Bott LC, Kimonis V, Yao TP, Dantuma NP, Taylor JP. VCP/p97 is essential for maturation of ubiquitin-containing autophagosomes and this function is impaired by mutations that cause IBMPFD. *Autophagy*. 2010;6(2):217-27. Epub 2010/01/28. doi: 10.4161/auto.6.2.11014. PubMed PMID: 20104022; PMCID: PMC2929010.
384. Campbell CA, Fursova O, Cheng X, Snella E, McCune A, Li L, Solchenberger B, Schmid B, Sahoo D, Morton M, Traver D, Espín-Palazón R. A zebrafish model of granulins deficiency reveals essential roles in myeloid cell differentiation. *Blood Adv*. 2021;5(3):796-811. Epub 2021/02/10. doi: 10.1182/bloodadvances.2020003096. PubMed PMID: 33560393; PMCID: PMC7876888 interests.
385. Solchenberger B, Russell C, Kremmer E, Haass C, Schmid B. Granulin knock out zebrafish lack frontotemporal lobar degeneration and neuronal ceroid lipofuscinosis pathology. *PLoS One*.

- 2015;10(3):e0118956. Epub 2015/03/19. doi: 10.1371/journal.pone.0118956. PubMed PMID: 25785851; PMCID: PMC4365039.
386. Doyle JJ, Maios C, Vranx C, Duhaime S, Chitramuthu B, Bennett HPJ, Bateman A, Parker JA. Chemical and genetic rescue of in vivo progranulin-deficient lysosomal and autophagic defects. *Proceedings of the National Academy of Sciences*. 2021;118(25):e2022115118. doi: 10.1073/pnas.2022115118.
387. Holler CJ, Taylor G, McEachin ZT, Deng Q, Watkins WJ, Hudson K, Easley CA, Hu WT, Hales CM, Rossoll W, Bassell GJ, Kukar T. Trehalose upregulates progranulin expression in human and mouse models of GRN haploinsufficiency: a novel therapeutic lead to treat frontotemporal dementia. *Mol Neurodegener*. 2016;11(1):46. Epub 2016/06/28. doi: 10.1186/s13024-016-0114-3. PubMed PMID: 27341800; PMCID: PMC4919863.
388. Davis SE, Roth JR, Aljabi Q, Hakim AR, Savell KE, Day JJ, Arrant AE. Delivering progranulin to neuronal lysosomes protects against excitotoxicity. *J Biol Chem*. 2021;297(3):100993. Epub 2021/07/24. doi: 10.1016/j.jbc.2021.100993. PubMed PMID: 34298019; PMCID: PMC8379502.
389. Almeida S, Zhang Z, Coppola G, Mao W, Futai K, Karydas A, Geschwind MD, Tartaglia MC, Gao F, Gianni D. Induced pluripotent stem cell models of progranulin-deficient frontotemporal dementia uncover specific reversible neuronal defects. *Cell Rep*. 2012;2(4):789-98.
390. Edwards MA, Loxley RA, Williams AJ, Connor M, Phillips JK. Lack of functional expression of NMDA receptors in PC12 cells. *Neurotoxicology*. 2007;28(4):876-85. Epub 2007/06/19. doi: 10.1016/j.neuro.2007.04.006. PubMed PMID: 17572500.
391. Gordon J, Amini S, White MK. General overview of neuronal cell culture. *Methods in molecular biology (Clifton, NJ)*. 2013;1078:1-8. Epub 2013/08/27. doi: 10.1007/978-1-62703-640-5_1. PubMed PMID: 23975816; PMCID: PMC4052554.
392. Bossolasco P, Cimini S, Maderna E, Bardelli D, Canafoglia L, Cavallaro T, Ricci M, Silani V, Marucci G, Rossi G. GRN^{-/-} iPSC-derived cortical neurons recapitulate the pathological findings of both frontotemporal lobar degeneration and neuronal ceroidlipofuscinosis. *Neurobiology of Disease*. 2022;175:105891. doi: <https://doi.org/10.1016/j.nbd.2022.105891>.
393. Lines G, Casey JM, Preza E, Wray S. Modelling frontotemporal dementia using patient-derived induced pluripotent stem cells. *Molecular and Cellular Neuroscience*. 2020;109:103553. doi: <https://doi.org/10.1016/j.mcn.2020.103553>.
394. Nuckols A. Comparison of two models of GRN-deficiency using quantitative proteomics Emory University; 2022.
395. Ishidoh K, Kominami E. Processing and activation of lysosomal proteinases. *Biol Chem*. 2002;383(12):1827-31. Epub 2003/01/30. doi: 10.1515/bc.2002.206. PubMed PMID: 12553719.
396. Reiser J, Adair B, Reinheckel T. Specialized roles for cysteine cathepsins in health and disease. *J Clin Invest*. 2010;120(10):3421-31. Epub 2010/10/06. doi: 10.1172/jci42918. PubMed PMID: 20921628; PMCID: PMC2947230.
397. Jung M, Lee J, Seo HY, Lim JS, Kim EK. Cathepsin inhibition-induced lysosomal dysfunction enhances pancreatic beta-cell apoptosis in high glucose. *PLoS One*. 2015;10(1):e0116972. Epub 2015/01/28. doi: 10.1371/journal.pone.0116972. PubMed PMID: 25625842; PMCID: PMC4308077.
398. Laurent-Matha V, Derocq D, Prébois C, Katunuma N, Liaudet-Coopman E. Processing of human cathepsin D is independent of its catalytic function and auto-activation: involvement of

- cathepsins L and B. *J Biochem.* 2006;139(3):363-71. Epub 2006/03/29. doi: 10.1093/jb/mvj037. PubMed PMID: 16567401; PMCID: PMC2376303.
399. Mehanna S, Suzuki C, Shibata M, Sunabori T, Imanaka T, Araki K, Yamamura K-i, Uchiyama Y, Ohmuraya M. Cathepsin D in pancreatic acinar cells is implicated in cathepsin B and L degradation, but not in autophagic activity. *Biochemical and Biophysical Research Communications.* 2016;469(3):405-11. doi: <https://doi.org/10.1016/j.bbrc.2015.12.002>.
400. Schröder BA, Wrocklage C, Hasilik A, Saftig P. The proteome of lysosomes. *Proteomics.* 2010;10(22):4053-76. Epub 2010/10/20. doi: 10.1002/pmic.201000196. PubMed PMID: 20957757.
401. Stoka V, Turk V, Turk B. Lysosomal cathepsins and their regulation in aging and neurodegeneration. *Ageing Res Rev.* 2016;32:22-37. doi: <https://doi.org/10.1016/j.arr.2016.04.010>.
402. Bunk J, Prieto Huarcaya S, Drobny A, Dobert JP, Walther L, Rose-John S, Arnold P, Zunke F. Cathepsin D Variants Associated With Neurodegenerative Diseases Show Dysregulated Functionality and Modified α -Synuclein Degradation Properties. *Front Cell Dev Biol.* 2021;9:581805. Epub 2021/03/09. doi: 10.3389/fcell.2021.581805. PubMed PMID: 33681191; PMCID: PMC7928348.
403. Drobny A, Prieto Huarcaya S, Dobert J, Kluge A, Bunk J, Schlothauer T, Zunke F. The role of lysosomal cathepsins in neurodegeneration: Mechanistic insights, diagnostic potential and therapeutic approaches. *Biochimica et Biophysica Acta (BBA) - Molecular Cell Research.* 2022;1869(7):119243. doi: <https://doi.org/10.1016/j.bbamcr.2022.119243>.
404. Telpoukhovskaia MA, Liu K, Sayed FA, Etcheagaray JI, Xie M, Zhan L, Li Y, Zhou Y, Le D, Bahr BA, Bogyo M, Ding S, Gan L. Discovery of small molecules that normalize the transcriptome and enhance cysteine cathepsin activity in progranulin-deficient microglia. *Scientific Reports.* 2020;10(1):13688. doi: 10.1038/s41598-020-70534-9.
405. Yadati T, Houben T, Bitorina A, Shiri-Sverdlov R. The Ins and Outs of Cathepsins: Physiological Function and Role in Disease Management. *Cells.* 2020;9(7). Epub 2020/07/17. doi: 10.3390/cells9071679. PubMed PMID: 32668602; PMCID: PMC7407943.
406. Hughes CS, Burden RE, Gilmore BF, Scott CJ. Strategies for detection and quantification of cysteine cathepsins-evolution from bench to bedside. *Biochimie.* 2016;122:48-61. doi: <https://doi.org/10.1016/j.biochi.2015.07.029>.
407. Serim S, Haedke U, Verhelst SH. Activity-based probes for the study of proteases: recent advances and developments. *ChemMedChem.* 2012;7(7):1146-59. Epub 2012/03/21. doi: 10.1002/cmdc.201200057. PubMed PMID: 22431376.
408. Oresic Bender K, Ofori L, van der Linden WA, Mock ED, Datta GK, Chowdhury S, Li H, Segal E, Sanchez Lopez M, Ellman JA, Figdor CG, Bogyo M, Verdoes M. Design of a highly selective quenched activity-based probe and its application in dual color imaging studies of cathepsin S activity localization. *J Am Chem Soc.* 2015;137(14):4771-7. Epub 2015/03/19. doi: 10.1021/jacs.5b00315. PubMed PMID: 25785540; PMCID: PMC4747655.
409. Fukuda M. Lysosomal membrane glycoproteins. Structure, biosynthesis, and intracellular trafficking. *J Biol Chem.* 1991;266(32):21327-30. Epub 1991/11/15. PubMed PMID: 1939168.
410. Schwake M, Schröder B, Saftig P. Lysosomal Membrane Proteins and Their Central Role in Physiology. *Traffic.* 2013;14(7):739-48. doi: <https://doi.org/10.1111/tra.12056>.
411. Siintola E, Topcu M, Aula N, Lohi H, Minassian BA, Paterson AD, Liu X-Q, Wilson C, Lahtinen U, Anttonen A-K, Lehesjoki A-E. The Novel Neuronal Ceroid Lipofuscinosis Gene

MFSD8 Encodes a Putative Lysosomal Transporter. The American Journal of Human Genetics. 2007;81(1):136-46. doi: 10.1086/518902.

412. Isolation of a novel gene underlying Batten disease, CLN3. The International Batten Disease Consortium. Cell. 1995;82(6):949-57. Epub 1995/09/22. doi: 10.1016/0092-8674(95)90274-0. PubMed PMID: 7553855.

413. Mathew E, Elizabeth T, Haydn W, Sukhwinder Singh S, Chris W. Increased expression of Lysosomal-associated membrane protein 1 (LAMP-1) found in small airway epithelium of COPD may have functional consequence and role in autophagy. European Respiratory Journal. 2017;50(suppl 61):OA507. doi: 10.1183/1393003.congress-2017.OA507.

414. Wang Q, Yao J, Jin Q, Wang X, Zhu H, Huang F, Wang W, Qiang J, Ni Q. LAMP1 expression is associated with poor prognosis in breast cancer. Oncol Lett. 2017;14(4):4729-35. Epub 2017/11/01. doi: 10.3892/ol.2017.6757. PubMed PMID: 29085473; PMCID: PMC5649640.

415. Eskelinen E-L. Roles of LAMP-1 and LAMP-2 in lysosome biogenesis and autophagy. Molecular aspects of medicine. 2006;27(5-6):495-502.

416. Kaushik S, Cuervo AM. Chaperone-mediated autophagy: a unique way to enter the lysosome world. Trends Cell Biol. 2012;22(8):407-17. Epub 2012/07/04. doi: 10.1016/j.tcb.2012.05.006. PubMed PMID: 22748206; PMCID: PMC3408550.

417. Yogalingam G, Bonten EJ, van de Vlekkert D, Hu H, Moshiah S, Connell SA, d'Azzo A. Neuraminidase 1 is a negative regulator of lysosomal exocytosis. Dev Cell. 2008;15(1):74-86. Epub 2008/07/09. doi: 10.1016/j.devcel.2008.05.005. PubMed PMID: 18606142; PMCID: PMC2664108.

418. Martina JA, Chen Y, Gucek M, Puertollano R. mTORC1 functions as a transcriptional regulator of autophagy by preventing nuclear transport of TFEB. Autophagy. 2012;8(6):903-14. Epub 2012/05/12. doi: 10.4161/auto.19653. PubMed PMID: 22576015; PMCID: PMC3427256.

419. Radulovic M, Schink KO, Wenzel EM, Nähse V, Bongiovanni A, Lafont F, Stenmark H. ESCRT-mediated lysosome repair precedes lysophagy and promotes cell survival. The EMBO Journal. 2018;37(21):e99753. doi: <https://doi.org/10.15252/embj.201899753>.

420. Caron A, Richard D, Laplante M. The roles of mTOR complexes in lipid metabolism. Annual review of nutrition. 2015;35:321-48.

421. Ballabio A, Gieselmann V. Lysosomal disorders: from storage to cellular damage. Biochimica et Biophysica Acta (BBA)-Molecular Cell Research. 2009;1793(4):684-96.

422. Meikle Peter J, Duplock S, Blacklock D, Whitfield Phillip D, Macintosh G, Hopwood John J, Fuller M. Effect of lysosomal storage on bis(monoacylglycero)phosphate. Biochemical Journal. 2008;411(1):71-8. doi: 10.1042/bj20071043.

423. Drizyte-Miller K, Schott MB, McNiven MA. Lipid Droplet Contacts With Autophagosomes, Lysosomes, and Other Degradative Vesicles. Contact. 2020;3:2515256420910892. doi: 10.1177/2515256420910892.

424. Olzmann JA, Carvalho P. Dynamics and functions of lipid droplets. Nat Rev Mol Cell Biol. 2019;20(3):137-55. Epub 2018/12/14. doi: 10.1038/s41580-018-0085-z. PubMed PMID: 30523332; PMCID: PMC6746329.

425. Turkish AR, Sturley SL. The genetics of neutral lipid biosynthesis: an evolutionary perspective. Am J Physiol Endocrinol Metab. 2009;297(1):E19-27. Epub 2009/01/01. doi: 10.1152/ajpendo.90898.2008. PubMed PMID: 19116372; PMCID: PMC2711666.

426. Farmer BC, Walsh AE, Kluemper JC, Johnson LA. Lipid Droplets in Neurodegenerative Disorders. Front Neurosci. 2020;14:742. Epub 2020/08/28. doi: 10.3389/fnins.2020.00742. PubMed PMID: 32848541; PMCID: PMC7403481.

427. Horton JD, Goldstein JL, Brown MS. SREBPs: activators of the complete program of cholesterol and fatty acid synthesis in the liver. *The Journal of clinical investigation*. 2002;109(9):1125-31.
428. Migita T, Okabe S, Ikeda K, Igarashi S, Sugawara S, Tomida A, Soga T, Taguchi R, Seimiya H. Inhibition of ATP citrate lyase induces triglyceride accumulation with altered fatty acid composition in cancer cells. *International Journal of Cancer*. 2014;135(1):37-47. doi: <https://doi.org/10.1002/ijc.28652>.
429. Kang S, Seo JH, Heo T-H, Kim S-J. Batten disease is linked to altered expression of mitochondria-related metabolic molecules. *Neurochemistry International*. 2013;62(7):931-5. doi: <https://doi.org/10.1016/j.neuint.2013.03.007>.
430. Jones SF, Infante JR. Molecular Pathways: Fatty Acid Synthase. *Clin Cancer Res*. 2015;21(24):5434-8. Epub 2015/11/01. doi: 10.1158/1078-0432.Ccr-15-0126. PubMed PMID: 26519059.
431. Chandak PG, Radovic B, Aflaki E, Kolb D, Buchebner M, Fröhlich E, Magnes C, Sinner F, Haemmerle G, Zechner R, Tabas I, Levak-Frank S, Kratky D. Efficient phagocytosis requires triacylglycerol hydrolysis by adipose triglyceride lipase. *J Biol Chem*. 2010;285(26):20192-201. Epub 2010/04/29. doi: 10.1074/jbc.M110.107854. PubMed PMID: 20424161; PMCID: PMC2888432.
432. Vanier MT. Niemann-Pick disease type C. *Orphanet journal of rare diseases*. 2010;5:1-18.
433. Li X, Saha P, Li J, Blobel G, Pfeffer SR. Clues to the mechanism of cholesterol transfer from the structure of NPC1 middle luminal domain bound to NPC2. *Proc Natl Acad Sci U S A*. 2016;113(36):10079-84. Epub 2016/08/24. doi: 10.1073/pnas.1611956113. PubMed PMID: 27551080; PMCID: PMC5018801.
434. Lloyd-Evans E, Platt FM. Lipids on Trial: The Search for the Offending Metabolite in Niemann-Pick type C Disease. *Traffic*. 2010;11(4):419-28. doi: <https://doi.org/10.1111/j.1600-0854.2010.01032.x>.
435. Wassall SR, Brzustowicz MR, Shaikh SR, Cherezov V, Caffrey M, Stillwell W. Order from disorder, corralling cholesterol with chaotic lipids. The role of polyunsaturated lipids in membrane raft formation. *Chem Phys Lipids*. 2004;132(1):79-88. Epub 2004/11/09. doi: 10.1016/j.chemphyslip.2004.09.007. PubMed PMID: 15530450.
436. Kolter T, Sandhoff K. Principles of lysosomal membrane digestion: stimulation of sphingolipid degradation by sphingolipid activator proteins and anionic lysosomal lipids. *Annu Rev Cell Dev Biol*. 2005;21:81-103. Epub 2005/10/11. doi: 10.1146/annurev.cellbio.21.122303.120013. PubMed PMID: 16212488.
437. Chypre M, Zaidi N, Smans K. ATP-citrate lyase: a mini-review. *Biochemical and biophysical research communications*. 2012;422(1):1-4.
438. Wellen KE, Hatzivassiliou G, Sachdeva UM, Bui TV, Cross JR, Thompson CB. ATP-citrate lyase links cellular metabolism to histone acetylation. *Science*. 2009;324(5930):1076-80.
439. Szutowicz A, Bielarczyk H, Jankowska-Kulawy A, Pawełczyk T, Ronowska A. Acetyl-CoA the Key Factor for Survival or Death of Cholinergic Neurons in Course of Neurodegenerative Diseases. *Neurochemical Research*. 2013;38(8):1523-42. doi: 10.1007/s11064-013-1060-x.
440. Arrese EL, Saudale FZ, Soulages JL. Lipid Droplets as Signaling Platforms Linking Metabolic and Cellular Functions. *Lipid Insights*. 2014;7:7-16. Epub 2014/09/16. doi: 10.4137/lpi.S11128. PubMed PMID: 25221429; PMCID: PMC4161058.

441. Zehmer JK, Huang Y, Peng G, Pu J, Anderson RG, Liu P. A role for lipid droplets in intermembrane lipid traffic. *Proteomics*. 2009;9(4):914-21. Epub 2009/01/23. doi: 10.1002/pmic.200800584. PubMed PMID: 19160396; PMCID: PMC2676673.
442. Cabodevilla AG, Sánchez-Caballero L, Nintou E, Boiadjeva VG, Picatoste F, Gubern A, Claro E. Cell survival during complete nutrient deprivation depends on lipid droplet-fueled β -oxidation of fatty acids. *J Biol Chem*. 2013;288(39):27777-88. Epub 2013/08/14. doi: 10.1074/jbc.M113.466656. PubMed PMID: 23940052; PMCID: PMC3784694.
443. Hamilton JA, Hillard CJ, Spector AA, Watkins PA. Brain uptake and utilization of fatty acids, lipids and lipoproteins: application to neurological disorders. *J Mol Neurosci*. 2007;33(1):2-11. Epub 2007/09/29. doi: 10.1007/s12031-007-0060-1. PubMed PMID: 17901539.
444. Henrietta Lacks: science must right a historical wrong. *Nature*. 2020;585(7823):7. Epub 2020/09/03. doi: 10.1038/d41586-020-02494-z. PubMed PMID: 32873976.
445. The Legacy of Henrietta Lacks: The Importance of HeLa Cells: Johns Hopkins Medicine; 2023 [cited 2023 May 5]. Available from: <https://www.hopkinsmedicine.org/henrietalacks/importance-of-hela-cells.html>.
446. Skloot R. *The Immortal Life of Henrietta Lacks*. New York Broadway Books; 2010.
447. Collins F. NIH Director's Lof [Internet]. Morgan K, editor: National Institutes of Health. 2013. [cited 2023]. Available from: <https://directorsblog.nih.gov/2013/08/07/hela-cells-a-new-chapter-in-an-enduring-story/>.
448. Zhou P, Yang XL, Wang XG, Hu B, Zhang L, Zhang W, Si HR, Zhu Y, Li B, Huang CL, Chen HD, Chen J, Luo Y, Guo H, Jiang RD, Liu MQ, Chen Y, Shen XR, Wang X, Zheng XS, Zhao K, Chen QJ, Deng F, Liu LL, Yan B, Zhan FX, Wang YY, Xiao GF, Shi ZL. A pneumonia outbreak associated with a new coronavirus of probable bat origin. *Nature*. 2020;579(7798):270-3. Epub 2020/02/06. doi: 10.1038/s41586-020-2012-7. PubMed PMID: 32015507; PMCID: PMC7095418.
449. Bhopatkar AA, Ghag G, Wolf LM, Dean DN, Moss MA, Rangachari V. Cysteine-rich granulin-3 rapidly promotes amyloid-beta fibrils in both redox states. *Biochem J*. 2019;476(5):859-73. Epub 2019/02/21. doi: 10.1042/BCJ20180916. PubMed PMID: 30782973.
450. Horinokita I, Hayashi H, Oteki R, Mizumura R, Yamaguchi T, Usui A, Yuan B, Takagi N. Involvement of Progranulin and Granulin Expression in Inflammatory Responses after Cerebral Ischemia. *Int J Mol Sci*. 2019;20(20):5210. PubMed PMID: doi:10.3390/ijms20205210.
451. Bateman A, Bennett HP. The granulin gene family: from cancer to dementia. *Bioessays*. 2009;31(11):1245-54. Epub 2009/10/02. doi: 10.1002/bies.200900086. PubMed PMID: 19795409.
452. Kim WD, Wilson-Smillie M, Thanabalasingam A, Lefrancois S, Cotman SL, Huber RJ. Autophagy in the Neuronal Ceroid Lipofuscinoses (Batten Disease). *Front Cell Dev Biol*. 2022;10:812728. Epub 2022/03/08. doi: 10.3389/fcell.2022.812728. PubMed PMID: 35252181; PMCID: PMC8888908.
453. Jabs S, Quitsch A, Käkälä R, Koch B, Tyynelä J, Brade H, Glatzel M, Walkley S, Saftig P, Vanier MT, Braulke T. Accumulation of bis(monoacylglycero)phosphate and gangliosides in mouse models of neuronal ceroid lipofuscinosis. *J Neurochem*. 2008;106(3):1415-25. Epub 2008/05/24. doi: 10.1111/j.1471-4159.2008.05497.x. PubMed PMID: 18498441.
454. Walkley SU, Vanier MT. Secondary lipid accumulation in lysosomal disease. *Biochim Biophys Acta*. 2009;1793(4):726-36. Epub 2008/12/30. doi: 10.1016/j.bbamcr.2008.11.014. PubMed PMID: 19111580; PMCID: PMC4382014.

455. Laqtom NN, Dong W, Medoh UN, Cangelosi AL, Dharamdasani V, Chan SH, Kunchok T, Lewis CA, Heinze I, Tang R, Grimm C, Dang Do AN, Porter FD, Ori A, Sabatini DM, Abu-Remaileh M. CLN3 is required for the clearance of glycerophosphodiester from lysosomes. *Nature*. 2022;609(7929):1005-11. doi: 10.1038/s41586-022-05221-y.
456. Goursot A, Mineva T, Bissig C, Gruenberg J, Salahub DR. Structure, dynamics, and energetics of lysobisphosphatidic acid (LBPA) isomers. *J Phys Chem B*. 2010;114(47):15712-20. Epub 2010/11/09. doi: 10.1021/jp108361d. PubMed PMID: 21053942.
457. Showalter MR, Berg AL, Nagourney A, Heil H, Carraway KL, 3rd, Fiehn O. The Emerging and Diverse Roles of Bis(monoacylglycero) Phosphate Lipids in Cellular Physiology and Disease. *Int J Mol Sci*. 2020;21(21). Epub 2020/11/04. doi: 10.3390/ijms21218067. PubMed PMID: 33137979; PMCID: PMC7663174.
458. Schlame M, Rua D, Greenberg ML. The biosynthesis and functional role of cardiolipin. *Prog Lipid Res*. 2000;39(3):257-88. Epub 2000/05/09. doi: 10.1016/s0163-7827(00)00005-9. PubMed PMID: 10799718.
459. Petersen NH, Olsen OD, Groth-Pedersen L, Ellegaard AM, Bilgin M, Redmer S, Ostenfeld MS, Ulanet D, Dovmark TH, Lønborg A, Vindeløv SD, Hanahan D, Arenz C, Ejsing CS, Kirkegaard T, Rohde M, Nylandsted J, Jäättelä M. Transformation-associated changes in sphingolipid metabolism sensitize cells to lysosomal cell death induced by inhibitors of acid sphingomyelinase. *Cancer Cell*. 2013;24(3):379-93. Epub 2013/09/14. doi: 10.1016/j.ccr.2013.08.003. PubMed PMID: 24029234.
460. Abe A, Shayman JA. The role of negatively charged lipids in lysosomal phospholipase A2 function. *J Lipid Res*. 2009;50(10):2027-35. Epub 2009/03/27. doi: 10.1194/jlr.M900008-JLR200. PubMed PMID: 19321879; PMCID: PMC2739751.
461. Du H, Yang C, Nana AL, Seeley WW, Smolka M, Hu F. Progranulin inhibits phospholipase sPLA2-IIA to control neuroinflammation. *bioRxiv*. 2023. Epub 2023/04/18. doi: 10.1101/2023.04.06.535844. PubMed PMID: 37066328; PMCID: PMC10104136 (9987-01-US) for methods using sPLA2-IIA inhibition to treat FTLN-GRN and other neurodegenerative diseases.
462. Chen J, Cazenave-Gassiot A, Xu Y, Piroli P, Hwang R, Jr., DeFreitas L, Chan RB, Di Paolo G, Nandakumar R, Wenk MR, Marquer C. Lysosomal phospholipase A2 contributes to the biosynthesis of the atypical late endosome lipid bis(monoacylglycero)phosphate. *Commun Biol*. 2023;6(1):210. Epub 2023/02/25. doi: 10.1038/s42003-023-04573-z. PubMed PMID: 36823305; PMCID: PMC9950130 current employee and shareholder of Denali Therapeutics Inc. The other authors declare no competing financial interests.
463. Locatelli-Hoops S, Rimmel N, Klingenstein R, Breiden B, Rossocha M, Schoeniger M, Koenigs C, Saenger W, Sandhoff K. Saposin A mobilizes lipids from low cholesterol and high bis(monoacylglycerol)phosphate-containing membranes: patient variant Saposin A lacks lipid extraction capacity. *J Biol Chem*. 2006;281(43):32451-60. Epub 2006/08/15. doi: 10.1074/jbc.M607281200. PubMed PMID: 16905746.
464. Schueler U, Kolter T, Kaneski C, Blusztajn J, Herkenham M, Sandhoff K, Brady R. Toxicity of glucosylsphingosine (glucopsychosine) to cultured neuronal cells: a model system for assessing neuronal damage in Gaucher disease type 2 and 3. *Neurobiology of disease*. 2003;14(3):595-601.
465. van Eijk M, Ferraz Maria J, Boot Rolf G, Aerts Johannes MFG. Lyso-glycosphingolipids: presence and consequences. *Essays in Biochemistry*. 2020;64(3):565-78. doi: 10.1042/ebc20190090.

466. Matsumoto S-i, Sato S, Otake K, Kosugi Y. Highly-sensitive simultaneous quantitation of glucosylsphingosine and galactosylsphingosine in human cerebrospinal fluid by liquid chromatography/tandem mass spectrometry. *Journal of Pharmaceutical and Biomedical Analysis*. 2022;217:114852. doi: <https://doi.org/10.1016/j.jpba.2022.114852>.
467. Surface M, Balwani M, Waters C, Haimovich A, Gan-Or Z, Marder KS, Hsieh T, Song L, Padmanabhan S, Hsieh F, Merchant KM, Alcalay RN. Plasma Glucosylsphingosine in GBA1 Mutation Carriers with and without Parkinson's Disease. *Mov Disord*. 2022;37(2):416-21. Epub 2021/11/07. doi: 10.1002/mds.28846. PubMed PMID: 34741486; PMCID: PMC8840974.
468. Orvisky E, Park JK, LaMarca ME, Ginns EI, Martin BM, Tayebi N, Sidransky E. Glucosylsphingosine accumulation in tissues from patients with Gaucher disease: correlation with phenotype and genotype. *Mol Genet Metab*. 2002;76(4):262-70. Epub 2002/09/05. doi: 10.1016/s1096-7192(02)00117-8. PubMed PMID: 12208131.
469. Taguchi YV, Liu J, Ruan J, Pacheco J, Zhang X, Abbasi J, Keutzer J, Mistry PK, Chandra SS. Glucosylsphingosine Promotes α -Synuclein Pathology in Mutant GBA-Associated Parkinson's Disease. *J Neurosci*. 2017;37(40):9617-31. Epub 2017/08/30. doi: 10.1523/jneurosci.1525-17.2017. PubMed PMID: 28847804; PMCID: PMC5628407.
470. Lukas J, Cozma C, Yang F, Kramp G, Meyer A, Neßlauer A-M, Eichler S, Böttcher T, Witt M, Bräuer AU. Glucosylsphingosine causes hematological and visceral changes in mice—evidence for a pathophysiological role in gaucher disease. *Int J Mol Sci*. 2017;18(10):2192.
471. Lloyd-Evans E, Pelled D, Riebeling C, Bodenec J, de-Morgan A, Waller H, Schiffmann R, Futerman AH. Glucosylceramide and Glucosylsphingosine Modulate Calcium Mobilization from Brain Microsomes via Different Mechanisms *. *Journal of Biological Chemistry*. 2003;278(26):23594-9. doi: 10.1074/jbc.M300212200.
472. Lloyd-Evans E, Platt FM. Lysosomal Ca(2+) homeostasis: role in pathogenesis of lysosomal storage diseases. *Cell Calcium*. 2011;50(2):200-5. Epub 2011/07/05. doi: 10.1016/j.ceca.2011.03.010. PubMed PMID: 21724254.
473. Pišlar A, Bolčina L, Kos J. New Insights into the Role of Cysteine Cathepsins in Neuroinflammation. *Biomolecules*. 2021;11(12). Epub 2021/12/25. doi: 10.3390/biom11121796. PubMed PMID: 34944440; PMCID: PMC8698589.
474. Kos J, Sekirnik A, Premzl A, Zavasnik Bergant V, Langerholc T, Turk B, Werle B, Golouh R, Repnik U, Jeras M, Turk V. Carboxypeptidases cathepsins X and B display distinct protein profile in human cells and tissues. *Exp Cell Res*. 2005;306(1):103-13. Epub 2005/05/10. doi: 10.1016/j.yexcr.2004.12.006. PubMed PMID: 15878337.
475. Sun Y, Zamzow M, Ran H, Zhang W, Quinn B, Barnes S, Witte DP, Setchell KDR, Williams MT, Vorhees CV, Grabowski GA. Tissue-specific effects of saposin A and saposin B on glycosphingolipid degradation in mutant mice. *Human Molecular Genetics*. 2013;22(12):2435-50. doi: 10.1093/hmg/ddt096.
476. Rorman EG, Scheinker V, Grabowski GA. Structure and evolution of the human prosaposin chromosomal gene. *Genomics*. 1992;13(2):312-8. Epub 1992/06/01. doi: 10.1016/0888-7543(92)90247-p. PubMed PMID: 1612590.
477. Matsuda J, Vanier MT, Saito Y, Tohyama J, Suzuki K, Suzuki K. A mutation in the saposin A domain of the sphingolipid activator protein (prosaposin) gene results in a late-onset, chronic form of globoid cell leukodystrophy in the mouse. *Hum Mol Genet*. 2001;10(11):1191-9. Epub 2001/05/24. doi: 10.1093/hmg/10.11.1191. PubMed PMID: 11371512.
478. Spiegel R, Bach G, Sury V, Mengistu G, Meidan B, Shalev S, Shneur Y, Mandel H, Zeigler M. A mutation in the saposin A coding region of the prosaposin gene in an infant presenting as

Krabbe disease: first report of saposin A deficiency in humans. *Mol Genet Metab.* 2005;84(2):160-6. Epub 2005/03/19. doi: 10.1016/j.ymgme.2004.10.004. PubMed PMID: 15773042.

479. Ho MW, O'Brien JS. Gaucher's disease: deficiency of 'acid' -glucosidase and reconstitution of enzyme activity in vitro. *Proc Natl Acad Sci U S A.* 1971;68(11):2810-3. Epub 1971/11/01. doi: 10.1073/pnas.68.11.2810. PubMed PMID: 5288260; PMCID: PMC389531.

480. Schnabel D, Schröder M, Sandhoff K. Mutation in the sphingolipid activator protein 2 in a patient with a variant of Gaucher disease. *FEBS Lett.* 1991;284(1):57-9. Epub 1991/06/17. doi: 10.1016/0014-5793(91)80760-z. PubMed PMID: 2060627.

481. Azuma N, O'Brien JS, Moser HW, Kishimoto Y. Stimulation of acid ceramidase activity by saposin D. *Archives of biochemistry and biophysics.* 1994;311(2):354-7.

482. Radha Rama Devi A, Kadali S, Radhika A, Singh V, Kumar MA, Reddy GM, Naushad SM. Acute Gaucher Disease-Like Condition in an Indian Infant with a Novel Biallelic Mutation in the Prosaposin Gene. *J Pediatr Genet.* 2019;8(2):81-5. Epub 2019/05/08. doi: 10.1055/s-0038-1675372. PubMed PMID: 31061751; PMCID: PMC6499618.

483. Li S, Sonnino S, Tettamanti G, Li Y. Characterization of a nonspecific activator protein for the enzymatic hydrolysis of glycolipids. *Journal of Biological Chemistry.* 1988;263(14):6588-91.

484. Wilkening G, Linke T, Uhlhorn-Dierks G, Sandhoff K. Degradation of membrane-bound ganglioside GM1: stimulation by bis (monoacylglycero) phosphate and the activator proteins SAP-B and GM2-AP. *Journal of Biological Chemistry.* 2000;275(46):35814-9.

485. Harzer K, Paton BC, Christomanou H, Chatelut M, Levade T, Hiraiwa M, O'Brien JS. Saposins (sap) A and C activate the degradation of galactosylceramide in living cells. *FEBS letters.* 1997;417(3):270-4.

486. Ahn VE, Leyko P, Alattia JR, Chen L, Privé GG. Crystal structures of saposins A and C. *Protein Sci.* 2006;15(8):1849-57. Epub 2006/07/11. doi: 10.1110/ps.062256606. PubMed PMID: 16823039; PMCID: PMC2242594.

487. Gebai A, Gorelik A, Nagar B. Crystal structure of saposin D in an open conformation. *Journal of Structural Biology.* 2018;204(2):145-50. doi: <https://doi.org/10.1016/j.jsb.2018.07.011>.

488. Wendt W, Schulten R, Stichel CC, Lübbert H. Intra- versus extracellular effects of microglia-derived cysteine proteases in a conditioned medium transfer model. *J Neurochem.* 2009;110(6):1931-41. Epub 2009/07/25. doi: 10.1111/j.1471-4159.2009.06283.x. PubMed PMID: 19627446.

489. Kingham PJ, Pocock JM. Microglial secreted cathepsin B induces neuronal apoptosis. *J Neurochem.* 2001;76(5):1475-84. Epub 2001/03/10. doi: 10.1046/j.1471-4159.2001.00146.x. PubMed PMID: 11238732.

490. Anes E, Pires D, Mandal M, Azevedo-Pereira JM. Spatial localization of cathepsins: Implications in immune activation and resolution during infections. *Front Immunol.* 2022;13:955407. Epub 2022/08/23. doi: 10.3389/fimmu.2022.955407. PubMed PMID: 35990632; PMCID: PMC9382241.

491. Pišlar A, Božić B, Zidar N, Kos J. Inhibition of cathepsin X reduces the strength of microglial-mediated neuroinflammation. *Neuropharmacology.* 2017;114:88-100. Epub 2016/11/28. doi: 10.1016/j.neuropharm.2016.11.019. PubMed PMID: 27889490.

492. Pišlar A, Tratnjek L, Glavan G, Zidar N, Živin M, Kos J. Neuroinflammation-Induced Upregulation of Glial Cathepsin X Expression and Activity in vivo. *Front Mol Neurosci.* 2020;13:575453. Epub 2020/12/18. doi: 10.3389/fnmol.2020.575453. PubMed PMID: 33328882; PMCID: PMC7714997.

493. Gómez-Sintes R, Ledesma MD, Boya P. Lysosomal cell death mechanisms in aging. *Ageing Res Rev.* 2016;32:150-68.
494. Okeke EB, Louttit C, Fry C, Najafabadi AH, Han K, Nemzek J, Moon JJ. Inhibition of neutrophil elastase prevents neutrophil extracellular trap formation and rescues mice from endotoxic shock. *Biomaterials.* 2020;238:119836. Epub 2020/02/12. doi: 10.1016/j.biomaterials.2020.119836. PubMed PMID: 32045782; PMCID: PMC7075277.
495. Stock AJ, Kasus-Jacobi A, Pereira HA. The role of neutrophil granule proteins in neuroinflammation and Alzheimer's disease. *Journal of Neuroinflammation.* 2018;15(1):240. doi: 10.1186/s12974-018-1284-4.
496. Pham CTN. Neutrophil serine proteases: specific regulators of inflammation. *Nature Reviews Immunology.* 2006;6(7):541-50. doi: 10.1038/nri1841.
497. Repnik U, Starr AE, Overall CM, Turk B. Cysteine Cathepsins Activate ELR Chemokines and Inactivate Non-ELR Chemokines. *J Biol Chem.* 2015;290(22):13800-11. Epub 2015/04/03. doi: 10.1074/jbc.M115.638395. PubMed PMID: 25833952; PMCID: PMC4447957.
498. Wolf Y, Yona S, Kim KW, Jung S. Microglia, seen from the CX3CR1 angle. *Front Cell Neurosci.* 2013;7:26. Epub 2013/03/20. doi: 10.3389/fncel.2013.00026. PubMed PMID: 23507975; PMCID: PMC3600435.
499. Vizovišek M, Fonović M, Turk B. Cysteine cathepsins in extracellular matrix remodeling: Extracellular matrix degradation and beyond. *Matrix Biology.* 2019;75-76:141-59. doi: <https://doi.org/10.1016/j.matbio.2018.01.024>.
500. Campden RI, Warren AL, Greene CJ, Chiriboga JA, Arnold CR, Aggarwal D, McKenna N, Sandall CF, MacDonald JA, Yates RM. Extracellular cathepsin Z signals through the $\alpha 5$ integrin and augments NLRP3 inflammasome activation. *Journal of Biological Chemistry.* 2022;298(1):101459. doi: <https://doi.org/10.1016/j.jbc.2021.101459>.
501. Schuster DJ, Dykstra JA, Riedl MS, Kitto KF, Belur LR, McIvor RS, Elde RP, Fairbanks CA, Vulchanova L. Biodistribution of adeno-associated virus serotype 9 (AAV9) vector after intrathecal and intravenous delivery in mouse. *Front Neuroanat.* 2014;8:42. Epub 2014/06/25. doi: 10.3389/fnana.2014.00042. PubMed PMID: 24959122; PMCID: PMC4051274.
502. Mackenzie IRA, Baker M, Pickering-Brown S, Hsiung G-YR, Lindholm C, Dwosh E, Gass J, Cannon A, Rademakers R, Hutton M, Feldman HH. The neuropathology of frontotemporal lobar degeneration caused by mutations in the progranulin gene. *Brain.* 2006;129(11):3081-90. doi: 10.1093/brain/awl271.
503. Bhandari V, Palfree RG, Bateman A. Isolation and sequence of the granulin precursor cDNA from human bone marrow reveals tandem cysteine-rich granulin domains. *Proc Natl Acad Sci U S A.* 1992;89(5):1715-9. Epub 1992/03/01. doi: 10.1073/pnas.89.5.1715. PubMed PMID: 1542665; PMCID: PMC48523.
504. Altmann C, Vasic V, Hardt S, Heidler J, Häussler A, Wittig I, Schmidt MHH, Tegeder I. Progranulin promotes peripheral nerve regeneration and reinnervation: role of notch signaling. *Mol Neurodegener.* 2016;11(1):69. Epub 2016/10/25. doi: 10.1186/s13024-016-0132-1. PubMed PMID: 27770818; PMCID: PMC5075406.
505. Dong T, Tejwani L, Jung Y, Kokubu H, Luttik K, Driessen TM, Lim J. Microglia regulate brain progranulin levels through the endocytosis/lysosomal pathway. *JCI Insight.* 2021;6(22). Epub 2021/10/08. doi: 10.1172/jci.insight.136147. PubMed PMID: 34618685; PMCID: PMC8663778.

506. Petkau TL, Kosior N, de Asis K, Connolly C, Leavitt BR. Selective depletion of microglial progranulin in mice is not sufficient to cause neuronal ceroid lipofuscinosis or neuroinflammation. *Journal of Neuroinflammation*. 2017;14(1):225. doi: 10.1186/s12974-017-1000-9.
507. Petkau TL, Blanco J, Leavitt BR. Conditional loss of progranulin in neurons is not sufficient to cause neuronal ceroid lipofuscinosis-like neuropathology in mice. *Neurobiol Dis*. 2017;106:14-22. Epub 2017/06/26. doi: 10.1016/j.nbd.2017.06.012. PubMed PMID: 28647554.
508. de Majo M, Koontz M, Marsan E, Salinas N, Ramsey A, Kuo YM, Seo K, Li H, Dräger N, Leng K, Gonzales SL, Kurnellas M, Miyaoka Y, Klim JR, Kampmann M, Ward ME, Huang EJ, Ullian EM. Granulin loss of function in human mature brain organoids implicates astrocytes in TDP-43 pathology. *Stem Cell Reports*. 2023;18(3):706-19. Epub 2023/02/25. doi: 10.1016/j.stemcr.2023.01.012. PubMed PMID: 36827976; PMCID: PMC10031303.
509. Kim S, Moon GJ, Oh Y-S, Park J, Shin W-H, Jeong JY, Choi KS, Jin BK, Kholodilov N, Burke RE, Kim H-J, Ha CM, Lee S-G, Kim SR. Protection of nigral dopaminergic neurons by AAV1 transduction with Rheb(S16H) against neurotoxic inflammation in vivo. *Experimental & Molecular Medicine*. 2018;50(2):e440-e. doi: 10.1038/emm.2017.261.
510. Mosher KI, Andres RH, Fukuhara T, Bieri G, Hasegawa-Moriyama M, He Y, Guzman R, Wyss-Coray T. Neural progenitor cells regulate microglia functions and activity. *Nat Neurosci*. 2012;15(11):1485-7. Epub 2012/10/23. doi: 10.1038/nn.3233. PubMed PMID: 23086334; PMCID: PMC3495979.
511. Jin X, Yamashita T. Microglia in central nervous system repair after injury. *The Journal of Biochemistry*. 2016;159(5):491-6. doi: 10.1093/jb/mvw009.
512. Chakrabarty P, Ceballos-Diaz C, Lin WL, Beccard A, Jansen-West K, McFarland NR, Janus C, Dickson D, Das P, Golde TE. Interferon- γ induces progressive nigrostriatal degeneration and basal ganglia calcification. *Nat Neurosci*. 2011;14(6):694-6. Epub 2011/05/17. doi: 10.1038/nn.2829. PubMed PMID: 21572432; PMCID: PMC3780582.
513. Aschauer DF, Kreuz S, Rumpel S. Analysis of transduction efficiency, tropism and axonal transport of AAV serotypes 1, 2, 5, 6, 8 and 9 in the mouse brain. *PLoS One*. 2013;8(9):e76310. Epub 2013/10/03. doi: 10.1371/journal.pone.0076310. PubMed PMID: 24086725; PMCID: PMC3785459 KG, which partly funded this study. There are no patents, products in development or marketed products to declare. This does not alter the authors' adherence to all the PLOS ONE policies on sharing data and materials.
514. Zhao X, Lin Y, Liou B, Fu W, Jian J, Fannie V, Zhang W, Setchell KDR, Grabowski GA, Sun Y, Liu CJ. PGRN deficiency exacerbates, whereas a brain penetrant PGRN derivative protects, GBA1 mutation-associated pathologies and diseases. *Proc Natl Acad Sci U S A*. 2023;120(1):e2210442120. Epub 2022/12/28. doi: 10.1073/pnas.2210442120. PubMed PMID: 36574647; PMCID: PMC9910439.
515. Mathiesen SN, Lock JL, Schoderboeck L, Abraham WC, Hughes SM. CNS Transduction Benefits of AAV-PHP.eB over AAV9 Are Dependent on Administration Route and Mouse Strain. *Molecular Therapy - Methods & Clinical Development*. 2020;19:447-58. doi: 10.1016/j.omtm.2020.10.011.
516. Ravindra Kumar S, Miles TF, Chen X, Brown D, Dobрева T, Huang Q, Ding X, Luo Y, Einarsson PH, Greenbaum A, Jang MJ, Deverman BE, Gradinaru V. Multiplexed Cre-dependent selection yields systemic AAVs for targeting distinct brain cell types. *Nature Methods*. 2020;17(5):541-50. doi: 10.1038/s41592-020-0799-7.

517. Hordeaux J, Wang Q, Katz N, Buza EL, Bell P, Wilson JM. The Neurotropic Properties of AAV-PHP.B Are Limited to C57BL/6J Mice. *Mol Ther*. 2018;26(3):664-8. Epub 2018/02/13. doi: 10.1016/j.ymthe.2018.01.018. PubMed PMID: 29428298; PMCID: PMC5911151.
518. Matsuzaki Y, Konno A, Mochizuki R, Shinohara Y, Nitta K, Okada Y, Hirai H. Intravenous administration of the adeno-associated virus-PHP. B capsid fails to upregulate transduction efficiency in the marmoset brain. *Neuroscience letters*. 2018;665:182-8.
519. Hordeaux J, Yuan Y, Clark PM, Wang Q, Martino RA, Sims JJ, Bell P, Raymond A, Stanford WL, Wilson JM. The GPI-linked protein LY6A drives AAV-PHP. B transport across the blood-brain barrier. *Molecular Therapy*. 2019;27(5):912-21.
520. Huang Q, Chan KY, Tobey IG, Chan YA, Poterba T, Boutros CL, Balazs AB, Daneman R, Bloom JM, Seed C. Delivering genes across the blood-brain barrier: LY6A, a novel cellular receptor for AAV-PHP. B capsids. *PLoS One*. 2019;14(11):e0225206.
521. Song R, Pekrun K, Khan TA, Zhang F, Paşca SP, Kay MA. Selection of rAAV vectors that cross the human blood-brain barrier and target the central nervous system using a transwell model. *Molecular Therapy - Methods & Clinical Development*. 2022;27:73-88. doi: 10.1016/j.omtm.2022.09.002.
522. Wu Y, Shao W, Todd TW, Tong J, Yue M, Koga S, Castanedes-Casey M, Librero AL, Lee CW, Mackenzie IR, Dickson DW, Zhang YJ, Petrucelli L, Prudencio M. Microglial lysosome dysfunction contributes to white matter pathology and TDP-43 proteinopathy in GRN-associated FTD. *Cell Rep*. 2021;36(8):109581. Epub 2021/08/26. doi: 10.1016/j.celrep.2021.109581. PubMed PMID: 34433069; PMCID: PMC8491969.
523. Raitano S, Ordovàs L, De Muyenck L, Guo W, Espuny-Camacho I, Geraerts M, Khurana S, Vanuytsel K, Tóth BI, Voets T, Vandenberghe R, Cathomen T, Van Den Bosch L, Vanderhaeghen P, Van Damme P, Verfaillie CM. Restoration of progranulin expression rescues cortical neuron generation in an induced pluripotent stem cell model of frontotemporal dementia. *Stem Cell Reports*. 2015;4(1):16-24. Epub 2015/01/06. doi: 10.1016/j.stemcr.2014.12.001. PubMed PMID: 25556567; PMCID: PMC4297877.
524. Cheng XT, Xie YX, Zhou B, Huang N, Farfel-Becker T, Sheng ZH. Characterization of LAMP1-labeled nondegradative lysosomal and endocytic compartments in neurons. *J Cell Biol*. 2018;217(9):3127-39. Epub 2018/04/27. doi: 10.1083/jcb.201711083. PubMed PMID: 29695488; PMCID: PMC6123004.
525. Vázquez CL, Colombo MI. Assays to assess autophagy induction and fusion of autophagic vacuoles with a degradative compartment, using monodansylcadaverine (MDC) and DQ-BSA. *Methods Enzymol*. 2009;452:85-95. Epub 2009/02/10. doi: 10.1016/s0076-6879(08)03606-9. PubMed PMID: 19200877.
526. Zhang Y, Zhao Y, Wu Y, Zhao B, Wang L, Song B. Hemicyanine based naked-eye ratiometric fluorescent probe for monitoring lysosomal pH and its application. *Spectrochimica Acta Part A: Molecular and Biomolecular Spectroscopy*. 2020;227:117767. doi: <https://doi.org/10.1016/j.saa.2019.117767>.
527. DiCiccio JE, Steinberg BE. Lysosomal pH and analysis of the counter ion pathways that support acidification. *J Gen Physiol*. 2011;137(4):385-90. Epub 2011/03/16. doi: 10.1085/jgp.201110596. PubMed PMID: 21402887; PMCID: PMC3068279.
528. Barral DC, Staiano L, Guimas Almeida C, Cutler DF, Eden ER, Futter CE, Galione A, Marques ARA, Medina DL, Napolitano G, Settembre C, Vieira OV, Aerts JMFG, Atakpa-Adaji P, Bruno G, Capuozzo A, De Leonibus E, Di Malta C, Escrevente C, Esposito A, Grumati P, Hall MJ, Teodoro RO, Lopes SS, Luzio JP, Monfregola J, Montefusco S, Platt FM, Polishchuck R, De

- Risi M, Sambri I, Soldati C, Seabra MC. Current methods to analyze lysosome morphology, positioning, motility and function. *Traffic*. 2022;23(5):238-69. doi: <https://doi.org/10.1111/tra.12839>.
529. Abu-Remaileh M, Wyant GA, Kim C, Laqtom NN, Abbasi M, Chan SH, Freinkman E, Sabatini DM. Lysosomal metabolomics reveals V-ATPase- and mTOR-dependent regulation of amino acid efflux from lysosomes. *Science (New York, NY)*. 2017;358(6364):807-13. Epub 2017/10/26. doi: 10.1126/science.aan6298. PubMed PMID: 29074583.
530. Hasan S, Fernandopulle MS, Humble SW, Frankenfield AM, Li H, Prestil R, Johnson KR, Ryan BJ, Wade-Martins R, Ward ME, Hao L. Multi-modal Proteomic Characterization of Lysosomal Function and Proteostasis in Progranulin-Deficient Neurons. *bioRxiv*. 2023. Epub 2023/03/04. doi: 10.1101/2023.02.24.529955. PubMed PMID: 36865171; PMCID: PMC9980118.
531. Patel S, Docampo R. Acidic calcium stores open for business: expanding the potential for intracellular Ca²⁺ signaling. *Trends Cell Biol*. 2010;20(5):277-86. Epub 2010/03/23. doi: 10.1016/j.tcb.2010.02.003. PubMed PMID: 20303271; PMCID: PMC2862797.
532. Feng X, Yang J. Lysosomal Calcium in Neurodegeneration. *Messenger (Los Angel)*. 2016;5(1-2):56-66. Epub 2016/06/01. doi: 10.1166/msr.2016.1055. PubMed PMID: 29082116; PMCID: PMC5659362.
533. Kawamoto EM, Vivar C, Camandola S. Physiology and pathology of calcium signaling in the brain. *Front Pharmacol*. 2012;3:61. Epub 2012/04/21. doi: 10.3389/fphar.2012.00061. PubMed PMID: 22518105; PMCID: PMC3325487.
534. McQuade A, Coburn M, Tu CH, Hasselmann J, Davtyan H, Blurton-Jones M. Development and validation of a simplified method to generate human microglia from pluripotent stem cells. *Mol Neurodegener*. 2018;13(1):67. Epub 2018/12/24. doi: 10.1186/s13024-018-0297-x. PubMed PMID: 30577865; PMCID: PMC6303871.
535. Garcia-Reitboeck P, Phillips A, Piers TM, Villegas-Llerena C, Butler M, Mallach A, Rodrigues C, Arber CE, Heslegrave A, Zetterberg H, Neumann H, Neame S, Houlden H, Hardy J, Pocock JM. Human Induced Pluripotent Stem Cell-Derived Microglia-Like Cells Harboring TREM2 Missense Mutations Show Specific Deficits in Phagocytosis. *Cell Rep*. 2018;24(9):2300-11. doi: <https://doi.org/10.1016/j.celrep.2018.07.094>.
536. Lindner B, Burkard T, Schuler M. Phagocytosis assays with different pH-sensitive fluorescent particles and various readouts. *BioTechniques*. 2020;68(5):245-50. doi: 10.2144/btn-2020-0003. PubMed PMID: 32079414.
537. Götzl JK, Brendel M, Werner G, Parhizkar S, Sebastian Monasor L, Kleinberger G, Colombo A-V, Deussing M, Wagner M, Winkelmann J, Diehl-Schmid J, Levin J, Fellerer K, Reifschneider A, Bultmann S, Bartenstein P, Rominger A, Tahirovic S, Smith ST, Madore C, Butovsky O, Capell A, Haass C. Opposite microglial activation stages upon loss of PGRN or TREM2 result in reduced cerebral glucose metabolism. *EMBO Mol Med*. 2019;11(6):e9711. doi: 10.15252/emmm.201809711.